DOE/PC/90287--T15

Further Studies of the Effects of Oxidation on the Surface Properties of Coal and Coal Pyrite

by

Miguel Nicolas Herrera

B.S. (Universidad de Chile-Chile) 1984
M.S. (Universidad de Chile-Chile) 1988

A dissertation submitted in partial satisfaction of the requirements for the degree of

Doctor of Philosophy

in

Engineering - Materials Science and Mineral Engineering

in the

GRADUATE DIVISION

of the

UNIVERSITY of CALIFORNIA at BERKELEY

Committee in charge:

Professor Fiona M. Doyle
Professor Douglas Fuerstenau
Professor William Nazaroff

1994

TO BENJAMIN, SEBASTIAN AND MARTA

TABLE OF CONTENTS

TABLE OF CONTENTS (CONTINUED)

TABLE OF CONTENTS (CONTINUED)

TABLE OF CONTENTS (CONTINUED)

LIST OF FIGURES

LIST OF TABLES

ACKNOWLEDGEMENTS

I want to express my thanks to Professor Fiona M. Doyle for her guidance, suggestions, and encouragement throughout the course of my study at Berkeley. Special thanks to Professor D.W. Fuerstenau and Professor W. Nazaroff for reviewing my dissertation.

I thank to Jianli Diao who has always taken time to discuss my study and give suggestions. Thanks to Abbas Mirza and Saskia Duyvesteyn. Also, special thanks to Alexandre Monteiro for being my best colleague and friend.

I thank all my professors at Berkeley for their useful lectures, discussions and guidance.

The financial support of the U. S. Department of Energy under grant number DE-FG22-90PC90287 is gratefully acknowledged. I thank the California Mining and Mineral Resources Research Institute, under grant number G1134206 for their financial support during the last stage of my study. Also, thank to the contributors of the Jane Lewis Fellowship.

Finally, I thank my wife for her sacrifices and my sincere thanks are due to my mother in law for her support.

I. INTRODUCTION

Due to the continuous depletion of world oil reserves, the global demand for coal as an energy source has been continuously increasing for the last two decades. According to the International Energy Agency, coal demand by the year 2005 in more than 20 member countries of the Organization for Economic Cooperation and Development (OECD) will be 1.4 times the demand in 1985, and coal use as a percentage of total energy requirements will be approximately 30%, the same as oil. Most of this growth is expected to occur in steam coal used to produce electricity[1]. In the United States there is an increasing demand for coal from the electric utilities, which consumed about 84% of the total coal produced in 1992.[2]

The United States has the largest coal resources in the world, with a mineable reserve of about 318 billions tons, of coals of different ranks, with high to low sulfur content.[3] This provides a good energy alternative, to reduce the excessive dependence on imported oil. However, there still several technical problems associated with coal conversion and utilization. One of the most important problems is the release of SO_2 to the atmosphere on combustion. In 1986, gaseous SO_2 emissions were 30 times greater than in 1860 and were expected to be 40 times greater by the year 2000.[4]

Although the basic attraction of coal remains its low cost and great abundance, the greatest obstacle to expansion of coal-fired power generation plants is the cost of environmental protection. In the United States, about 40% of the capital cost and 35% of the operating cost of new plants can be accounted for by their pollution control systems.[6] In an effort to reduce the detrimental effects of SO_2 on the environment, the 1990 Clean Air Act established a maximum emission level of 2.5 lb SO_2/MBtu to go into effect by 1995 and 1.2 lb SO_2/MBtu to go into effect by 2000. Under these circumstances, there is

a crucial need for clean and cost-effective coal technologies that can improve coal use and its environmental acceptability.

Pyrite (FeS_2) is the major inorganic form in which sulfur occurs in coal and it comprises 30 to 70% of total sulfur in most coals. Understanding the oxidation of coal and coal pyrite is extremely important considering the devastating effects that their oxidation has on the environment. When pyrite is oxidized in the presence of water and oxygen, it produces sulfuric acid, dissolved ferrous iron and heat. In some cases, this reaction can be dramatically accelerated by Thiobacillus ferrooxidans, an iron oxidizing bacteria that catalyze the oxidation of ferrous to ferric iron in the low pH range and provides appropriate solution potential conditions for pyrite oxidation. Thus, the oxidation of pyrite is significantly accelerated and an autocatalytic process named acid mine drainage is established which is extremely difficult to halt.

The sulfuric acid generated by pyrite oxidation, provides the appropriate conditions for the leaching of trace toxic metals from ash minerals present in coal, and other minerals that the acid can contact. The solution produced contains toxic metals that may spread and contaminate, lakes, surface water streams and aquifer systems. It can also pose threats to wildlife and public health. In the United States, acid mine drainage is the most severe and widespread water pollution problem encountered with inactive and abandoned coal and base metal mines.

The increasing application of flotation and oil agglomeration technologies[7] would produce significant amounts of pyrite wastes in future. Considering that there is no agreement on what strategies are required to prevent pyrite from oxidation, it is expected that some preventing measures would not be effective. Under these circumstances, the

generation of acidic discharges in coal preparation plants could be another serious environmental problem for the coal industry in the future.

The oxidation behavior of coal pyrite is by no mean completely understood, and considering that acid mine drainage is an environmental problem of significant magnitude, it is extremely important to make efforts to further understand the mechanisms of its formation. Environmental assessment and effective use of remediation strategies, require an in-depth understanding of pyrite oxidation. This knowledge also provides a basis for predicting how changing conditions within mining waste facilities alter the long term release rates of trace metals and other contaminants.

Another factor related with the noxious effect of the oxidation of coal and coal pyrite on the environment is associated with coal conversion and utilization. One of the most important problems associated with coal combustion is the release of SO_2 to the atmosphere. In the atmosphere, SO_2 undergoes chemical conversion and reacts with other atmospheric species to form a variety of compounds, the most important being sulfuric acid and ammonium sulfate.[5] Also, SO_2 can corrode the boiler section of power plants, while inorganic sulfur compounds present in coal can poison catalysts in coal liquefaction processes.

The separation of pyrite from coal is crucial in addressing the reduction of the detrimental effects of SO_2 on the environment. However, it is very difficult to achieve reliable separation from coal. In pre-combustion coal desulfurization, pyrite can either be oxidatively leached or physically separated from coal using such technologies as froth flotation and selective oil agglomeration.[7] The effectiveness of these processes is strongly dependent on the surface properties of coal and the mineral matter associated with it. However, the surface properties of coal and coal pyrite can be significantly affected by

oxidation that reduce the hydrophobicity of coal, and affects the interaction of pyrite with depressants in flotation and bridging agents in oil agglomeration.

Despite its crucial importance, the role of oxidation on the surface properties of coal and coal pyrite is still not fully understood. Therefore, in order to improve the environmental acceptability of coal, it is necessary to have more fundamental knowledge on the effects of oxidation on the surface properties of coal and coal pyrite. This information will provide a foundation for predicting how oxidation can control the behavior of coal and coal pyrite in coal cleaning processes.

II. SCOPE OF THIS INVESTIGATION

Coal oxidation has been studied extensively; however, still there is no general agreement concerning the mechanisms of oxidation. Moreover, coal and mineral matter oxidation behavior have been regarded as separate processes and the resulting changes in surface properties are notoriously difficult to predict. Greater understanding of the effect of oxidation on the surface properties of coal and coal mineral matter is essential for process improvement. The objective of this research, therefore, was to investigate the oxidation behavior of coal and coal pyrite and to correlate the changes in the surface properties induced by oxidation, along with the intrinsic physical and chemical properties of these organic and inorganic materials, with the behavior in physical coal cleaning processes. This provide more fundamental knowledge for understanding the way in which different factors interact in a medium as heterogeneous as coal.

Fourteen coal samples of different ranks ranging from high to medium sulfur content were studied by dry oxidation tests at different temperatures and humidities, and by wet oxidation tests using different oxidizing agents. The concentration of surface oxygen functional groups was determined by ion-exchange methods. The changes in the coal composition with oxidation were analyzed by spectroscopic techniques. The wettability of as-received and oxidized coal and coal pyrite samples was assessed by film flotation tests. The electrokinetic behavior of different coals and coal pyrite samples was studied by electrokinetic tests using electrophoresis. Possible oxidation mechanisms have been proposed to explain the changes on the coal surface induced by different oxidation treatments.

Flotation tests were done on different coals under controlled pH and solution potential to investigate the effect of polarization on the flotation of coal, and the ability to

separate pyrite from coal by selective flotation of either coal or pyrite. The results were related to selected rank parameters from the proximate, sulfur and oxygen group analysis. to identify any parameter that correlated well with flotation response, either positively or negatively.

The electrochemical behavior of polished and etched coal pyrite samples was investigated from pH 1.0 to 10.5 by rest potential measurements and cyclic voltammetry. Also, the effect of the electrode potential on the wetting behavior of coal pyrite was investigated by contact angle measurements on polarized coal pyrite electrode.

The reliability and suitability of standard test methods used to determine the pyrite content of coal and mineral wastes, and their propensity to release acidic drainage were studied. The kinetics of coal pyrite dissolution were also investigated by using aqueous solutions of hydrogen peroxide and nitric acid.

III. LITERATURE REVIEW

A. COAL CHARACTERISTICS

A.1. Origin and Coalification

Coal is a material composed of organic chemical substances and inorganic minerals, derived from decomposed plant matter. The chemical composition and physical properties changes with coalification. Coalification is the progressive enrichment in organically bound carbon; starting from decomposed plant and through a series of changes, the decomposed plant is transformed sequentially into peat, lignite, sub-bituminous coal, bituminous coal and finally anthracite. The stage of coalification of a coal is denoted by its rank, with lignite and sub-bituminous coals being commonly referred as low-rank coal, and bituminous and anthracite coals being considered high-rank coals.

The diversity of the original materials and the degree of coalification of coals lead to a wide range in the behavior of coals. As the rank increases, the composition and physical properties of the coal constituents change. These are of vital importance in determining the properties and potential behavior of a coal and an optimum use of coal can be made according to its rank. The rank of a coal is determined by its fixed carbon, volatile matter and BTU content. Table 1 shows the main characteristics of coals of different rank.

A.2. Chemical Composition

The chemical composition of coal is usually determined by proximate analysis, and by elemental or ultimate analysis. Proximate analysis is a simple gravimetric procedure

Table 1: Approximate values of some coal properties in different rank. (adapted from ref. 127)

Rank	Fixed Carbon	Volatile Matter	Moisture	Calorific Value	Hydrogen	Oxygen
	%, dmmf *	%, dmmf	%, As-rec'd	Btu/lb	%, dmmf	%, dmmf
Lignite	65-72	40-50	70-90	7000	4-5	30
Sub-bituminous C	65-75	49-50	30-40	9000	4-5	20
Sub-bituminous B	70-75	47-49	20-30	10000	4-5	17
Sub-bituminous A	70-75	42-45	20-30	11000	5-6	16
HV bituminous C	76-78	34-45	1-20	12000	5-6	13
HV bituminous B	78-80	30-40	1-20	13500	5-6	10
HV bituminous A	80-87	31-40	1-20	14500	5-6	4-10
MV bituminous	89-90	20-31	1-20	15000	4-5	3-4
LV bituminous	90-93	10-20	1-20	15800	3-4	3
Semi-anthracite	90-93	15-10	1.5-3.5	15400	2-3	3
Anthracite	93	<10	1.5-3.5	15200	2-3	3

*% by mass

*dmmf : dry mineral matter free

that determines moisture, volatile matter and ash. Moisture is water that is driven off when coal is heated to 106°C. It can be present in two forms: free moisture that can be removed by air drying, and bound moisture that is physically-held water in the smaller capillaries or pores. Volatile matter varies qualitatively and quantitatively according to the rank and petrographic composition of coal. It consists of a wide spectrum of hydrocarbons, carbon monoxide, carbon dioxide and chemically combined water formed

by thermal decomposition of coal. Ash corresponds to the residues left behind when weighed test samples are completely incinerated in air at about 725°C. It should be noted that the ash content is not identical to mineral matter in coal, because minerals may undergo compositional changes during incineration.

Ultimate analysis is an elemental chemical analysis that yields the percentages of carbon, hydrogen, nitrogen and sulfur. Oxygen is obtained by difference. The American Society for Testing and Materials (A.S.T.M.) has developed standard testing procedures for the proximate and ultimate analysis of coals.[8,9]

A.3. Coal Components and Their Structure

Coal is composed mainly of two types of materials: organic carbonaceous macerals and inorganic crystalline minerals.

A.3.1. Organic Material

The organic material in coal is composed of small units called macerals, which are the combustible part of coal. They can be distinguished by their morphology and are very different in their physical and chemical properties, and therefore, in their reactivities. Based on their petrographic properties, macerals are divided in three groups, namely vitrinite, exinite and inertinite.[10]

Vitrinite group. This maceral group is medium dark to light grey with occasional botanical structure. Vitrinite reflectance increases with coalification. Among the important properties of vitrinite are its tendency to shows fissures and cracks, and excellent coking ability due to its high swelling properties and plasticity. Vitrinite is easily

hydrogenated in low rank coals whereas high rank coals require special processes. Vitrinite is very easily oxidized, leading to spontaneous combustion. Due to its brittleness and fissuring, it represent a large proportion of mine dust.[10]

Exinite group. This maceral group has low reflectivity and high volatile matter content. The exinite macerals are the most valuable component in coals because they produce tar. Exinite produces the highest yield of byproducts in coal, over 25% volatile matter (low rank coals). Exinites have no tendency to spontaneous combustion, and their toughness restricts fissuring and dust formation.[10]

Inertinite group. This is the highest reflecting component and may be distinguished by a higher relief than other macerals on polished surfaces. Inertinite possesses a higher carbon and lower volatile matter content than vitrinite, but it is richer in oxygen than vitrinite or exinite.[10]

A.3.2. Mineral Matter

In recent years, the mineral components of coal have been studied extensively, because they strongly influence the behavior of coal during storage and processing.[11-16] Minerals in coal have different origins and on this basis are divided in two groups, syngenetic and epigenetic.[10] Syngenetic minerals were either formed or accumulated in coal swamps up to the time of peatification; they usually display intimate intergrowth of mineral with the macerals, and are more difficult to remove in coal preparation. Epigenetic minerals were deposited in cleats and fissures and may be primary minerals or secondary transformations of primary minerals. They are easier to remove by grinding, crushing and washing operations.

Typical minerals present in coals are shown in Table 2. The most common are silicates that constitute about 60 to 70 percent of the coal mineral matter. The most frequent types are kaolinite and illite. Other important minerals found in excess of 1% include disulfides and carbonates[10]. Disulfide minerals are extremely important owing to the harmful effects of sulfur in corrosion, catalyst poisoning and air pollution. The principal disulfides in coal are pyrite and marcasite. Syngenetic pyrite is very rare, with the epigenetic pyrite being more abundant. Carbonates may be syngenetic or occur as spars in cleats and fissures. Ash fusibility can be strongly influenced by the presence of calcium, iron and magnesium. Too high a magnesium content may cause clinkering.

A.4. Porosity and Surface Area

By studying the penetration of mercury into coals as a function of pressure, Zwieterling and van Krevelen[18] established that coal contains a macropore and micropore system. They were able to establish the existence of pores with radii in the range from 30000 to 250 Å. Lin *et al.*[19] found micropores with average diameter of 20 and 30 Å, and mesopores with diameters between 200 and 500 Å. In general, macropores are dominant in coals with carbon contents below 75%, whereas micropores are dominant in coals with carbon contents about 85 - 90%.[20] This delicate structured porous system reflects the spatial arrangement of the large, complex molecules in coals and influences the behavior of coal in many applications.

The pore structure and surface area of coals are determined using different techniques, with carbon dioxide and nitrogen adsorption being the most commonly used.[21,22,23] Other techniques include mercury intrusion [24], heat of wetting[25], X-ray scattering (SAXS)[26], methanol adsorption[27] and transmission electron microscopy (TEM).[28]

Table 2. Common minerals in coal (adapted from ref. 17)

Major	Silicates	Clay Minerals	Kaolinite	$Al_2Si_2O_5(OH)_4$
			Illite	Illite-montmorillonite
			Mixed Layer	
			Chlorite	$(MgFeAl)_6(SiAl)_4O_{10}(OH)_8$
			Quartz	SiO_2
		Carbonates	Calcite	$CaCO_3$
			Dolomite	$Ca.Mg(CO_3)_2$
			Ankerite	$Ca(FeMg)CO_3$
			Siderite	$FeCO_3$
		Disulfides	Pyrite	FeS_2 (cubic)
			Marcasite	FeS_2 (orthorhombic)
Minor		Sulfates	Coquimbite	$Fe_2(SO_4)_3.9H_2O$
			Szmolnokite	$FeSO_4.H_2O$
			Gypsum	$CaSO_4.2H_2O$
			Bassanite	$CaSO_4.1/2H_2O$
			Anhydrite	$CaSO_4$
			Jarosite	$KFe_3(SO_4)_2(OH)_6$
		Feldspars	Plagioclase	$(NaCa)Al(AlSi)Si_2O_8$
			Orthoclase	$KAlSi_3O_8$
		Sulfides	Sphalerite	ZnS
			Galena	PbS
			Pyrrhotite	FeS
Trace			Trace Minerals	

Carbon dioxide adsorption at 298 K, followed by analysis using the Dubinin-Polanyi equation, has become a common practice for determining surface areas of coals. Working with different coals, Marsh and Siemieniewska[20] found discrepancies among the surface areas predicted by the Dubinin-Polanyi equation and those predicted using either the B.E.T. or Langmuir equations. For example, for a coal from Brora, Scotland, they found that the Dubinin-Polanyi equation predicted a surface area of 196 m^2/g whereas the B.E.T. equation predicted a surface area of 271 m^2/g.[20] They suggested that Dubinin-Polanyi equation takes into account capillary condensation at low pressures, and depending on the nature of the adsorbent and adsorbate, may give more accurate estimates of surface area. It has been proposed that carbon dioxide adsorption measurements

determine the total available surface area, whereas nitrogen adsorption gives only the external area because of shrinkage of the pores at low temperature (77 K) or the fact that the high activation energy for diffusion of nitrogen into the very fine pores is unavailable at this low temperature.[26,29] Surface areas of coals determined by carbon dioxide vary from 50 to 410 m^2/g[22,30] whereas those measured by nitrogen adsorption vary from 1 to 32 m^2/g.[22]

B. COAL BENEFICIATION

Coal preparation or cleaning is the process of removing undesirable minerals from a run-of-mine coal. Coal preparation plants in general use the same separation techniques used in mineral plants, consisting mostly of gravity concentration and to some extent flotation, complemented by screening and solid/liquid auxiliary processes.[31,32] In the United States about 94% of the coal preparation plants use simple gravity processes, which separate coal (specific gravity of 1.2 to 1.8) from denser clays, feldspar, etc. (specific gravity of about 2.5) and pyrite (specific gravity of 5.0). About 5% of the preparation plants use processes based on differences in surface properties namely froth flotation and oil agglomeration. Although the proportion of flotation and oil agglomeration plants is relatively small, the number of these plants has increased in recent years.[7] Only about 1% of the preparation plants use pneumatic separation. Gravity processes can separate the 7900-500 μm fraction and mainly include the use of jigs, heavy media methods, concentration tables, hydrocyclones, etc. For the minus 500 μm (-28 mesh) fraction, froth flotation and oil agglomeration are the major means of processing. In froth flotation system, gas bubbles are introduced into an aqueous slurry of the mixture of coal and coal minerals to be separated. An efficient separation depends on the formation of a stable bond between coal and the gas phase in the suspension and the

simultaneous adhesion to water of undesirable minerals. Air-adhering coal particles are then floated to the surface of the slurry and removed as a concentrate. This process also involves the use of suitable reagents that modify the interaction between water molecules and the surface of the particles. Fundamentals of flotation have been discussed by Fuerstenau and Healy,[33] the thermodynamic aspects has been presented by Fuerstenau and Raghavan[34], and the chemistry of flotation and a review of flotation reagents are given by Fuerstenau[35] and Fuerstenau and Herrera-Urbina[36] respectively.

The agglomeration process involves either bridging between particles by polymers or oil droplets, or the process involves coagulation by reduction of surface forces. Water soluble polymers contain polar functional groups that are available for bridging to a gangue particle (undesirable material) when they absorb on the coal surface. Therefore, the use of polymers has the drawback of not being very selective. The problem can be overcomed by using a hydrocarbon oil as a bridging agent. Coal and its associated mineral matter are slurried with a hydrocarbon bridging agent allowing agglomeration of coal particles to occur whereas the hydrophilic gangue particles remain dispersed. Then, the agglomerated coal can be retained by screening whereas the suspended gangue material passes through.[37] Aplan and Fuerstenau[38] have presented a review of agglomeration flotation practice and fundamentals. The most recent advances in coal cleaning processes including advanced froth flotation, selective agglomeration and advanced cycloning has been discussed by Feeley and McLean.[7]

Coal desulfurization using different oxidizing agents has been explored by several authors as an alternative route for coal cleaning.[39,40-47] The use of aqueous ferric chloride and ferric sulfate solutions led to the development of the Mayer process.[39] Others oxidizing agents used include hydrogen peroxide[40-45], nitric acid.[46,47] These procedures have the potential advantage over the physical methods that they can act

simultaneously on the inorganic and the organic sulfur in coal. Although some progress has been made, no simple, rapid, low temperature and inexpensive technique has been found to remove organic sulfur from coal.

Other chemical desulfurization approaches include the use of aqueous base solutions,[41,47] however, they generally can remove only pyritic sulfur. Moreover, there are problems associated with the high temperature and pressure involved, and the removal and recovery of the base from the desulfurized coal.[48] These factors make these processes economically unattractive.

The effect of aqueous chemical oxidation on the behavior of coal during flotation has been studied by Fuerstenau *et al.*[96,143] By using hydrogen peroxide as an oxidizing agent, it was found that oxidation severely reduce the floatability of coals and that wet oxidation occur at the external surface of the coal particles.[96]

C. COAL OXIDATION

Coal and coal pyrite are very susceptible to oxidation, which strongly affects their physical and chemical properties, along with the surface properties that govern the surface based processes used in coal beneficiation plants.[31,49-51] There are different situations during which coal oxidation can occur: in the seam, when fresh coal surfaces are exposed to the atmosphere; during storage and transport; and in processing. In each of these situations, the conditions of oxidation and/or weathering are different.

Oxidation changes the organic and inorganic components of coals to different extents, inducing changes in the physical structure. These changes can dramatically modify the behavior of coals in beneficiation and utilization processes. The structural

changes induced by oxidation can induce loss of coking properties.[52-55] Coal oxidation also adversely affects the yield and quality of liquids obtained in direct liquefaction,[56,57] and reduces the efficiency of coal cleaning.[58,59] The effect of oxidation on the combustion behavior of coals is not well understood;[60-62] however, a reduction in heats of combustion and calorific values has been reported.[63,64] Oxidized bituminous coal may be largely beneficial for gasification, mainly because oxidation enhances char reactivity.[62] Oxidation increases the number of cyclic structures containing oxygen. In general, these structures are very reactive and provide new sites for chemical reactions and catalyst binding.[63] Oxidation also alters the fundamental physical structure of coals in addition to the chemical composition.[65] Consequently, oxidation has an indirect effect on coal chemical reactions through alteration of mass and thermal transport through the solid coal.

Coal oxidation has been studied for many years; however there is not agreement concerning the mechanisms and products of oxidation. This is probably because different coals have widely different compositions and properties, and therefore exhibit different oxidation behaviors. There is a general agreement on the complexity of oxidation and the diversity of associated reactions. van Krevelen[66] proposed three stages for low temperature oxidation: 1. fixation of oxygen by chemisorption, 2. decomposition of the chemisorbed complex, 3. formation of oxycoal. At relatively low temperatures (below 100°C) in the presence of oxygen, Grossman[67] observed the evolution of molecular hydrogen that depends linearly on the amount of oxygen consumed by the coal. The source of the molecular hydrogen was the C-H bonds of the coal macromolecules. Liotta *et al.*[68] considered that all of the chemically incorporated oxygen eventually formed ether bonds; hydroperoxides were detected as intermediates in the early stages of oxidation. Swaan *et al.*[69] found that the main oxidation products close to ambient temperature were carbonyl, carboxyl and phenolic groups. A decrease in the aliphatic C-H along with the increase in oxygenated species, mainly carbonyl and carboxyl have been detected.[70,71]

Oxidation rates and oxidation stages differed among different coals indicating that oxidation strongly depend upon the origin and chemistry of the selected coals.[71] Clemens *et al.*[72] studied the low temperature oxidation of coals of different ranks; the chemical reactions responsible for self-heating of coals were apparently the same for all coals. The reactions involved the formation of hydroperoxides followed by their decomposition into carboxylic acid and aldehyde species.

Studying the oxidation of coals at temperatures near 100°C, Gethner[73] proposed the formation and decomposition of hydroperoxide, and the simultaneous competitive thermolysis reaction involving decarbonylation or decarboxylation. The formation of carbonyl groups with concurrent loss of aliphatic C-H have been reported at 100°C,[52] 60-140°C,[74] 130°C.[75] It was proposed that the initial step of oxidation involves the formation of hydroperoxides, and the decomposition of hydroperoxides leads to alcohols and carboxylic acids.[52] High rank coals had marked changes in the aromatic structure.[75] By using spin resonance spectroscopy, changes in the free radical content produced by oxidation of coals at room temperature and 105°C have been detected.[76] Free radicals are molecules that contain an odd number of electrons and are very important intermediates in many organic reactions. It was postulated that free radicals were produced in the basic first step of oxidation, then they react with coal to form hydroperoxide compounds that easily decomposed to form phenolic and carboxylic groups.[76] MacPhee *et al.*[77] found that the evolution of CO, CO_2, and CH_4 from bituminous coals during oxidation appear to be more pronounced for low rank coals and to be a function of the oxygen uptake. Painter *et al.*[78] studied the oxidation of a coking coal by FTIR; the results indicated the formation of carbonyl groups. They suggested that the formation of ester crosslinks was responsible for the loss of swelling characteristic and coking properties in the oxidized samples.

The formation of humic acids and anhydrides during coal oxidation at temperatures between 120 and 190°C has been reported.[79,80] Moreover, Azik *et al.*[81] found that oxidation not only affects the organic structure of coals but also the inorganic matter at different stages of oxidation. The functional groups produced by oxidation included ketones, carboxyls, and anhydrides, but the major groups produced were aryl esters. Iron sulfate was the only inorganic oxidation product. Huai *et al.*[82] examined the changes in the morphology of coal particles that had undergo oxidation with air at 150°C using SEM. Oxidation occurred randomly on the coal surface. Large cracks developed after eight to twenty four hours of oxidation, but cracking could not be attributed unambiguously to either reaction or thermal stress.

Coal oxidation at temperatures higher than 200°C induces major modification on the coal structure independently of the coal rank.[83] Coals lose volatiles in parallel with oxidation.[84,85] A significant buildup in carboxylic and phenolic functionalities[86] along with evolution of carbon oxides was observed after 12 h of oxidation at 200°C.[84] The formation of ethers groups was also detected.[87]

In the mining, storage, and processing of coals, a number of problems arise that are connected with their uptake of moisture. There is consensus that moisture in coal affects low-temperature oxidation; however, there are contradictory opinions concerning the mechanisms involved.[40,88-92] Some workers state that moisture is a necessary component and activates the oxidation process,[88-91] while others consider that it does not increase the rate of the reaction of coal with atmospheric oxygen, and instead inhibits the oxidation process.[89]

Chen *et al.*[88] suggested that water accelerates the oxidation of coals through the rapid formation of peroxide complexes. Panaseiko[89] concluded that in some cases water

retards, and in others accelerates, the oxidation of coal. An interaction between water molecules and the functional groups on the surface of coal was proposed as a mechanism that activates the oxidation of coal. Huggins *et al.*[90] studied the oxidation of coal at 50°C in moist air, and found that ether and carbonyl functional groups were the main products of oxidation. Also, the formation of sulfuric acid as a by-product of pyrite oxidation was detected. Not only does this acid promote the dissolution and leaching of other minerals in the coal, but it can also catalyze and possible initiate oxidation of C-H bonds to oxygen-bearing functional groups. Mossbauer spectroscopy studies[91] show that pyrite in coal was readily transformed to ferrous sulfate at 50°C and 65% relative humidity, while α-iron oxyhydroxide was the principal oxidation product in stockpiled samples. Weak carbonyl bands and enhancement of ether bands were detected by diffuse reflectance infrared fourier transform analysis (DRIFT) in coals oxidized longer than 167 days at 50°C and 65% relative humidity. Petit[92] studied the water vapor/coal system at temperatures between 40 to 250°C. Water vapor interacted with the organic matter of coal in a similar way as with activated carbon and carbon black. At ambient temperature, coal first underwent a reversible adsorption of water that prevented oxygen access to the micropores, then the most reactive oxygen groups on the surface were chemically altered, leading to a drastic change on coal surface evidenced by CO_2 formation.

The interaction of coal with different oxidizing agents in aqueous solutions has been studied in the context of desulfurization and wet oxidation studies. As mentioned earlier, various chemical desulfurization approaches have been applied to coal; however, there are contradictory opinions concerning the mechanisms involved.[40-46,93-96] Aqueous hydrogen peroxide-sulfuric acid solutions are of interest for desulfurizing coal.[40-43] Working at ambient temperature and pressure, complete remotion of sulfate and pyritic sulfur with unaltered coal matrix has been reported.[40] However, no organic sulfur was removed. Ali *et al.*[41] studied the removal of sulfur by using different oxidizing

agents, namely, copper chloride, hydrogen peroxide, glacial acetic acid, ammonium hydroxide, potassium dichromate and sodium hydroxide. Working at room temperature they found that the only effective reagent was hydrogen peroxide that removed about 50 to 90% of the sulfur from coal with a minimum destruction of the coal structure. Under similar conditions, it was postulated that organic sulfur was oxidized to sulphonic acid and then removed by desulphonation.[42] Using hydrogen peroxide at different concentration and at different temperatures (15-40°C), Ahnonkitpanit *et al.*[43] found that most of the inorganic sulfur and a small portion of organic sulfur were removed, and ash was substantially reduced. Working with solutions of 30% H_2O_2 at different pH ranging from pH=0 to pH=11.5 at room temperature, Heard *et al.*[44] found that the oxidation of the organic matter was minimal and was observed only at very low pH (<1.5).

Other chemical desulfurization approaches have been tried. A mixture of hydrogen peroxide in acetic acid has been reported to remove the majority of pyritic sulfur and some organic sulfur.[45] From infrared spectroscopy analysis Czuchajowsky[93] determined that different coals have different propensities to be oxidized by hydrogen peroxide and nitric acid. Three types of oxidation products were generally detected, namely, products not soluble in either acids or alkalis, representing the most weakly oxidized part of the coal, carboxyl and hydroxyl groups or humic acids soluble in alkaline solutions, and finally benzenocarboxylic acids. Kinney *et al.*[46] studied the nitric acid oxidation of bituminous coal; about 80% of the carbon of the coal was converted to alkali-soluble humic acids.

The kinetics of oxidation and desulfurization by ferric chloride over the temperature range 333 to 363 K has been reported.[94] Over 90% of ferric ions were

consumed during oxidation of the organic matrix of coal whereas the remaining 10% was consumed in the pyrite oxidation. A kinetic model based on the Langmuir-Hinshelwood form was proposed assuming that the coal matrix involves two different reactive sites which are oxidized consecutively. The reaction rate was reported to be independent of coal particle size. These results are not in agreement with those reported by Oshinowo and Ofi.[95] They found that working at temperatures ranging from 60 to 102°C, the kinetic of oxidation increased by reducing the particle size and increasing the temperature. The overall kinetic was chemically controlled.

Dry thermal and wet chemical oxidation of coal using hydrogen peroxide have been compared.[96] It was concluded that oxidation, whether thermal or chemical, makes coal more hydrophilic and reduces its floatability markedly. However, it was suggested that wet oxidation occurs mainly at the external surface of coal, whereas dry thermal oxidation takes place on both the external and internal surfaces of the coal particles.

D. OXIDATION MECHANISMS OF COAL

The mechanisms of oxidation can be interpreted in terms of classical autooxidation reactions in which the first step of oxidation is the formation of peroxide compounds by the oxidation of the aliphatic, olefinic, and ether structures that link the aromatic units present in coal. These reactions are commonly invoked. [68,74,97] Peroxides, although frequently proposed [98-99], are extremely difficult to detect directly on coal surface by any method unless an *in-situ* technique is used, because they easily decompose at the experimental oxidation temperature. Once peroxide has decomposed and released more radicals into the system, the range of reaction possibilities becomes extensive and choosing among them is somewhat speculative. However, the presence of some products of oxidation can be consistently explained according to coherent reaction sequences.

The basic first step of oxidation is believed to be as follows:[76,87,97-99]

$$RH + O_2 \rightarrow R\cdot + \cdot OOH \quad (1)$$

$$R\text{-}CH_2\text{-}R + R\cdot \rightarrow R\text{-}C\cdot H\text{-}R + RH \quad (2)$$

$$R\text{-}C\cdot H\text{-}R + O_2 \rightarrow R\text{-}\underset{\displaystyle O\text{-}O\cdot}{\underset{|}{C}}H\text{-}R \quad (3)$$

$$R\text{-}\underset{\displaystyle O\text{-}O\cdot}{\underset{|}{C}}H\text{-}R + RH \rightarrow R\text{-}\underset{\displaystyle O\text{-}OH}{\underset{|}{C}}H\text{-}R + R\cdot \quad (4)$$

Decomposition of the peroxide can produce various oxygen-containing compounds such as acids, alcohols, ketones, aldheydes, esters and ethers. The following reaction sequence explains the generation of carboxylic acid and aldehyde groups on coal oxidation:[74,87,100]

$$R\text{-}\underset{\displaystyle O\text{-}OH}{\underset{|}{C}}H\text{-}R \rightarrow R\text{-}\underset{\displaystyle O\cdot}{\underset{|}{C}}H\text{-}R + \cdot OH \quad (5)$$

$$R\text{-}\underset{\displaystyle O\cdot}{\underset{|}{C}}H\text{-}R \rightarrow R\text{-}\underset{\displaystyle H}{\underset{|}{C}}{=}O + R\cdot \quad (6)$$

aldehyde

Aldehydes are oxidized to carboxylic acids with great ease. In the case of oxidation by air, the initial oxidation product is a peroxycarboxylic acid generated by a free radical process.[100] A possible mechanism is as follows:

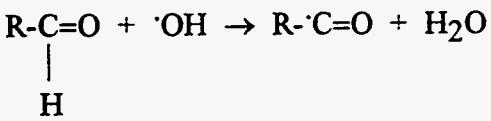

(7)

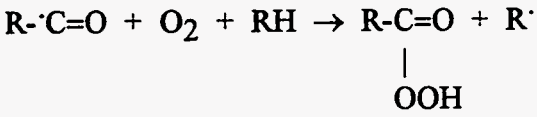

(8)

peroxycarboxylic acid

The second stage could be the oxidation of aldehyde by the initially formed peroxycarboxylic acid. The probable course of this oxidation is shown in the following reactions:

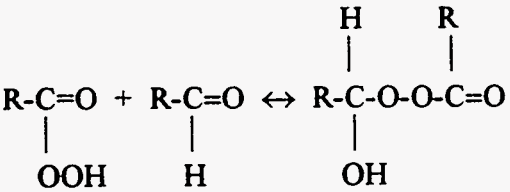

(9)

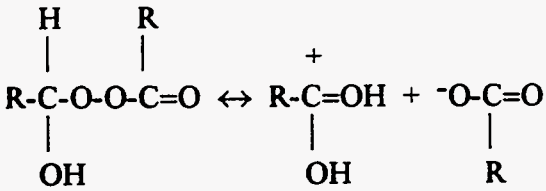

(10)

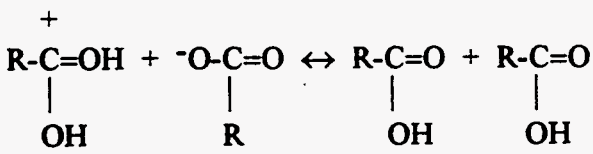

(11)

carboxylic acids

In the foregoing reactions, R can be aliphatic or aromatic. If R is aromatic, the oxidation probably occurs at the carbon α in the aromatic ring.[101]

More extensive oxidation can form ester and anhydride functionalities. The formation of an ester might take place by the following mechanism:

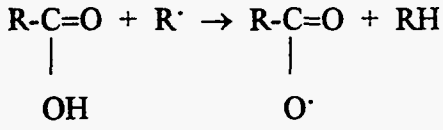

(12)

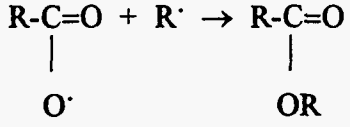

(13)

ester

On the other hand, the generation of anhydride from the same is given by:

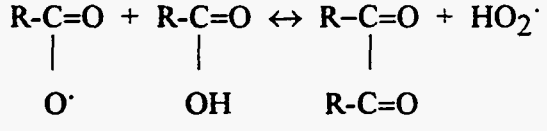

(14)

anhydride

The amount of phenolic groups in general increases with oxidation. It has been suggested that when peroxide is formed on the carbon α to an aromatic ring, phenols are produced as illustrated by Albers *et al.*[101], and Markova:[102]

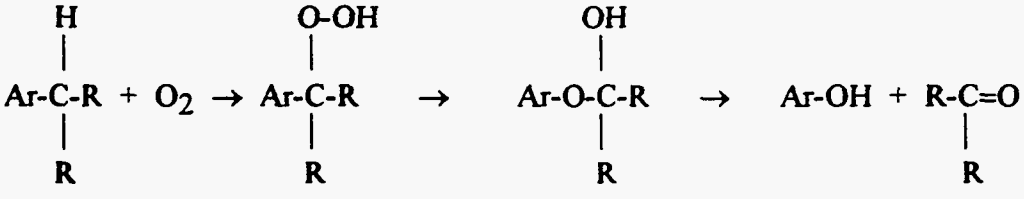

(15)

The phenolic structures can be further oxidized to quinone structures.

It has been demonstrated that during adsorption of oxygen on solid surfaces different forms of molecular and ionic oxygen can be formed,[103] namely: $(O:)_{ads}$; $(O_2^+)_{ads}$; $(O_2^-)_{ads}$; $(O_2^{2-})_{ads}$; etc. These ionic forms of oxygen have the capacity to react with water to form hydroxide ions and radicals:

$$(O_2^-)_{ads} + H_2O \leftrightarrow HO_2^{\cdot} + OH^- \qquad (16)$$

The resulting active compound $HO_2^{\cdot}$ is an oxidizing agent that can participate in the formation of hydroperoxide compounds and free radicals. Subsequent reactions can proceed to oxidize the surface of coal, generating oxygen group functionalities. Thus, water enhances oxidation of coal by catalyzing the formation of free radicals.

Mineral components present in coal are active water sorbents. It has been suggested that water can adsorb via the formation of hydrogen bonds with the oxygen of the =Si=O group and at the expense of unsaturated silicon atoms on the surface.[104] Other minerals among the coal components can also sorb water. Particularly in the case of pyrite, the interaction with oxygen and water might occur through sorption of the latter[103]:

$$FeS_2 + 7/2(O_2)_{ads} + (H_2O)_{ads} \rightarrow Fe^{2+} + 2SO_4^{2-} + 2H^+ \qquad (17)$$

The sulfuric acid generated during pyrite oxidation is very important because its alters other minerals that might be stable. In general, mineral oxidation and maceral oxidation have been regarded as more or less separate processes, but it should be noted that the acidification of coal resulting from pyrite oxidation will probably catalyze and sometime initiate maceral oxidation. Several synthetic pathways for ether, esters and

carbonyl functional groups are possible in the presence of sulfuric acid.[105] Also, reactions involving hydroperoxides are dependent upon the pH of the system.[68]

During oxidation of coal by hydrogen peroxide, the latter decomposes spontaneously on coal surfaces with the formation of water and oxygen according to the reaction:

$$H_2O_2 \rightarrow H_2O + \tfrac{1}{2}O_2 \qquad (18)$$

However, in acidic solutions having a redox potential between about 0.7 and 1.0 V (Standard Hydrogen Electrode, SHE), H_2O_2 undergoes catalytic reduction and oxidation simultaneously by metallic ions such as Fe^{3+} and Fe^{2+}. Thus, the following reactions (Fenton mechanism) might take place in the presence of iron ions[44]:

$$Fe^{2+} + H_2O_2 \rightarrow Fe^{3+} + OH\cdot + OH^- \qquad (19)$$

$$Fe^{2+} + OH\cdot \rightarrow Fe^{3+} + OH^- \qquad (20)$$

$$H_2O_2 + Fe^{3+} \rightarrow Fe^{2+} + HO_2\cdot + H^+ \qquad (21)$$

$$Fe^{3+} + HO_2\cdot \rightarrow Fe^{2+} + H^+ + O_2 \qquad (22)$$

The OH· and HO_2· radicals produced by these reactions are strong oxidizing agents. Although either radical can attack coal, Draginac, J.G. and Draginac, Z.D.[106] considered that OH· is the primary oxidizing agent. Barb *et al.*[107] proposed that in the presence of ferrous and ferric salts the decomposition of hydrogen peroxide is described by reactions 19 and 23 to 26:

$$Fe^{2+} + OH\cdot \rightarrow Fe^{3+} + OH^- \qquad (23)$$

$$OH\cdot + H_2O_2 \rightarrow HO_2\cdot + H_2O \qquad (24)$$

$$HO_2\cdot + Fe^{2+} \rightarrow HO_2^- + Fe^{3+} \quad (25)$$

$$HO_2\cdot + Fe^{3+} \rightarrow O_2 + H^+ + Fe^{2+} \quad (26)$$

The initial stage is the reduction of Fe^{3+} to Fe^{2+} by the HO_2^- ions that are present in equilibrium with H_2O_2:

$$Fe^{3+} + HO_2^- \rightarrow Fe^{2+} + HO_2\cdot \quad (27)$$

$$H_2O_2 \leftrightarrow H^+ + HO_2^- \quad (28)$$

The hydroxyl radicals formed in Reaction 19 can then react with organic structures present in coal by either splitting off hydrogen from them or by adding to unsaturated fragments:[108]

$$RH + OH\cdot \rightarrow R\cdot + H_2O \quad (29)$$

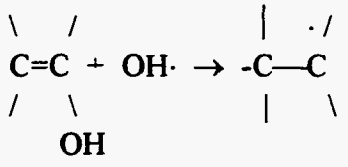

(30)

Hydroxyl radicals have also been used to perform processes of oxidative condensation:[108]

$$RH + OH\cdot \rightarrow R\cdot + H_2O \quad (31)$$

$$R\cdot + R\cdot \rightarrow R—R \quad (32)$$

According to the foregoing mechanisms, it is possible to hydroxylate organic structures with the aid of Fenton reagents. Thus, benzene can be converted into phenol and biphenol by a mechanism discussed by Walton.[108]

Also, as described earlier, the radicals in reaction (31) can undergo ulterior reaction to produce hydroperoxides and different types of functional groups:

$$R\cdot + O_2 \rightarrow RO_2\cdot \quad (33)$$

$$RO_2\cdot + H_2O_2 \rightarrow ROOH + HO_2\cdot \quad (34)$$

$$RO_2\cdot + RO_2\cdot \rightarrow \text{aldheydes, carboxylic acids, etc.} \quad (35)$$

According to the above mechanisms, the oxidation of coal by hydrogen peroxide, in general, involves its decomposition assisted by the presence of ferrous and ferric ions to produce free radicals and hydroperoxides. These products react with the organic structure of coal to produce different functional groups, including phenolic, carbonyl and carboxylic among others.

The interaction between coal and nitric acid involves complex mechanisms characterized by a series of reactions such as oxidation of the organic and inorganic fractions of coal, and nitration. van Krevelen[109] suggests that the oxidation of coals by nitric acid involves two stages: first, there is the oxidation of non-aromatic groups of the aliphatic coal chain to form carboxylic acids with the concurrent oxidation of aromatic rings to quinone structures. Second, there is an opening of the quinone configuration to produce carboxylic groups. Kinney *et al.*[46] proposed that at low temperatures the initial reaction of the coal involves the addition of nitric acid to unsaturated structures and the cleavage of other structures, such as phenolic ether linkages, possibly forming nitrophenols.

The reactions of pyrite with nitric acid are very complex and sensitive to temperature and concentration. Under moderate conditions the following reactions could occur[47,110]:

$$2FeS_2 + 10{\cdot}HNO_3 \rightarrow Fe_2(SO_4)_3 + H_2SO_4 + 10NO + 4H_2O \quad (36)$$

$$FeS_2 + 2{\cdot}HNO_3 \rightarrow Fe(NO_3)_2 + H_2S + S \quad (37)$$

$$2FeS_2 + 6{\cdot}HNO_3 \rightarrow 2Fe(NO_3)_3 + 3H_2S + S \quad (38)$$

although other reactions also take place in the process.

The oxidation of coal by acidic ferric sulfate solutions involves the presence of a redox couple Fe^{3+}/Fe^{2+} that determines the oxidation capacity of the solution. Thus, the reduction of Fe^{3+} on the surface of either coal or coal pyrite is given by the following cathodic reaction:

$$Fe^{3+} + e \rightarrow Fe^{2+} \quad (39)$$

where the redox potential is determined by the equation:

$$E = 0.771 + 0.0591{\cdot}\log (Fe^{3+}/ Fe^{2+}) \quad (40)$$

On the coal surface the group that is able to undergo a reversible redox reaction in the potential range of the Fe^{3+}/Fe^{2+} couple is the quinone/hydroquinone system proposed by Vetter.[111] As the hydroxyl species are consumed, sites with higher oxidation states are produced on the coal surface and other oxidation reactions could occur, leading for example to the formation of carboxylic groups.[112]

Ferric iron can also oxidize coal pyrite according to the reaction[113]:

$$FeS_2 + 14Fe^{3+} + 8H_2O \rightarrow 15Fe^{2+} + 16H^+ + 2SO_4^{2-} \quad (41)$$

The functional groups generated on the coal by oxidation can interact with both ferric iron as well as ferrous iron generated by the oxidation of coal pyrite (Reaction 41). In the specific case of carboxylic acid the following reactions could occur:[114]

$$\text{Coal-COOH} \leftrightarrow \text{Coal-COO}^- + \text{H}^+ \quad (42)$$

$$\text{Fe}^{2+} + 2\text{Coal-COO-} \leftrightarrow (\text{Coal-COO})_2\text{Fe} \quad (43)$$

$$\text{Fe}^{3+} + 3\text{Coal-COO}^- \leftrightarrow (\text{Coal-COO})_3\text{Fe} \quad (44)$$

Reaction (42) represents the dissociation of the carboxylic acid on the coal surface and reactions (43) and (44) represent the attachment of the ferrous and ferric ions respectively to the deprotonated coal surface by ion exchange at the carboxylic group to form metal carboxylates. A similar ion-exchange reaction may take place with phenolic acid groups, although this is questionable because phenolic groups are much less acidic than carboxylic groups.

E. ELECTROKINETIC BEHAVIOR OF COAL.

When two phases are in contact, a potential difference is developed between them. For a solid surface in contact with an aqueous electrolyte solution, there is generally an excess of charge of one sign at the solid surface, and this will be balanced by charge of the opposite sign distributed in the liquid region close to the surface. This separation of charge at the interface is known as the electrical double layer.[115] In the specific case of coal, the electric charge on its surface is probably generated by the dissociation of functional groups such as carboxylic (-COOH) and phenolic (-COH) or by adsorption of ions from solution.[116] When a solid surface and a fluid are moving relatively to each other, the plane close to the solid surface within which the fluid is assumed stationary is called the shear plane and the potential at that plane is called the zeta potential. The composition of the coal surface and the concentration and valence of ions in the solution

contribute to the sign and value of the zeta potential. The condition where the shear plane is uncharged is called the PZR (point of zeta potential reversal), and is commonly used to characterize the nature of the solid surface.[117]

Flotation of coal is based on differences in the surface properties of coal and gangue particles. Zeta potential measurements carried out under low solids concentrations can provide important information relevant to the surface properties of coal particles. Due to the complex nature of the coal surface composition and the strong tendency to be modified by interaction with different environments, the variation of the coal surface charge and hence its zeta potential are difficult to delineate. PZR values have been reported and depend on the rank of coal as shown in Table 3.[116-126] In general, PZR values for lignite, sub-bituminous and oxidized coals are at acidic pH, attributed to the contribution of strongly acidic functional groups, whereas bituminous and anthracite coals generally show PZR values situated close to the neutral pH range.[117,118,120] However, it should be emphazised that the presence of a high content of ash minerals having low PZR values (such as silica and clay), also contributes to lower observed PZR values of coals.[117]

In the specific case of oxidation, the PZR of coal and its zeta potential are decreased because of the generation of oxygen functional groups by oxidation. In general, depending of the degree of oxidation, the PZR's of oxidized coal decreased by 1 to 3 units compared with those of unoxidized coal.[116,118,127]

F. WETTING BEHAVIOR OF COAL

Wetting is defined as the displacement of one fluid from a surface by another fluid, and involves three phases, of which at least two must be fluid.[128] The wetting behavior

Table 3. Some published PZR values of coals.

Coal Rank	PZR	Method	Reference
Lignite	2.1	Electrophoresis	Kelebek *et al.*[118]
Lignite	2.3	Electrophoresis	Wen and Sun[119]
Sub-bituminous	3.6	Electrophoresis	Fuerstenau and Pradip[120]
Bituminous	4.5	Electrophoresis	Wen and Sun[119]
Low-ash bituminous	<2.0	Electrophoresis	Fuerstenau *et al.*[117]
High-ash bituminous	4.5	Electrophoresis	Fuerstenau *et al.*[117]
High vol. bituminous	5.2	Electrophoresis	Rubin and Kramer[121]
Bituminous	5.1	Electrophoresis	Kelebek *et al.*[118]
Bituminous	4.1	Electrophoresis	Yarar[122]
Bituminous	1.5	Electrophoresis	Coca *et al.*[123]
Bituminous	2.5	Electrophoresis	Coca *et al.*[123]
Bituminous	~2.0	Electrophoresis	Celik and Somasundaran[124]
Bituminous	4.6	Streaming potential	Campbell and Sun[125]
Anthracite	5.0	Electrophoresis	Wen and Sun[119]
Anthracite	3.5	Electrophoresis	Ferrell and Huang[126]
High-ash anthracite	2.8	Electrophoresis	Fuerstenau *et al.*[117]
Low-ash anthracite	4.5	Electrophoresis	Fuerstenau *et al.*[117]
Oxidized anthracite	2.5	Electrophoresis	Fuerstenau *et al.*[117]

of coal is extremely important because it controls froth flotation, oil agglomeration and dewatering methods used in coal preparation plants.[129] The wetting behavior of coal depends upon different factors, the most important being rank, mineral matter and degree of oxidation,[127] and, because of its critical role, should be assessed in the most reliable manner. Several techniques have been developed to characterize the wetting properties of coal, including contact angle measurements,[127,130] measurements of immersion time,[131,132] advancing solidification front,[133] heats of immersion[134], and film flotation.[135-139]

The contact angle is defined as the angle formed through the liquid phase at the three-phase interface when either a bubble is contacted with a solid surface in a liquid medium or a droplet is contacted with a solid surface in a vapor medium. In a solid/liquid/vapor system, the contact angle is zero when the surface is completely wetted by the liquid, whereas the contact angle is 180^{o} when the solid repels the liquid phase. The critical wetting surface tension of a solid (γ_c), as defined by Zisman, is the surface tension of the liquid (γ_{LV}) that just forms a zero contact angle on the solid.[128] It is an important parameter that can be used as an index of the wettability of the solid. The value of γ_c is obtained from extrapolation of a plot of cos θ versus γ_{LV} at cos θ =1 using homologous liquids or solutions of different surface tension. Using this approach, a critical surface tension of 45 mN/m was measured for a series of coals with different ranks, ranging from lignite to anthracite.[130] Using the same technique, Yang[140] found a value of 23 mN/m both for raw and oxidized coals ranging from sub-bituminous to anthracite in solutions of alcohol and water. The latter observation is surprising considering that oxidation strongly modifies the surface properties of coal. Horsley and Smith[141] found that a plot of contact angle as a function of carbon content in coal exhibited a maximum at about 88% carbon, attributed to a graphite-like structure of high rank coals coupled with a high proportion of wax hydrocarbons, which are more hydrophobic than graphite. The percentage of these waxy hydrocarbons is lower in anthracite coals, resulting in a lower contact angle.

Because of their heterogeneity, coal particles may vary widely in composition and consequently each particle may have its own unique set of surface properties. Considering this factor, Fuerstenau *et al.*[135-139] developed the film flotation technique that permits determination of the fraction of particles that sink (called lyophilic) or float (called lyophobic) on liquids of different surface tensions, from which the distribution of wetting surface tensions can be assessed. Particles sink under the condition when the contact

angle is just zero. These tests provide a surface tension versus lyophobic (hydrophobic) fraction diagram from which the mean critical wetting surface tension of the coal particles can be estimated. Fuerstenau *et al.*[142] studied the effect of particle size on the film flotation tests of coal. Working with various particle sizes from 53 to 425 μm they found that for all size fractions, the partition curves were identical, suggesting that the mean critical surface tension does not significantly depend on particle size. Working with coals ranging from lignite to anthracite, Fuerstenau *et al.*[143] found that the mean critical wetting surface tension ranged from 31 to 69 mN/m, respectively, with an average of 43 mN/m and standard deviation of 9 mN/m. Using the same technique, Fuerstenau *et al.*[139] found critical surface tension values of 43 and 67 mN/m for an as-received and oxidized Cambria #78 coal, respectively. Clearly, oxidation makes the coal surface less hydrophobic. It has been demonstrated that measurements of the critical wetting surface tension can be used to quantify the contact angle of coal particles as well as the distribution of hydrophobic sites on the surface of coal particles.[139]

In general, there are discrepancies in the contact angle measurements on different coals, mainly due to the heterogeneous nature of coal, contact angle hysteresis produced by the surface roughness, and the distribution of sites with different degrees of hydrophobicity on the coal surface. Gutierrez-Rodriguez *et al.*[144] studied the hydrophobicity of different coals by contact-angle measurements and the work of adhesion equation. Based on the water-sessile-drop contact angle, the hydrophobicity percentage of coals was about 20% for lignite, and increased with rank up to a maximum of 70% for low and medium volatile bituminous coals, then decreased for anthracite. Using the captive-bubble technique, the calculated hydrophobicity ranged from 0% (below HVA bituminous coals) to a maximum of 55% for LV-MV bituminous coals. Rosenbaum and Fuerstenau[145] expressed the change in the contact angle with rank in terms of Cassie's relation.[146] Assuming that different coals contain different amounts of hydrophobic and

hydrophilic sites, the contact angles of different coals as a function of carbon content were determined. The results were in excellent agreement with experimental measurements reported by Brown.[147]

A comparative study of contact angle measurements on three different coals by using film flotation, sessile-drop and captive-bubble techniques has been reported.[148] Excellent agreement was found among contact angles obtained directly by sessile-drop and captive-bubble measurements and those calculated from film flotation results. Also, the effect of weathering on the hydrophobicity of coal particles was investigated by film flotation response and induction time measurements. The results indicated that as a consequence of oxidation, the hydrophobicity of coal stored in open atmosphere is smaller than that for coal stored in inert atmosphere for similar periods of weathering.

The effects of coal rank, particle size and the mineral matter content of coal on its heat of immersion were investigated by Fuller,[149] who observed higher heats of immersion for low rank coals, high mineral matter contents and small particle sizes. The higher heats of immersion of low rank coals compared with high rank coals were attributed to the higher concentration of oxygen functional groups on low rank coals. Mineral matter present on the coal surface rendered it more hydrophilic. Small particles have larger surface area, providing greater access of water to the internal surface.

During flotation practice, because of their heterogeneity, coal particles can be partially hydrophobic and consequently interact with water molecules to form a liquid film that may exhibit some stability over a finite period. The minimum time required for thinning and rupture of the liquid film leading to a stable bubble-particle contact is called the induction time. Through measurements of the induction time of raw and oxidized coal particles, Ye and Miller[150] studied the effect of coal rank and oxidation of low rank coals

on their wettability. A minimum induction time was observed for a LV bituminous coal whereas anthracite and low rank coals exhibited larger induction times. They also found that oxidation at 130°C for 50 hours increased the hydrophobicity of coal whereas oxidation for longer time periods increased the induction time. These results are in partial agreement with the results of Diao,[127] who observed that oxidation at temperatures ranging from 100 to 244°C for 24 hours always increased the induction time. Yang[140] found that a sub-bituminous coal oxidized in air at 150°C was more hydrophobic than as-received coal. This anomalous behavior was attributed to the high moisture content of the as received coal. When coal was heated, the moisture content was reduced and consequently the coal surface becomes more hydrophobic.

In general, the wettability of different coals shows a minimum for LV bituminous coals whereas low rank and anthracite coals exhibit higher wettability.[144,147,150] Oxidation increases the wettability of coal samples due to the generation of oxygen functional groups on the coal surface.[139,149] Mineral matter also contributes to increase the wettability.[149]

G. ELECTROCHEMISTRY OF PYRITE

FeS_2 occurs in nature in two crystalline forms, cubic pyrite and orthorombic marcasite. Although both forms are present in coal, pyrite is much more abundant than marcasite.[151] Pyrite (FeS_2) is the major inorganic form in which sulfur occurs in coal; but because of its fine particle size, it is generally very difficult to separate from the coal matrix. The surface properties of pyrite are the subject of renewed interest because of the increasing awareness of the environmental hazard associated with the release of sulfur dioxide during coal combustion.[4] Currently, efforts are being made to improve flotation and oil agglomeration, which are based on differences in surface properties for removing pyrite from coal.[7] Oxidation of pyrite, which affects its surface properties, when pyrite is

exposed to water and oxygen, may occur in hardly natural mines and waste dumps, or during oxidative processing, such as hydrometallurgical treatment of pyritic gold ores. Pyrite oxidation, also leads to the formation of sulfuric acid and ferric hydroxide in mine drainage waters, which constitutes a significant environmental problem.[152] By electrochemical studies on coal pyrite samples Tao *et al.*[153] found that the surface of pyrite become more hydrophobic due to the formation of iron polysulfide by superficial oxidation.

The oxidation of pyrite is controlled by mixed potential, corrosion-type electrochemical reactions, in which pyrite undergoes anodic oxidation while oxygen or another oxidizing agent is cathodically reduced. In this context, electrochemical techniques offer a tool for quantitatively studying the redox behavior of different pyrite samples in different environments. This provide insight into the behavior that can be expected during flotation, or during chemical or biochemical leaching of pyrite.

Figure 1 shows the structure of pyrite, which is cubic with octahedrally coordinated metal atoms at the corners and face centers. Disulfide atoms, S_2^{2-}, lie at the center of the cube and the midpoints of the cell edges. The midpoint of the S_2 group occupies the Cl sites of an NaCl structure, whereas the Fe atoms occupy the Na positions.

Knowledge of the thermodynamics of the iron- and sulfur-containing species system is essential for predicting the possible reactions that pyrite can undergo under different conditions. Figure 2 shows the Eh-pH diagram for the Fe-S-H_2O system at 25°C, for activities of dissolved Fe and sulfur species of 10^{-3} M.

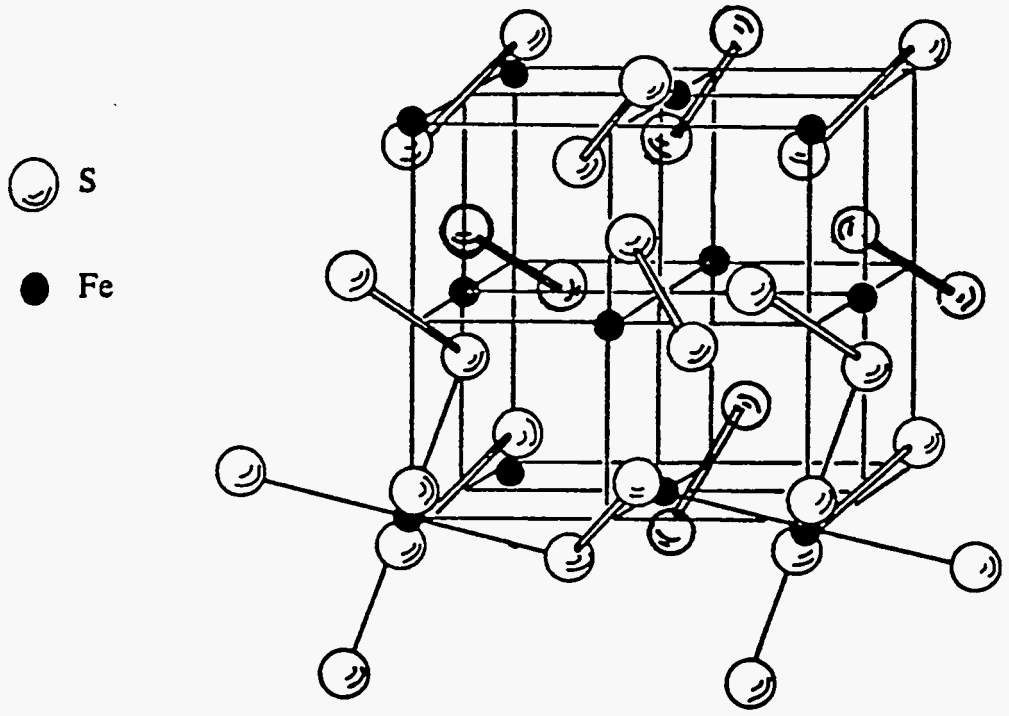

Figure 1: Structure of pyrite (FeS_2).[152]

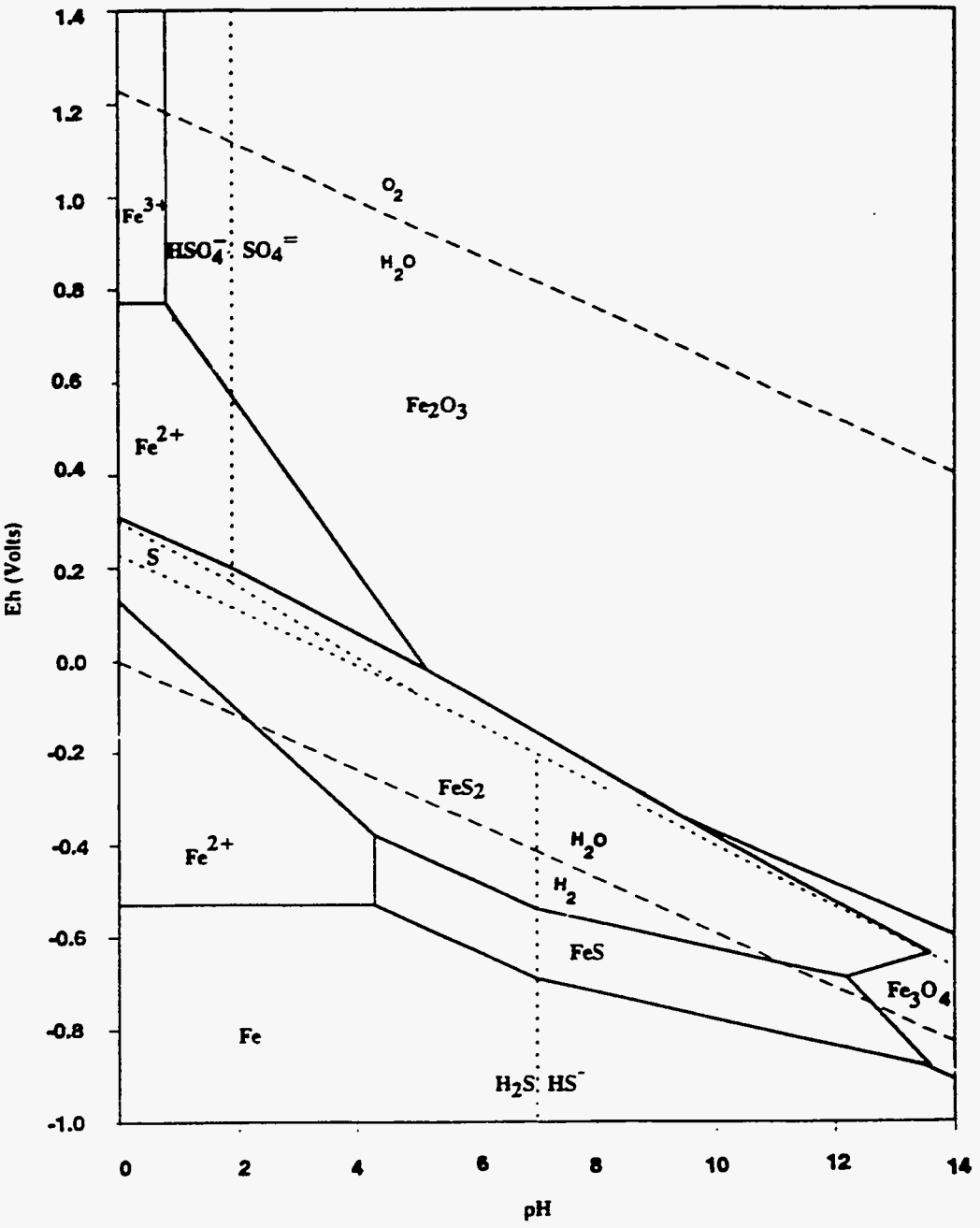

Figure 2: Eh-pH diagram for the Fe-S-H_2O system at 25°C. Activities of soluble Fe and S species: 10^{-3} M. (Data taken from ref. 154)

From Figure 2, pyrite would be expected to oxidize to Fe^{2+} and HSO_4^- at the most acidic pH values, and Fe^{2+} and SO_4^{2-} above pH 2. At high potentials, Fe^{3+} would be expected rather than Fe^{2+}. At higher pH, Fe_2O_3 and sulfate are predicted. Figure 2 predicts that pyrite should be reduced to Fe^{2+} and H_2S below pH 4, to FeS and H_2S from pH 4 to 7, and to FeS and HS^- above pH 7, with a pH-dependent reduction potential. Clearly, a variety of redox products can form on pyrite, depending on its redox history. The surface properties of the solid products vary substantially, and hence the behavior of pyrite in physical coal cleaning is expected to be sensitive to its redox history.

Pyrite is a semiconductor, and therefore the electrical conduction is due to the motion of either electrons in the normally empty conduction band (n-type), or holes in the normally full valence band (p-type). Holes are positive charges, to which the net current due to the lack of electrons in an almost-full band is conventionally attributed.[155] In a solid, the Fermi level is defined as the energy level for which the probability of occupancy by the electrons is 1/2. It is the same as the electrochemical potential of electrons in the solid. In a n-type semiconductor, the Fermi level is near the conduction band edge, whereas in a p-type semiconductor it is near the valence band edge. Thus, the work of electron release for a p-type semiconductor is greater than that for a n-type semiconductor by nearly the width of the band gap.[155] Depending on its deviation from stoichiometry and the impurity type and content, pyrite exhibits either n-type or p-type semiconduction with a 0.9 ± 0.1 eV band gap. In non-stoichiometric pyrite, an Fe excess (sulfur deficiency) correspond to a donor defect (n-type) and a Fe deficiency (sulfur excess) corresponds to an acceptor defect (p-type).[152] The electron donors more frequently found in n-type pyrite are Cu, Ni, Co and Ag. The more common electron acceptors found in p-type pyrite are As and Bi.[156] Donors provide free electrons to the conduction band, whereas acceptors produce an acceptor level located near the top of the valence band. Electrons can be promoted across the band gap by a redox couple with an

appropriate electronic distribution, or by photons. Conduction electrons are nearly two orders of magnitude more mobile than holes, and n-type pyrite statistically has a lower resistivity than p-type pyrite.[155] Coal pyrite is usually p-type whereas ore pyrite is n-type.[152,157] However, Lai *et al.*[158] based on cyclic voltammetry and X-ray photoelectron spectroscopy studies, found that coal pyrite behaved as an n-type semiconductor and mineral pyrite behaved as a p-type semiconductor.

Numerous studies have been made on the electrochemical behavior of ore and coal pyrite at different pH's, Table 4 summarizes the conditions used in these studies and the results obtained. Comparison of Table 4 and Figure 2 shows that many of the experimental studies of pyrite oxidation are not fully consistent with the behavior predicted by thermodynamics for the appropriate pH. Moreover, because cyclic voltammetry is a kinetic experimental procedure, there is hysteresis between oxidation and reduction peaks, and the peak potential varies with scan rate.[159,160] Most studies reported that the behavior of pyrite in the first cycle of cyclic voltammetry differed from the behavior in the subsequent cycles. Coal pyrite generally passed higher current densities than ore pyrite, and showed lower rest potentials, reflecting a higher susceptibility to oxidation.[160-162] There were also differences between different samples within each class. These differences have been discussed extensively, but the reasons for them are not fully understood. Mirza[152] suggested that the formation of a reverse biased n-p junction in ore pyrite samples is responsible for the lower current densities passed during cyclic voltammetry studies. Chander and Briceno[163] postulated that passivation was responsible for the differences in electrochemical behavior between ore and coal pyrite. However, passivation can not explain the fact that coal pyrite passes anodic current over potentials where ore pyrite passes a cathodic current.[152] Biegler[164] proposed that the differences in redox behavior among different pyrite samples were due

Table 4: Summary of previous work on electrochemical studies on mineral and coal pyrite

Technique	pH	Scan Rate mV/sec	Potential V(SHE)	Rest Pot. V(SHE)	Anodic Peak V(SHE)	Cathodic Peak V(SHE)	Products	Ref
Polarization, Cyclic Voltammetry	1.0	20.0	-0.26 to 0.65	Ore FeS_2 0.60	0 24	0.06	Oxidation: - Reduction: $FeS_{(1-x)}$, H_2S	164
Cyclic Voltammetry	0.0	4.0	-0.80 to 1.60	Ore FeS_2 0.62	-	-	Oxidation: Fe^{3+}, SO_4^{2-}, H^+ Reduction: Oxygen reduction	157
Polarization, Cyclic Voltammetry	0.0	0.1-5.0	-0.80 to 1.04	Ore FeS_2 0.60 Coal FeS_2 0.02	Coal FeS_2 0.25	Coal FeS_2 0.19	Oxidation: - Reduction: $FeS_{(1-x)}$, H_2S	161
Cyclic Voltammetry AC Impedance	9.3	20.0	-0.60 to 0.30	Ore FeS_2 0.15 Coal FeS_2 -0.30	Ore FeS_2 -0.1 (cycle 10) Coal FeS_2 -0.1 (cycle 10)	Ore FeS_2 -0.30 Coal FeS_2 -0.50	Passivating oxide layer formed only on ore pyrite surface	157
Cyclic Voltammetry	1.0	0.2 and 20.0	-0.40 to 0.10	Ore FeS_2 0.56-0.67	0.72 (cycle 1-5)	0.64,-0.06,0.02 (cycles 1-5)	Oxidation: Fe^{3+}, SO_4^{2-}, H^+ Reduction: $FeS_{(1-x)}$, H_2S	156
Cyclic Voltammetry AC Impedance	9.3	2.0 to 100.0	-0.50 to 0.20	Ore FeS_2 0.18	-0.1 (cycle 10)	-0.30 (cycle 10)	Oxidation: $Fe(OH)_3$ Reduction: $Fe(OH)_2$, OH^-	159
Cyclic Voltammetry	9.2	-	-0.60 to 0.20	-	0.1 (cycle 1)	-0.30 (cycle 10)	Oxidation: $Fe(OH)_3$ and metal polysulfide (FeSn)	153 169
Cyclic Voltammetry	4.6-13.0	20.0	-0.50 to 1.00	Ore FeS_2 -0.04(pH:4.6) -0 17(pH:9.2) -0.42(pH:13.0)	0.4,0.0(pH:4.6) 0.0 (pH:9.2) -0.2(pH:13.0) (cycle 1)	-0.18,0.25(pH:4.6) -0.27(pH:9.2) -0.65(pH:13.0) (cycle 1)	Oxidation: $Fe(OH)_3$, S^o, SO_4^{2-} and H^+ Reduction: FeS, OH^-, $Fe(OH)_2$, H_2S	167
Cyclic Voltammetry	9.3	20.0 to 200.0	-1.20 to 1.10	-	Ore FeS_2 -0.56,0.15,0.75 Coal FeS_2 -0.50,0.15 (cycle 1)	Ore FeS_2 -1.06,-0.76,-0.36 Coal FeS_2 -0.5, -0.15 (cycle 1)	Oxidation: $Fe(OH)_3$, S^o, SO_4^{2-} Reduction: FeS, Fe^o, $Fe(OH)_2$ and HS^-	160
Cyclic Voltammetry	9.2	100.0	0.65 to 1.05	-	-0.6,0.2,0.8 (cycle 1)	-0.3,-0.8 (cycle 1)	Oxidation: $Fe(OH)_3$, S^o, SO_4^{2-} Reduction: Sulfur intermediates, Fe^o, $Fe(OH)_2$ and HS^-	168 170

to differences in impurity contents and semiconductor properties, and that a sub-stoichiometric pyrite rather than FeS formed during cathodic reduction:

$$FeS_2 + 2xH^+ + 2xe \leftrightarrow FeS_{2-x} + xH_2S \qquad 0<x\leq 1 \qquad (45)$$

Peters and Majima[113] found that at the high potential where pyrite actually oxidized in acidic conditions, Fe^{3+} and SO_4^{2-} were the principal products:

$$FeS_2 + 8H_2O \leftrightarrow Fe^{3+} + 2SO_4^{2-} + 16H^+ + 15e \qquad (46)$$

It was suggested that pyrite is in a "passive" state after exposure to air, and the surface film formed may be adsorbed oxygen or an oxygen-sulfur compound.[113] The adsorbed oxygen participates in the xanthate oxidation to dixantogen during flotation according to a mechanism originally proposed by Fuerstenau *et al.*[165]

The rest potential of ore pyrite was generally higher than that of coal pyrite, attributed to the presence of some species such as an iron oxide surface layer, adsorbed oxygen, or an oxygen-sulfur compound, on ore pyrite that is absent on coal pyrite[161] or to differences in semiconductor properties.[157] Differences between different mineral pyrite samples in acidic conditions were correlated with differences in the semiconductor properties, which in turn were related to the concentration of impurities and the S/Fe ratio in the samples.[156] Higher cathodic and anodic currents were observed for samples with the higher charge carrier concentration.

Under basic conditions, pyrite has been found to produce $Fe(OH)_3$, S^o, SO_4^{2-} and FeS_n (the latter is commonly referred to as polysulfide, and forms by preferential leaching of Fe from the pyrite lattice).[159,160,162,166-170] Mineral pyrite produced surface films

of iron hydroxide with charge transfer resistance and other characteristics specific to each pyrite sample.[159] Reduction under basic conditions produced FeS, OH^-, $Fe(OH)_2$ and Fe.[159,167,170]

Both elemental sulfur and sulfate have been detected on oxidation of ore pyrite,[167] although the appearance of sulfur is not predicted by thermodynamics. The proportion of hydrophobic elemental sulfur decreased with increasing pH and potential, as would be expected from Figure 2. Wadsworth and colleagues found that oxidation of mineral pyrite in basic media at high potential produced elemental sulfur and iron oxides, which in turn influenced the anodic and cathodic behavior at lower potentials.[160] Coal pyrite shown similar behavior, albeit with higher current densities. Sulfur was detected using an *in-situ* Raman technique during oxidation of both coal and ore pyrite in acidic, neutral and weakly alkaline conditions; however polysulfide was only detected for ore pyrite.[162] Tao *et al.*[153], found that the rates of oxidation and reduction of coal pyrite are higher than those of mineral pyrite, which may be attributed to its high surface area and coal inclusions. Due to the high surface area, reactions took place internally in the pores and hindered diffusion of soluble products to the external electrode surface. At very high potentials, in the so-called transpassive region, ferric oxides, sulfate ion, and partially oxidized sulfur intermediates were produced. The latter dramatically affected subsequent oxidation at lower potentials.[168,170] Aplan[171] indicated that there is a wide variation in coal pyrite morphology from source to source. Ore pyrite in general, shows smooth surfaces whereas coal pyrite can shows samples with porous grains, granular masses, spherical masses and framboids. The effect of oxidation on the hydrophobicity of coal pyrite was studied by Tao *et al.*[160] using freshly fractured pyrite electrodes. They found that pyrite itself oxidizes to form ferric hydroxide (hydrophilic) and iron polysulfide (hydrophobic). Freshly fractured electrodes prevent the pre-oxidation of the surfaces during sample preparation.

It is clear that the behavior of pyrite depends upon different factors including the nature of the source, semiconductor properties, porosity, surface area and chemical composition. An understanding of the behavior of pyrite surfaces under different conditions may allow modification and improvement of methods for separating pyrite from coal.

IV. EXPERIMENTAL MATERIALS AND METHODS

A. MATERIALS

A.1. Coal Samples

Fourteen coals were used in this study. They came from different geographical locations in the United States and vary in rank from lignites to anthracites, each having different sulfur contents. One sample of freshly mined Upper Freeport coal was obtained from the Troutville #2 Mine, Clearfield County, Pennsylvania and stored under argon. Monosized fractions were prepared using a mortar and pestle, followed by sieving. Storage, grinding and sieving were done in an argon-filled glove box, to prevent oxidation. The other coals were obtained from the Pennsylvania State Coal Sample Bank. The sample designations used to refer to the samples are those used by the Coal Bank. The source, type and proximate analyses of these coals are tabulated in Table 5.

A.2. Coal Pyrite Samples

Two coal pyrite samples were used in this study: Upper Freeport and Pittsburgh coal pyrite. Upper Freeport coal pyrite samples were hand picked from crushed Upper Freeport coal obtained from the Troutville #2 Mine, Clearfield County, Pennsylvania. Pittsburgh coal pyrite samples were provided by the U.S. Bureau of Mines, Pittsburgh Research Center, Pennsylvania. One of the pieces of each sample was used to determine chemical composition, another for oxidation and electrokinetic studies, and a third for making electrodes to be used for electrochemical experiments.

A.3. Chemicals and Other Materials

Reagent grade chemicals were used in all experiments. Triply distilled water was used in preparing all solutions. Argon 99.995% pure was used to maintain an inert

atmosphere in the glove box and in the electrochemical experiments. The same argon and 99.7% pure nitrogen were used to deoxygenate solutions.

B. METHODS

B.1 Proximate and Elemental Analysis

Proximate analysis[8] of Upper Freeport coal was carried out using a LECO-MAC-400 proximate analyzer. One gram of coal sample was loaded into a crucible, then the temperature was increased to 106°C under nitrogen to release moisture. The samples were weighed continuously inside the equipment until the sample weight stopped decreasing. The percent moisture was computed from the difference between the initial and the final value. The crucible was then covered and the temperature was increased to 950°C under nitrogen to drive off the volatile matter. The computing procedure was identical to that used in the moisture determination. Then, the temperature was decreased to 600°C and the crucible covers were removed. Finally, the temperature was increased to 750°C under oxygen and the coal sample was burned. The weight loss was attributed to fixed carbon and the remaining material was considered ash. The results were computed on an as-received base and on a dry basis. The proximate analyses of the others coal samples was provided by the Pennsylvania State Coal Sample Bank. The proximate analyses of the coals studied are presented in Table 5. The accuracy of the proximate analysis is ±0.5%.

Ultimate analysis[9] of Upper Freeport coal was carried out using a LECO CHN-600 elemental analyzer by burning about 0.15 g of coal samples at 950°C under oxygen atmosphere in a combustion tube.

Table 5. Proximate analysis of coal samples studied.

Sample	Origin	Rank	Proximate (As-rec'd, %)			
			Ash	Volatile Matter	Fixed Carbon	Moisture
PSOC-1442	Darco, Texas	Sub-bituminous C	7.60	45.42	14.38	32.60
PSOC-1538	Bottom, Texas	Sub-bituminous C	11.07	33.18	25.75	30.00
PSOC-1486	Big Dirty, Washington	Sub-bituminous B	15.45	34.47	29.94	20.13
PSOC-1487	Adaville #1, Wyoming	Sub-bituminous A	4.55	34.67	41.78	18.99
PSOC-1539	Illinois #6, Illinois	HVC Bituminous	14.77	34.16	40.93	10.43
PSOC-1497	Illinois #2, Illinois	HVC Bituminous	10.13	35.70	40.74	13.44
PSOC-1494	Kentucky #9, Kentucky	HVB Bituminous	10.97	35.77	46.14	7.12
PSOC-1481	Upper Clarion, Pennsylvania	HVA Bituminous	8.76	38.73	50.79	1.73
DECS-12	Pittsburgh #8, Pennsylvania	HVA Bituminous	10.00	35.16	52.44	2.40
U.F.*	Upper Freeport, Pennsylvania	MV Bituminous	17.59	27.05	55.35	1.50
PSOC-1527	Upper Freeport, Pennsylvania	MV Bituminous	30.30	23.14	46.10	0.46
PSOC-1516	Lower Kittanning, Pennsylvania	LV Bituminous	10.11	17.38	70.54	1.97
PSOC-1515	Penn. Anthracite, Pennsylvania	Semi Anthracite	28.46	8.23	60.87	2.44
PSOC-1461	Mammot, Pennsylvania	Anthracite	23.44	3.89	69.61	3.06

*Measured by the author.

The amount of carbon dioxide and water produced by combustion was measured by carbon and hydrogen infrared detectors, whereas NOx was first reduced to N_2 by hot copper and a N-catalyst, then measured by a thermal conductivity cell.

The total sulfur content was determined using a LECO SC-132 Sulfur Analyzer. The coal samples were combusted at 1370°C under oxygen to oxidize sulfur to sulfur dioxide. The water vapor was removed by magnesium perchlorate and the sulfur dioxide was measured by an infrared detector. Finally, the oxygen content was calculated by difference (%O = 100. - %(C + H + N + S + Ash))

The ultimate analyses of the others coal samples was provided by the Pennsylvania State Coal Sample Bank. The elemental analyses of the coals studied are presented in Table 6. The accuracy of the elemental analysis is ±0.5%

Table 6. Elemental analysis (dry basis) of coal samples studied .

Sample	Origin	Rank	Carbon	Hydrogen	Nitrogen	Oxygen	Sulfur	Ash
			%	%	%	%	%	%
PSOC 1442	Darco Texas	Sub-bituminous C	65.46	4.00	1.53	16.96	0.78	11.27
PSOC 1538	Bottom Texas	Sub-bituminous C	62.53	4.75	1.23	14.69	0.99	15.81
PSOC 1486	Big Dirty Washington	Sub-bituminous B	59.12	4.77	1.07	14.75	0.94	19.35
PSOC 1487	Adaville #1 Wyoming	Sub-bituminous A	71.55	5.05	1.04	15.43	1.31	5.62
PSOC 1539	Illinois #6 Illinois	HVC Bituminous	65.49	4.56	1.11	8.16	4.52	16.16
PSOC 1497	Illinois #2 Illinois	HVC Bituminous	69.17	4.06	1.32	7.82	5.93	11.70
PSOC 1494	Kentucky #9 Kentucky	HVB Bituminous	70.33	4.28	1.23	7.50	4.85	11.81
PSOC 1481	Upper Clarion Pennsylvania	HVA Bituminous	73.40	4.68	1.28	6.91	4.82	8.91
DECS 12	Pittsburgh #8 Pennsylvania	HVA Bituminous	74.78	5.11	1.23	7.51	1.12	10.25
U.F+.	Upper Freeport Pennsylvania	MV Bituminous	NA *	NA	NA	NA	1.12	17.59
PSOC 1527	Upper Freeport Pennsylvania	MV Bituminous	NA	NA	NA	NA	2.02	30.44
PSOC 1516	Lower Kittann. Pennsylvania	LV Bituminous	79.67	4.20	1.47	2.95	1.40	10.31
PSOC 1515	Penn.Anthracite Pennsylvania	Semi Anthracite	62.38	2.77	0.80	4.30	0.58	29.17
PSOC 1461	Mammot. Pennsylvania	Anthracite	70.87	1.45	0.87	1.89	0.74	24.18

*NA: Not available. In the case of Upper Freeport coal (U.F) there was not equipment available in our laboratory, whereas in the case of PSOC-1527 coal the analysis was not provided by the Pennsylvania Coal State Bank..

+Measured by the author.

B.2 Pyritic Sulfur Analysis

The pyritic sulfur analysis was done by using the nitric acid extraction method[172](ASTM D2492-84). In this method 2-5 g of Upper Freeport coal was introduced into a 250 ml beaker. Fifty ml of HCl, with an HCl:H_2O volume ratio of 2:3,

was then added. The solution was heated and boiled for 30 minutes on a hot plate, then cooled to room temperature. The solution was filtered, and the residue washed with 250 ml distilled water, to transfer all the HCl to the beaker. The remaining residue and filter paper were transferred into a 250 ml beaker. Fifty ml of 1.97 M HNO_3 (HNO_3:H_2O volumen ratio of 1:7) was then added, and agitated to disintegrate the filter paper and wet the coal. The new solution was then boiled for 30 minutes. After boiling, it was again cooled to room temperature and filtered with 250 ml of distilled water. Two ml of 30% H_2O_2 was added and the solution was boiled again for 5 minutes, to oxidize any organic material that might have dissolved during the extraction. Finally the solution was immersed in an ice bath, in order to cool it to room temperature, and made up to 250 ml with distilled water. The solution was then analyzed for iron by atomic absorption spectrophotometry. The pyritic sulfur analyses of the others coal samples was provided by the Pennsylvania State Coal Sample Bank. The pyritic sulfur analyses of the coals is shown in Table 7.

B.3 Sulfatic Sulfur Analysis

In this analysis[172] the filtrate obtained after the treatment of coal with HCl in the pyritic sulfur analysis was used. The filtrate was treated with 5 ml of bromine water and boiled for 5 minutes to oxidize iron and expel any excess of bromine. Iron was then precipitated by adding ammonium hydroxide. The solution was filtered and made up to 400 ml whereas the filter paper was washed with a hot ammoniacal solution (1 vol. ammonia/ 10 vol. water). Two to three drops of methyl orange were added to the filtrate, and the HCl was added until the solution turned pink. The solution was boiled and 10 ml of barium chloride solution (100g/l) was added. The solution was then filtered and washed with hot water. The filter paper containing $BaSO_4$ was put into a crucible and burnt. Then, the amount of sulfur sulfate was obtained gravimetrically.

Table 7. Sulfur analysis (dry basis) of the coal samples studied.

Sample	Origin	Rank	Sulfatic %	Organic %	Pyritic %	Total %
PSOC-1442	Darco, Texas	Sub-bituminous C	0.02	0.65	0.11	0.78
PSOC-1538	Bottom, Texas	Sub-bituminous C	0.02	0.86	0.11	0.99
PSOC-1486	Big Dirty, Washington	Sub-bituminous B	0.01	0.68	0.25	0.94
PSOC-1487	Adaville #1, Wyoming	Sub-bituminous A	0.01	1.27	0.03	1.31
PSOC-1539	Illinois #6, Illinois	HVC Bituminous	0.01	2.24	2.27	4.52
PSOC-1497	Illinois #2, Illinois	HVC Bituminous	0.35	2.07	3.51	5.93
PSOC-1494	Kentucky #9, Kentucky	HVB Bituminous	0.02	1.69	3.14	4.85
PSOC-1481	Upper Clarion, Pennsylvania.	HVA Bituminous	0.20	1.42	3.20	4.82
DECS-12	Pittsburgh #8, Pennsylvania.	HVA Bituminous	0.01	0.73	0.38	1.12
U.F.	Upper Freeport, Pennsylvania.	MV Bituminous	0.01	0.45	0.66	1.12
PSOC-1527	Upper Freeport, Pennsylvania.	MV Bituminous	0.05	0.34	1.63	2.02
PSOC-1516	Lower Kittanning, Pennsylvania	LV Bituminous	0.01	0.78	0.61	1.40
PSOC-1515	Penn. Anthracite, Pennsylvania.	Semi Anthracite	0.00	0.48	0.10	0.58
PSOC-1461	Mammot, Pennsylvania.	Anthracite	0.02	0.36	0.36	0.74

Finally, the organic sulfur content was calculated by difference:

%Organic sulfur = %Total sulfur - (%Pyritic sulfur + %Sulfatic sulfur)

The sulfatic and organic sulfur analyses of the other coal samples was provided by the Pennsylvania State Coal Sample Bank. The sulfatic and organic sulfur analyses of the coals are shown in Table 7.

B.4 Coal Oxidation Methods

B.4.1 Thermal Oxidation

Upper Freeport coal samples were thermally oxidized in a mechanical convection oven, Model 26 manufactured by Precision Scientific Groups. Five gram samples of -75 +63 μm particles, spread to a depth of about 1 mm, were oxidized at 100, 150, 200 and 230^{o}C for 24 hours, to investigate the effect of oxidation temperature. Samples were also oxidized at 230^{o}C for 1, 2, 4, 8 and 24 hours, to investigate the oxidation rate. For

thermal oxidation of the coals from the Pennsylvania State Coal Bank, five gram samples of each coal were oxidized at 230°C for 1, 2, 4, 8 and 25 hours.

Five g samples of -75 +63 μm Upper Freeport coal particles, were also oxidized in a convection oven at 95°C, or at room temperature (mean 20°C) for extended time periods. Room temperature tests were done with uncontrolled (about 50-70%) humidity, dry (in a dessicator), or at about 100% humidity (in a dessicator, with liquid water present). To avoid oxygen depletion, the dessicator was left slightly open. Coal samples from the Pennsylvania State Coal Bank were also oxidized at room temperature (mean 20°C) for extensive time periods at about 100% humidity, and under uncontrolled (but low) humidity.

The extent of oxidation for each of the above experiments was assessed by analyzing the concentration of carboxylic and phenolic groups by ion-exchange methods, which will be described in the oxygen functional group analysis section.

B.4.2 Wet Oxidation

a. Acidic Ferric Sulfate

Twenty gram samples of -75 +63 μm (200x250 mesh) Upper Freeport coal particles were oxidized for 24 hours at room temperature in a well stirred, Pyrex vessel, through which argon was passed continuously, using 600 ml of 0.0094 M, 0.0187 M, and 0.0374 M $Fe_2(SO_4)_3$ solutions, all adjusted to pH 1.00±0.05. This correspond to 50%, 100%, and 200% of the stoichiometric Fe(III) requirement for oxidizing all the pyrite in each sample. Ten ml samples of the slurry were withdrawn periodically, filtered immediately, and the coal was washed with water to remove all ferric ions, to halt oxidation. Both the coal and the liquid fraction were stored under argon. Solution samples were analyzed by atomic absorption spectrophotometry, to determine the total

iron concentration in solution. The ferric:ferrous ratio was determined from the solution potential, using calibration curves.[209] These calibration curves were prepared for different total iron concentrations, using ferric solutions standarized by atomic absorption, and ferrous solutions standarized by potassium permanganate titration.

b. Nitric Acid

Twenty gram samples of -75 +63 μm (200x250 mesh) Upper Freeport coal particles were oxidized for 24 hours at room temperature in a well-stirred, Pyrex vessel, using 600 ml of 0.10 M or 3.00 M HNO_3. Samples were taken and treated as described above. The total iron in solution was determined by atomic absorption spectrophotometry.

c. Hydrogen Peroxide

Twenty gram samples of -75 +63 μm (200x250 mesh) Upper Freeport coal particles were oxidized for 6 hours at room temperature in a well stirred, Pyrex vessel, using 600 ml of 5.0%, 10% and 15% H_2O_2, all adjusted to pH 1.0. Ten ml slurry samples were withdrawn periodically and filtered immediately. The coal was washed to remove residual H_2O_2 and stored under argon. The liquid fractions were refrigerated, then were analyzed by atomic absorption spectrophotometry to determine the total iron in solution, and hence the extent of pyrite oxidation.

d. Wet Oxidation of Coal Samples from the Pennsylvania State Coal Bank

In the case of coal samples from the Pennsylvania State Coal Bank, 10 gram samples of each coal were oxidized for 5 hours at room temperature in a well stirred, Pyrex vessel through which argon was passed continuously, using 500 ml of 10% H_2O_2 at

pH 1.0, 1.0 M HNO_3 or 0.05 M $Fe_2(SO_4)_3$ at pH 1.0. These concentrations provided solution potentials of about 700 mV. Ten ml samples of slurry were withdrawn periodically and filtered immediately. The coal was washed carefully, dried under vacuum, then stored under argon at room temperature.

The extent of oxidation of each coal sample in the above experiments was assessed by analyzing the carboxylic and phenolic group concentration.

e. Chemical Oxidation of Coal Pyrite

Two standard methods for determining the pyrite content of coal and mineral wastes, and their propensity to release acidic drainage, were evaluated. One is the nitric acid oxidation-extraction method (ASTM D2492-84)[172] described earlier in this chapter and the other one is the peroxide oxidation method.[173,174]

i. Peroxide Oxidation Method

About 3 g of Upper Freeport coal was placed in a funnel fitted with filter paper. To remove oxidized iron that might dissolve during peroxide treatment, the sample was first leached with 300 ml HCl solution, with an HCl:H_2O volume ratio of 2:3. The sample was then washed with distilled water until the filtrate was free of chloride, as detected by a 10% silver nitrate solution. The filter paper and acid-leached sample were dried in a convection air oven at 75°C. About 2 gram of the dried sample was then placed in a 500 ml beaker and 24 ml of 30% H_2O_2 was added, and the mixture was heated to 40°C, then allowed to cool for 30 minutes, or until the reaction went to completion. About 12 ml of H_2O_2 was then added to the beaker, and left for 30 minutes. The mixture was heated to about 95°C for 30 minutes to decompose any unreacted H_2O_2. The solution volume was made up to 100 ml, then heated to boiling to drive off any dissolved CO_2. It was then

cooled to room temperature and analyzed for iron by atomic absorption analysis, and for acidity by titration with NaOH solution.

ii. Modifications to the Peroxide Oxidation Method

When the peroxide method was performed exactly as prescribed, very little pyrite appeared to dissolve; this is because the reaction of 30% H_2O_2 with either coal or ore pyrite is strongly exothermic. The temperature reached values as high as 95°C within a few minutes of the initial addition of H_2O_2. Hydrogen peroxide decomposes rapidly at such high temperature, hence there is limited oxidation of pyrite. In order to devise a more reliable and reproducible analytical procedure that eliminated the thermal decomposition of the hydrogen peroxide, two modifications of this method were investigated.

1. As soon as the solution temperature reached 40°C, the beaker was immersed in an ice-water bath and cooled to room temperature. The beaker was then removed from the ice-water bath, and the reaction was allowed to proceed until the temperature again reached 40°C, when the mixture was cooled again. Five cycles were usually needed to allow the reaction go to completion; at that point, the standard procedure was followed. This method is referred to as PO:40, whereas the unmodified peroxide oxidation method, in which the temperature was uncontrolled, is denoted as PO:U.

2. The beaker with coal and hydrogen peroxide was held in an ice-water bath. While the exothermic reaction between the pyrite and hydrogen peroxide was occurring, the temperature of the solution stayed at 10 to 12°C. Once the reaction slowed down, and the temperature dropped to 7 to 8°C, the standard procedure was followed. This method is referred to as PO:10.

B.5 Oxygen Functional Group Analysis

As-received and oxidized coal samples were analyzed by the sodium acetate ion-exchange method to determine the surface carboxylate species, and by the barium hydroxide ion-exchange method to determine the total acidic species (carboxylate and phenolic). Both methods are described in detail by Brooks and Sternhell.[175]

The sodium acetate ion-exchange method assumes that all the surface carboxylic acid groups will be converted to their solution salts on exposure to a large excess of sodium acetate, releasing hydrogen ions into solution according to the reaction:

$$RCOOH(s) + CH_3COONa \leftrightarrow RCOONa(s) + CH_3COOH \quad (47)$$

A gram of sample was purged with nitrogen, and shaken with 100 ml of 3.0M sodium acetate solution for 24 hours. The solution was filtered and after the filtration step, 30 ml of the filtrate was pipetted into the titrator beaker, which already contained 50 ml of CO_2-free, triply-distilled water. This solution was then potentiometrically titrated with 0.2 N NaOH using a Fisher computer-aided titrimeter Model 455.

The barium hydroxide ion-exchange method assumes that Ba^{2+}exchanges with H^+ in the carboxylic and phenolic groups, forming insoluble compounds on the coal surface and releasing hydrogen ions into the solution:

$$2RCOOH(s) + Ba(OH)_2 \leftrightarrow (RCOO)_2Ba(s) + 2H_2O \quad (48)$$

$$2ArOH(s) + Ba(OH)_2 \leftrightarrow (ArO)_2Ba(s) + 2H_2O \quad (49)$$

where (s) denotes a surface species.

A gram of sample was purged with nitrogen, and shaken with 100 ml of 0.3 N $Ba(OH)_2$ solution for 24 hours. The solution was filtered, 30 ml of the filtrate was immediately pipetted into the titrator beaker, which already contained 31 ml of 0.3N HCl and 10 ml CO_2 free, triply-distilled (3D) water. This solution was titrated with 0.2 N NaOH using the same equipment described above. The phenolic group concentration is found by difference from the carboxylic and total acid concentrations.

B.6 Film Flotation Tests

The wettability of as-received, oxidized coal and coal pyrite samples was assessed by film flotation.[135-139] Closely sized particles were gently sprinkled onto the surface of solutions with different surface tensions. At any given surface tension, those particles that do not sink into the wetting liquid are called lyophobic (hydrophobic), whereas those that are imbibed into the liquid are called lyophilic (hydrophilic). The weight percentage of each fraction was determined gravimetrically, and the percentage of lyophobic particles was plotted as a function of the surface tension of the solutions. It should be emphasized that this method provides information on the averaged surface properties of individual particles. Each particle has a critical surface tension, which depends upon the relative concentration of lyophobic and lyophilic groups on the particle surface. Film flotation tests reveal the distribution of critical surface tension. The mean critical surface tension of each entire coal sample (the surface tension at which 50% of the sample is lyophobic) can be obtained from the distribution curve.

B.7 Zeta Potential Measurements

In order to study the effect of pH on the zeta potential of coal and coal pyrite samples, particles were ground to minus 400 mesh (<38 μm) with a mortar and pestle in

an argon-filled glove box. A 0.002M sodium nitrate solution was used as electrolyte, because nitrate ions do not form complexes with metal ions commonly found in coal suspensions. Sodium hydroxide and nitric acid were used to adjust the pH. Samples containing 0.02 gram of either coal or coal pyrite with 100 ml of electrolyte solution were conditioned for 16 hours, then redispersed ultrasonically. The zeta potential of each sample was measured in a Model 501 Lazer Zee Meter, using 25 ml of coal or coal pyrite suspension and a potential of 100 mV. Triplicate measurements were made for each sample. The results reported here correspond to the average of three measurements versus the final pH after conditioning.

B.8 Scanning Electron Microscopy (SEM) and Energy Dispersive X-ray (EDX) Analysis

SEM/EDX analysis was done to study the morphology and the elemental composition of raw coals, oxidized coals, coal pyrite samples and humic acids extracted from coals. Samples were mounted on bronze sample holders and coated with carbon for SEM examination using a JOEL JSM-35SF scanning electron microscope with a KEVEX energy dispersive X-ray analyzer. The analyses were carried out at an accelerating voltage of 10 kV and a beam current of 10 nA with an X-ray take off angle of 28^{o}. The SEM instrument has a resolution of the order of 40-60 Å.

B.9 Diffuse Reflectance Infrared Fourier Transform Analysis (DRIFT)

Coal and coal pyrite samples were prepared for DRIFT analysis by grinding a small amount of either coal or coal pyrite in an argon atmosphere to -400 mesh. Spectra were obtained using a computer-controlled Perkin Elmer 1750 Fourier transform infrared spectrometer employing a liquid nitrogen-cooled MCT (Hg-Cd-Te) detector and operated at nominal resolution of 4 cm^{-1}. Prior to each analysis, samples were thoroughly mixed

with KBr powder and transferred into a 10 mm aluminum cup. This cup was mounted in a beam condensing accessory. Typically 400 interferogram scans were combined to obtain each spectrum. Each spectrum was ratioed to the spectrum of finely powdered KBr.

B.10 Surface Area Determinations

In gas adsorption experiments a quantity V of volume of gas sorbed at constant temperature is determined at different relative pressures (P/P_0), and the surface area is evaluated from the value of volume at which the entire available surface is covered by a monolayer of sorbate and from the cross-sectional area of the sorbate molecule in its adsorbed state.[30] In this study a Micromeritics Surface Area/Pore Volume Analyzer (Model 2100D) was employed for gas adsorption experiments. In this apparatus, the quantity of adsorbed gas is determined from volume measurements before and after each adsorption step. The operating and data analysis procedures for the instrument are described in the Micromeritics Operating Manual.[176] CO_2 adsorption experiments, followed by analysis using the Dubunin-Polanyi equation were used in the present study. The relevant equation is:

$$\log V = \log V_0 - (BT^2/\beta) \log^2(P_0/P) \qquad (50)$$

where V is the volume of gas adsorbed, in cm^3 adsorbate per gram of adsorbent, V_0 is the micropore capacity (cm^3/g), P is the pressure, P_0 is the saturation vapor pressure of the adsorbate at temperature T (K), β is the affinity coefficient of the adsorbate relative to nitrogen, and B is a constant. Thus, a plot of logV vs $\log^2(P_0/P)$ should yield a straight line, with intercept of $\log V_0$ and slope $-BT^2/\beta$. Using the calculation procedures described in the instrument manual,[176] the gas volumes V and V_0 are reduced to S.T.P.

The applicability of equation (50) is limited to microporous materials, where the majority of the pore diameters are a few times the effective diameter of the adsorbing gas molecules. For such systems, monolayer adsorption may be assumed, so that V_o may be used to estimate the surface area from the equation:

$$S = N_A V_o S_a v^{-1} 10^{-20} \tag{51}$$

where S is the specific surface area (m^2/g), N_A is Avogadro's number, v is the specific volume of the adsorbing gas, and S_a is the effective specific surface area per molecule of the gas at the appropriate temperature. The specific volume of CO_2 at S.T.P. is $2.23 \cdot 10^4$ cm^3/mole and S_a has been taken as 25.3 $Å^2$/molecule at 298 K.[176] The factor 10^{-20} accounts for unit transformations. For all adsorption experiments the samples were outgassed for 48 hours. The entire evacuation procedure was performed by the mechanical vacuum pump in the gas adsorption apparatus at a vacuum of about 10^{-3} mm Hg. The adsorption experiments were carried out at room temperature (about 20°C) by placing a water-filled Dewar flask around the sample bulb. The time to reach equilibrium between measurements varied from coal to coal, but was usually between 1.5 and 2.0 hours. In general, 4 different volume values were measured for each coal by using pressure values ranging from 300 to 800 mm Hg. Sample weights of 1.0 to 2.0 g weighed to four decimal points were used, and duplicate measurements were made for each coal sample.

B.11 Surface Tension Measurements

The surface tension of methanol-water solutions used in the film flotation tests was measured with a Fisher Scientific Surface Tensiomat, Model 21, using the du Nouy ring

method.[177] This method is suitable for solutions that achieve surface tension equilibrium rapidly, which is the case of methanol-water solutions. Three readings were taken on each solution, with the average being utilized as the final value. Errors estimated from the average differences in the triplicate measurements, were ± 0.30 mN/m.

B.12 Hallimond Tube Flotation Tests

In these experiments no organic frother or collector was used. Instead, the so-called "salt flotation" method was used.[178] In this technique, the pH of the liquid phase is controlled and a high concentration of non-specifically adsorbing electrolyte is used as a bubble-size modifier and frother. The advantage of this method is that surfactant adsorption effects at the solid-liquid and liquid-gas interfaces are negligible. Moreover, the froth formed is of very low persistency, which minimizes the holdup of material at the air-liquid surface. The salt flotation tests were made using a modified Hallimond tube.[179] Before each test, 1 L of a 0.5M NaCl solution was purged with 99.7% nitrogen for 1 hour, followed by 99.995% argon for 1 hour. One gram of 28 x 65 mesh (-590 + 210 μm) coal sample was then conditioned with 175 ml of deoxygenated 0.5M NaCl solution for 10 minutes. After conditioning, the slurry was added to the Hallimond tube. At this point the nitrogen flow through the glass frit in the bottom of the Hallimond tube was turned on at a flow rate of 30 ml/min and flotation was allowed to proceed for 3 minutes (designated as a flotation time), unless otherwise stated. Throughout the entire conditioning and flotation period the sample was magnetically stirred at constant speed. Nitrogen bubbles floated hydrophobic solid particles to the air-liquid surface and as the bubbles broke, the particles fell into the concentrate stem. At the end of each test the fraction of material in the concentrate stem and the material remaining in the cell above the frit were collected separately, filtered, washed, dried and weighed, to determine the flotation yield.

B.13 Electrochemical Experiments

B.13.1 Electrode Preparation

Upper Freeport coal pyrite samples about 5.0x5.0x7.0 mm in size were hand picked from crushed coal, and cleaned, first with hot hydrochloric acid, to remove acid-soluble impurities, then with pyridine, to remove coal impurities. A Pittsburgh coal pyrite sample was prepared from a natural pyrite sample, which was dried at 80°C for 30 minutes in air, then transferred to a vacuum chamber to evacuate the pores. After 10 minutes the sample was coated with 302-2 epoxy resin in the vacuum chamber, allowing the resin to penetrate all pores. After 20 minutes the pyrite sample was removed from the vacuum chamber, cured at 90°C for 6 hours, then cut to size, avoiding inclusions, cracks and voids.

Copper wires 1 mm in diameter were connected to the Upper Freeport and Pittsburgh coal pyrite samples using silver epoxy, then each copper wire was shrouded in an insulating plastic capillary tube. The sample and base of the plastic tube were then encased in cold-setting resin, to expose only the bottom of the pyrite sample. Because of the porous, irregular nature of the pyrite electrodes, the exposed surface areas were estimated by mapping a magnified image. These areas, 0.2 cm^2 for the Upper Freeport and 0.187 cm^2 for the Pittsburgh coal pyrite, were used to calculate the current densities.

The method used in the preparation of the Pittsburgh coal pyrite electrode was adopted to overcome some difficulties observed during preliminary electrochemical tests. Upper Freeport coal samples were very porous, irregular and likely with high surface area. These physical characteristics allowed the electrolyte solution to penetrate the internal surface of the electrode with the consequent damage of the connection between the

copper wire and the pyrite samples. The method also allows to have a more realistic value of the surface area used in the calculation of current densities.

B.13.2 Electrochemical Cell and Instrumentation

A three compartment electrochemical cell was used for all the electrochemical experiments. A schematic diagram of the experimental set-up is shown in Figure 3. The tubular furnace shown in Figure 3 was used to purify argon of any residual oxygen. Argon passed over pellets containing activated copper, heated to 120°C. Activated copper on the pellets reacts with oxygen in the argon to form copper oxide. Any CO_2 trace in argon was removed by using calcium hydroxide pellets. Figure 4 shows details of the electrochemical cell used in this study.

An EG&G Model 273 potentiostat was used for all the electrochemical experiments. It was interfaced with an IBM computer (PC/XT). The electrode potentials were controlled and the current measurements were made using the electrochemistry software package, HEADSTRT, provided with the Model 273 potentiostat. The programs used to run the electrochemistry experiments were written using a code system provided by the software package HEADSTRT.[152]

B.13.3 Rest Potential Measurements and Cyclic Voltammetry Tests

Before each electrochemical experiment a fresh pyrite surface was exposed by wet grinding on a 600 grit silicon carbide paper using deoxygenated triply distilled water under an argon atmosphere in a glove box. The surface was etched for a minute in a 2:1:1 mixture of HNO_3:HF:CH_3COOH by volume (70% W/W assay HNO_3, 52% W/W HF, and 99.7% CH_3COOH), to dissolve any oxidized layers and surface debris. The electrode was transferred to the electrochemical cell inside the glove box, to prevent oxidation. The potentials were measured against a saturated calomel electrode using an EG&G Model

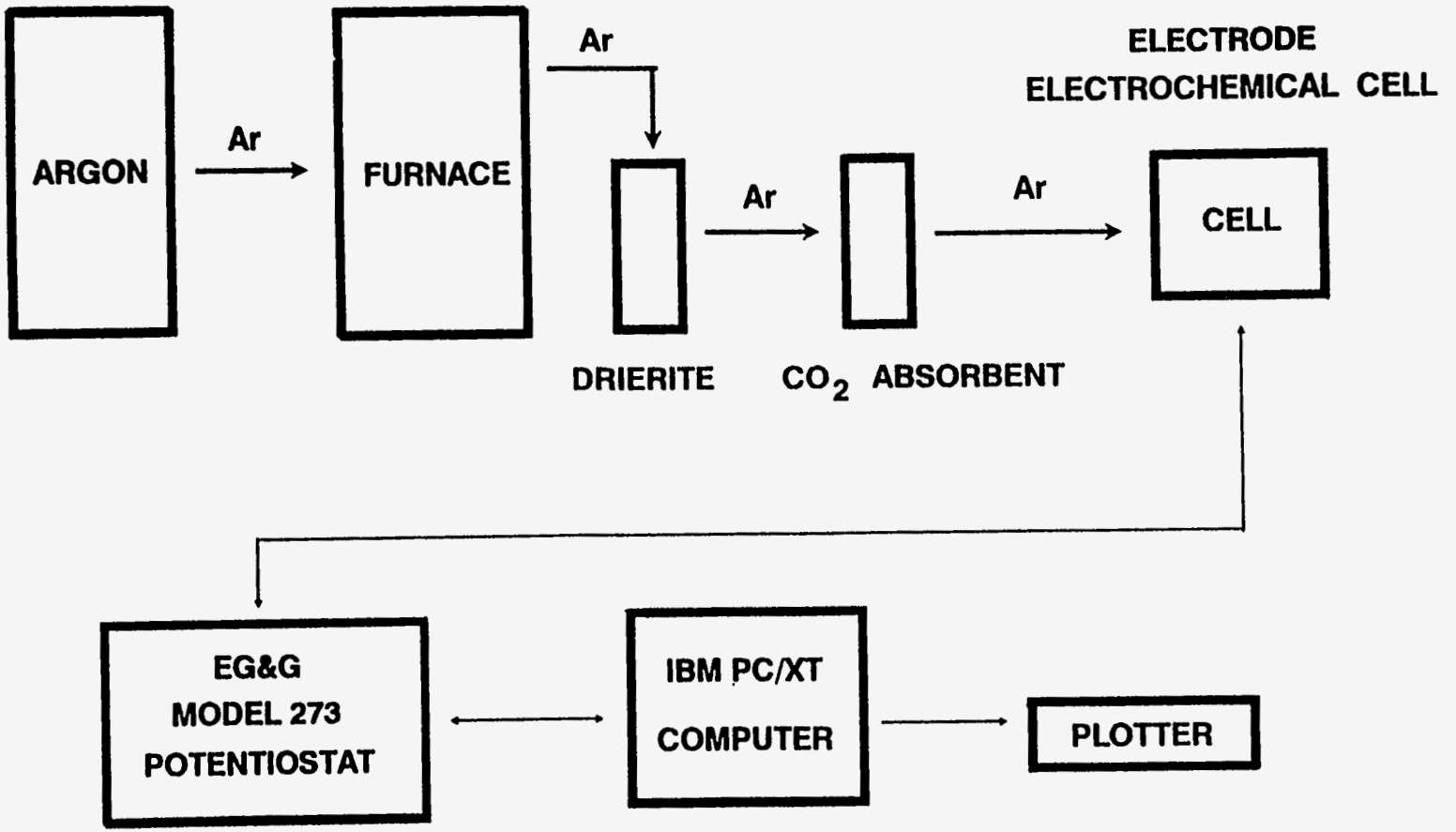

Figure 3. Experimental set-up for electrochemical experimental work.

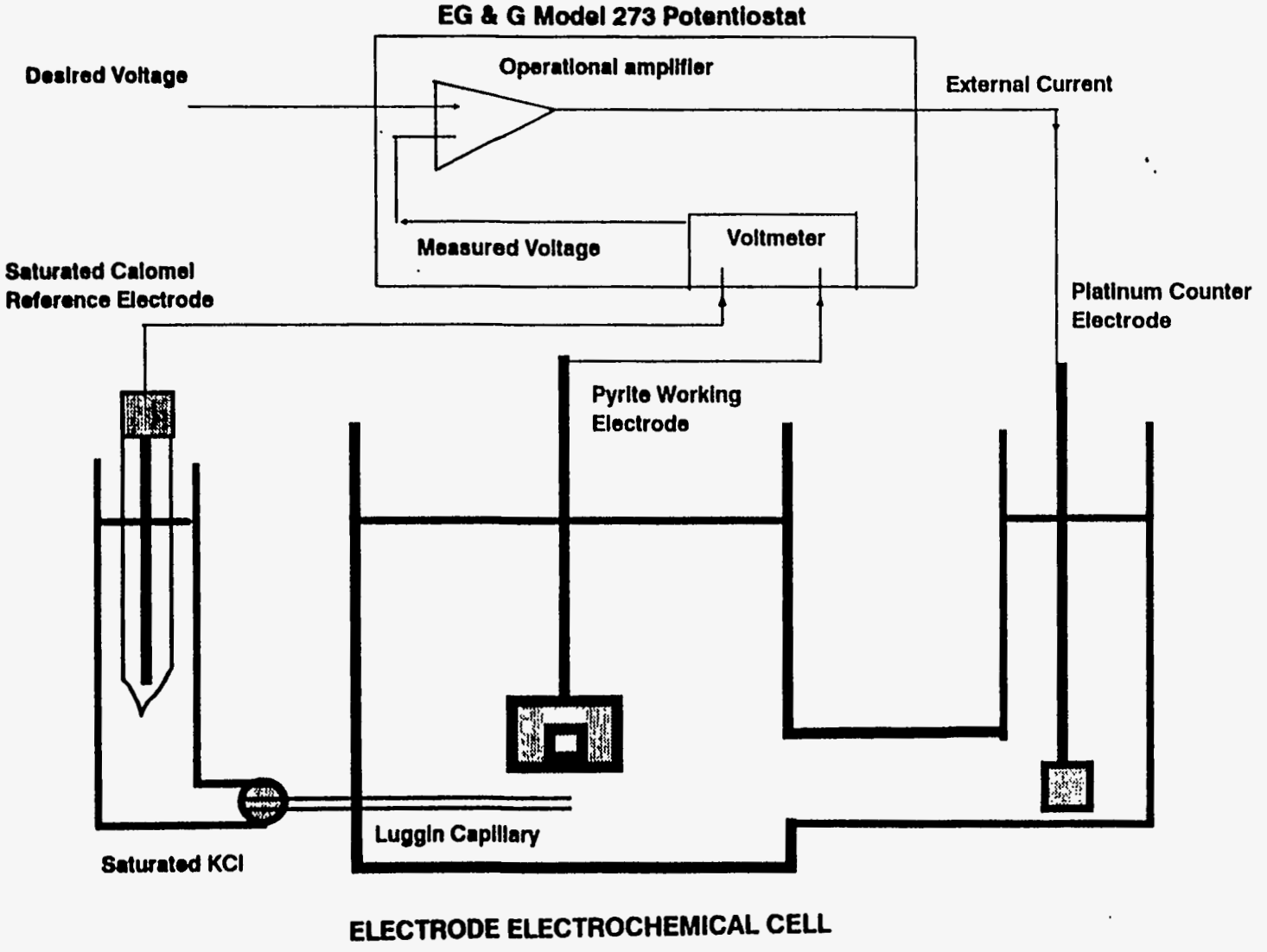

Figure 4. Electrochemical cell used in the electrochemical experimental work

273 potentiostat, and then converted to the SHE scale. The counter electrode was a platinum gauze, 12 cm^2 in area.

In the rest potential measurements, the potential of coal pyrite electrodes was measured as a function of time for 24 hours, in a pH 1.0 H_2SO_4 solution, a pH 7.4 phosphate buffer (0.008695 M KH_2PO_4, 0.03043 M Na_2PO_4), a pH 9.3 borate buffer (0.025M $Na_2B_4O_7.10H_2O$) and a pH 10.5 borate buffer (0.0125M $Na_2B_4O_7.10H_2O$ in 0.02425M NaOH). In the cyclic voltammetry experiments the samples were contacted with the selected buffer for either 2 or 24 hours, then scanned at 20.0 or 2.0 mV/s for five cycles in each test, starting in the anodic direction from the rest potential. A potential range of -0.43 to 1.05 V(SHE) was used at pH 1.0 whereas at higher pH values, a potential range of -0.75 to 0.75 V(SHE) was used.

B.13.4 Contact Angle Measurements

The contact angles were measured in the same electrochemical cell used in the rest potential measurements and cyclic voltammetry experiments, with an extra hole in the cell cover to accommodate a curve-tipped capillary. A nitrogen bubble was placed onto the surface of the coal pyrite electrode, using the capillary and a syringe, then the capillary was removed from the surface. The bubble generally attached easily to the surface of the coal pyrite when the contact angle exceeded 10^o. For contact angles below 10^o, the bubbles did not have strong affinity for the surface of coal pyrite and often rolled off the surface. The dependence of contact angle on the potential was assessed by stepping the potential from the rest potential to the desired value, letting the electrode equilibrate for 5 minutes, then measuring the contact angle of three bubbles on each side of the bubble profile. After measuring the contact angle, the potential was stepped to the next potential.

V. RESULTS AND DISCUSSION

A. Oxidation Studies on Upper Freeport Coal

A.1. Dry oxidation studies

The reaction of coal with oxygen is a complex process accompanied by a change in the composition and properties. This chapter reports the compositional and structural changes to the organic and inorganic material of the coals, caused by oxidation. The effect of these changes on the subsequent behavior of coals, and the implications of the results for practical situations are also discussed.

Five gram samples of -75 +65 μm Upper Freeport coal, spread to a depth of about 1 mm, were oxidized in a convection oven at 100, 150, 200 and 230°C for 24 hours to investigate the effect of oxidation temperature. Samples were also oxidized at 230°C for 1, 2, 4, 8 and 24 hours, to investigate the oxidation rate.

A.1.1. Acidic Group Analyses

In this study the extent of oxidation was assessed by analyzing the concentration of carboxylic and phenolic groups by ion-exchange methods[175] and by infrared spectroscopy. The reproducibilities between duplicate analyses of the acid-treated coals were good. Errors, estimated from the average differences in the duplicate runs, were ± 0.05 Wt% group oxygen for the carboxyl determinations and ±0.15Wt% group oxygen for the total acid determinations. Figure 5 shows that the majority of the acidic oxygen groups are phenolic in the as-received coal and coal oxidized at temperatures up to 150°C. At higher oxidation temperatures there is a dramatic increase in the total percentage of acid groups oxygen in the coal, but the majority of this is present as more

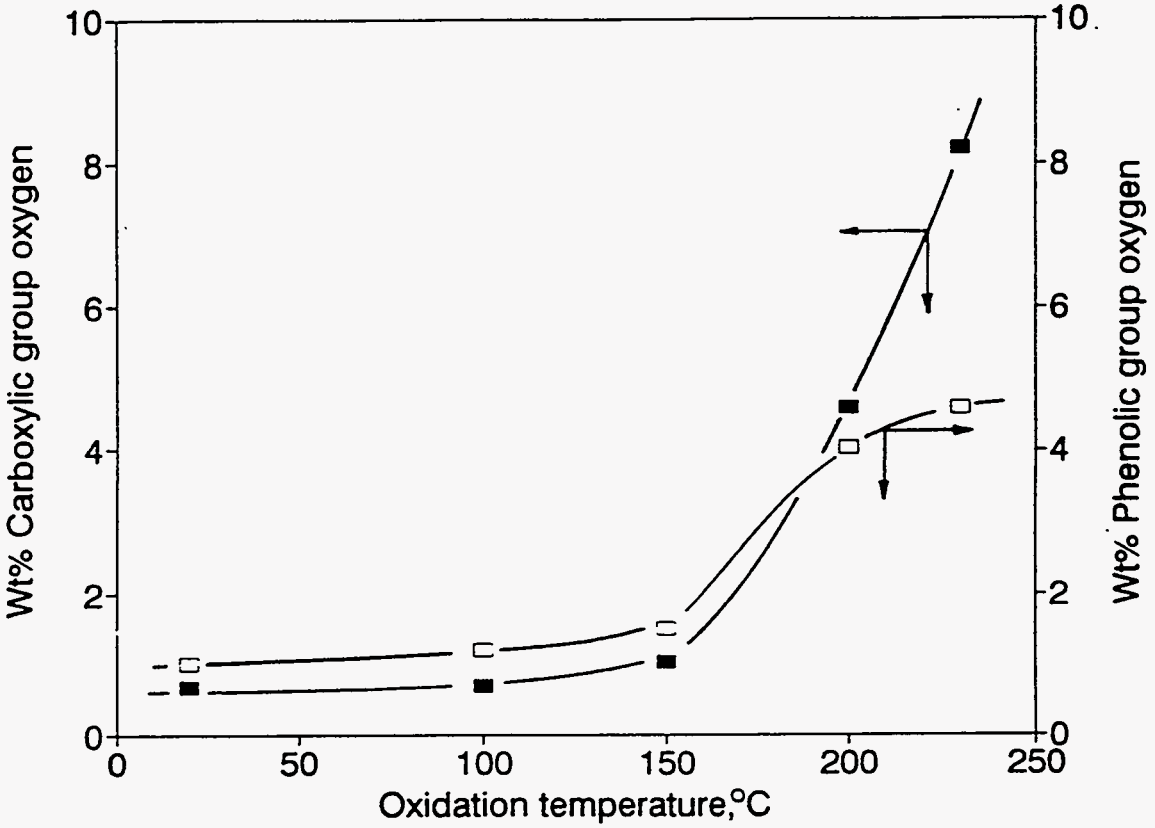

Figure 5. Effect of oxidation temperature on weight percent oxygen in the form of carboxylic and phenolic groups during oxidation of Upper Freeport coal for 24 hours.

highly oxidized carboxylic groups. Higher oxidation temperatures have been reported to produce carboxylic group preferentially,[84,127,180,181] although higher concentration of phenolic groups has been also reported.[143] Figure 6 shows that Upper Freeport coal oxidized at 230°C for less than five hours has a majority of phenolic groups, whereas the concentration of carboxylic acid groups increases steadily with oxidation time, exceeding that of phenolic groups after five hours, suggesting that the oxidation product after more extensive periods is carboxylic groups and phenolic groups are also transformed to carboxilic groups. These results are in good agreement with results reported by other researchers.[79,127,182]

Figures 7 and 8 show the rate of generation of carboxylic and phenolic groups, respectively. The rate of carboxylic group generation shows a maximum after two hours whereas the rate of phenolic group generation shows a maximum at about two hours, but is negative after about 4 hours, then increases again after 8 hours. These results suggest that initially, the oxidation of coal may be dominated by the chemical adsorption of oxygen molecules on the coal surface; thus, the generation of carboxylic and phenolic groups is relatively slow. As oxidation progresses, more surface area is available (discussed later) likely due to release of volatile matter and opening up of pores with thermal treatment. Thus, a high concentration of oxygen on the coal surface is achieved and chemical reactions leading to the formation of carboxylic and phenolic take place. At this stage, the rate of oxidation increases substantially until it reaches a maximum. The decrease in the total percentage of phenolic groups observed after about 4 hours suggests that generation with concurrent transformation to carboxylic groups or to other functional groups could take place. After 8 hours more oxidation occurs to form more phenolic and carboxylic groups, but the rate of increase in carboxylic groups decreases with oxidation time.

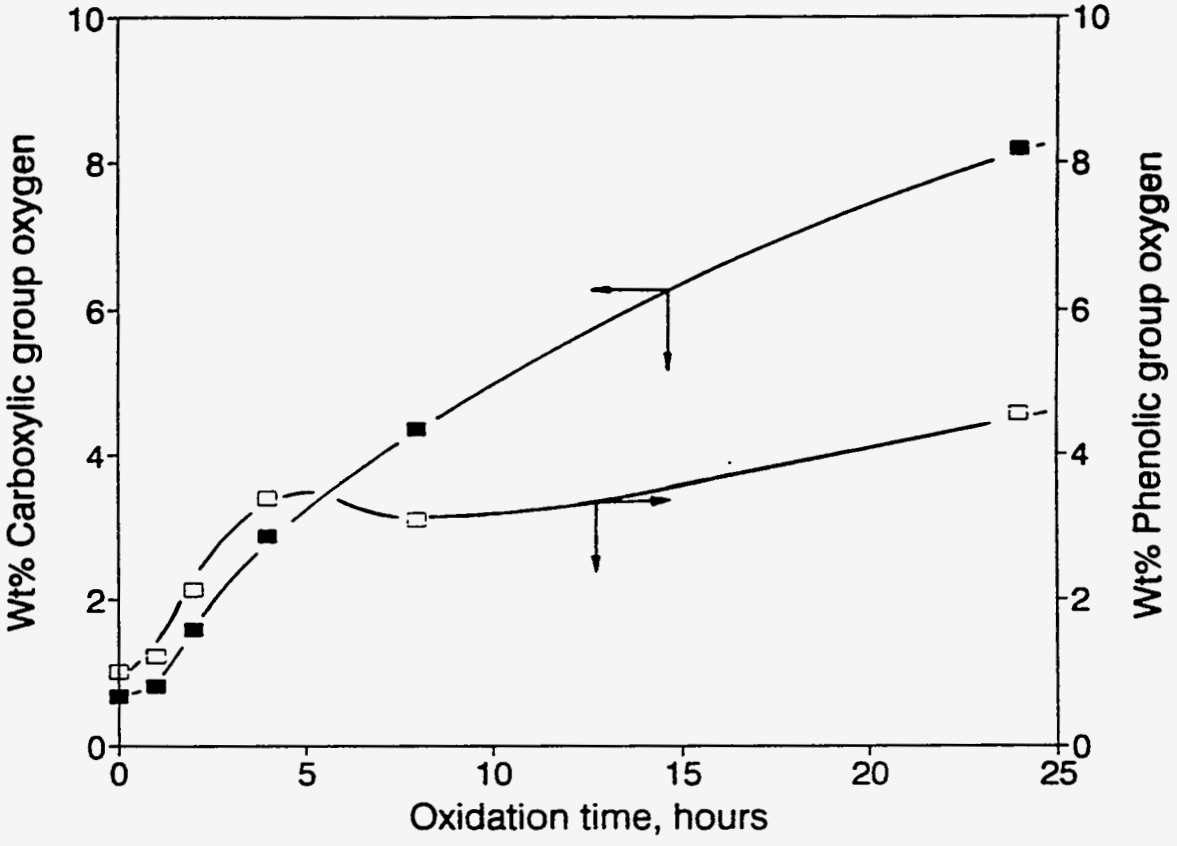

Figure 6. Effect of oxidation time on weight percent oxygen in the form of carboxylic and phenolic groups in Upper Freeport coal oxidized at 230°C.

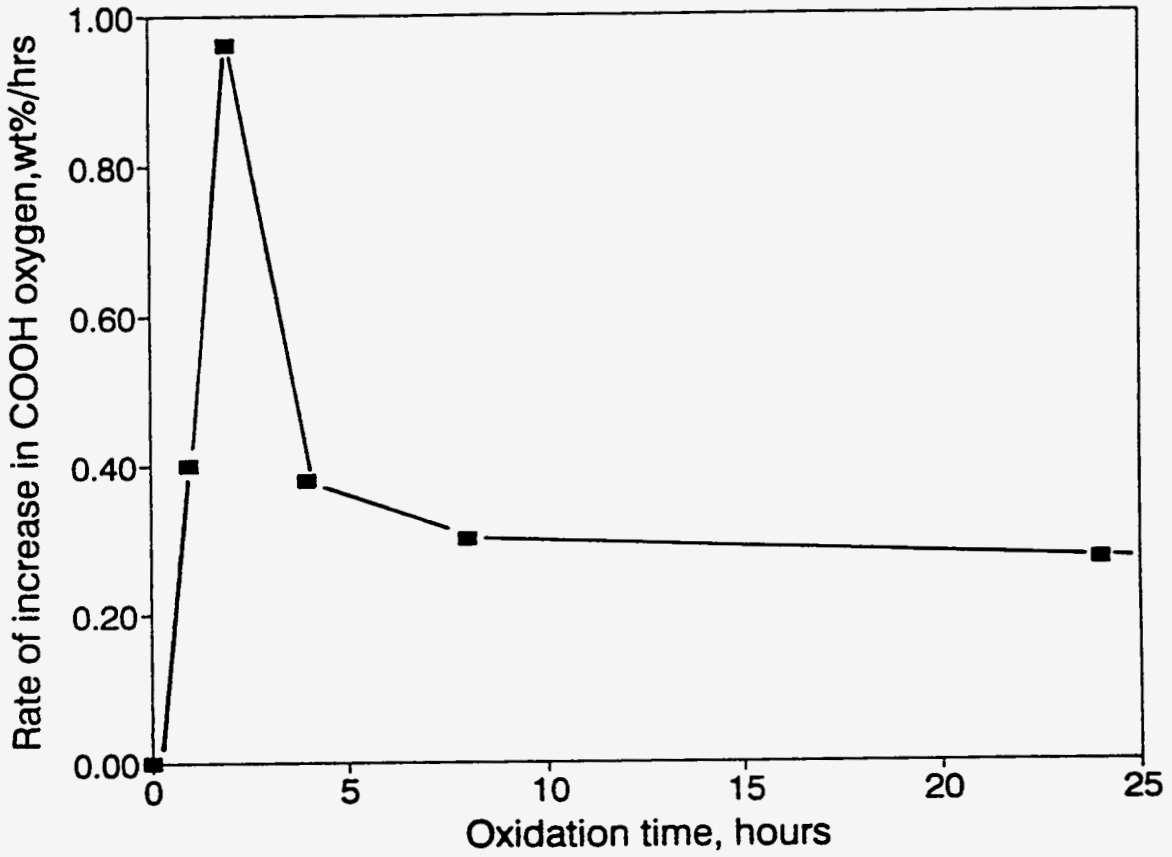

Figure 7. Rate of increase in weight percent oxygen in the form of carboxylic group in Upper Freeport coal oxidized at 230°C.

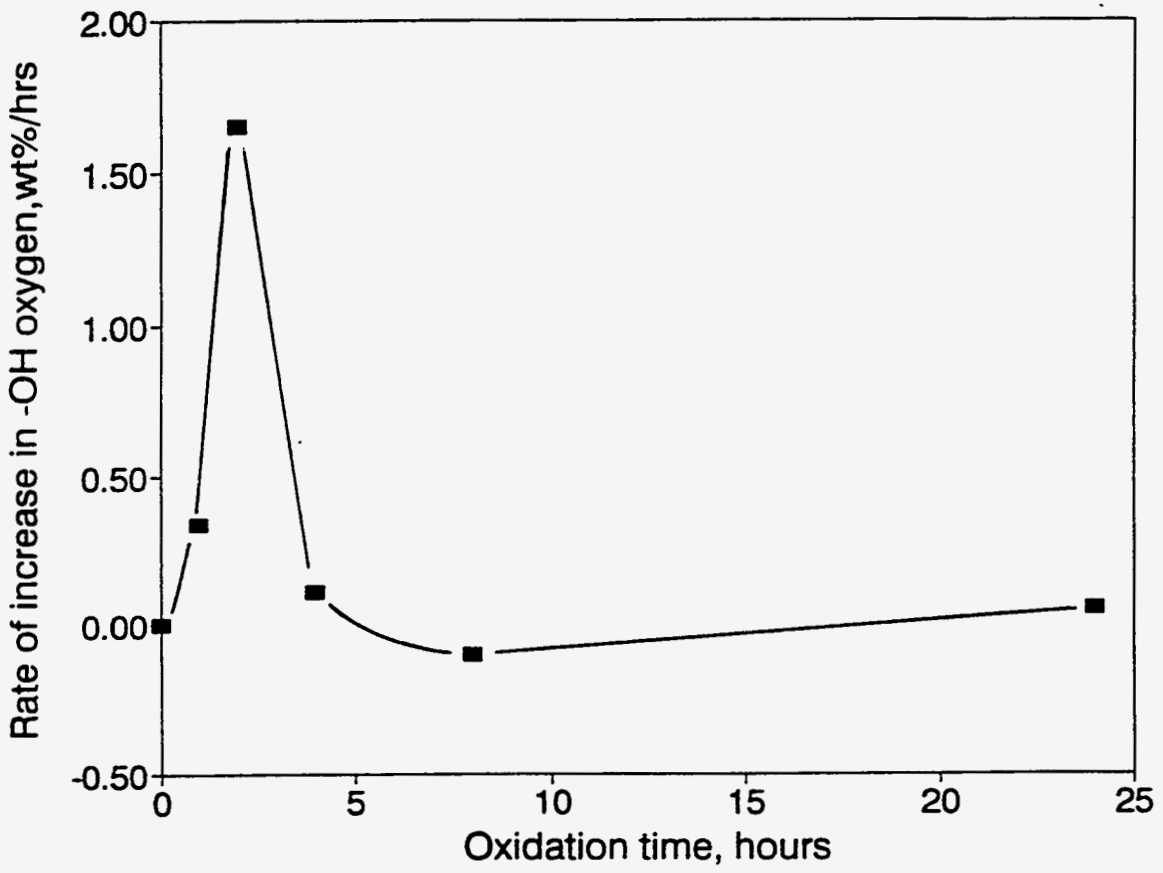

Figure 8. Rate of increase in weight percent oxygen in the form of phenolic group in Upper Freeport coal oxidized at 230°C.

A.1.2 Film Flotation Tests

The wettability of as-received coal, and samples subjected to various degree of thermal oxidation for 24 hours was assessed by film flotation,[135-139] using solutions with surface tensions between that of distilled water (72.8 mN/m) and pure methanol (22.5mN/m). Figure 9 shows the film flotation partition curves of raw coal and coal oxidized at different temperatures and Figure 10 shows the mean critical surface tensions derived from these curves. It is clear that there is a distribution in the wettability of coal particles. For the sample oxidized at 230°C, the mean critical surface tension was obtained by extrapolation, and hence is only approximate. The critical surface tension increased dramatically with increasing oxidation temperature, corresponding to a decrease in the hydrophobicity of the coal samples with oxidation and loss of volatiles and therefore less coal would be floated during cleaning with increasing extent of oxidation. These results are similar to those observed previously.[96,127,129] Figure 11 indicates that at 230°C, the partition curves shifted to higher surface tension values with increasing oxidation times as compared with that of as-received coal particles. Figure 12 shows that at 230°C there is a rapid increase in the mean critical surface tension for oxidation times of less than 5 hours. After 5 hours, the mean critical surface tension appears to increase more slowly, although there is less certainty in these values, since they are extrapolated; it would be expected that the surface tension would reach a maximum value, corresponding to complete surface oxidation. Figure 13 shows that the mean critical surface tension of coal samples appears to be directly related to the total concentration of acidic functional group oxygen; these groups increase the hydrophilicity of the coal surface due to strong interaction with water molecules. The observed increases in hydrophilicity could also be due to evolution of volatile matter during oxidation. Figure 13 also indicates that complete external surface oxidation has not been achieved, even

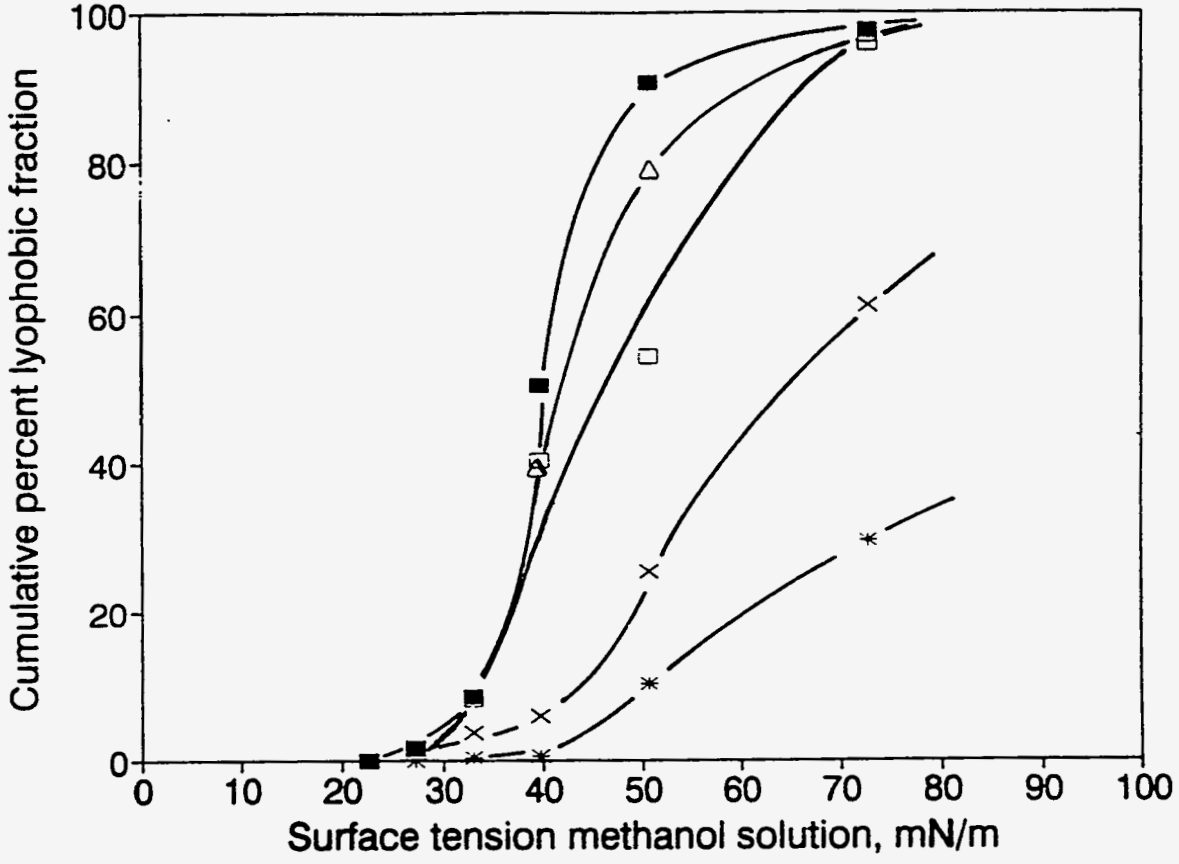

Figure 9. Film flotation partition curves of as-received Upper Freeport coal and oxidized for 24 hours. ■:as-received; Δ: oxidized at 100°C; ❑: oxidized at 150°C; ×: oxidized at 200°C; *: oxidized at 230°C.

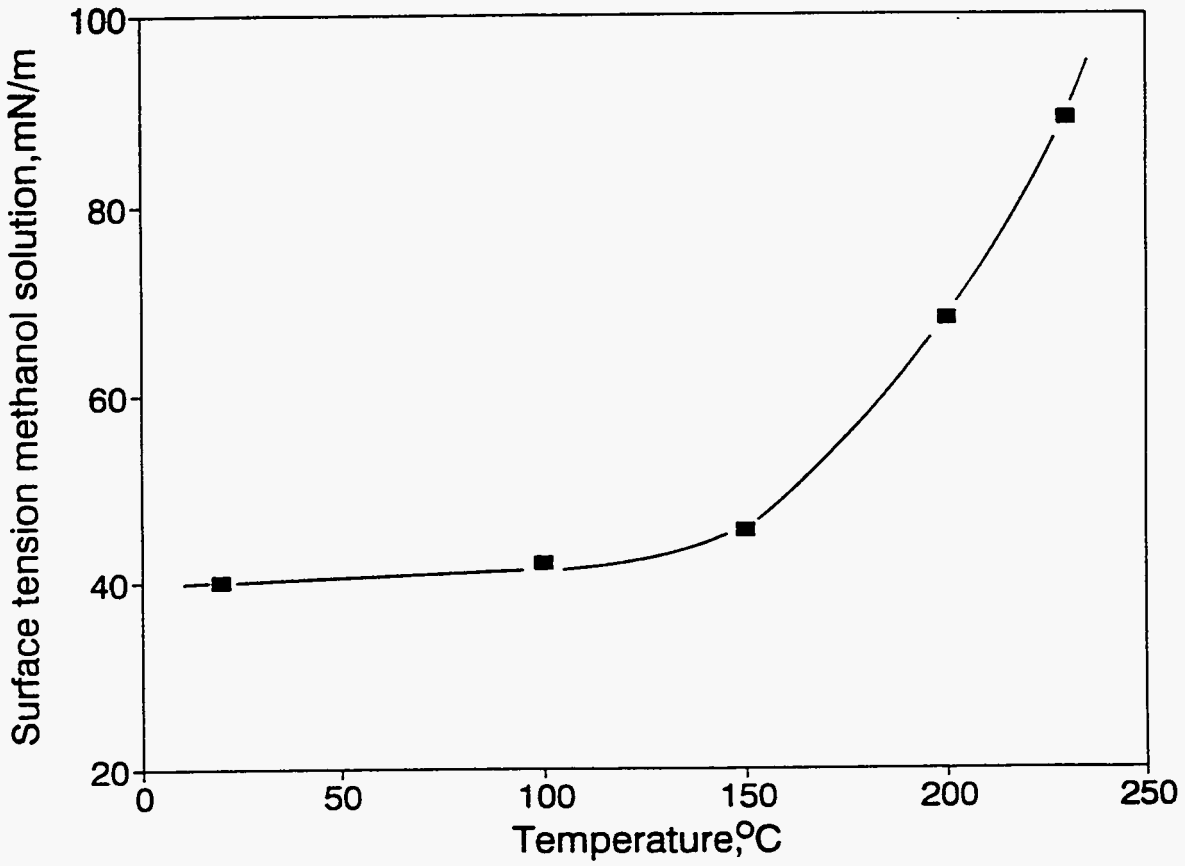

Figure 10. Mean critical surface tension of as-received and oxidized Upper Freeport coal for 24 hours as a function of oxidation temperature.

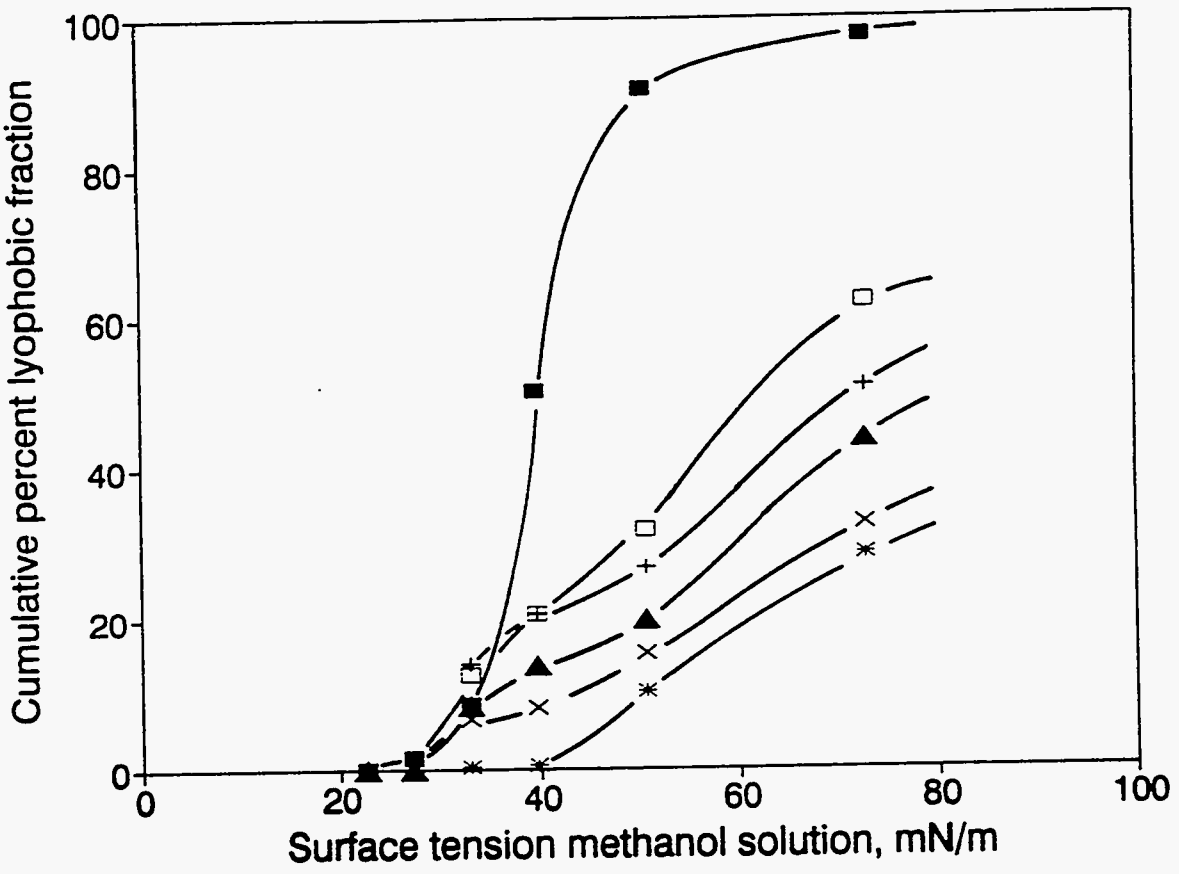

Figure 11. Film flotation partition curves of Upper Freeport coal oxidized at 230°C for different time periods: ■:0 hour; ❑:1 hour; +:2 hours; ▲:4 hours; ×:8 hours; *: 24 hours.

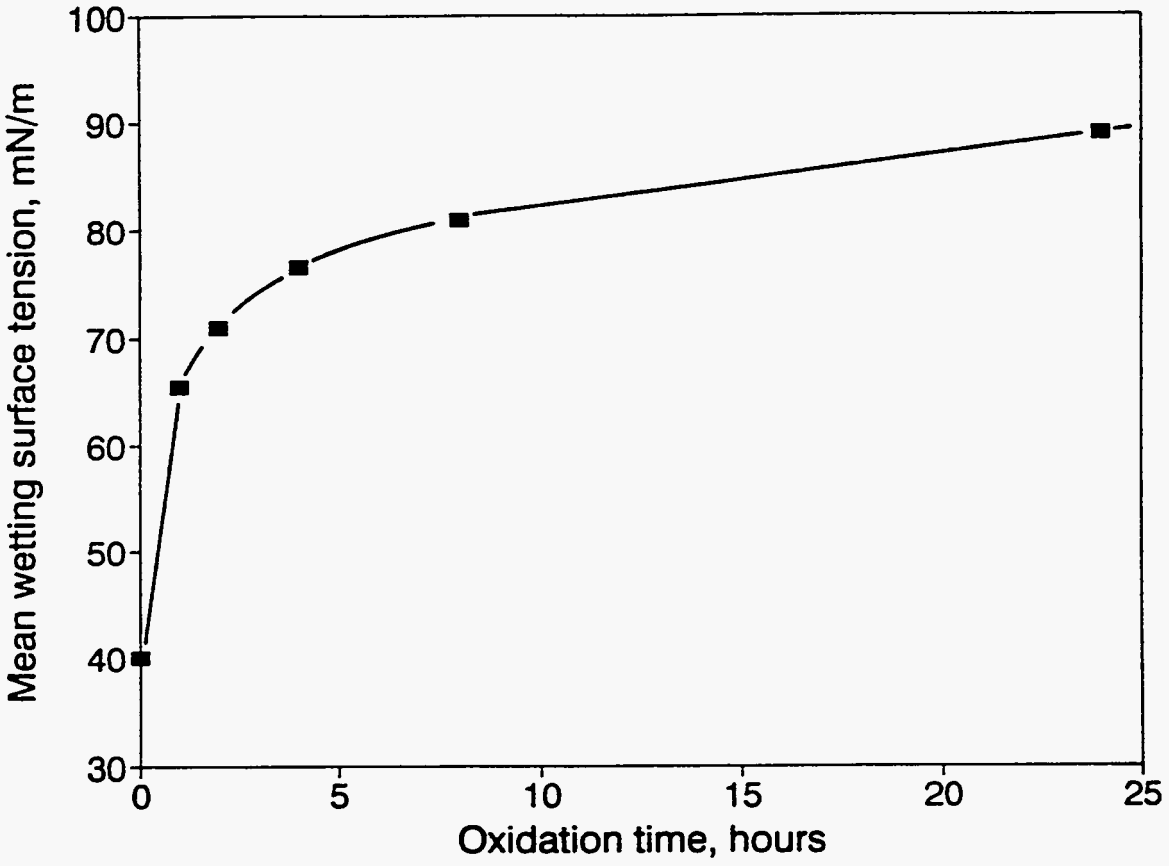

Figure 12. Mean critical surface tension versus oxidation time of as-received Upper Freeport coal and oxidized at 230°C.

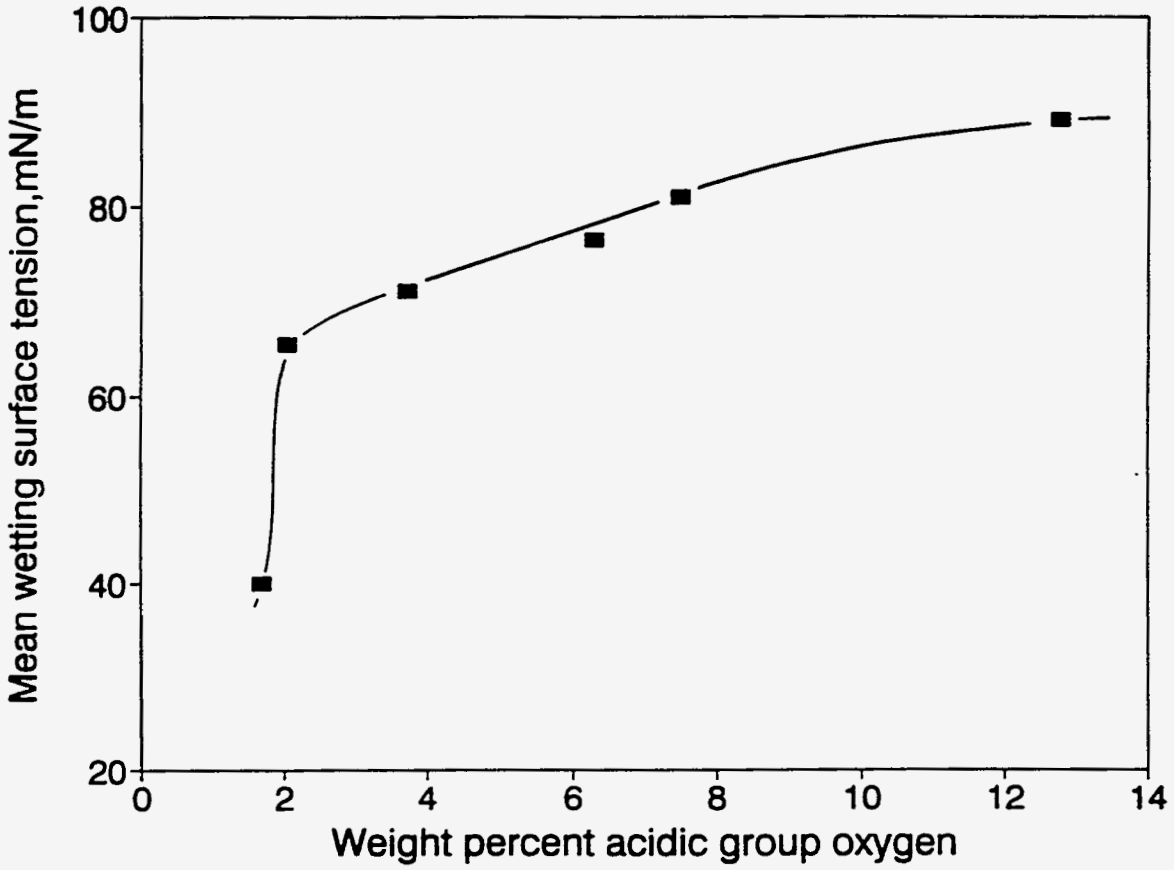

Figure 13. Mean critical surface tension versus weight percent acidic group oxygen in as-received Upper Freeport coal and oxidized at 230°C for 1,2,4,8,and 24 hours.

after twenty four hours at 230°C as indicated by the slow decrease in the slope of the curve.

For low temperature oxidation, a slight decrease in the hydrophobicity of the coal samples was observed, but this effect is moderate. The results are consistent with the increase in total acid oxygen percentage (discussed later).

A.1.3 Electrokinetic Studies

The zeta potentials of the as-received Upper Freeport coal and of the samples oxidized at different temperatures were determined as a function of pH in 0.002 M $NaNO_3$ solution after conditioning for 16 hours. Triplicate measurements were made for each sample and the results reported correspond to the average of three measurements versus the final pH after conditioning.

Figure 14 shows that increasing the oxidation temperature decreased the zeta potential in acidic and slightly alkaline solutions. For coal oxidized at 150°C for 24 hours, the PZR dropped from its original value of pH 4.8 to about pH 2.8. Samples oxidized at higher temperatures were negatively charged at all pH values tested. This is attributed to the formation on oxidation of acidic surface functional groups that are dissociated even at low pH. The results are in agreement with the findings of other authors.[116,127] Although the origins of coals are very different, the PZR value of the as received coal is in agreement with those of bituminous coals shown in Table 3.

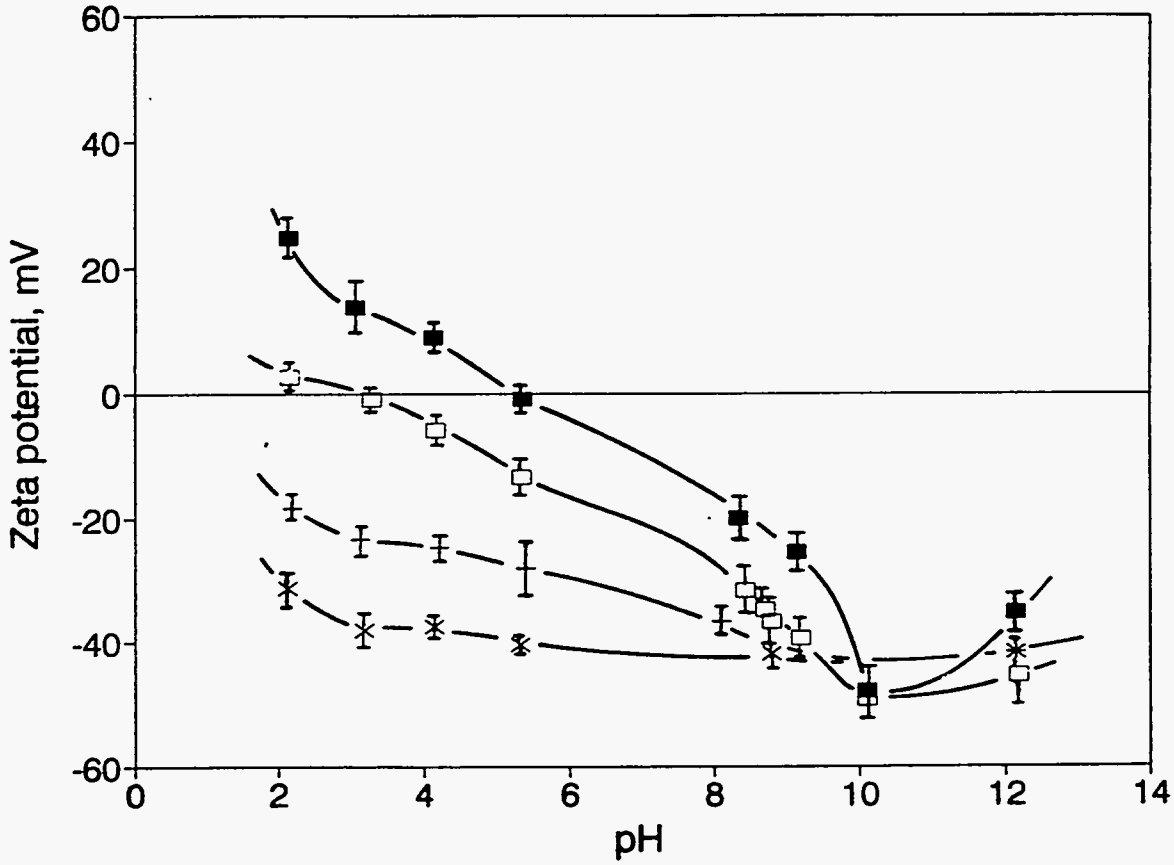

Figure 14. Effect of oxidation on the zeta potential of Upper Freeport coal (-400 mesh) in 0.002M $NaNO_3$ solution as a function of pH: ■:as-received; ❑:oxidized at 150°C; +:oxidized at 200°C; ×:oxidized at 230°C.

A.1.4 Humic Acid Extraction Test

Humic acids have been found to form by thermal oxidation of coal.[79,80,183-185] Humic acids are a complex mixture of highly functionalized macromolecules having a moderately high aromatic carbon content (65-75%), acidic functional groups (for example, phenolic and carboxylic) and average molecular weights between 300,000 and 50,000.[185] These acids are highly soluble in alkaline solutions.

During electrokinetic experimentation at pH 12 of coal samples that had been oxidized at 200 and 230°C, the pulp acquired an intense brown color, attributed to the dissolution of humic acids. Dissolution and readsorption of humic acids might also be responsible for the fact that the zeta potential of these samples remained constant in the alkaline range, whereas that of the less oxidized samples continued to become more negative. However, at pH greater than 10 there is possible a combined effect of dissociation of humic acids and adsorption of sodium ions. In order to study the effect of humic acids on the wetting behavior of coal, humic acid was extracted from 0.3 g of Upper Freeport coal, that had been previously oxidized at 230°C for 24 hours, by shaking with 500 ml of 0.1 M NaOH solution in an inert atmosphere at room temperature for 16 hours, decanting and filtering. The filtrate was then acidified with 0.1 M HCl solution to pH 2.0. After shaking for 16 hours, the humic acid precipitate was separated by centrifuging and filtering. This precipitate was washed repeatedly with distilled water to remove any HCl or NaCl, until the filtrate was nearly colorless. The removal of HCl and NaCl was also verified by additions of a few drops of silver nitrate to the filtrate until no formation of a AgCl precipitate was observed. Then the humic acid was dried overnight at room temperature in a dessicator under vacuum, to minimize oxidation.

Humic acid formed on the coal surface during oxidation makes the coal surface more hydrophilic. Figure 15 shows the film flotation partition curves of as-received coal,

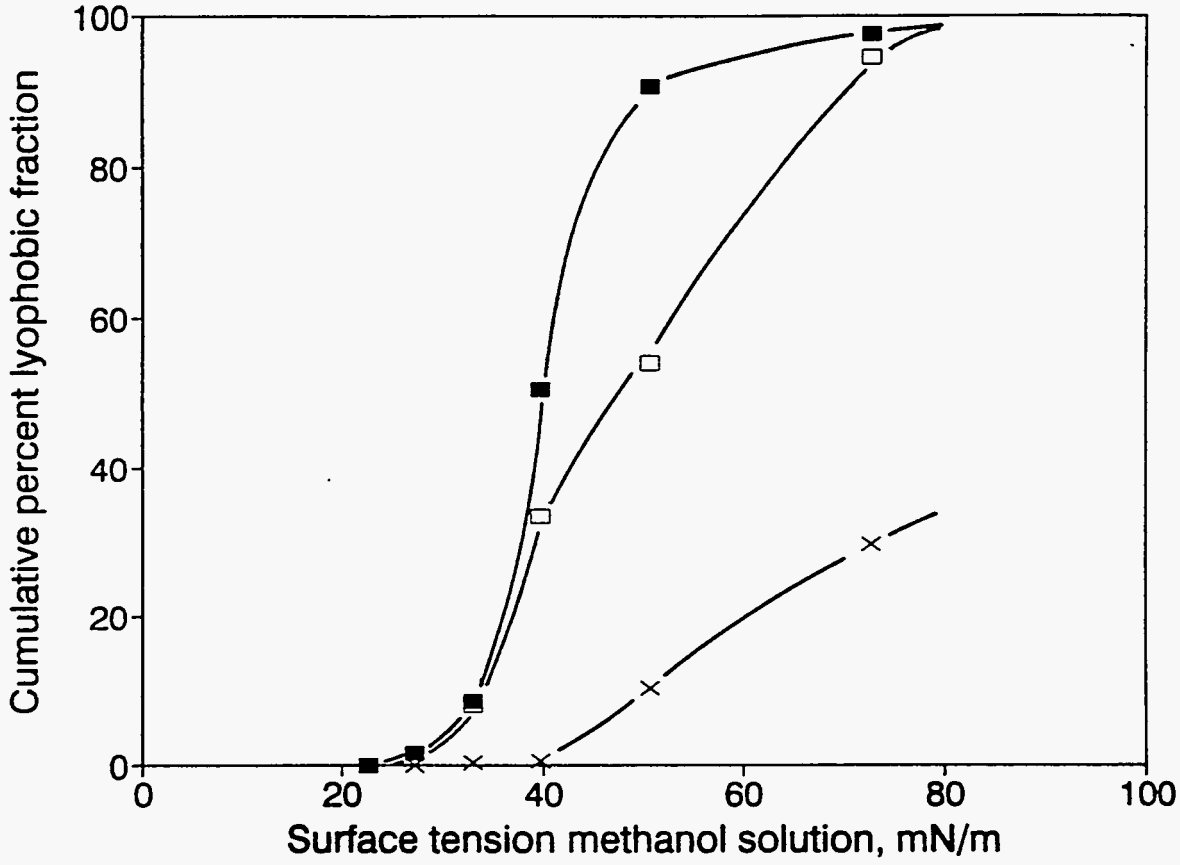

Figure 15. Film flotation partition curves of Upper Freeport coal: ■: as received; ×: oxidized at 230°C; ❑: after humic acid extraction.

coal oxidized at 230°C and coal oxidized at 230°C after extraction of humic acids. The removal of the hydrophilic humic acids clearly restores most of the intrinsic wettability of the coal.

The generation of humic acid by oxidation is the final result of a series of chemical reactions. The chemical modifications of the coal structure that are responsible for conversion to humic acids are in general consistent with a preferential oxidation of the aliphatic structure of coal, leading to a more aromatic product and concomitant formation of various oxygenated functional groups that make the coal surface more hydrophilic.[84,185,186]

A.1.5 Scanning Electron Microscopy (SEM) and Energy Dispersive X-ray (EDX) analysis

SEM/EDX analysis was done on Upper Freeport coal to study the morphology and the elemental composition of raw coal, oxidized coal, oxidized coal after extraction of humic acid and humic acids. Microscopy alone yielded information of limited use.

A small sample of -75 +63 μm particles of each coal was used for analysis. For each coal or humic acid sample, one particle was selected for EDX analysis. EDX analysis gives only qualitative information for elements of atomic number 6 and above. Figure 16 shows the energy dispersive spectrum of as-received coal. C, O, Al, Si and S are clearly visible. The carbon, oxygen and sulfur are from the coal; and the aluminum and silicon are from the ash minerals, although the latter were not visible under microscopy. Copper and zinc were from the SEM sample holder. Any iron was below the detection limit of 1.0 %wt. Figure 17 shows the energy dispersive spectrum of coal oxidized at 230°C for 24 hours. Comparing Figure 16 with Figure 17, there is a marked increase in the intensity of the oxygen peak, demonstrating the formation of oxygen containing functional groups by

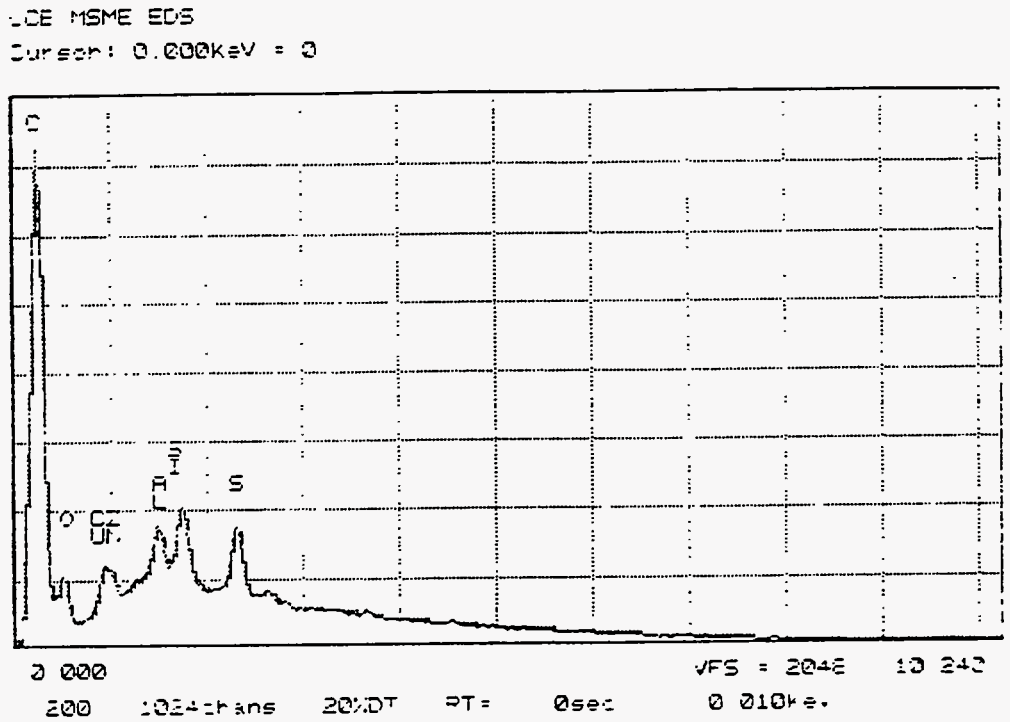

Figure 16. Energy dispersive spectrum of as-received Upper Freeport coal.

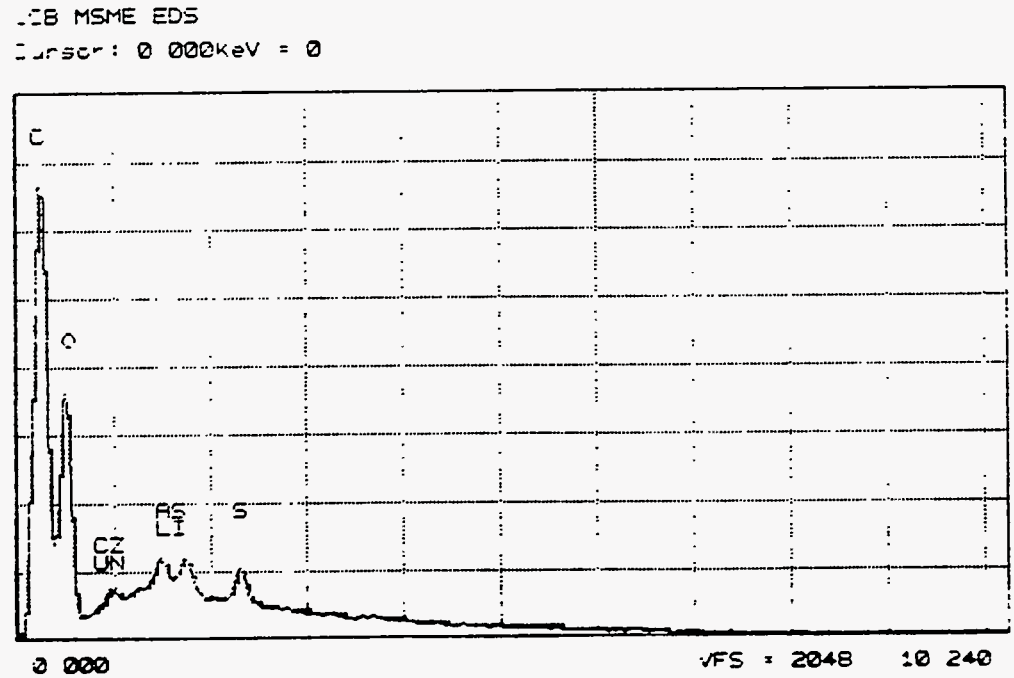

Figure 17. Energy dispersive spectrum of Upper Freeport coal, oxidized for 24 hours at 230°C

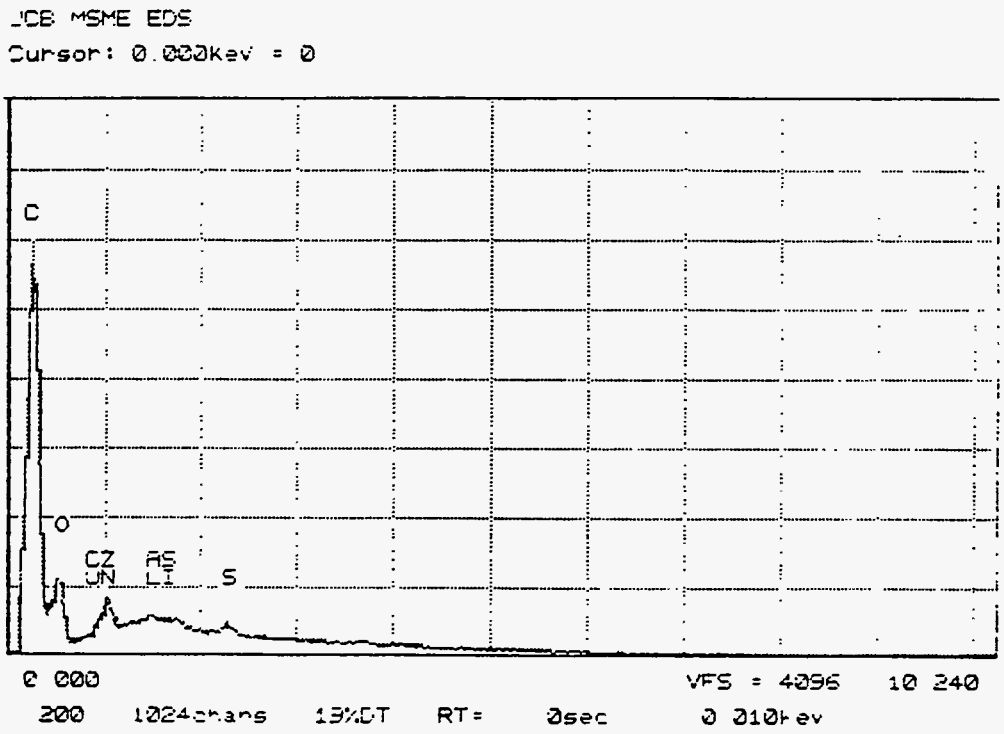

Figure 18. Energy dispersive spectrum of Upper Freeport coal, oxidized for 24 hours at 230°C, after extraction of humic acids.

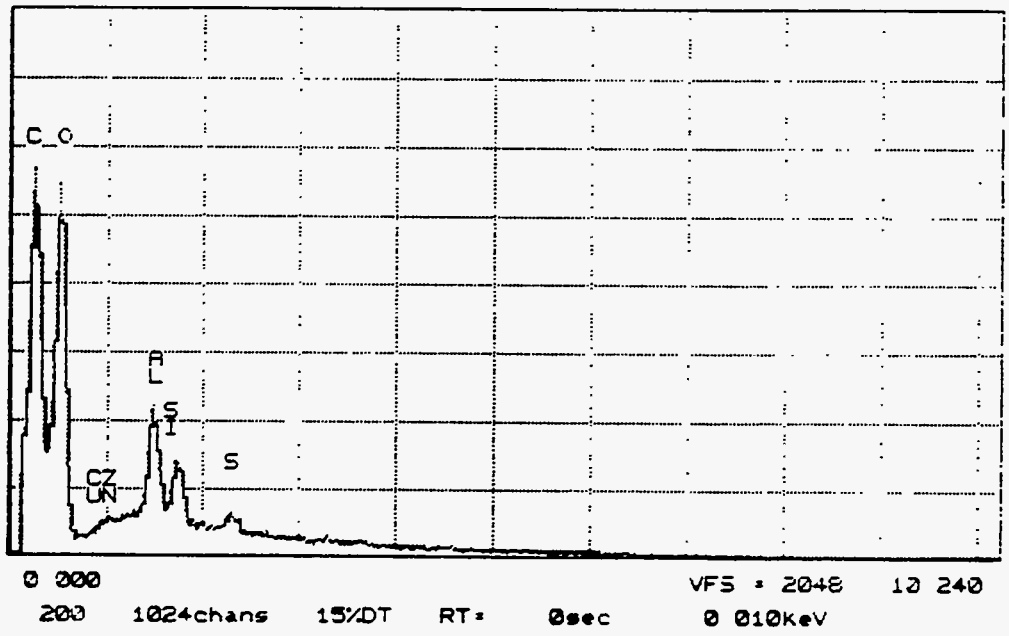

Figure 19. Energy dispersive spectrum of humic acid extracted from Upper Freeport coal, after oxidation for 24 hours at 230°C.

oxidation. Figure 18 shows the energy dispersive spectrum of coal oxidized at 230°C for 24 hours after extraction of humic acids. The oxygen peak is dramatically lower than in Figure 17, due to the removal of carboxylate groups of the humic acids. This is consistent with the observation that the floatability of Upper Freeport coal was partially restored after remotion of humic acid (Figure 15). The energy dispersive spectrum of humic acid, shown in Figure 19, shows an oxygen peak that is very strong, comparable with the carbon peak, revealing the oxygen rich nature of humic acids. Comparing Figure 19 with Figure 18, there is a increase in the intensity of the aluminum and silicon peaks in the humic acid particles and a decrease of the respective peaks in the coal particles after extraction of humic acids. This could be due to the existence of organic-clay complexes in the as-received coal; these complexes show strong solubility in basic solutions[187] and were extracted simultaneously with humic acids.

A.1.6 Surface Area Measurements

The specific surface area of the as-received and oxidized coal samples was measured with a Micromeritics Surface Area/Pore Volume Analyzer (Model 2100D) using carbon dioxide as an absorbent at room temperature. Figure 20 shows the data for Upper Freeport coal plotted by the Dubinin-Polanyi method; an excellent fit to a straight line was obtained. A surface area of 120.5 m^2/g was obtained for as received Upper Freeport coal. This surface area increased by about 54% after oxidation at 230°C, mainly due to the opening of pores by evolution of gaseous compounds on heating. However, this effect was not visually observed by SEM analysis, suggesting that the increase in surface area is mainly associated with opening of micropores.

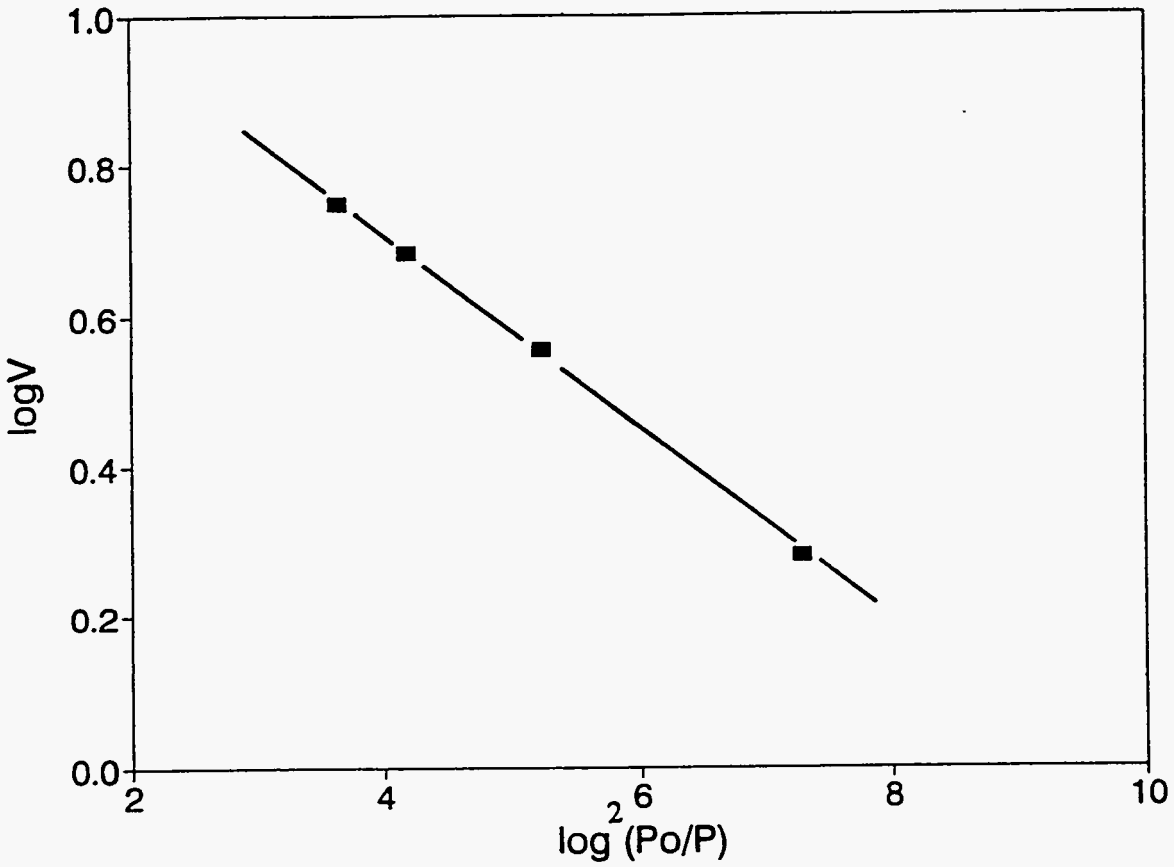

Figure 20. A Dubinin-Polanyi plot of as-received Upper Freeport coal as obtained by carbon dioxide adsorption at room temperature.

A.2 Low Temperature Oxidation of Upper Freeport Coal.

Upper Freeport coal samples were also oxidized in a convection oven at 95°C, or at room temperature (mean 21°C) for extensive time periods. The latter allows to simulate weathering conditions, which are not easy to control. Room temperature tests were done with uncontrolled (about 50-70%) humidity, dry (in a dessicator), or at 100% humidity (in a dessicator, with the desiccant replaced by water).

A.2.1 Acidic Group Analyses

Figure 21 shows that at 95°C there was rapid oxidation in the first few days, followed by steady, but much slower oxidation. At 21°C, there was relatively little oxidation when the samples were dry or under low humidity. After 20 days, oxidation under dry condition proceeded faster than oxidation under ambient conditions. At 100% humidity, oxidation appeared to proceed at steady, intermediate rate for the duration of the test and increased continously after 20 days. There are contradictory opinions in the literature in relation with the mechanisms involved[40,88-92], but, the results of the present study are in agreement with the observation of some authors.[88-91] As mentioned earlier, during adsorption of oxygen on solid surfaces ionic oxygen can be formed[103] and react with water to form hydroxyde ions and radicals that can participate in the formation of hydroperoxide compound and free radicals. Thus, water enhances oxidation of coal by promoting the formation of free radicals.

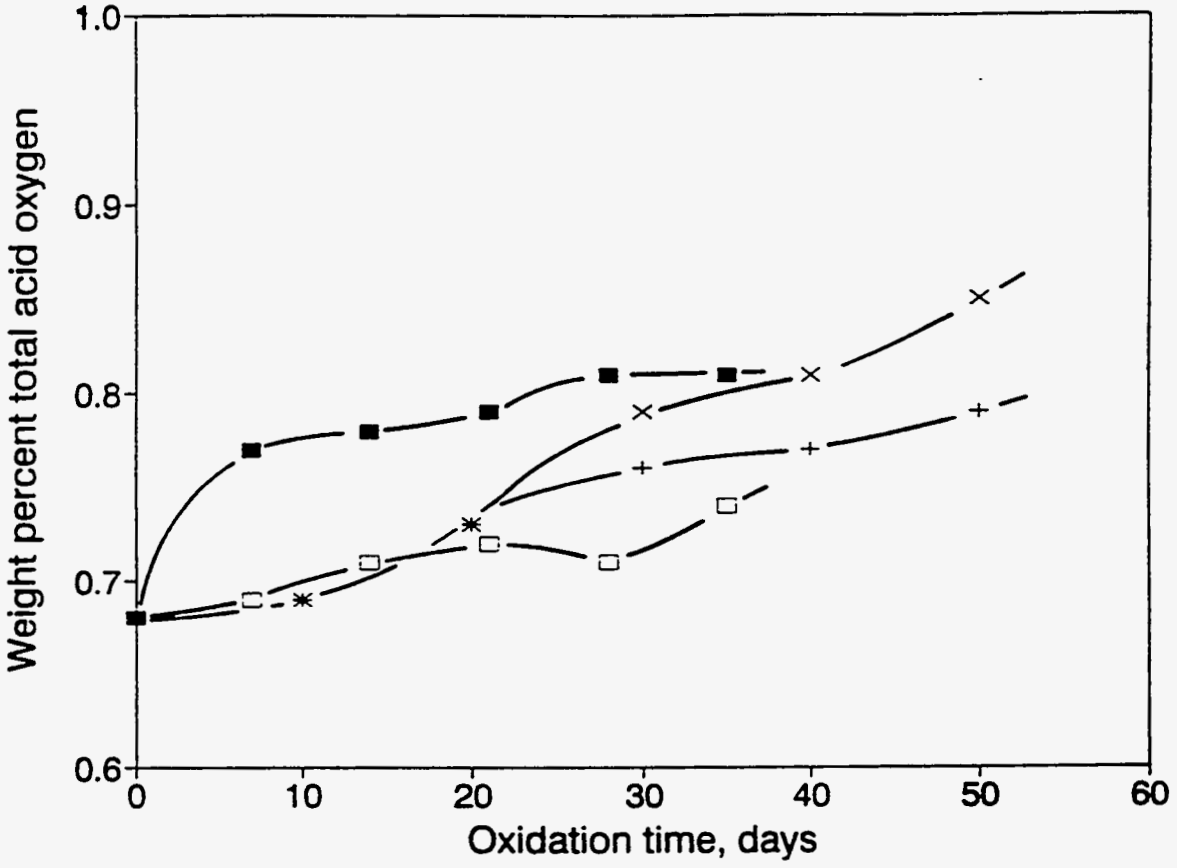

Figure 21. Effect of oxidation time on weight percent oxygen in the form of carboxylic groups on the surface of Upper Freeport coal oxidized under different humidity conditions: ■: oxidized at 95°C (low humidity); □: oxidized at 21°C (50-70% humidity); ×: oxidized at 21°C and 100% humidity; +:oxidized at 21°C and dry air.

A.2.2 Film Flotation Tests

Figure 22 shows the film flotation partition curves for coal oxidized under the conditions described above. The result are consistent with those in Figure 21; the increase in total acid oxygen produces a slight decrease in the hydrophobicity of the coal samples, but this effect is moderate.

A.3 Wet Chemical Oxidation of Upper Freeport Coal

In general, wet oxidation of coal studies has been studied to investigate the possibility of chemically removing sulfur from coal.[40-46,93-96] In this study, wet oxidation tests were done on Upper Freeport coal using different oxidizing agents to investigate the changes induced by oxidation on the surface properties of the coal. The ability of the different oxidizing agents to remove sulfur is also discussed.

A.3.1 Oxidation by Acidic Ferric Sulfate Solutions.

Twenty gram samples of Upper Freeport coal particles were oxidized for 24 hours at room temperature using 600 ml of 0.0094 M, 0.0187 M, and 0.0374 M $Fe_2(SO_4)_3$ solutions, all adjusted to pH 1.00±0.05. This correspond to 50%, 100%, and 200% of the stoichiometric Fe(III) requirement for oxidizing all the pyrite in each sample. In these experiments the ferric:ferrous ratio was determined from the solution potential, using calibration curves.[209] These calibration curves were prepared for different total iron concentrations, using ferric solutions standarized by atomic adsorption, and ferrous solutions standarized by potassium permanganate titration. The effect of the concentration of ferric sulfate on the solution potential during oxidation of Upper Freeport coal is shown in Figure 23. It is observed that in all three oxidation tests, the solution

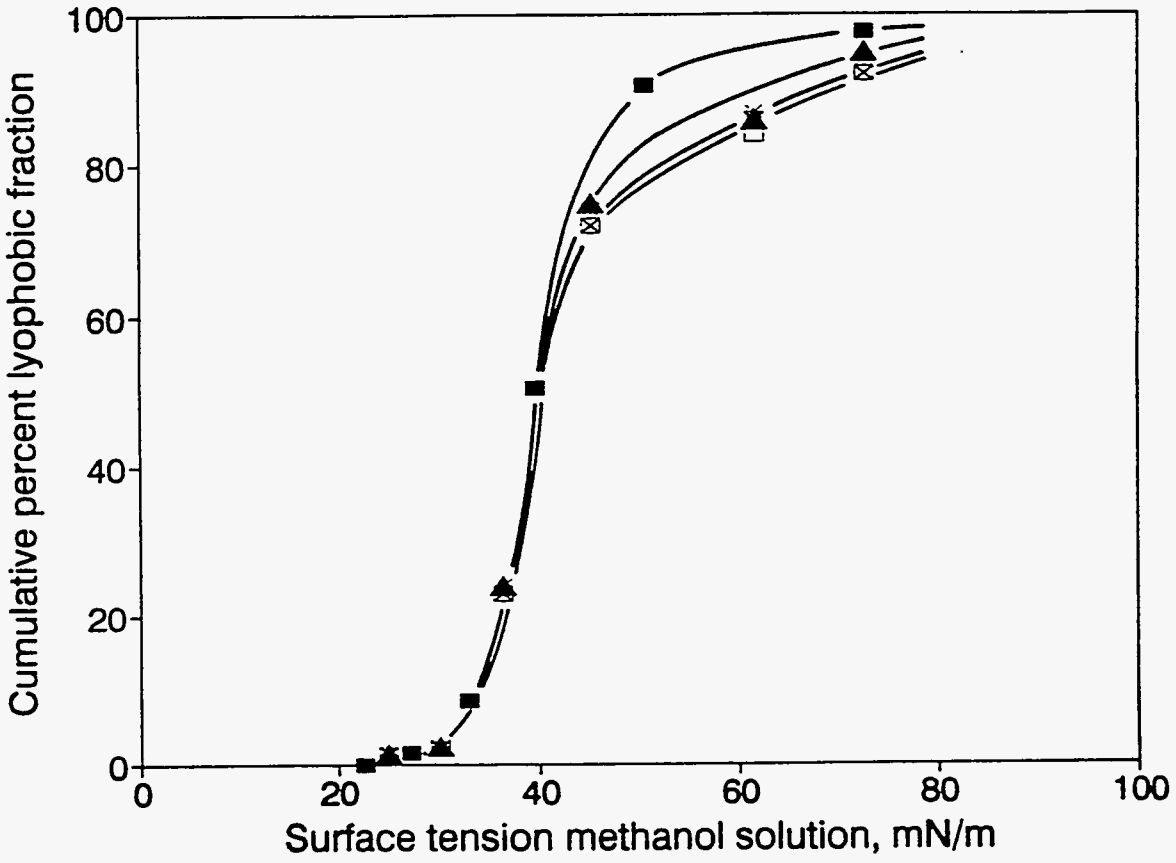

Figure 22. Film flotation partition curves of Upper Freeport coal samples oxidized at 95°C and 21°C for 35 days, oxidized at 21°C under dry and humid conditions for 50 days.: ■ as received; ▲:oxidized in dry air at 21°C; *:oxidized in ambient humid at 21°C (50-70% humidity); ×:oxidized at 95°C (low humidity); ❑:oxidized in saturated air at 21°C.

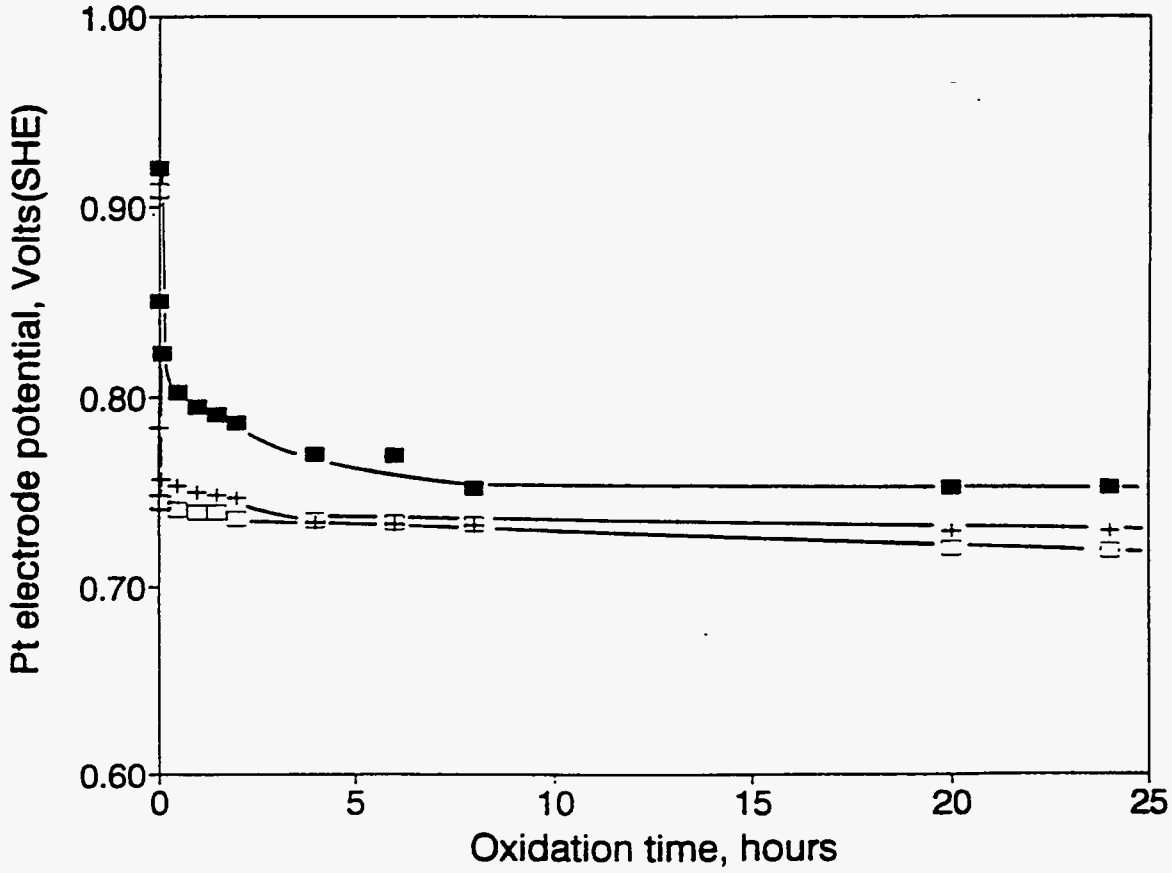

Figure 23. Effect of the ferric sulfate concentration on the solution potential during oxidation of 20 g of Upper Freeport coal at room temperature with 600 ml of solutions at pH 1.0 : ■: 0.0374M $Fe_2(SO_4)_3$; +: 0.0187M $Fe_2(SO_4)_3$; ❑: 0.0094M $Fe_2(SO_4)_3$.

potential, which in this medium reflects the ferric:ferrous ratio, decreased rapidly during the first few minutes, then continued to decrease more slowly over the 24-hour test period. Figure 24 shows that the Fe(III) concentration decreased markedly in the first few minutes, then remained almost constant, whereas the ferrous concentration increased steadily over 24 hours (Figure 25), accounting for the observed decline in the solution potential. The initial decrease in Fe(III) led to an overall decrease in total dissolved iron, and hence cannot be due only to reduction to Fe(II). It is thought that the iron loss, which has also been observed in other tests, is due to chemisorption on oxidized surface functional groups, or precipitation of a hydrolyzed phase. This hypothesis has been has also been observed in other tests, is due to chemisorption on oxidized surface functional groups, or precipitation of a hydrolyzed phase. This hypothesis has been recently confirmed by Eligwe and Okolue,[114] who found that adsorption of iron on the coal surface takes place by ion-exchange mechanisms involving carboxylic and phenolic groups. They also reported precipitation of metal hydroxides.

A.3.2 Oxidation by Nitric Acid Solutions.

Twenty gram samples of Upper Freeport coal were oxidized for 24 hours at room temperature, using 600 ml of 0.10 M or 3.00 M HNO_3. The percentage of carboxylate oxygen generated by oxidation of Upper Freeport coal by nitric acid solutions is shown in Table 8. 0.1M HNO_3 gave a slight increase in the carboxylate oxygen content of the coal, whereas 3.0M HNO_3 gave an appreciable increase. These results only partially reflect the oxidation of coal, since oxidation could have generated other functional groups. Figure 26 shows the film flotation partition curves for coal samples oxidized by 0.1M and 3.0M HNO_3 solutions. As expected, the surface tensions shifted to higher values with increasing nitric acid concentration. Table 9 shows the mean critical surface tension after both treatments.

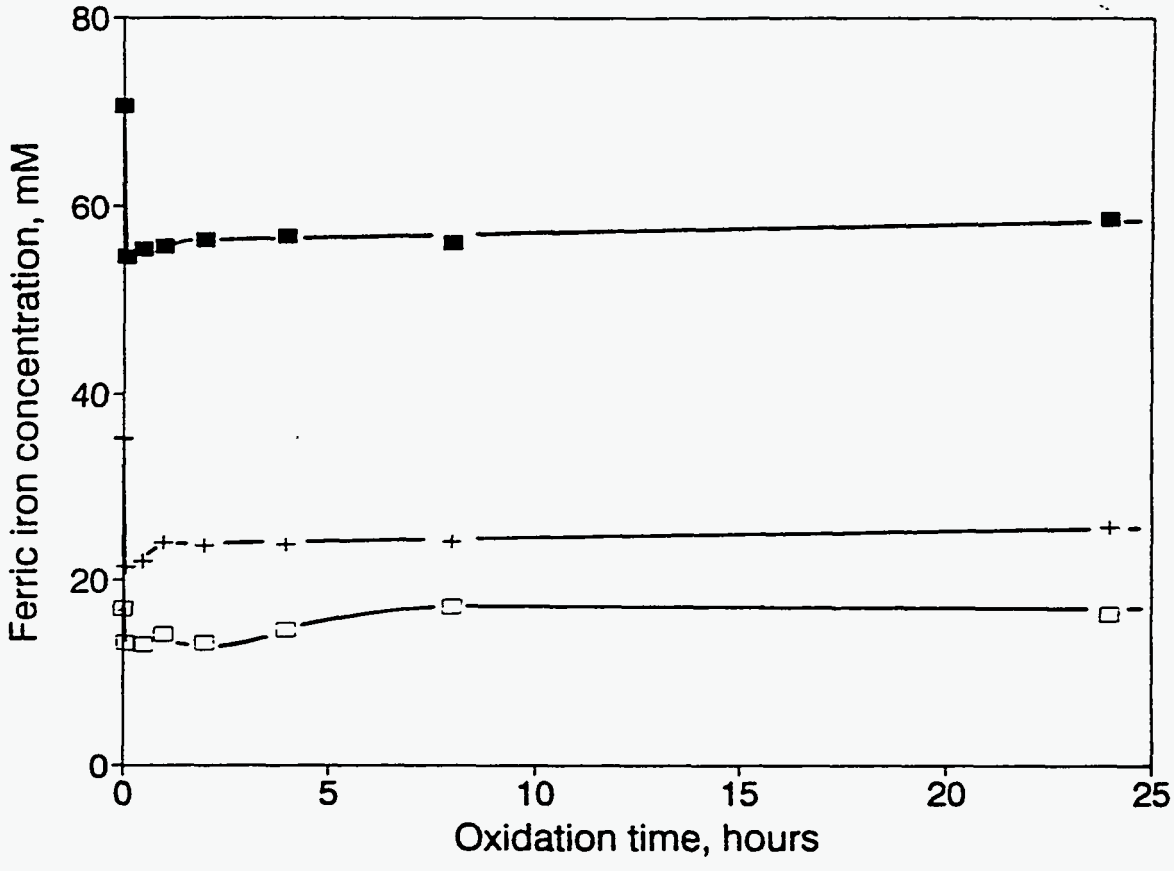

Figure 24. Concentration of ferric iron in solution as a function of time during oxidation of 20 g of Upper Freeport coal at room temperature with 600 ml of solutions at pH 1.0 :■: 0.0374M $Fe_2(SO_4)_3$; +: 0.0187M $Fe_2(SO_4)_3$; ❑: 0.0094M $Fe_2(SO_4)_3$.

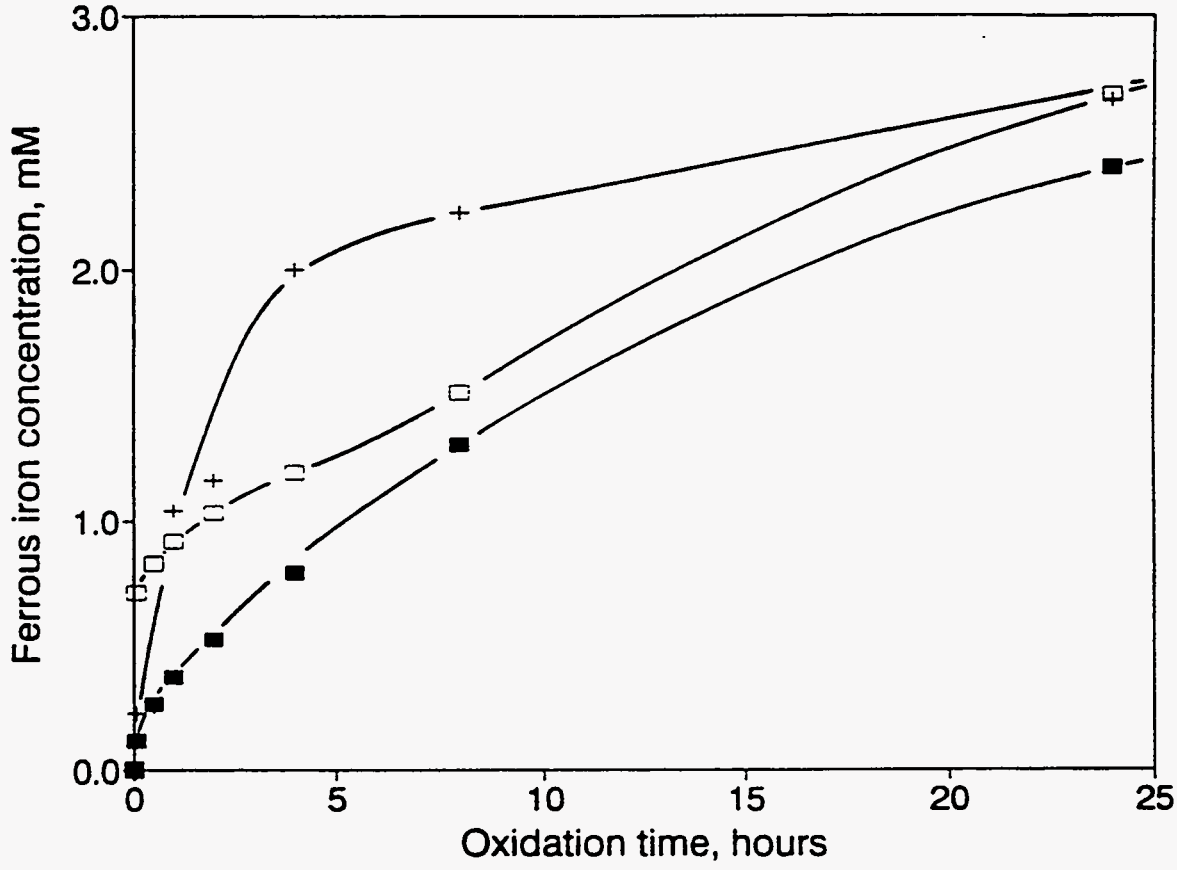

Figure 25. Concentration of ferrous iron in solution as a function of time during oxidation of 20 g of Upper Freeport coal at room temperature with 600 ml of solutions at pH 1.0 :■: 0.0374M $Fe_2(SO_4)_3$; +: 0.0187M $Fe_2(SO_4)_3$; ❑: 0.0094M $Fe_2(SO_4)_3$.

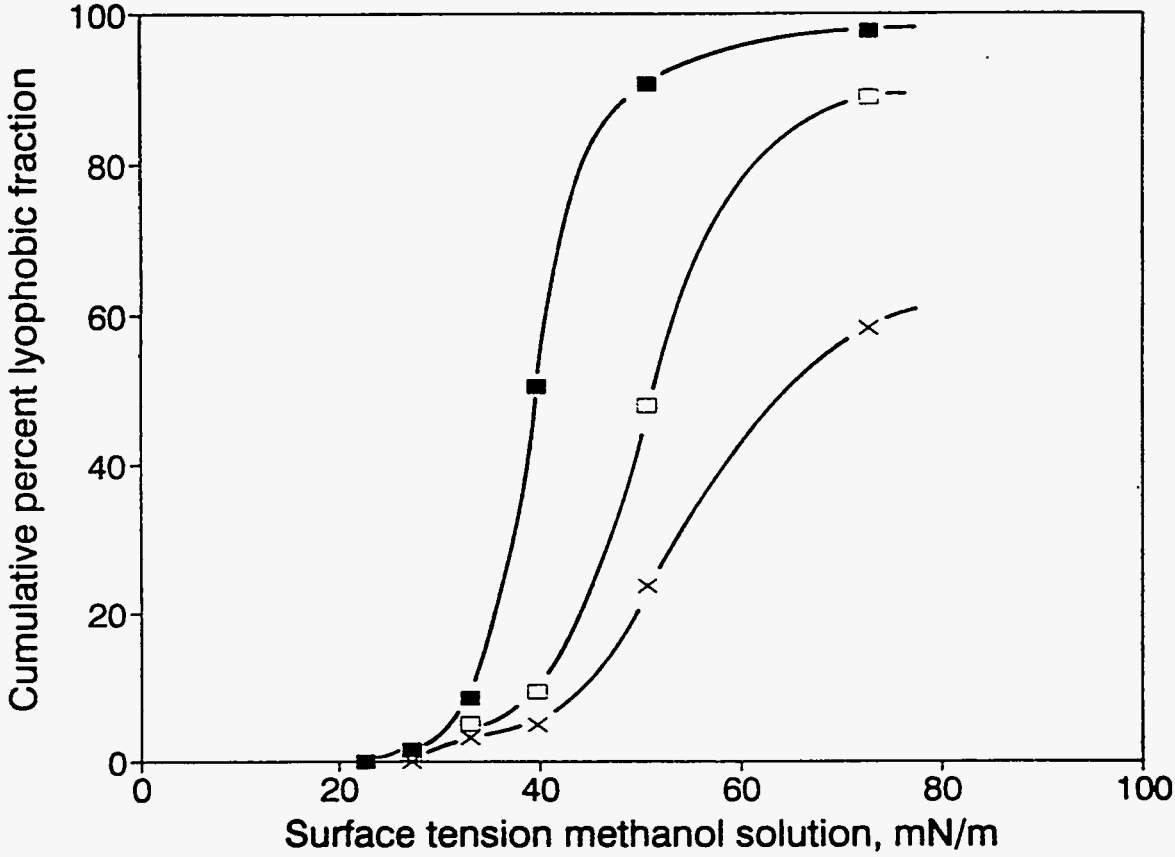

Figure 26. Film flotation partition curves of Upper Freeport coal oxidized by HNO_3 solutions for 24 hours: ■:as-received; ❑:oxidized with 0.1M HNO_3; ×:oxidized with 3.0M HNO_3.

Table 8. Weight percent carboxylate oxygen in Upper Freeport coal samples oxidized by nitric acid solutions

Coal Treatment	Weight % Carboxylate Oxygen
As-received coal	0.68
0.1M HNO_3, 24 hours	0.81
3.0M HNO_3, 24 hours	1.87

Table 9. Mean critical surface tension of coal samples oxidized by nitric acid.

Coal Treatment	Mean Critical Surface Tension, mN/m
As-received	40
0.1M HNO_3, 24 hours	51
3.0M HNO_3, 24 hours	65

Figure 27 shows the percentage of coal pyrite dissolved by HNO_3 as a function of time. At either 0.1 or 3.0M HNO_3 there was rapid initial oxidation; the former eventually oxidized 64% of all pyrite in the coal sample, whereas the latter had oxidized all pyrite within 5 hours. It is clear from the solution potentials in each case (Figure 28), that oxidation halted at the lower nitric acid concentration because of the low potential.

A.3.3 Oxidation by Hydrogen Peroxide Solutions.

Twenty gram samples of Upper Freeport coal were oxidized for 6 hours at room temperature, using 600 ml of 5.0%, 10% and 15% H_2O_2, all adjusted to pH 1.0 by using

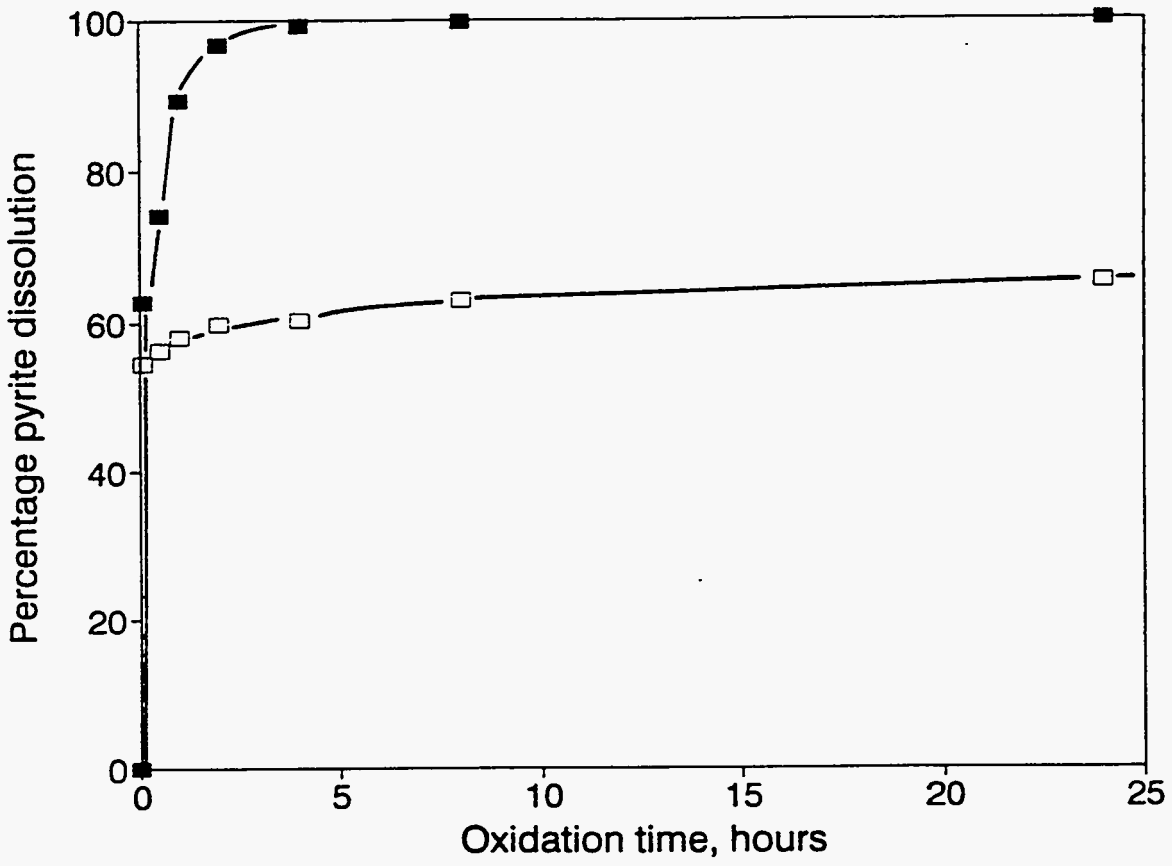

Figure 27. Percentage of Upper Freeport coal pyrite dissolved by: ❑ 0.1M HNO_3; ■: 3.0M HNO_3 at room temperature.

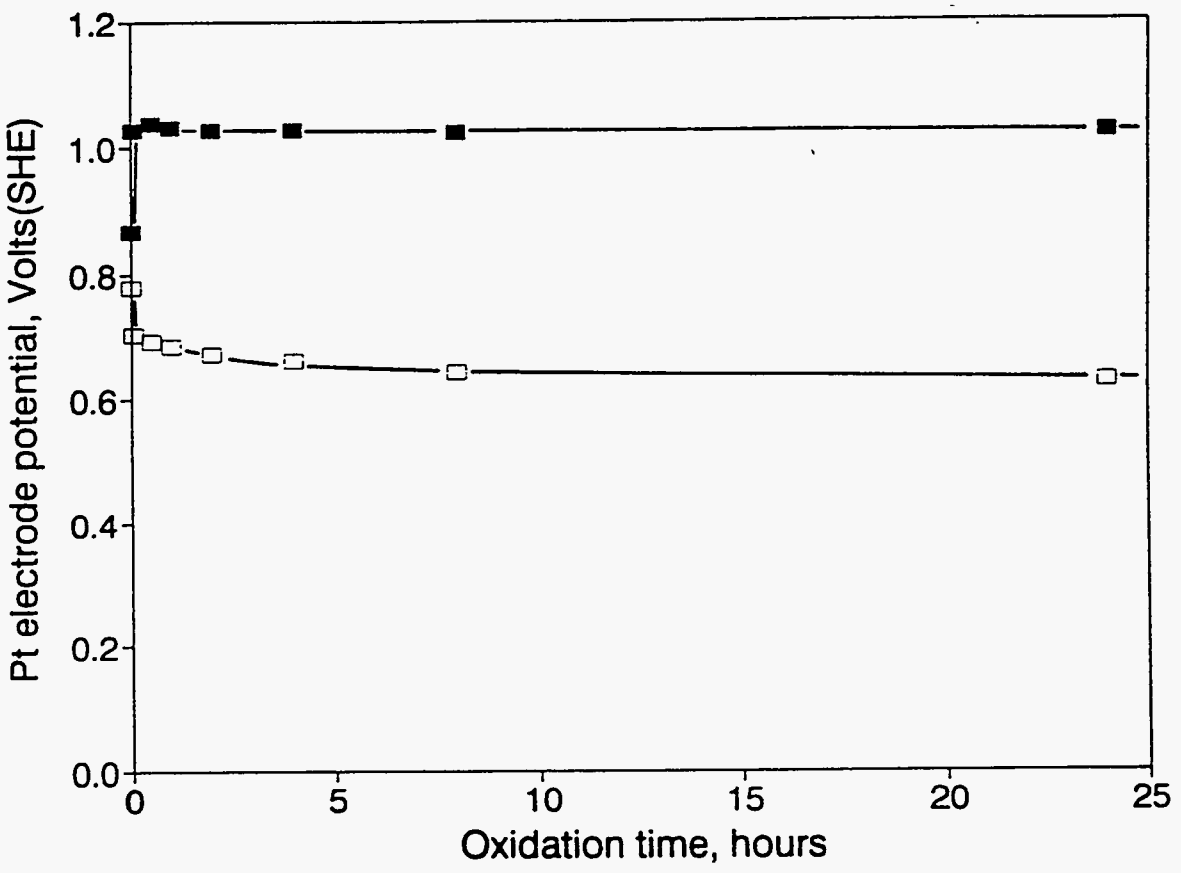

Figure 28. Solution potential as a function of time during oxidation of Upper Freeport coal by: ❑ 0.1M HNO_3; ■: 3.0M HNO_3 at room temperature.

sulfuric acid solutions. Figure 29 shows the percentage of coal pyrite dissolved by H_2O_2 as a function of time. About 88% and 92% of the coal pyrite was dissolved in 6 hours, using 10.0 and 15% H_2O_2 respectively, whereas 5.0% H_2O_2 dissolved only about 67% of the coal pyrite. These results show the suitability of hydrogen peroxide for removing inorganic sulfur from coal, as observed by different authors.[40-43] Figure 30 shows the variation of solution potential with time. It is clear that the potential increases only marginally with increasing H_2O_2 concentration. Table 10 shows the weight percent of carboxylate oxygen generated within 6 hours in each experiment. Comparing with Figure 21, it is clear that the peroxide dramatically accelerated oxidation; even 5% H_2O_2 gave more oxidation after 6 hours than occurred in 50 days at 21°C in humid air. This suggests that peroxide is, indeed a suitable oxidant for accelerated oxidation tests. The results in Figure 31 indicated that the use of high concentrations of peroxide strongly decreased the hydrophobicity of coal. This result are consistent with those obtained by Fuerstenau *et al.*[143,96] who found that oxidation of coal by using hydrogen peroxide markedly decreased the hydrophobicity of coals. The reactions involved in the chemical oxidation of coal by hydrogen peroxide are not well understood. Heard and Senfle[44] proposed a Fenton's reaction mechanism by which coal is oxidized on active centers to form phenol structures and carboxylic acids. Moreover, in the presence of pyrite, hydrogen peroxide dissociates to form OH· radicals that oxidize the coal surface.

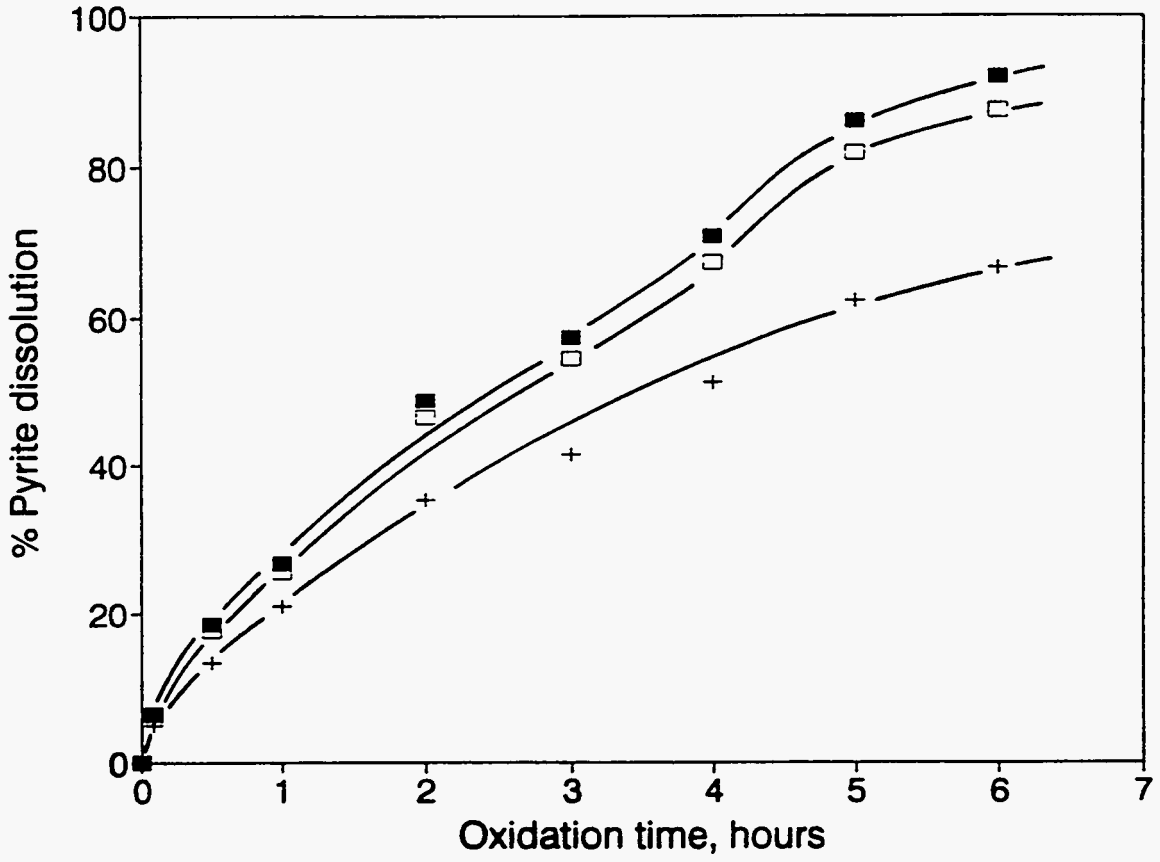

Figure 29. Percentage of Upper Freeport coal pyrite dissolved by: +: 5% H_2O_2; ❑: 10% H_2O_2; ■:15% H_2O_2 solutions.

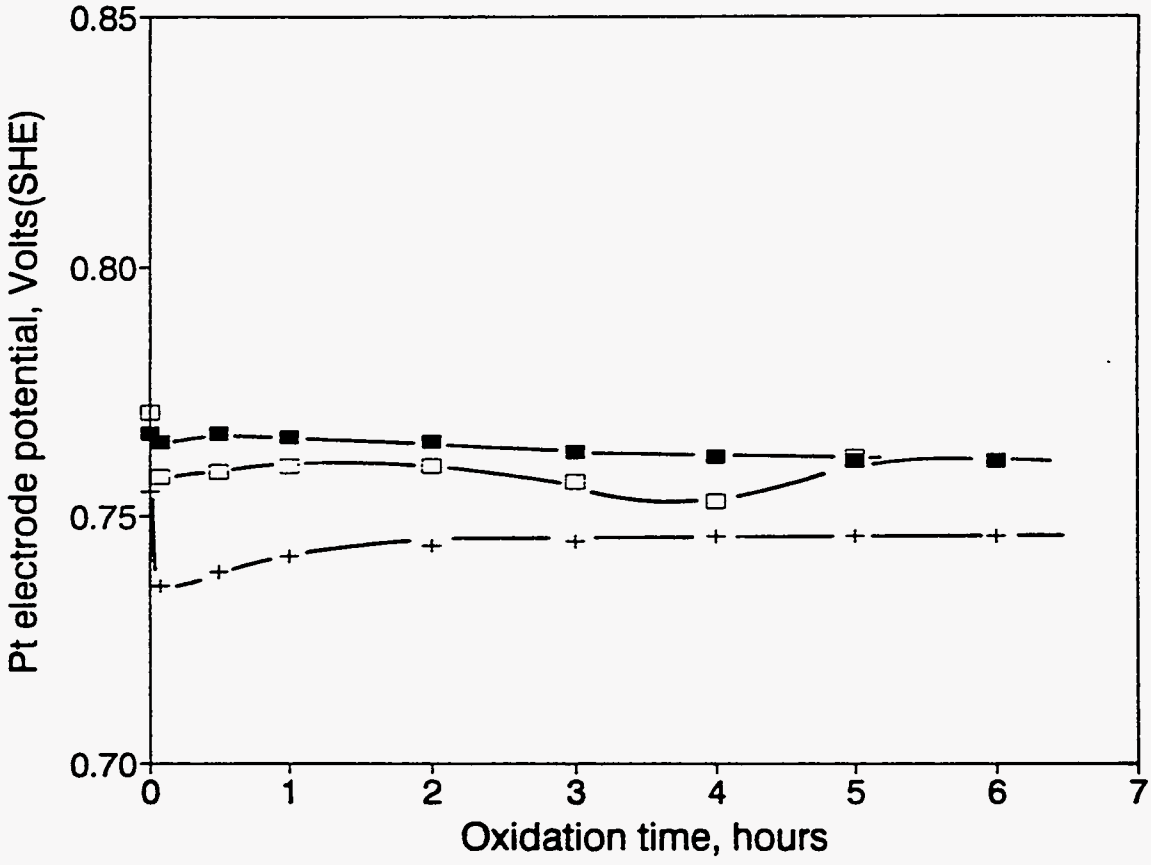

Figure 30. Solution potential as a function of time during oxidation of Upper Freeport coal by: +: 5% H_2O_2; ❑: 10% H_2O_2; ■:15% H_2O_2 solutions.

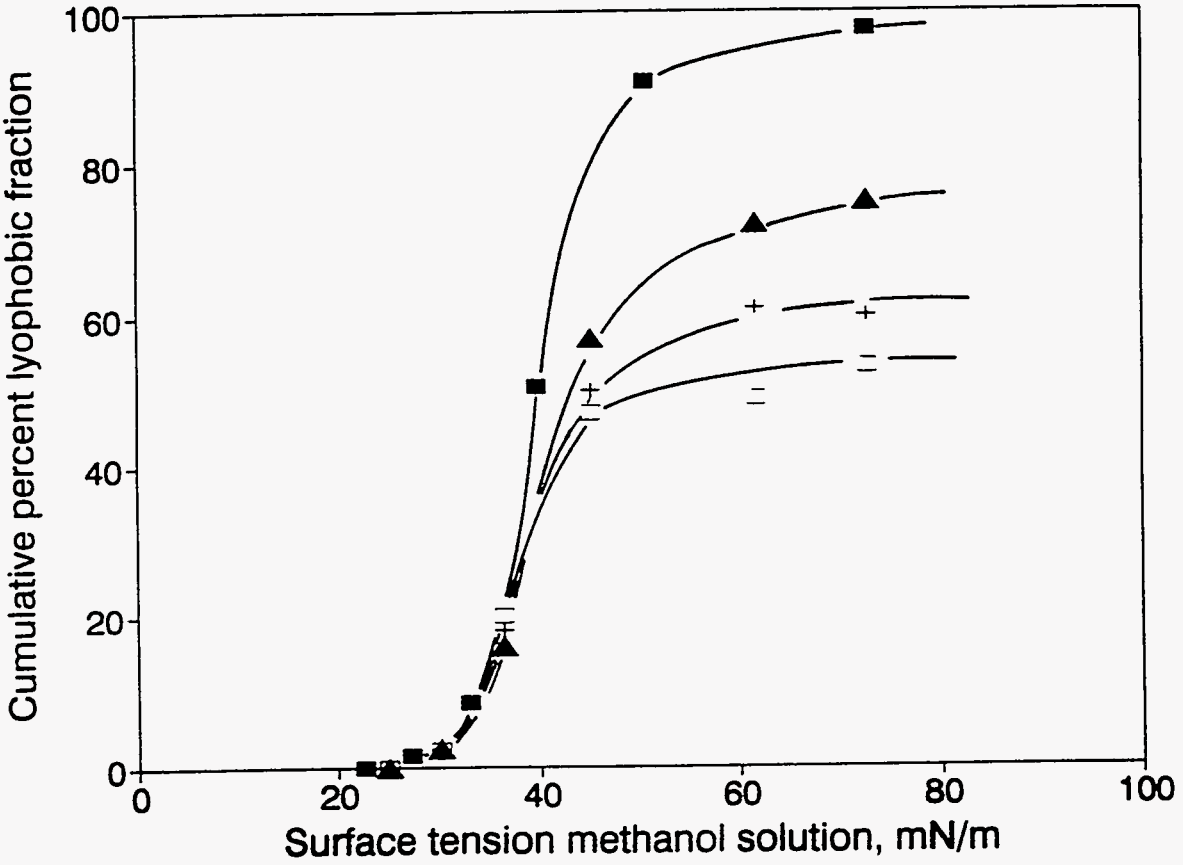

Figure 31 Film flotation partition curves of Upper Freeport coal oxidized by H_2O_2 solutions for 24 hours: ■: as-received; ▲: 5% H_2O_2; +: 10%H_2O_2 ; ❑: 15% H_2O_2.

Table 10. Weight percent carboxylate oxygen in Upper Freeport coal samples oxidized by by hydrogen peroxide solutions.

Coal Treatment	Weight % Carboxylate Oxygen
As-received	0.68
5.0% H_2O_2, 6 hrs	0.95
10.0% H_2O_2, 6 hrs	1.20
15.0% H_2O_2, 6 hrs	1.47

B. Oxidation Studies on Coals from Pennsylvania State Coal Bank

B.1. Dry Oxidation Studies

In the previous section, dry oxidation studies on Upper Freeport coal were performed at different temperatures ranging from 21 to 230°C. It was observed that severe oxidation of coal occurs at high temperature (230°C) in a relatively short time period. Oxidation tests were done on other coal samples at 230°C to minimize experimental time.

Coals with different rank and sulfur content obtained from Pennsylvania State Coal Bank were studied. Tables 5, 6, and 7 (Chapter IV) show the proximate, elemental and sulfur analysis of the coals studied. Five gram samples of each coal were oxidized in a convection oven at 230°C for 1, 2, 4, 8, and 24 hours. The extent of oxidation was assessed by analyzing the concentration of carboxylic and phenolic groups by ion-exchange methods, as described earlier.

Figure 32 shows the carboxylate and phenolic contents of three coals having different ranks: sub-bituminous (PSOC-1442), HVA bituminous (DECS-12) and anthracite (PSOC-1461) coals. The sub-bituminous coal experienced the greatest increase in total acidity (carboxylic plus phenolic) in 24 hours. With the exception of the anthracite coal, oxidation was fastest in the first few hours. The greater susceptibility to oxidation, of the sub-bituminous coal is consistent with the fact that lower rank coals are richer in aliphatic components that oxidize preferentially. The anthracite coal experienced negligible oxidation. Figure 33 shows the carboxylate and phenolic contents of LV bituminous (PSOC-1516), MV bituminous (PSOC-1527) and HVA bituminous (PSOC-1481) coals. The HVA bituminous coal (high sulfur) underwent the highest increase in total acidity whereas the lowest was experienced by the LV bituminous coal. Again, the

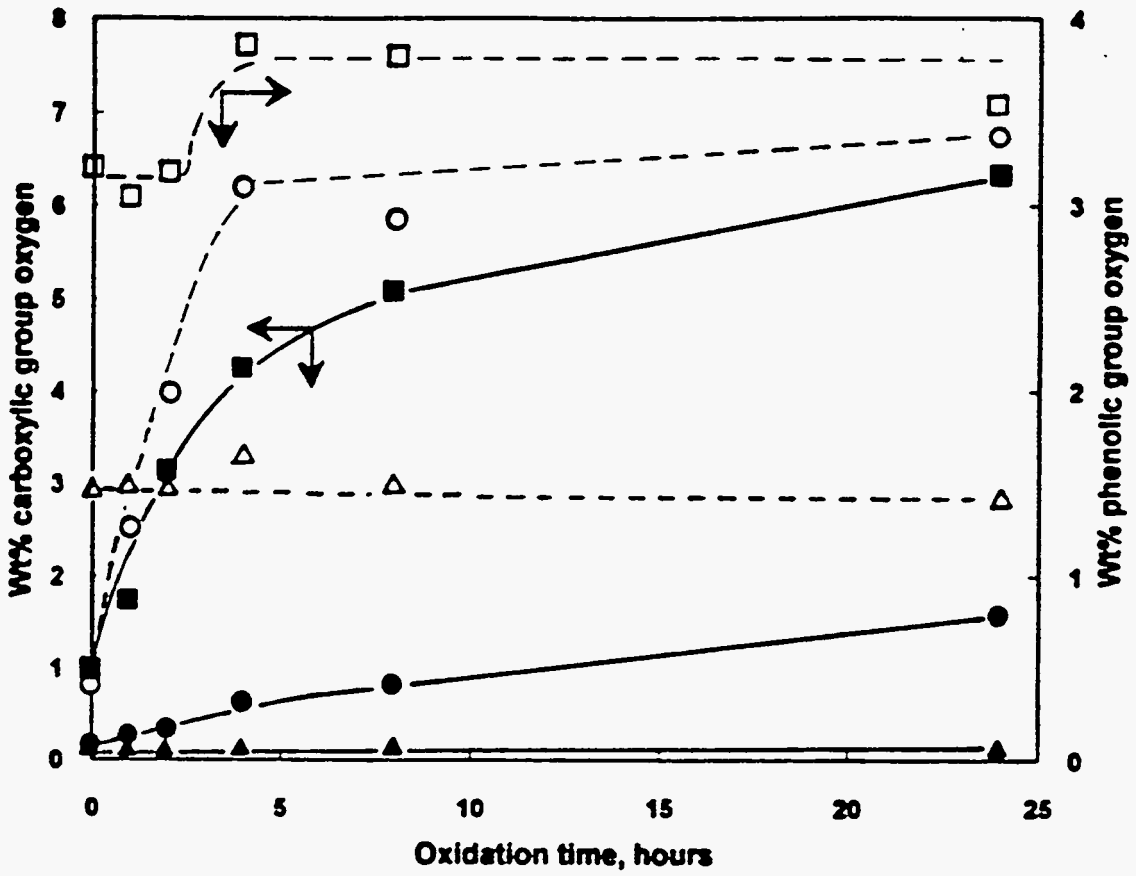

Figure 32. Wt% carboxylate and phenolic oxygen of coals oxidized at 230°C.
PSOC-1442 (Sub bituminous C): □ phenolic, ■ carboxylic;
DECS-12 (HVA Bituminous): ○ : phenolic, ● :carboxylic;
PSOC-1461 (Anthracite):Δ: phenolic, ▲: carboxylic.

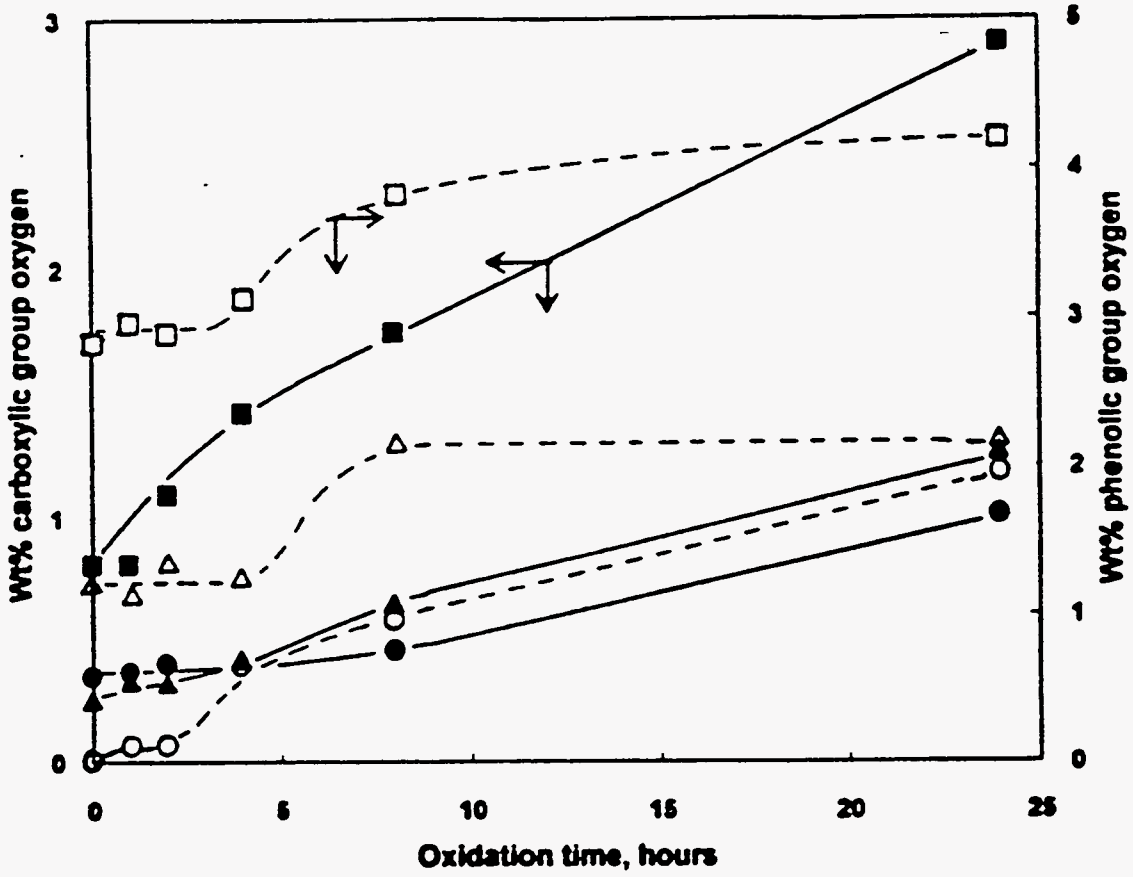

Figure 33. Wt% carboxylate and phenolic oxygen of coals oxidized at 230°C.
PSOC-1481 (HVA Bituminous): □ phenolic, ■ carboxylic;
PSOC-1527 (MV Bituminous):Δ: phenolic, ▲: carboxylic;
PSOC-1516 (LV Bituminous): ○ : phenolic, ● :carboxylic.

susceptibility of bituminous coals to oxidation is consistent with rank. Figures 32 and 33 show that PSOC-1481 was more susceptible to oxidation than the other HVA bituminous coal, DECS-12; this could be due to the higher sulfur content of the former, or to its higher volatile matter content. The results given in Figures 32 and 33 show that the percentage of phenolic group oxygen increased substantially in the first 5 hours in the case of HVA bituminous coal (DECS-12), whereas with the exception of anthracite, the percentage of phenolic groups increased only after 5 hours, thereafter increased only slightly, whereas the percentage of carboxylic group oxygen increased steadily over the entire oxidation period. These results suggest that phenolic groups are generated mostly during the first hours of oxidation. At longer oxidation periods, they probably can be further oxidized to quinone structures[101,102] or be converted to carboxylic groups. Carboxylic groups seem to be more stable at higher temperatures. Studying the oxidation of coal using X-ray photoelectron spectroscopy, Perry and Grint[188] observed that stable carboxylic groups were generated in high concentration at temperatures above 250°C. The comparison between the oxidation behavior of the freshly mined Upper Freeport coal (Figure 6) with the behavior of Upper Freeport coal from the Pennsylvania State Coal Bank (PSOC-1527 in Figure 33) indicates that the former experienced more extensive oxidation likely due to its higher moisture content. However, the effect of oxidation on the wettability (discussed later) was more severe in the PSOC-1527 sample attributed to its high ash content.

Figure 34 shows the carboxylate and phenolic contents of three sub-bituminous coals: sub-bituminous C (PSOC-1538), sub-bituminous B (PSOC-1486), and sub-bituminous A (PSOC-1487) coals. The sub-bituminous A coal experienced the greatest increase in total acidity (carboxylic plus phenolic) in 24 hours, suggesting that this coal has more propensity to be oxidized. It is observed that for all the coal samples, oxidation was fastest in the first few hours. The phenolic content was much greater than the carboxylic

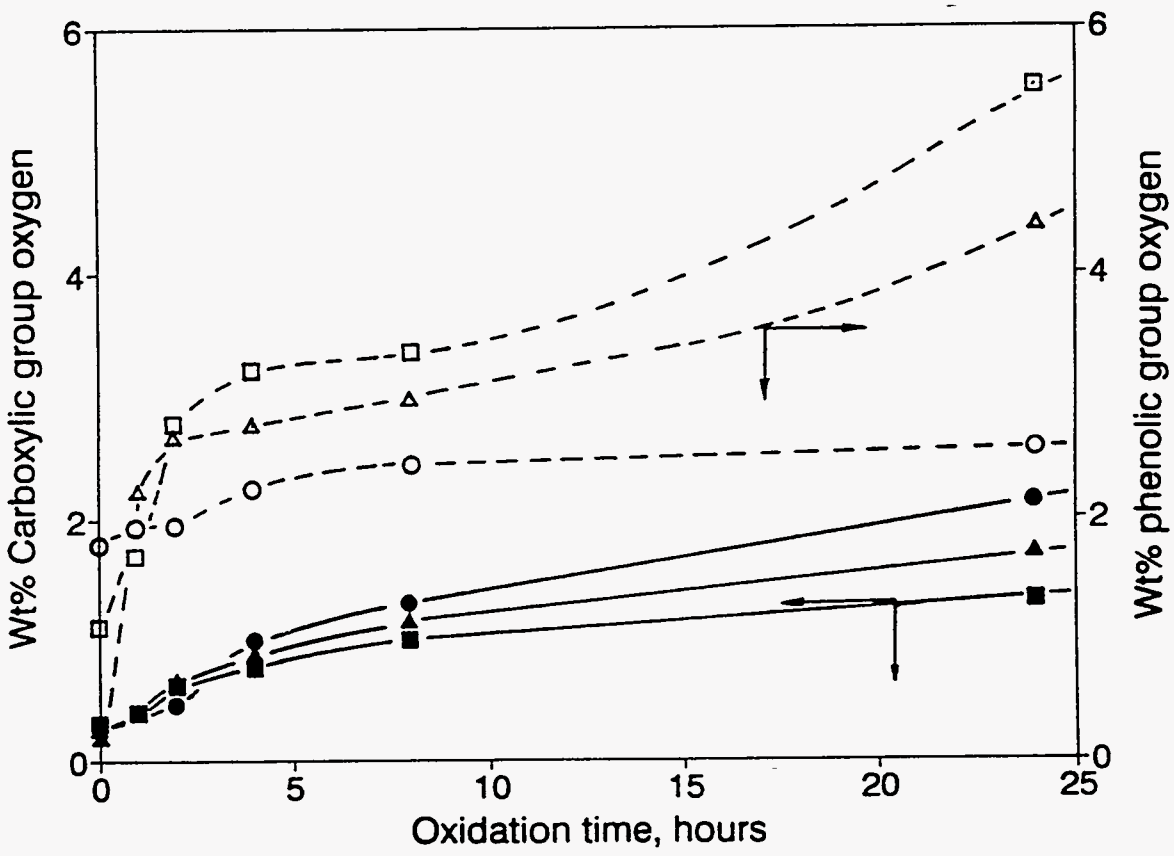

Figure 34. Wt% carboxylate and phenolic oxygen of coals oxidized at 230°C.
PSOC-1538 (Sub-bituminous C): □ phenolic, ■ carboxylic;
PSOC-1486 (Sub-bituminous B):○: phenolic, ●: carboxylic;
PSOC-1487 (Sub-bituminous A): Δ : phenolic, ▲ :carboxylic.

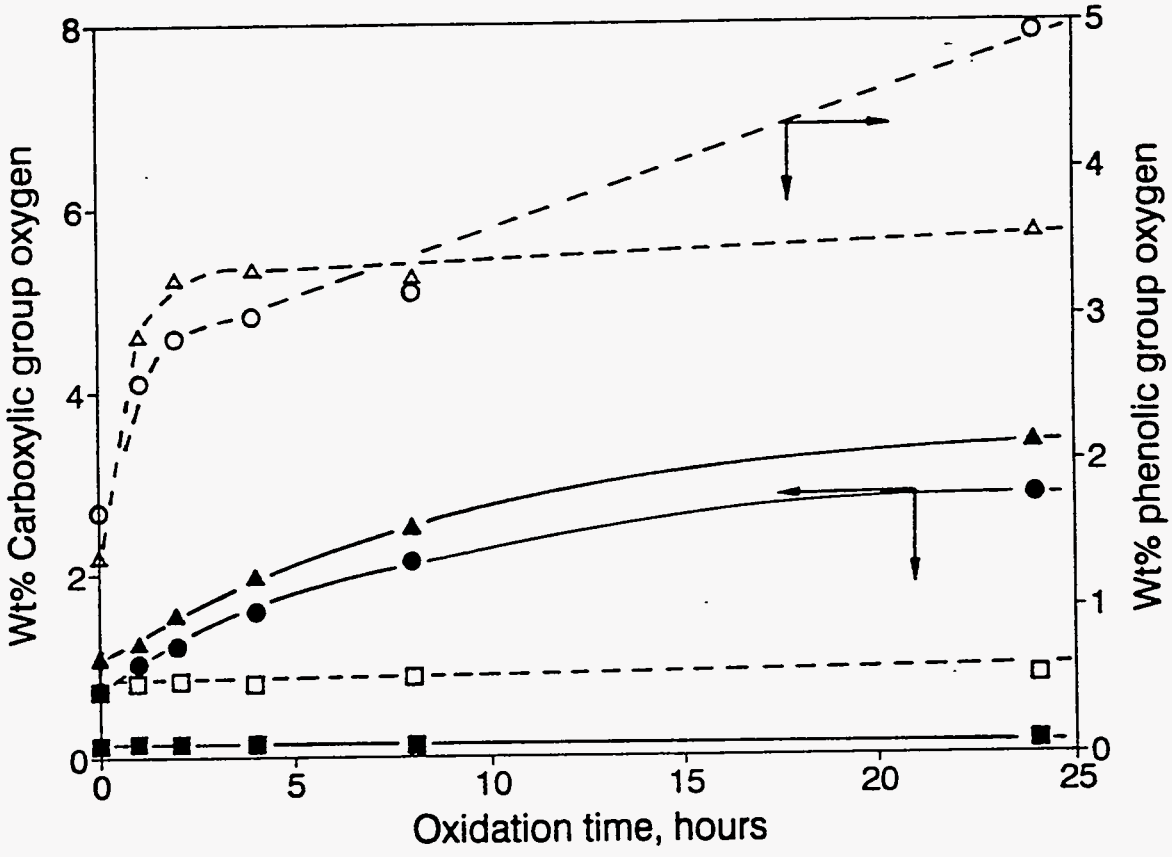

Figure 35. Wt% carboxylate and phenolic oxygen of coals oxidized at 230°C.
PSOC-1515 (Semi-anthracite): □ phenolic, ■ carboxylic;
PSOC-1539 (HVC Bituminous):○: phenolic, ●: carboxylic;
PSOC-1497 (HVC-Bituminous): Δ : phenolic, ▲ :carboxylic.

oxygen, indicating that there was more oxidation on the aromatic structure of coal. Figure 35 shows that the semi-anthracite coal (PSOC-1515) experienced negligible oxidation, whereas PSOC-1497 coal experienced slightly more oxidation than the other HVC bituminous coals (PSOC-1539), probably due to its higher moisture content.

B.2 Film Flotation Tests.

The wettability of the as-received and oxidized coals from the Pennsylvania State Coal Bank was assessed by film flotation. Figure 36 shows the film flotation curves of as-received and oxidized sub-bituminous (PSOC-1442), HVA bituminous (DECS-12) and anthracite (PSOC-1461) coals. The hydrophobicity of the sub-bituminous and bituminous coals was markedly reduced by oxidation, by both the increase in surface acid groups and the loss of volatile matter on heating. The decrease in hydrophobicity observed in anthracite coal after thermal treatment is probably due to the loss of volatile matter. As expected, Figure 36 shows that the shift of the partition curves decreased as the coal rank increases; this is consistent with the fact that lower rank coals are more susceptible to oxidation than higher rank coals. Figure 37 shows film flotation curves of as-received and oxidized LV bituminous (PSOC-1516), MV bituminous (PSOC-1527) and HVA bituminous (PSOC-1481) coals. The hydrophobicity of each coal was significantly reduced by the increase of acidic groups and the loss of volatile matter. The MV bituminous coal underwent a dramatic reduction in hydrophobicity due to its high ash content. Figure 38 shows that reduction in hydrophobicity of sub-bituminous coals was less severe than the reduction experienced by bituminous coals (Figure 37). It is possible that oxidation in bituminous coals took place more preferentially at the external surface of the coal particles.

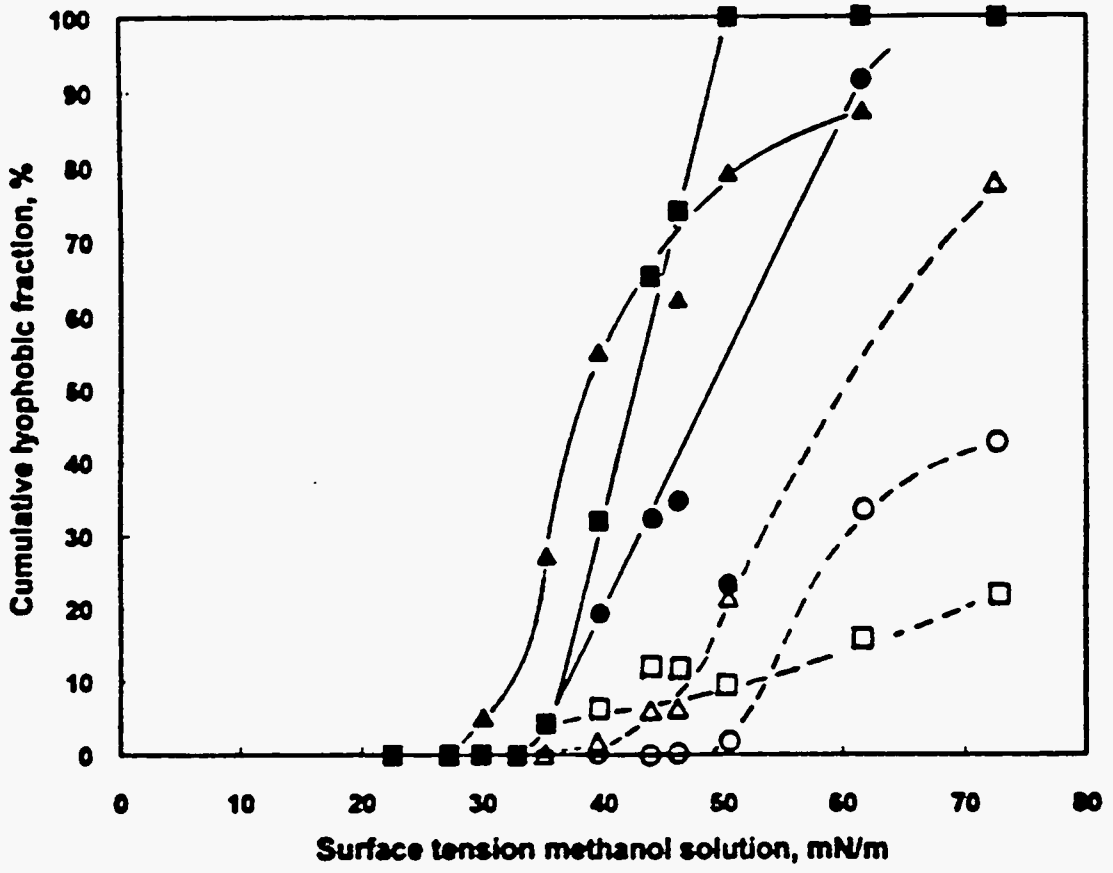

Figure 36. Film flotation curves of as-received and after oxidation at 230°C for 24 hours.
PSOC-1442 (Sub bituminous C): □ :oxidized, ■ :as-received;
DECS-12 (HVA Bituminous): ○ :oxidized, ● :as-received;
PSOC-1461 (Anthracite): Δ :oxidized, ▲ :as-received.

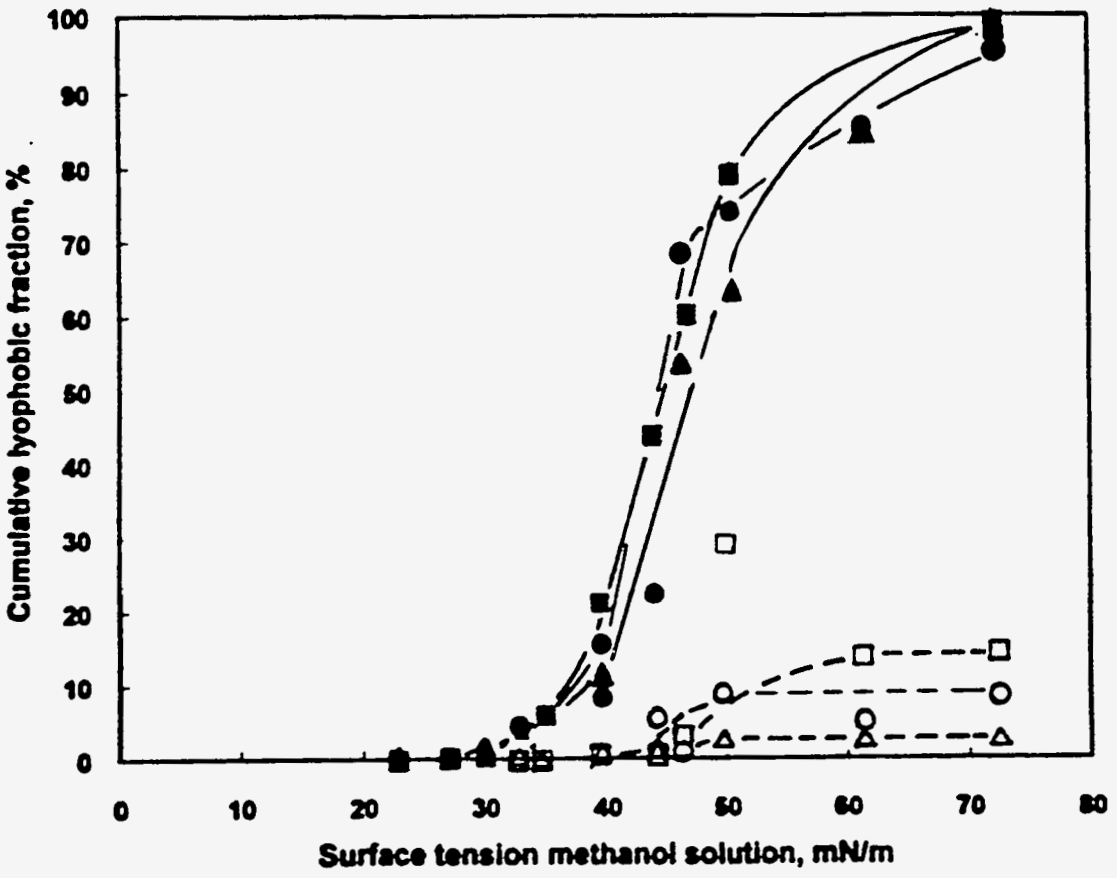

Figure 37. Film flotation curves of as-received and after oxidation at 230°C for 24 hours.
PSOC-1481 (HVA Bituminous): □ :oxidized, ■ :as-received;
PSOC-1527 (MV Bituminous): Δ :oxidized, ▲ :as-received;
PSOC-1516 (LV Bituminous): ○ :oxidized, ● :as-received

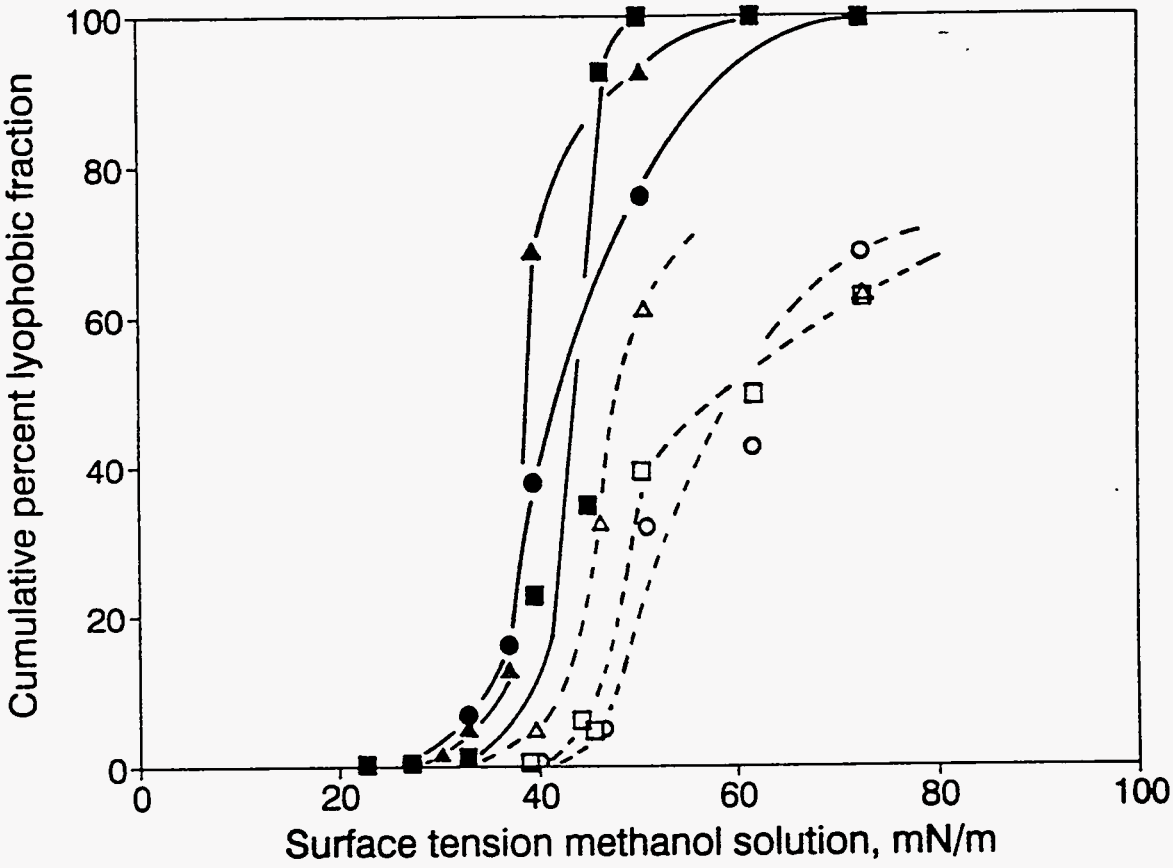

Figure 38. Film flotation curves of as-received and after oxidation at 230°C for 24 hours.
PSOC-1538 (Sub-bituminous C): □ :oxidized, ■ as-received;
PSOC-1486 (Sub-bituminous B): ○ :oxidized, ● :as-received;
PSOC-1487 (Sub-bituminous A): Δ :oxidized, ▲ :as-received.

B.3 Electrokinetic Studies

Electrokinetic tests were done on three coals with different rank: sub-bituminous (PSOC-1442), HVA bituminous (DECS-12) and anthracite (PSOC-1461). Zeta potential versus pH curves for each of the coals studied are given in Figures 39, 40, and 41. Figure 39 shows that oxidation at 230°C slightly increased the magnitude of the negative zeta potential of sub-bituminous coal (PSOC-1442) at pH values above 3.0. Also, the PZR decreased from about 2.1 (for as-received) to about 1.8 after oxidation and the zeta potential remained relatively insensitive to pH in the range 3 to 10 for both raw and oxidized coals. Similar results were obtained by Kelebek *et al.*[118] and Wen *et al.*[119] However, it was proposed[119] that hydronium and hydroxide ions were not the potential determining ions for sub-bituminous coal, since the zeta potential remained constant in the pH range between 4 and 8. Figure 40 shows that oxidation strongly affected the zeta potential of HVA bituminous coal (DECS-12) up to pH 10 or so; the PZR decreased from about 3.1 (for as-received) to about 2.3 after oxidation. Figure 41 shows that oxidation has no effect on the zeta potential of anthracite coal (PSOC-1461); this is consistent with the fact that this coal was not appreciably oxidized at 230°C for 24 hours (Figure 32) and suggests that the loss of volatile matter could be the major reason for its increase in wettability. The strongly negative zeta potential observed is probably due to the high ash content of this coal. About 56.5% of the ash content in this coal is silica. The PZR was found to lie at about 2.7, consistent with the presence of silica (PZR at about 1-2); similar PZR was found by Fuerstenau *et al*[117] working with high ash anthracite coal. Quast and Readett[182] found that the zeta potential of the residual ash from the proximate analysis of low rank coals remained negative in the pH range 2 to 12. Figures 39, 40, and 41 show that the coal surfaces are negatively charged except under strongly acidic conditions. This is consistent with the presence of acidic functional groups which are ionized, except at low values of pH. The reduction in the magnitude of the zeta potential at pH greater than 10

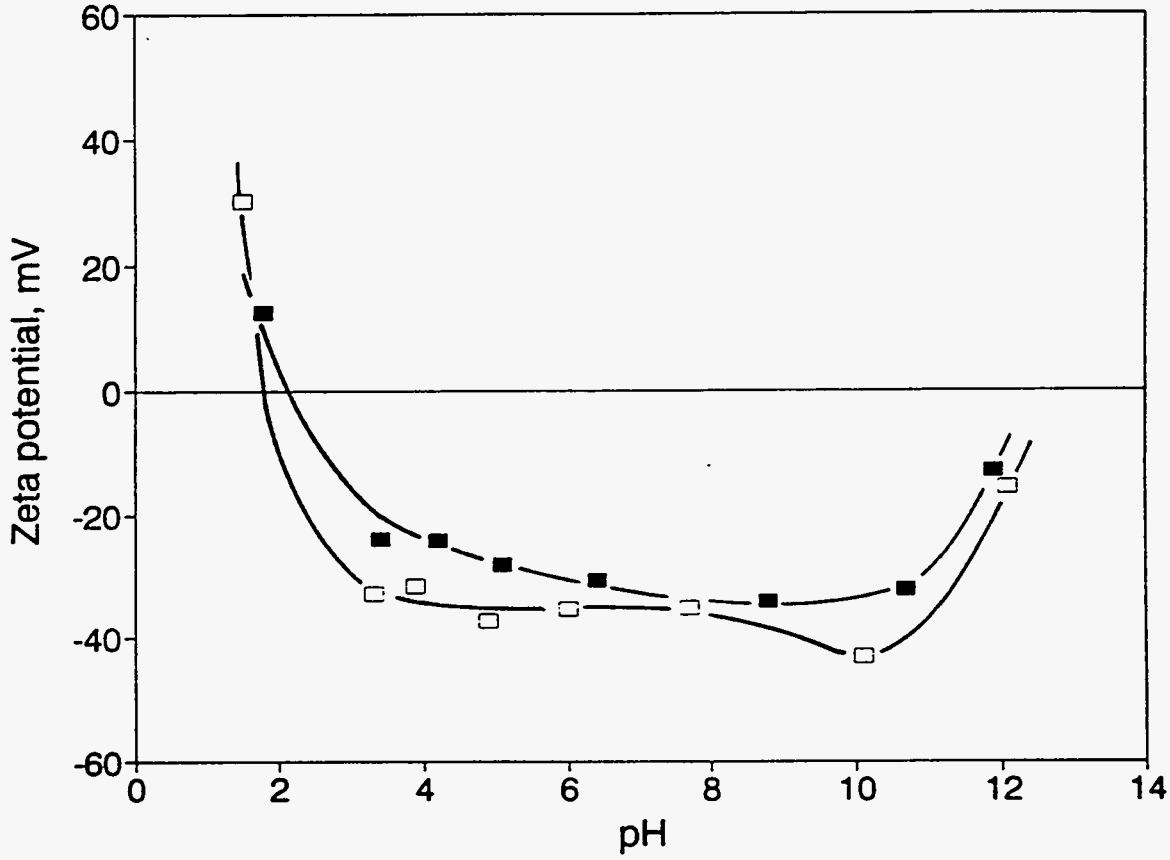

Figure 39. Electrokinetic measurements on PSOC-1442 (Sub-bituminous C) coal; □ :oxidized for 24 hours at 230°C, ■ :as-received.

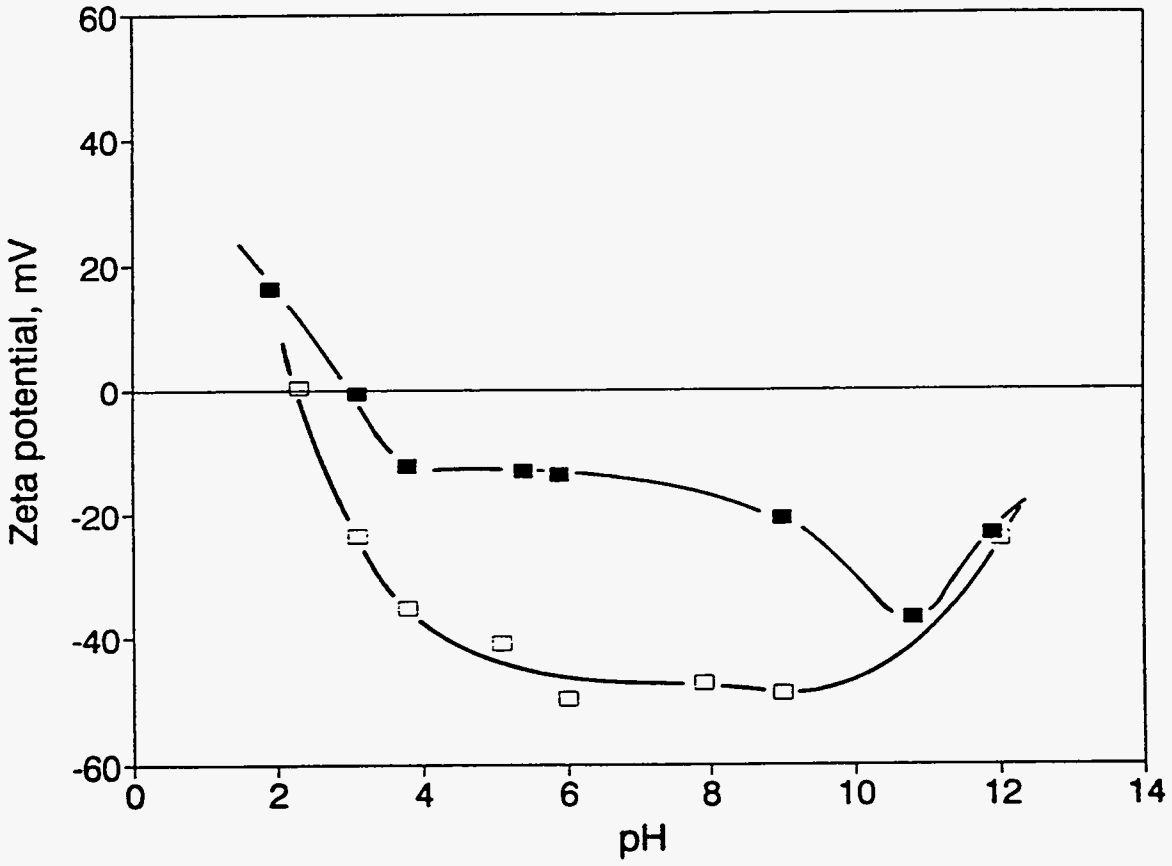

Figure 40. Electrokinetic measurements on DECS-12 (HVA bituminous) coal; □ :oxidized for 24 hours at 230°C, ■ :as-received.

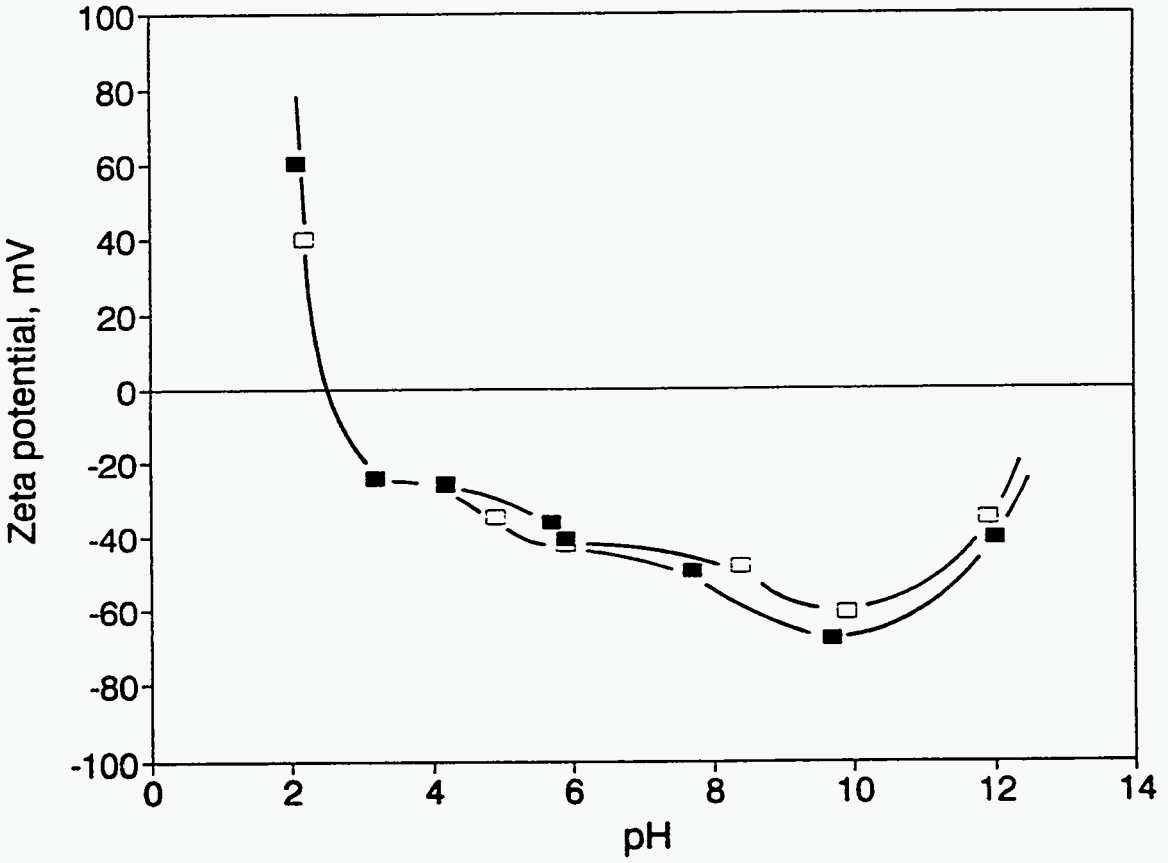

Figure 41. Electrokinetic measurements on PSOC-1461 (Anthracite) coal; □ :oxidized for 24 hours at 230°C, ■ :as-received.

Table 11. Summary of the PZR values of raw and oxidized coals

Sample	Rank	PZR	Oxidation Temperature	PZR
		as received	^{o}C	after oxidation for 24 hours
PSOC-1442	Sub-bituminous C	2.1	230	- 1.8
DECS-12	HVA Bituminous	3.1	230	2.3
U.F.*	MV Bituminous	4.8	150	2.8
PSOC-1461	Anthracite	2.7	230	2.7

* Freshly mined Upper Freeport coal.

is due to dissociation of humic acids at high pH values. However, the effect is also observed in the anthracite coal that underwent slight oxidation. It is possible that at high concentration of NaOH some adsorption of sodium ions could occur. Table 11 summarizes the results obtained in this investigation.

In summary, the results of this study indicate that in general, oxidation decreased the pH at which the zeta potential of a coal is reversed. This is due to the presence of acidic oxygen functional groups generated by oxidation. Also, oxidation generated a more negatively charged coal surface.

B.4 Surface Area Measurements

Carbon dioxide adsorption experiments at room temperature were conducted on as received coal samples from the Pennsylvania State Coal Bank. Duplicate samples were run and the mean surface area for each coal sample is shown in Table 12. It is observed that generally there is a decrease in surface area with increasing coal rank and indicates that in this study high rank coals have a more close pore structure. The surface area of Upper Freeport coal is smaller than others coals suggesting a less porous structure. A value of 136 m^2/g has been also reported for Upper Freeport coal.[148]

Table 12. Surface areas of coals measured by CO_2 adsorption at room temperature.

Sample	Rank	Mean Surface Area m^2/g
PSOC-1442	Sub-bituminous C	322
PSOC-1494	HVB Bituminous	290
PSOC-1481	HVA Bituminous	115
DECS-12	HVA Bituminous	245
PSOC-1527	MV Bituminous	234
PSOC-1516	LV Bituminous	216
PSOC-1461	Anthracite	181

B.5 Wet Oxidation Studies

Wet oxidation tests were done on all of the coal samples from the Pennsylvania State Coal Bank to investigate the changes induced by oxidation on the coal surface properties. Twenty gram samples of each coal sample were oxidized for 5 hours at room temperature using 600 ml of 10% H_2O_2 at pH 1.0, 1.0 N HNO_3 or 0.05 M $Fe_2(SO_4)_3$ at pH 1.0. The amounts of carboxylic and phenolic group oxygen generated by oxidation with different treatments are shown in Table 13, in which the coals are listed in order of increasing rank.

Table 13 indicates that generally the amount of carboxylic and phenolic groups increased after the oxidation procedures. The phenolic content of the anthracite coal (PSOC-1461) decreased slightly after oxidation in nitric acid, probably because of conversion to another functional group. The sub-bituminous (PSOC-1442) and MV bituminous (PSOC-1527) samples underwent much more extensive oxidation than the other samples. These differences could be due to the individual structures of each coal sample, or to the presence of different levels of ash and pyrite.

Table 13. Weight percentage of carboxylic and phenolic group oxygen of coal as-received, and oxidized in different solutions.

Sample	As-received		1.0 N HNO_3		10 % H_2O_2		0.05 M $Fe_2(SO_4)_3$	
	Carboxylic %	Phenolic %	Carboxylic %	Phenolic %	Carboxylic %	Phenolic %	Carboxylic %	Phenolic %
PSOC-1442	0.99	3.23	2.20	10.50	1.10	9.10	1.80	9.50
PSOC-1538	0.13	1.06	0.44	1.82	0.38	1.91	0.32	1.67
PSOC-1486	0.30	1.80	1.10	2.23	0.92	2.56	0.82	1.97
PSOC-1487	0.21	0.29	0.75	1.06	0.83	1.23	0.56	0.97
PSOC-1539	0.62	1.68	1.57	2.75	1.98	3.46	1.05	2.02
PSOC-1497	1.02	1.38	1.10	1.47	1.52	2.35	1.04	1.41
PSOC-1494	0.50	1.07	0.65	1.39	0.70	1.49	0.58	1.24
PSOC-1481	0.81	2.84	1.87	3.87	1.02	4.12	2.81	3.97
DECS-12	0.15	0.41	0.16	0.50	0.19	0.49	0.17	0.52
PSOC-1527	0.25	1.22	2.10	10.50	2.20	9.10	0.80	8.00
PSOC-1516	0.35	0.02	0.44	1.02	0.61	1.20	0.40	1.20
PSOC-1515	0.11	0.42	0.12	0.46	0.15	0.54	0.13	0.51
PSOC-1461	0.11	1.47	0.26	1.42	0.92	1.61	1.40	1.81

B.6 Film Flotation Tests on Wet Oxidized Samples

Figure 42 shows film flotation curves of as-received and oxidized sub-bituminous C coal (PSOC-1442). Table 13 shows that this sample has a strong sensitivity to oxidation, consistent with its low rank. Ferric sulfate markedly reduced the hydrophobicity of the coal, while hydrogen peroxide and nitric acid gave only a moderate reduction in hydrophobicity. Comparison with Table 13 shows that the change in surface properties cannot be due entirely to an increase in carboxylic and phenolic groups, since these were fairly comparable after oxidation with all three aqueous oxidizing agents. The reduction in hydrophobicity was much less dramatic than that observed for the same coal after thermal oxidation, which produced about the same weight percentage of carboxylic and phenolic groups (Figures 32 and 36). This supports the hypothesis that thermal treatment alters the surface properties of coals through loss of volatiles, as well as through surface oxidation.

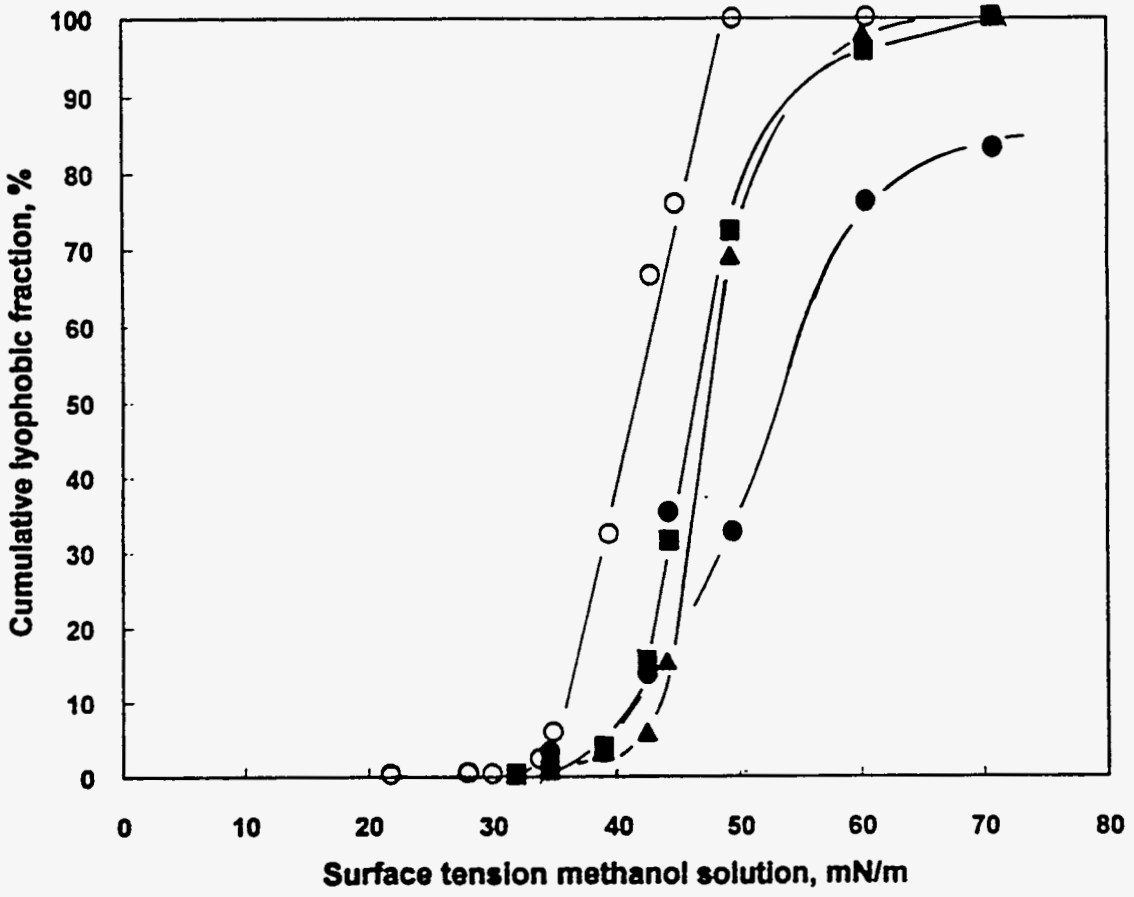

Figure 42. Film flotation partition curves of sub-bituminous C (PSOC-1442) coal after wet oxidation by different oxidizing agents for 5 hours. ○: as-received, ■:1.0 M HNO_3, ● :0.05M $Fe_2(SO_4)_3$, ▲ :10% H_2O_2, all at pH 1.0.

Figures 43 and 44 show film flotation curves for HVA bituminous coal samples (PSOC-1481 and DECS-12) respectively. None of the oxidizing procedures significantly affected the wetting behavior of these samples. Although this is somewhat consistent with the modest increase in carboxylic and phenolic concentrations experienced by these samples on oxidation, it is surprising that the differences in carboxylic and phenolic concentration of the different coals after oxidation did not give more marked differences in film flotation.

The film flotation curves for raw and oxidized MV bituminous (PSOC-1527) coal are presented in Figure 45. The hydrophobicity is markedly reduced at surface tensions higher than 40 mN/m, with oxidation by 10% H_2O_2 having the most severe effect, followed by ferric sulfate. As with Figure 42, comparison with Table 13 indicates that although the reduction in hydrophobicity is qualitatively consistent with an increase in carboxylic and phenolic groups, the agreement is not quantitative. The critical surface tension of LV bituminous coal (PSOC-1516) was not modified by the different oxidizing treatments (Figure 46), and the hydrophobicity was only modestly reduced at surface tensions exceeding 45 mN/m. This coal underwent moderate increases in phenolic group concentration on oxidation, and very minor increases in carboxylate groups.

Figure 47 shows film flotation curves of as-received and oxidized anthracite (PSOC-1461) using different oxidizing agents. Although this sample experienced only minor increases in carboxylic and phenolic group concentrations after treatment with the oxidants, the hydrophobicity was reduced markedly, particularly by 10% H_2O_2 and 0.05M $Fe_2(SO_4)_3$. This could not be due to loss of volatile material, because the wet oxidation tests were done at room temperature. Assuming that the ash content was

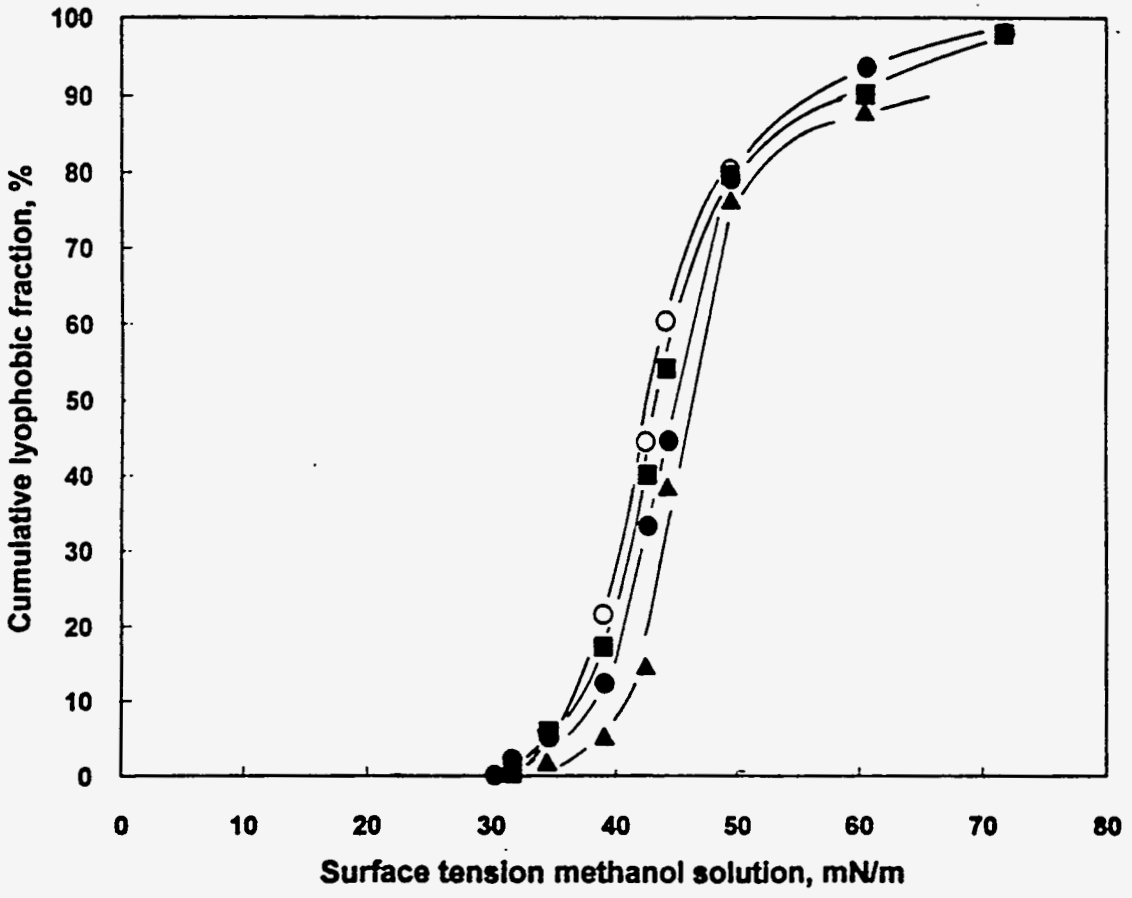

Figure 43. Film flotation partition curves of HVA bituminous (PSOC-1481) coal after wet oxidation by different oxidizing agents for 5 hours. ○: as-received, ■: 1.0 M HNO_3, ●: 0.05M $Fe_2(SO_4)_3$, ▲: 10% H_2O_2, all at pH 1.0.

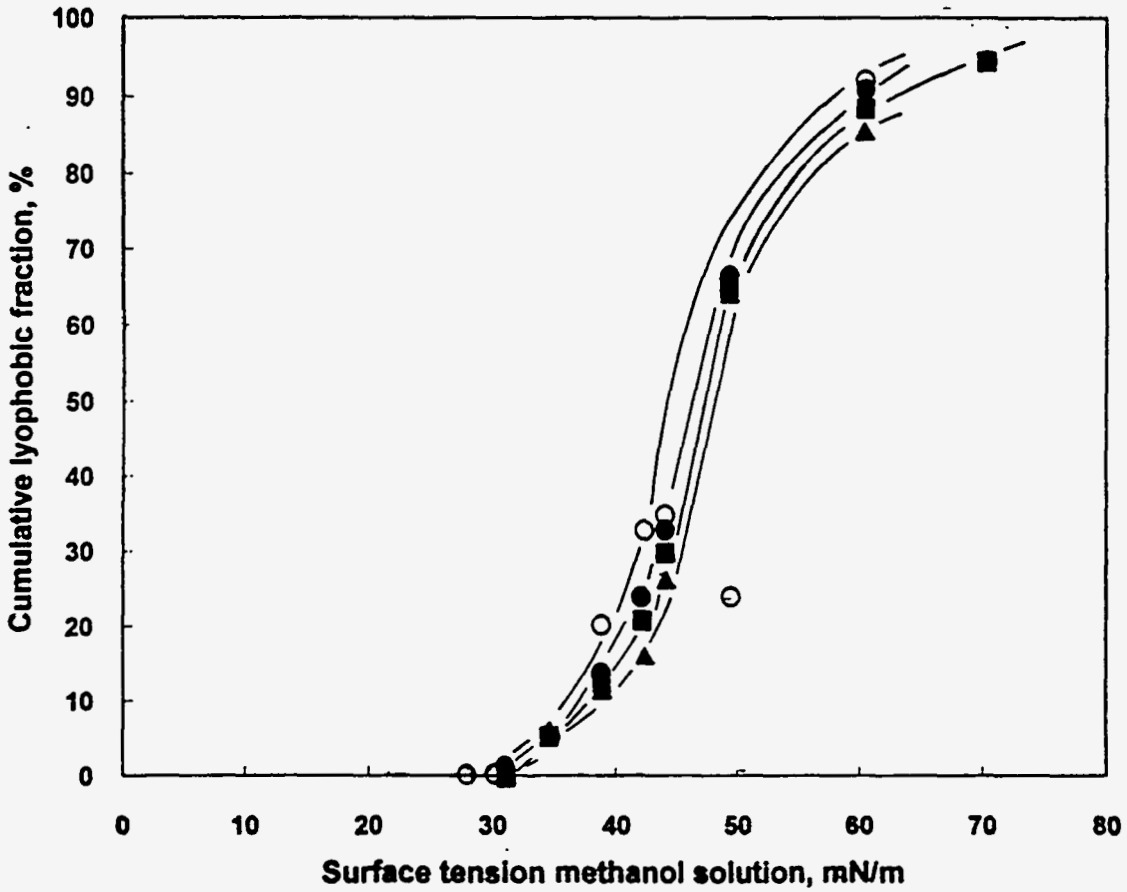

Figure 44. Film flotation partition curves of HVA Bituminous (DECS-12) coal after wet oxidation by different oxidizing agents for 5 hours. ○: as-received, ■: 1.0 M HNO_3, ●: 0.05M $Fe_2(SO_4)_3$, ▲: 10% H_2O_2, all at pH 1.0.

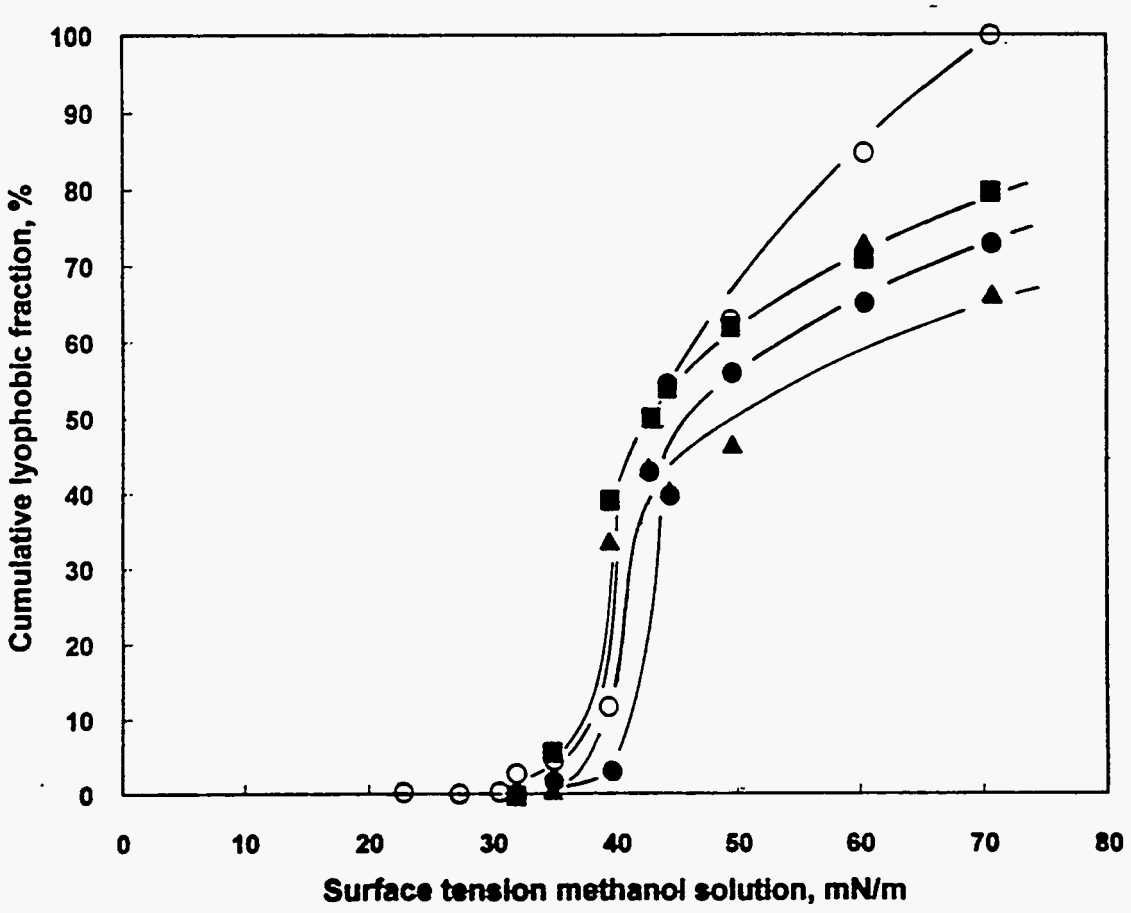

Figure 45. Film flotation partition curves of MV bituminous (PSOC-1527) coal after wet oxidation by different oxidizing agents for 5 hours. ○: as-received, ■: 1.0 M HNO_3, ●: 0.05M $Fe_2(SO_4)_3$, ▲: 10% H_2O_2, all at pH 1.0.

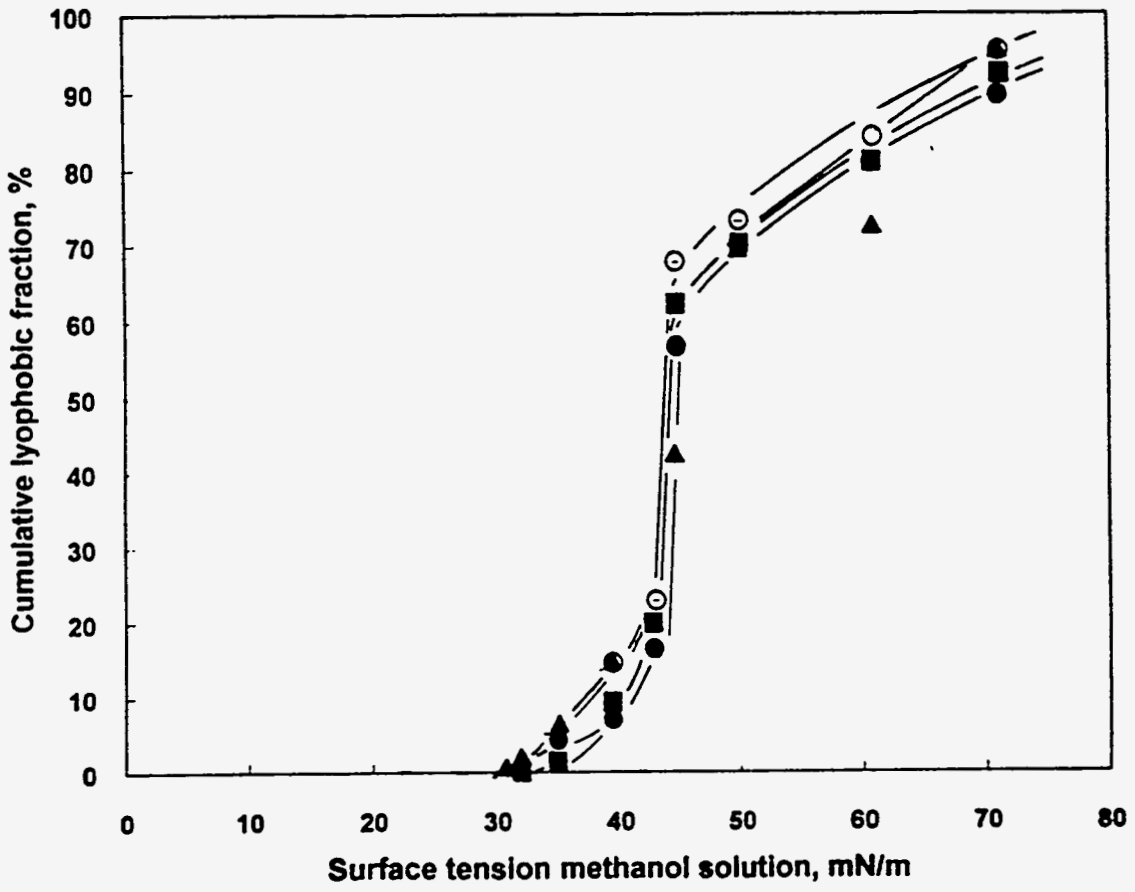

Figure 46. Film flotation partition curves of LV bituminous (PSOC-1516) coal after wet oxidation by different oxidizing agents for 5 hours. ○: as-received, ■: 1.0 M HNO_3, ●: 0.05M $Fe_2(SO_4)_3$, ▲: 10% H_2O_2, all at pH 1.0.

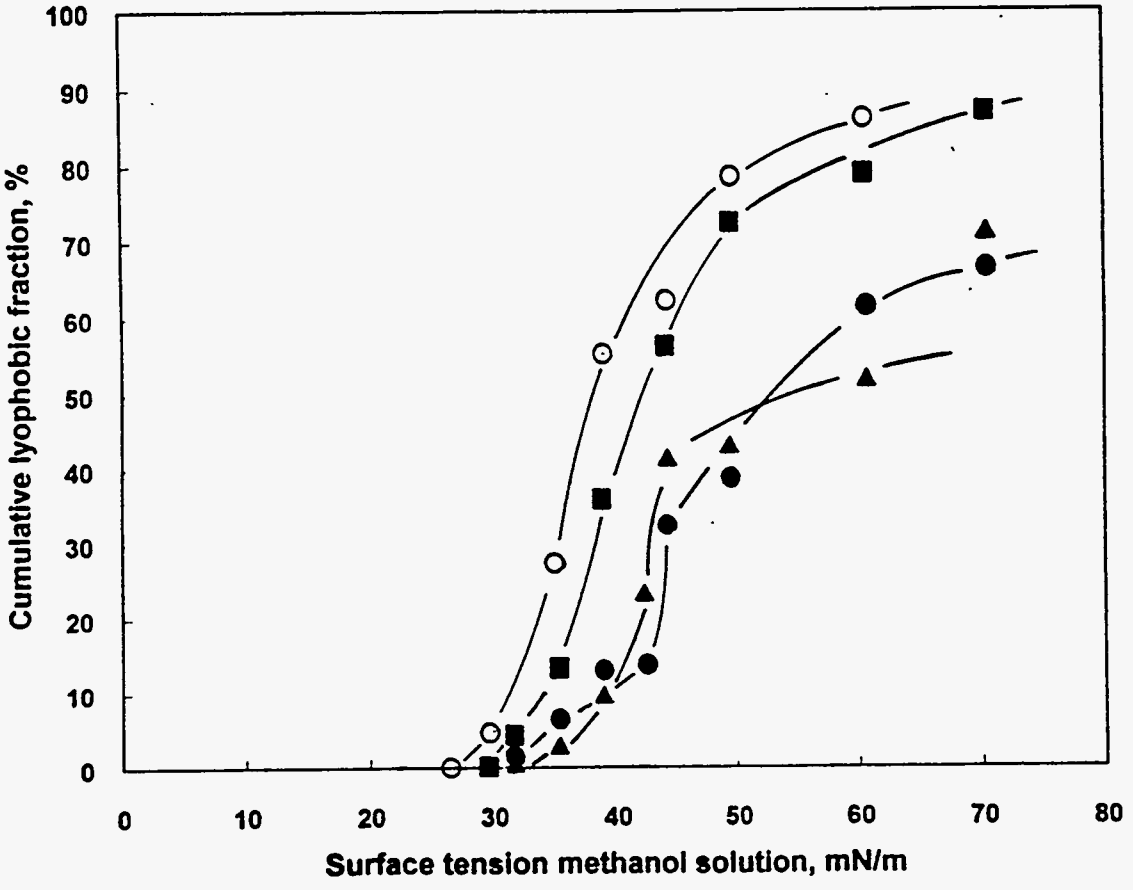

Figure 47. Film flotation partition curves of anthracite (PSOC-1461) coal after wet oxidation by different oxidizing agents for 5 hours. ○: as-received, ■: 1.0 M HNO_3, ●: 0.05M $Fe_2(SO_4)_3$, ▲: 10% H_2O_2, all at pH 1.0.

homogeneously distributed on the coal, it is possible to suggest that some ash compounds were modified during the oxidation to render more hydrophilic products.

Figure 48 compares the effect of 1.0M HNO_3 on the hydrophobicity of sub-bituminous C (PSOC-1442), HVA bituminous (DECS-12), and anthracite(PSOC-1461). The sub-bituminous coal and anthracite experienced the most significant reduction in hydrophobicity, especially at the lower surface tensions. Figures 49 and 50, which compare the behavior with 0.05M $Fe_2(SO_4)_3$ and 10% H_2O_2, show similar trends.

B.7 Diffuse Reflectance Infrared Fourier Transform Spectroscopy Analysis (DRIFT)

Spectroscopy is the measurement and interpretation of electromagnetic radiation adsorbed, scattered, or emitted by atoms, molecules, or other chemical species. This adsorption or emission is associated with changes in the energy states of the interacting chemical species and because each species has characteristic energy states, spectroscopy can be used to identify the interacting species.[190] Infrared spectroscopy involves examination of the twisting, bending, rotating, and vibrational motions of atoms in a molecule. Upon interaction with infrared radiation, portions of the incident radiation are absorbed at specific wavelengths. The multiplicity of vibrations occurring simultaneously produces a complex spectrum that is uniquely characteristic of the functional groups that make up the molecule and also of the overall configuration of the molecule.[190]

DRIFT spectroscopy was used to obtain information on the changes of the structure of coals during oxidation by different procedures. This technique is very sensitive for studying the chemical transformations undergone by the coal surface during oxidation.[91] Figures 51, 52, and 53 show the spectra of as-received and oxidized sub-

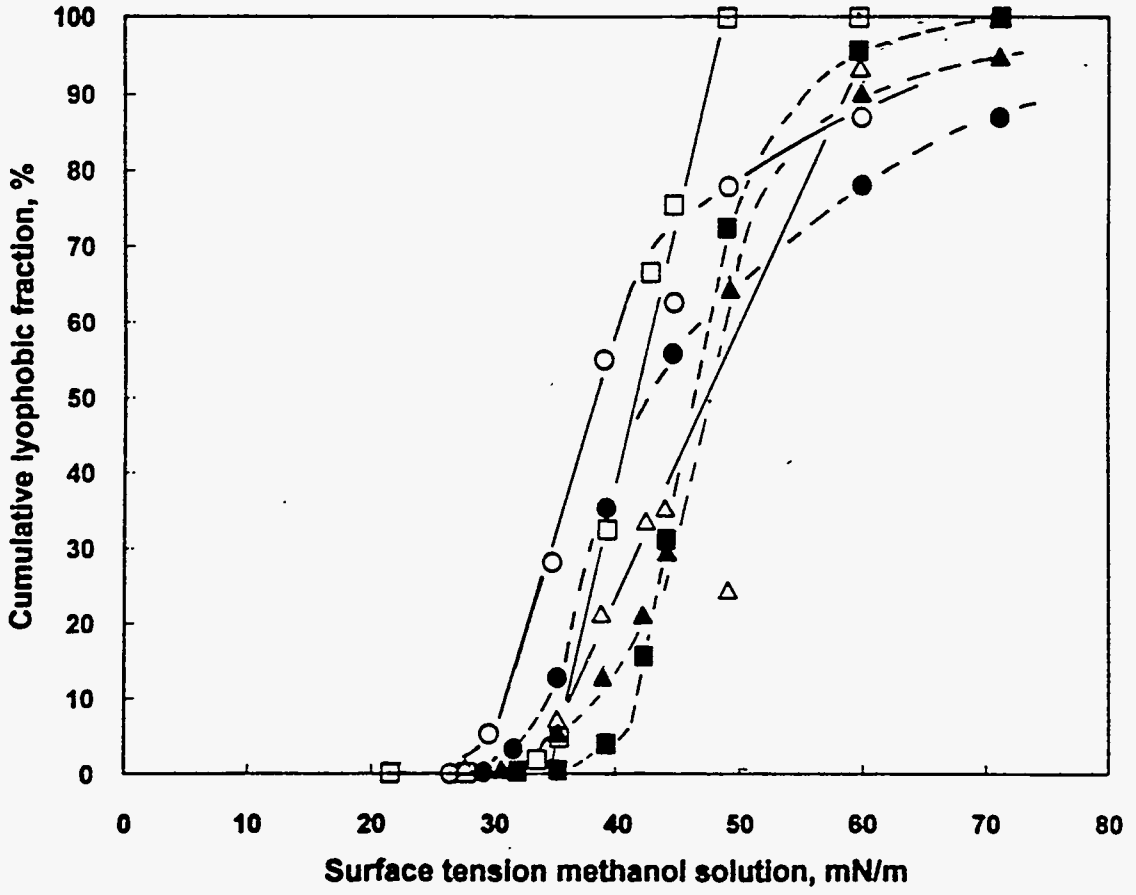

Figure 48. Film flotation partition curves of raw and after oxidation with 1.0M HNO_3 for 5 hours. Sub-bituminous (PSOC-1442): □: as-received, ■: oxidized; HVA bituminous (DECS-12): Δ: as-received, ▲: oxidized; Anthracite (PSOC-1461): ○: as-received, ●: oxidized.

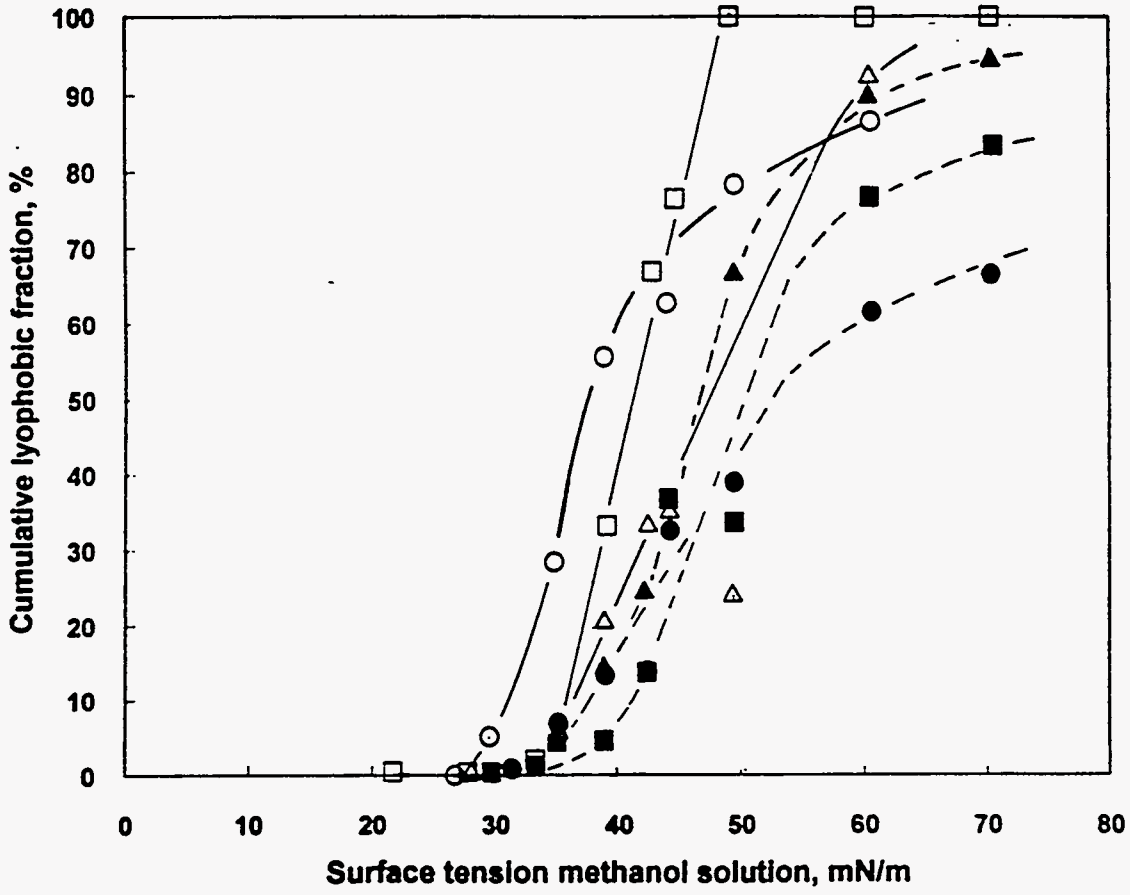

Figure 49. Film flotation partition curves of raw and after oxidation with 0.05 M $Fe_2(SO_4)_3$ at pH 1.0 for 5 hours. Sub-bituminous (PSOC-1442): □: as received, ■: oxidized; HVA bituminous (DECS-12): Δ: as-received, ▲: oxidized; Anthracite (PSOC-1461): ○: as-received, ●: oxidized.

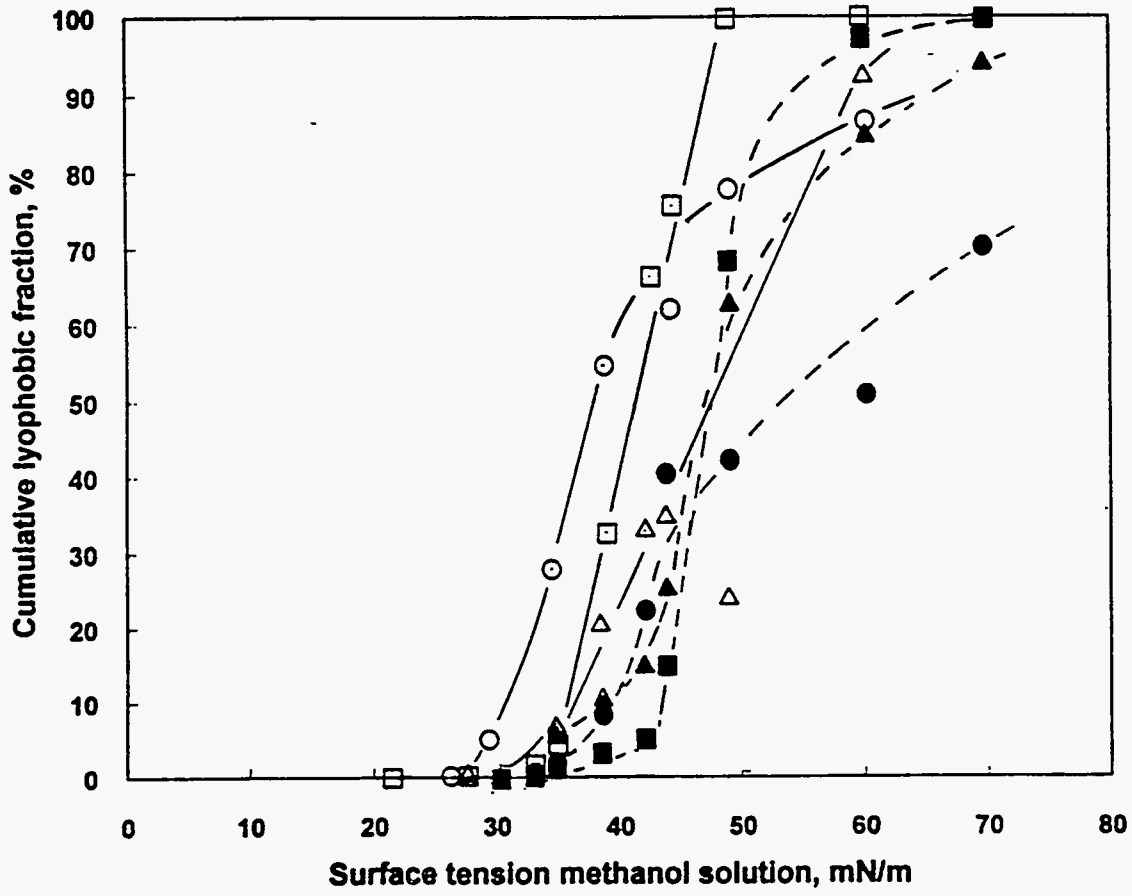

Figure 50. Film flotation partition curves of raw and after oxidation with 10% H_2O_2 at pH 1.0 for 5 hours. Sub-bituminous (PSOC-1442): □: as-received, ■: oxidized; HVA bituminous (DECS-12): Δ: as-received, ▲: oxidized; Anthracite (PSOC-1461): ○ as-received, ●:oxidized.

bituminous (PSOC-1442), HVA bituminous (DECS-12), and anthracite (PSOC-1461) coals respectively. The peaks at about 2900 cm^{-1} in the spectra of as-received PSOC-1442 and DECS-12 coals are characteristic of aliphatic -CH- and -CH2- groups. A significant decrease in the peak intensity was observed after thermal oxidation, indicating that the aliphatic structure was either severely oxidized or volatilized. As discussed earlier, the first step of oxidation is the formation of peroxide compounds by the oxidation of the aliphatic, olefinic, and ether structures that link the aromatic units present in coal. These reactions are commonly invoked[68,74,97] and are likely to be occurring in this study. The detected loss of aliphatic groups suggest that this would be the initial site of abstraction of hydrogen and subsequent peroxide formation. Peroxide products, are difficult to detect directly on coal surface by DRIFT (or any other method), because they easily decomposed at the experimental oxidation temperature. Figure 53 shows no peak at 2900 cm^{-1} for anthracite (PSOC-1461), which is consistent with the highly aromatic structure of high rank coals.

The 1900-1400 cm^{-1} region is of interest in oxidation studies because most of the oxygen functional groups absorb infrared radiation in this region. The shoulders at 1770 and 1840 cm^{-1} correspond to ester and anhydride functionalities respectively.[191] Ester and anhydrides are formed at high oxidation temperature according to reactions 17 to 19 (Section D, Chapter 3). A medium intensity peak at about 1726 $cm^{-1}$and 1720 cm^{-1}, corresponding to carboxylic acids, was observed in the spectra of oxidized PSOC-1442 and DECS-12 coals respectively. As discussed earlier, the formation of carboxylic groups probably occurs according to the reactions 10 to 16 (Section D, Chapter 3). Figure 32 indicates that the final percentage of carboxylic oxygen group of the HVA bituminous coal (DECS-12) was close to the initial percentage of the carboxylic oxygen group of sub-bituminous C (PSOC-1442) coal. Unexpectedly, these results are not consistent with those in Figures 51 and 52, because the peaks corresponding to carboxylic acids are only

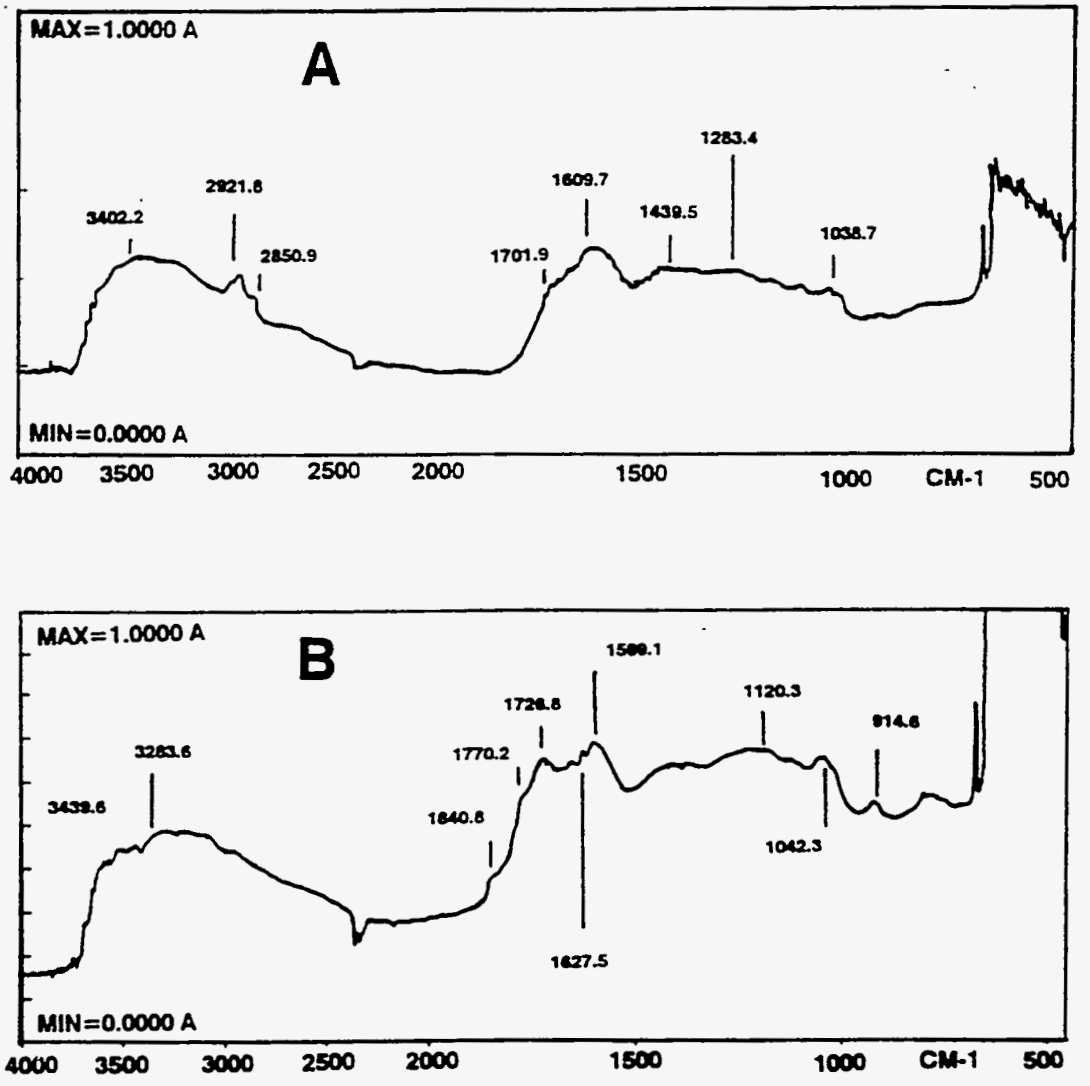

Figure 51. DRIFT spectra of sub-bituminous C coal (PSOC-1442); (A): as-received; (B): oxidized at 230°C for 24 hours.

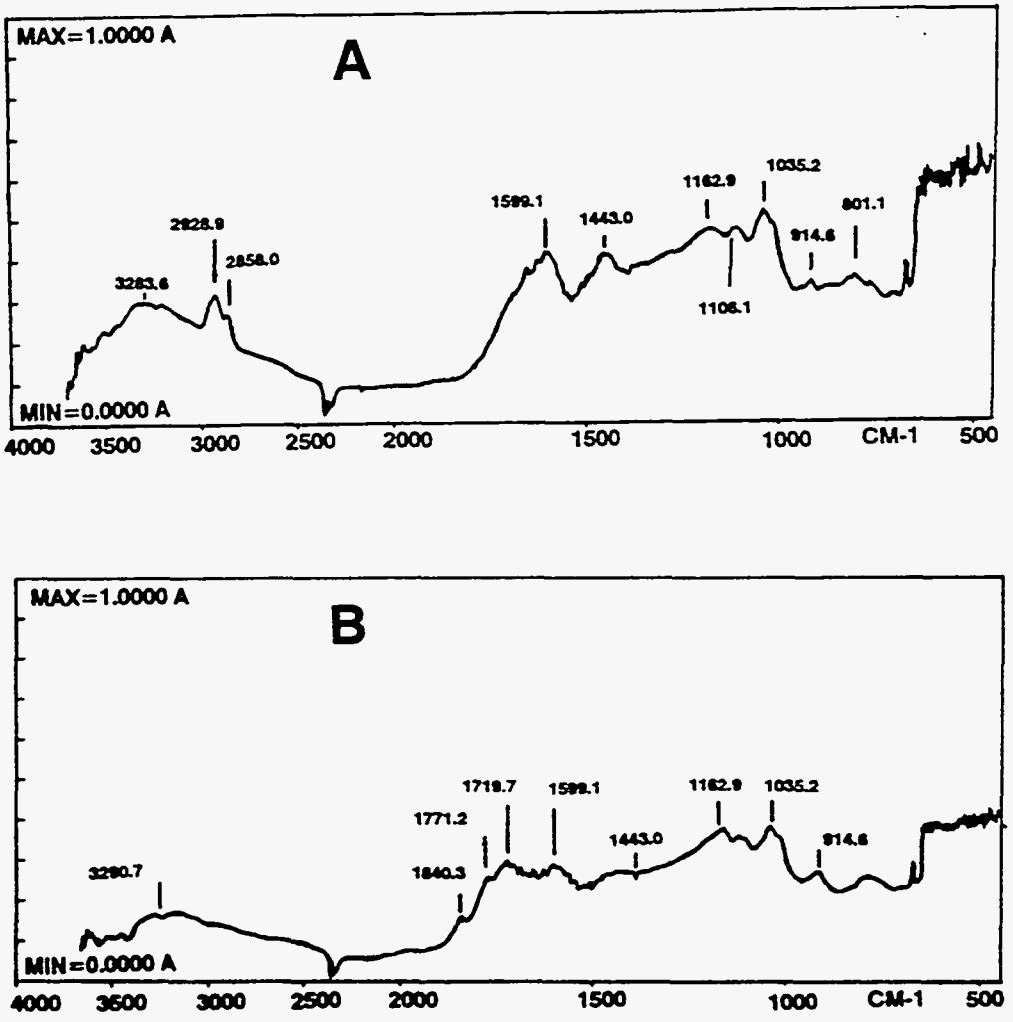

Figure 52. DRIFT spectra of HVA bituminous coal (DECS-12); (A): as-received; (B): oxidized at 230°C for 24 hours.

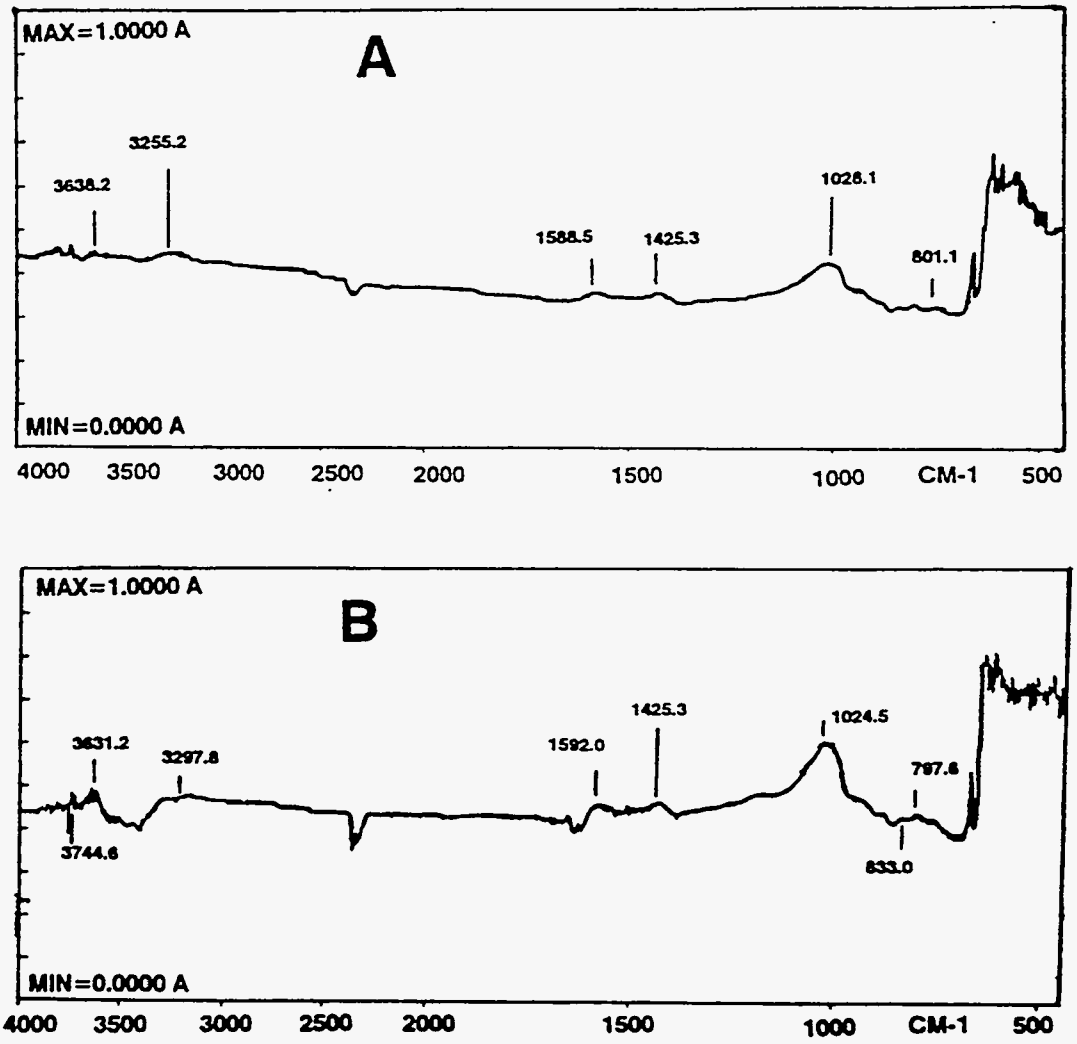

Figure 53. DRIFT spectra of anthracite coal (PSOC-1461); (A): as-received; (B): oxidized at 230°C for 24 hours.

observed in the spectrum of the HVA bituminous coal (DECS-12), whereas the spectrum of sub-bituminous coal shows a small shoulder at 1701.9 cm^{-1}. It is possible that the vibration of the oxygen functionalities in the as-received sub-bituminous C coal are in somehow diminished by the presence of other molecules.

The peak at about 1600 cm^{-1} probably corresponds to aromatic rings. The peak at about 1450 cm^{-1} is characteristic of aliphatic bending modes. The intensity of the peak at 1450 cm^{-1} was less intense in the spectrum of oxidized DECS-12 coal than for as-received coal, reflecting a loss of -CH2- and -CH3- groups with thermal oxidation. The broad band at 3300-3400 cm^{-1} in the spectra of as-received and oxidized PSOC-1442 and DECS-12 coals probably reflects the presence of phenolic groups. The spectra of as-received and oxidized anthracite coal in Figure 53 are characterized by a more uniform adsorption in the region between 3000-1500 cm^{-1}. The latter feature, is probably produced by free electrons associated with graphitic structures.[192] As expected, no significant differences between the spectra are evident; this is consistent with the negligible oxidation experienced by this coal. The peak present at about 3600 cm^{-1} is attributable to kaolinite.[191,193] Two peaks are evident at 1588.5 and 1425.3 cm^{-1} corresponding to C=C aromatic stretching. The former peak slightly shifted to 1592.0 with oxidation. The strong peaks at 1028.1 cm^{-1}(as-received coal) and 1024.5 cm^{-1}(oxidized coal) could correspond to the presence of kaolinite and quartz[156]. The ash of this coal contains 56.5 % of SiO_2 (wt% dry basis). The peaks at 1028.1 cm^{-1} and 3600 cm^{-1} were not significantly altered by any of the oxidation procedures. Peaks of medium to small intensity characteristic of out of plane aromatic C-H deformations are present between 900 and 650 cm^{-1}, consistent with the rich aromatic nature of anthracite coals.

In summary, in the case of sub-bituminous and bituminous coals, the organic structural changes caused by thermal oxidation are very similar, except for a few minor

differences. Anthracite coal shows a more uniform absorption in the 3000-1500 cm^{-1} region.

In a qualitatively analysis of as-received and oxidized coals using DRIFT spectroscopy Fuerstenau *et al.*[194] found similar characteristic peaks to those observed in this study. Oxidation of coal at 200°C for 30 minutes resulted in the appearance of a carbonyl peak in conjuction with a decrease in the intensity of aliphatic C-H groups. However, changes on the coal surface were only detected when coal was subjected to severe oxidation.

Coal samples oxidized by aqueous solutions of different oxidizing agents were also analyzed by DRIFT. Figures 54 and 55 show the spectra of as-received and oxidized sub-bituminous C (PSOC-1442) coal and Table 14 summarizes the most relevant peaks observed along with their intensities. The broad peak observed at about 3400 cm^{-1} corresponds to hydroxyl vibrations. This peak did not experience appreciable changes in the oxidized coal spectra and Table 14 shows that a slight increase in the intensity of this peak was observed with all oxidation treatments. Comparison with Table 13 shows that although increase in peak intensity is qualitatively consistent with an increase in carboxylic and phenolic groups, the agreement is not quantitative. The range between 3000 and 2800 cm^{-1} corresponds to the alkyl group region (CH, CH_2 and CH_3). As-received coal exhibited two principal peaks at 2921.8 and 2850.9 cm^{-1}. Although these were unchanged by treatment with 0.05 M $Fe_2(SO_4)_3$ and 10 % H_2O_2, the former shifted to 2928.9 cm^{-1} and the later to 2858.0 cm^{-1} by treatment with 1.0 N HNO_3. Table 14 indicates that the intensity of the peaks was slightly increased by treatment with 1.0 N HNO_3 and 0.05 M $Fe_2(SO_4)_3$ and decreased by treatment with 10% H_2O_2. These results contrast with the spectrum of the same coal oxidized by air at 230°C (Figure 51) where the intensity of these specific peaks was significantly decreased, and indicate that

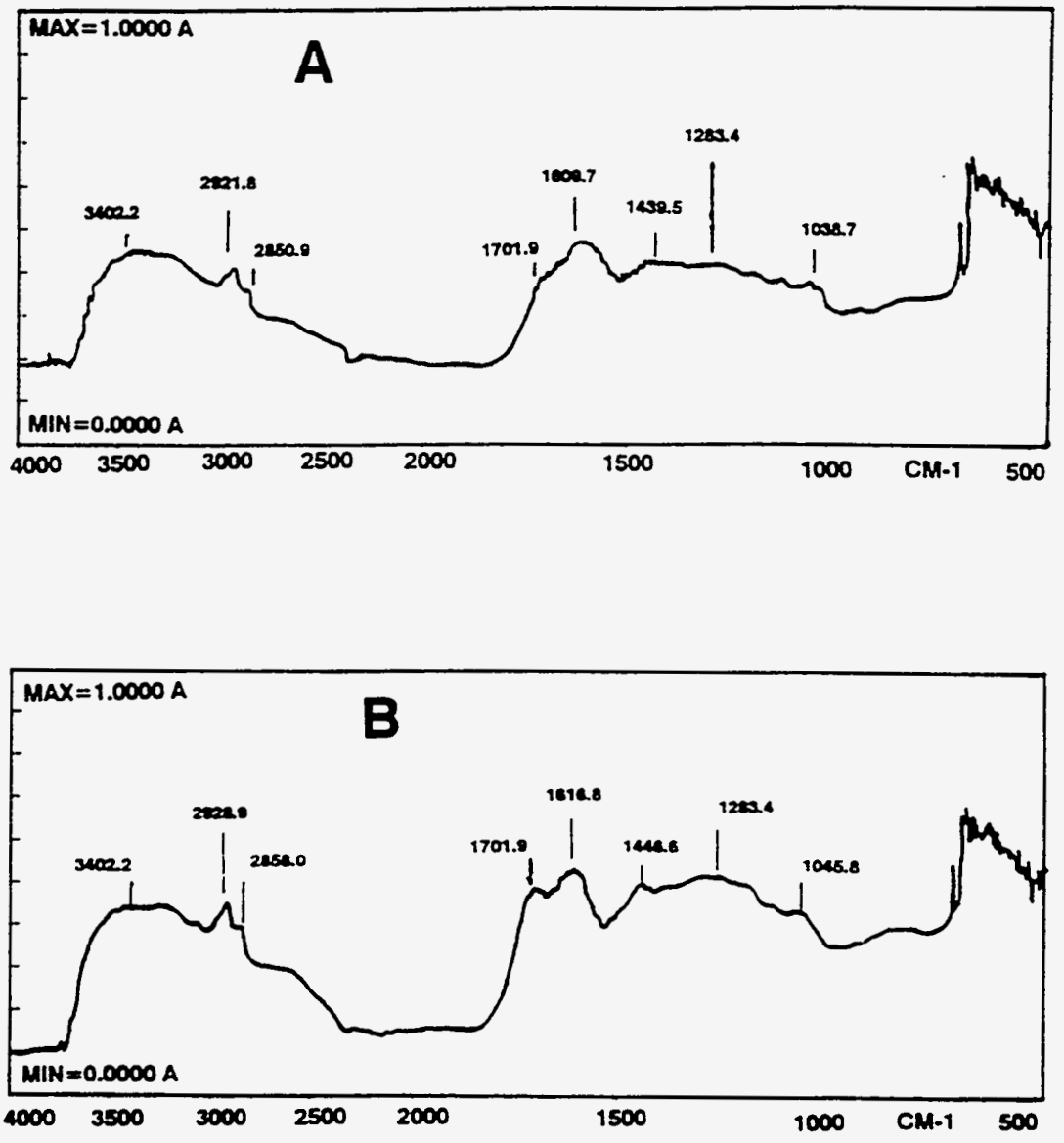

Figure 54. DRIFT spectra of sub-bituminous C coal (PSOC-1442); (A): as- received; (B) oxidized with 1.0M HNO_3 for 5 hours at room temperature.

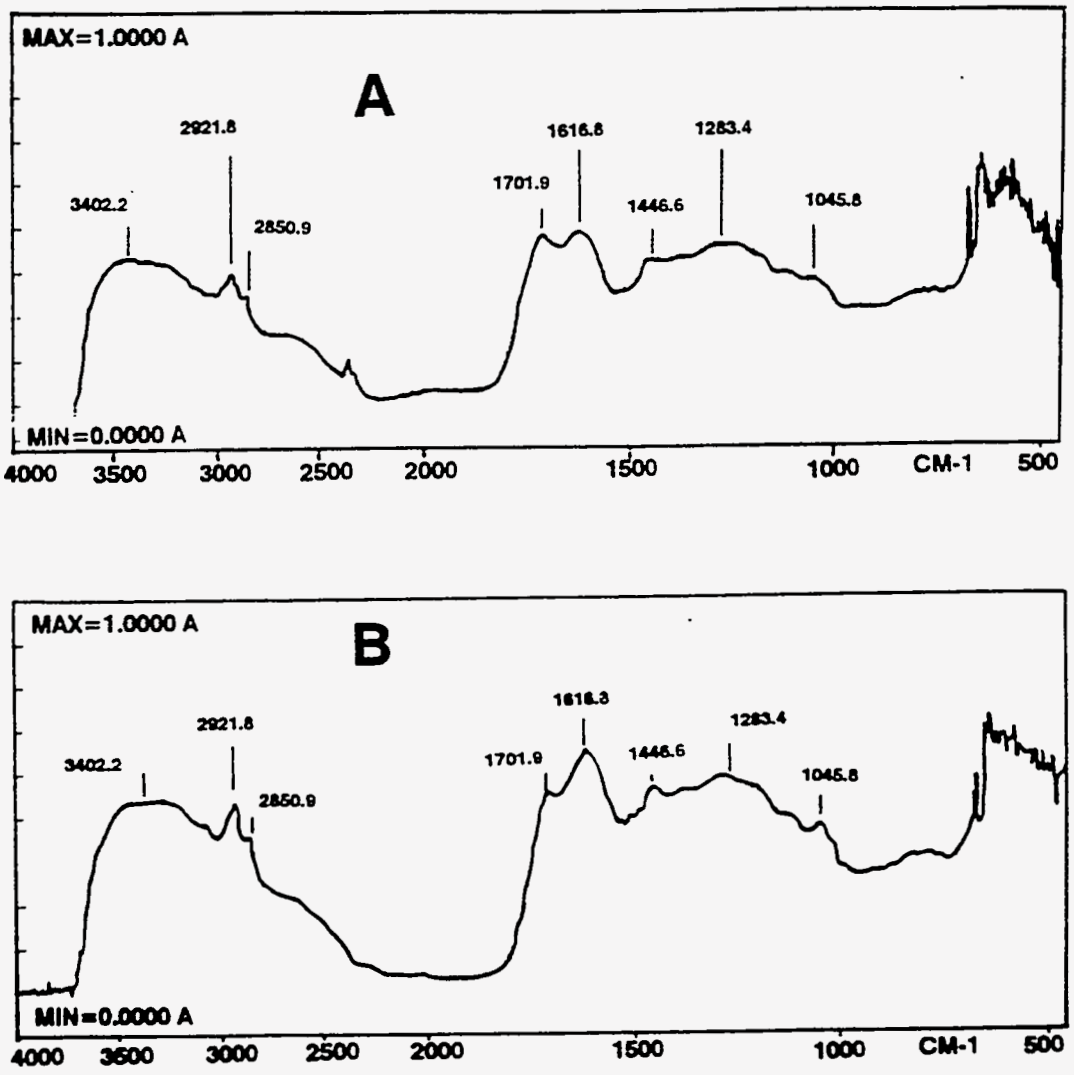

Figure 55. DRIFT spectra of sub-bituminous C coal (PSOC-1442); (A):oxidized with 10% H_2O_2; (B) oxidized with 0.05M $Fe_2(SO_4)_3$ for 5 hours at room temperature.

Table 14. DRIFT absorption peaks of as-received and oxidized sub-bituminous C (PSOC-1442) coal.

As-received		1.0 N HNO_3		10 % H_2O_2		0.05 $Fe_2(SO_4)_3$	
Peak cm^{-1}	Intensity	Peak cm^{-1}	Intensity	Peak cm^{-1}	Intensity	Peak cm^{-1}	Intensity
3402.2	0.44	3402.2	0.49	3402.2	0.48	3402.2	0.53
2921.8	0.41	2928.9	0.43	2921.8	0.40	2921.8	0.42
2850.9	0.36	2858.0	0.37	2850.9	0.35	2850.9	0.37
1701.9	0.38	1701.9	0.49	1701.9	0.48	1701.9	0.55
1609.7	0.47	1616.8	0.53	1616.8	0.49	1616.8	0.64
1439.5	0.42	1446.6	0.49	1446.6	0.42	1446.6	0.57
1283.4	0.38	1283.4	0.52	1283.4	0.46	1283.4	0.59
1038.7	0.38	1045.8	0.43	1045.8	0.38	1045.8	0.48

the mechanisms associated with wet oxidation do not involve the formation of peroxide compound by oxidation of the aliphatic and olefinic structures that link the aromatic units present in coal.

The as-received coal spectrum shows a shoulder at 1701.9 cm^{-1} and two peaks at 1609.7 and 1439.5 cm^{-1}. The shoulder at 1701.9 cm^{-1} corresponds to carbonyl absorption and it is consistent with the presence of carboxylic group on as-received coal. The peak at 1609.7 cm^{-1} corresponds to C=C aromatic stretching whereas the peak at 1439.5 cm^{-1} corresponds to aliphatic bending modes. Changes were observed in all spectra of wet oxidized coal. The most significant change is the enhanced carbonyl absorption at the 1701.9 cm^{-1} region that is in agreement with the increase of carboxylic group observed in Table 13 after oxidation with all three aqueous oxidants. The peak at 1609.7 cm^{-1} exhibits a shift towards 1616.8 cm^{-1} by treatment with 10% H_2O_2 and 0.05 M $Fe_2(SO_4)_3$ and it is due to aromatic hydrogen substitution patterns.[195] This fact suggests that the aromatic configuration would be the site of abstraction of hydrogen and subsequent peroxide formation. As discussed earlier, in the specific case of oxidation by hydrogen peroxide, the hydroxyl radicals formed by the Fenton mechanism[44] can react with the organic structure present in coal by either splitting off hydrogen from them or by

adding unsaturated fragments.[108] Furthermore, Table 14 shows that the intensity of this peak increased with all treatments and may be explained by the presence of more adjacent oxygen-containing functional groups, which induces an asymmetrical arrangement of C=C rings.[196] The peak at 1439.5 cm^{-1} corresponding to an in plane aromatic CH deformation shift to 1446.6 cm^{-1}, is likely due to substitution by OH groups in the ring structure.[195] Also, the peak intensity increases only by treatments with 0.05 M $Fe_2(SO_4)_3$ and 1.0 N HNO_3.

Consistent with the increase in the concentration of phenolic group with oxidation as is observed in Table 13, the intensity of the peak at 1283 cm^{-1} corresponding to C-O stretching (phenols) coupled with OH deformation increased for all oxidized samples. The mechanism of phenol formation has been discussed by Alberts *et al.*[101] and Markova.[102] The peak at 1038.7 cm^{-1}, which corresponds to C_{al}-O-C_{al} stretching[197] (al=aliphatic), shifts to 1045.8 cm^{-1} with all oxidation treatments, although the intensity was only increased by treatments with 0.05 M $Fe_2(SO_4)_3$ and 1.0 M HNO_3.

Figure 56 shows the spectra of HVA bituminous (PSOC-1481) coal, as-received and oxidized with 1.0 M HNO_3. Table 15 summarizes the wavenumbers and intensities associated of the major peaks observed in Figure 56.

The peaks observed for this bituminous coal are similar to those in Figures 54 and 55; the peak at about 3450 cm^{-1} corresponding to hydroxyl vibrations, and the peaks at 2921.8 cm^{-1} and 2858.0 cm^{-1} corresponding to alkyl region, were not changed by oxidation. Again, the most significant change was the increase in the peak absorbance at 1701.9 cm^{-1} corresponding to the formation of carboxylic groups on oxidation. The position and intensity of the peak at 1609.7 cm^{-1} was not altered by oxidation, whereas the peaks at 1443.0 cm^{-1} and 1191.2 cm^{-1} experienced a slight decrease in intensity. The peak at 1049.4 cm^{-1} increased after oxidation; this probably has its origin in the C-O

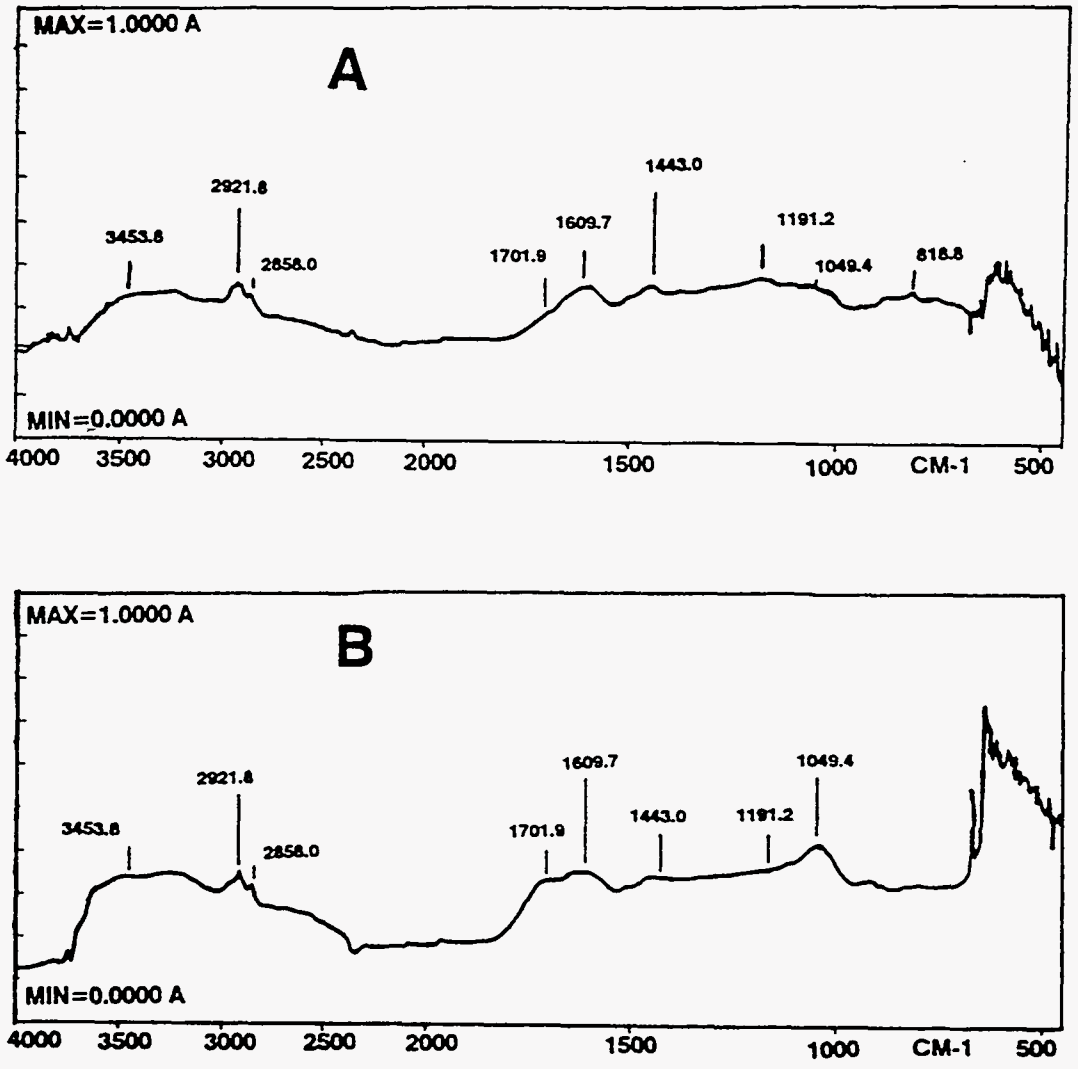

Figure 56. DRIFT spectra of HVA bituminous C coal (PSOC-1481); (A): as- received; (B) oxidized with 1.0M HNO_3 for 5 hours at room temperature.

Table 15: DRIFT absorption peaks of HVA bituminous (PSOC-1481) coal, as-received and oxidized with 1.0M HNO_3.

As-received		1.0 N HNO_3	
Peak cm^{-1}	Intensity	Peak cm^{-1}	Intensity
3453.8	0.34	3453.8	0.34
2921.8	0.36	2921.8	0.35
2858.0	0.33	2858.0	0.32
1701.9	0.28	1701.9	0.34
1609.7	0.36	1609.7	0.36
1443.0	0.36	1443.0	0.33
1191.2	0.38	1191.2	0.35
1049.4	0.35	1049.4	0.42

stretching of aliphatic ethers.[191] Similar spectra (not shown) were obtained for this coal oxidized with H_2O_2 and $Fe_2(SO_4)_3$.

Figures 57 and 58 show the spectra of as-received and oxidized MV bituminous (PSOC-1527) coal. Table 16 summarizes the principal features of these spectra. This coal showed a series of peaks at high wavenumbers, predominated by a peak at 3617.0 cm^{-1} that decreased after oxidation and shifted to 3624.1 cm^{-1} after treatment with 10 % H_2O_2. This feature is thought to be due to specific minerals (an ash analysis of this coal is not available). A similar peak has been assigned to kaolinite ($Al_2(Si_2O_5)(OH)_4$).[193,198] The broad hydroxyl peak at 3382.9 cm^{-1} decreased in intensity after all oxidation treatments, although there was a marked increase in the concentration of surface groups measured by ion-exchange. A peak at about 3042 cm^{-1} associated with aromatic C-H stretching was present, in addition to peaks corresponding to the alkyl groups (CH, CH_2 and CH_3); this is consistent with the fact that high rank coals have a more aromatic structure. The intensity of these peaks was slightly reduced by all wet oxidation procedures, however; Figure 59 shows that the same coal oxidized in air at 230°C experienced a dramatic decrease in intensity of the peaks corresponding to the alkyl

Table 16: DRIFT absorption peaks of as-received and oxidized MV bituminous (PSOC-1527) coal.

As-received		1.0 N HNO_3		10 % H_2O_2		0.05 $Fe_2(SO_4)_3$	
Peak cm^{-1}	Intensity	Peak cm^{-1}	Intensity	Peak cm^{-1}	Intensity	Peak cm^{-1}	Intensity
3617.0	0.45	3617.0	0.34	3624.1	0.38	3617.0	0.40
3382.9	0.53	3382.9	0.36	3382.9	0.40	3382.9	0.44
3042.4	0.51	3042.4	0.37	3042.4	0.38	3042.4	0.41
2928.9	0.57	2921.8	0.50	2921.8	0.51	2921.8	0.54
2858.0	0.51	2865.1	0.42	2872.2	0.42	2865.1	0.45
1652.3	0.40	1652.3	0.42	1652.3	0.42	1652.3	0.42
1609.7	0.53	1609.7	0.53	1609.7	0.55	1609.7	0.55
1453.7	0.53	1446.3	0.53	1439.5	0.57	1446.3	0.54
1191.2	0.54	1191.2	0.47	1191.2	0.53	1191.2	0.54
1099.0	0.61	1099.0	0.52	1099.0	0.63	1099.0	0.65
1028.1	0.67	1031.6	0.64	1028.1	0.77	1035.2	0.77
914.6	0.51	914.6	0.46	914.6	0.55	914.6	0.52
801.1	0.52	804.7	0.47	801.1	0.54	801.1	0.52

groups. This confirms the fact that dry oxidation severely modifies the aliphatic structure of coal. Figures 57 and 58 contain no carbonyl peak at about 1700 cm^{-1} . This is also inconsistent with results of ion-exchange (Table 13); the analytical data indicate a significant increase in the amount of oxygen functional groups with all wet oxidation procedures that was not reflected by an increase in the peak intensity at 1700 cm^{-1}. This inconsistency is not yet understood. It is possible that adsorption of ferric and ferrous iron by ion exchange at the carboxylic group[114] could changes the vibrational states of carboxylic groups; however, the effect should appears in all spectra of wet oxidized coals. A small shoulder at 1652.3 cm^{-1}, associated with highly conjugated carbonyl, most probably quinone type[78,87,199] appeared in all spectra of wet oxidized coal. Quinone structures are products of further oxidized phenolic groups.[101,102] On the coal surface the group that is able to undergo a reversible redox reaction in the potential range of the Fe^{3+}/Fe^{2+} couple is the quinone/hydroquinone system, as proposed by Vetter.[111]

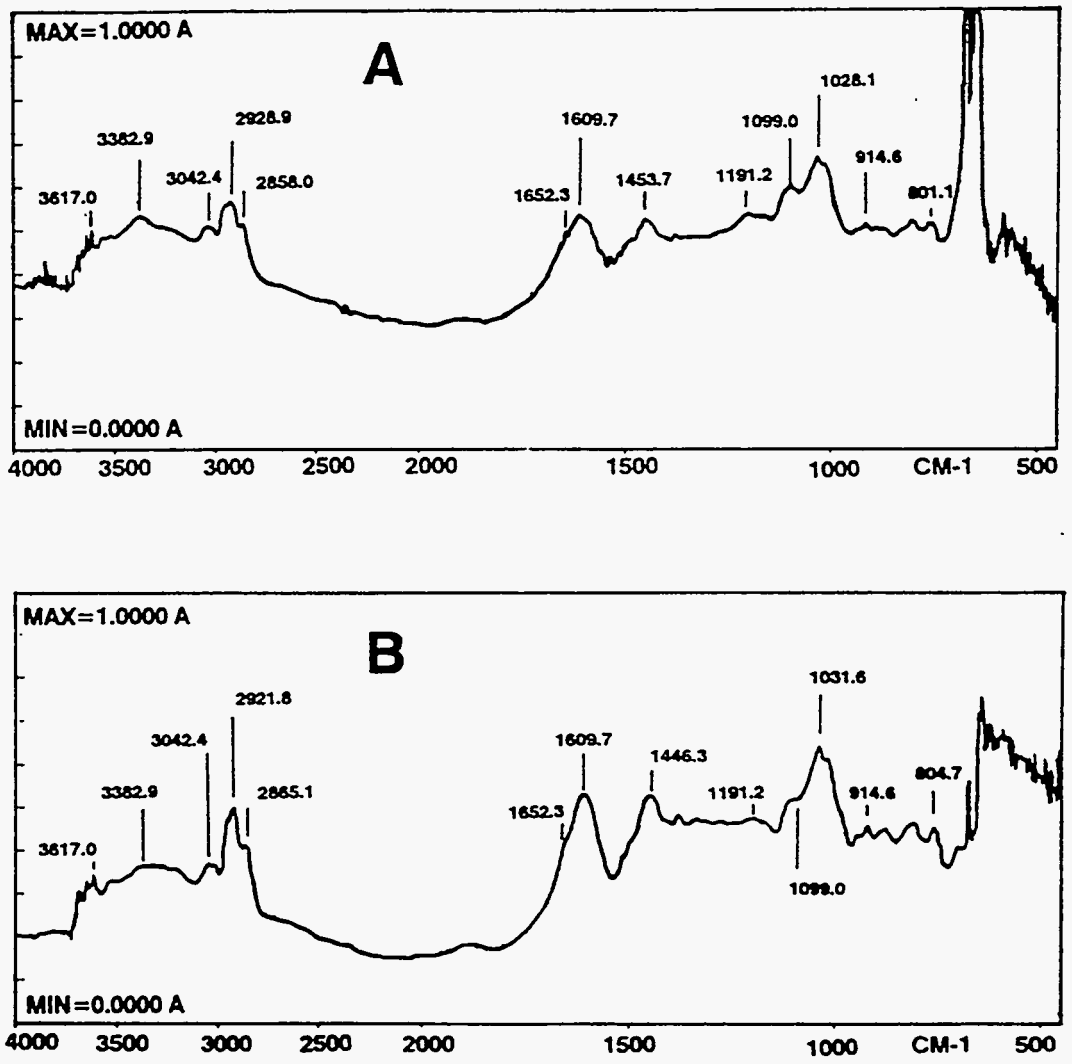

Figure 57. DRIFT spectra of MV bituminous coal (PSOC-1527); (A): as- received; (B) oxidized with 1.0M HNO_3 for 5 hours at room temperature.

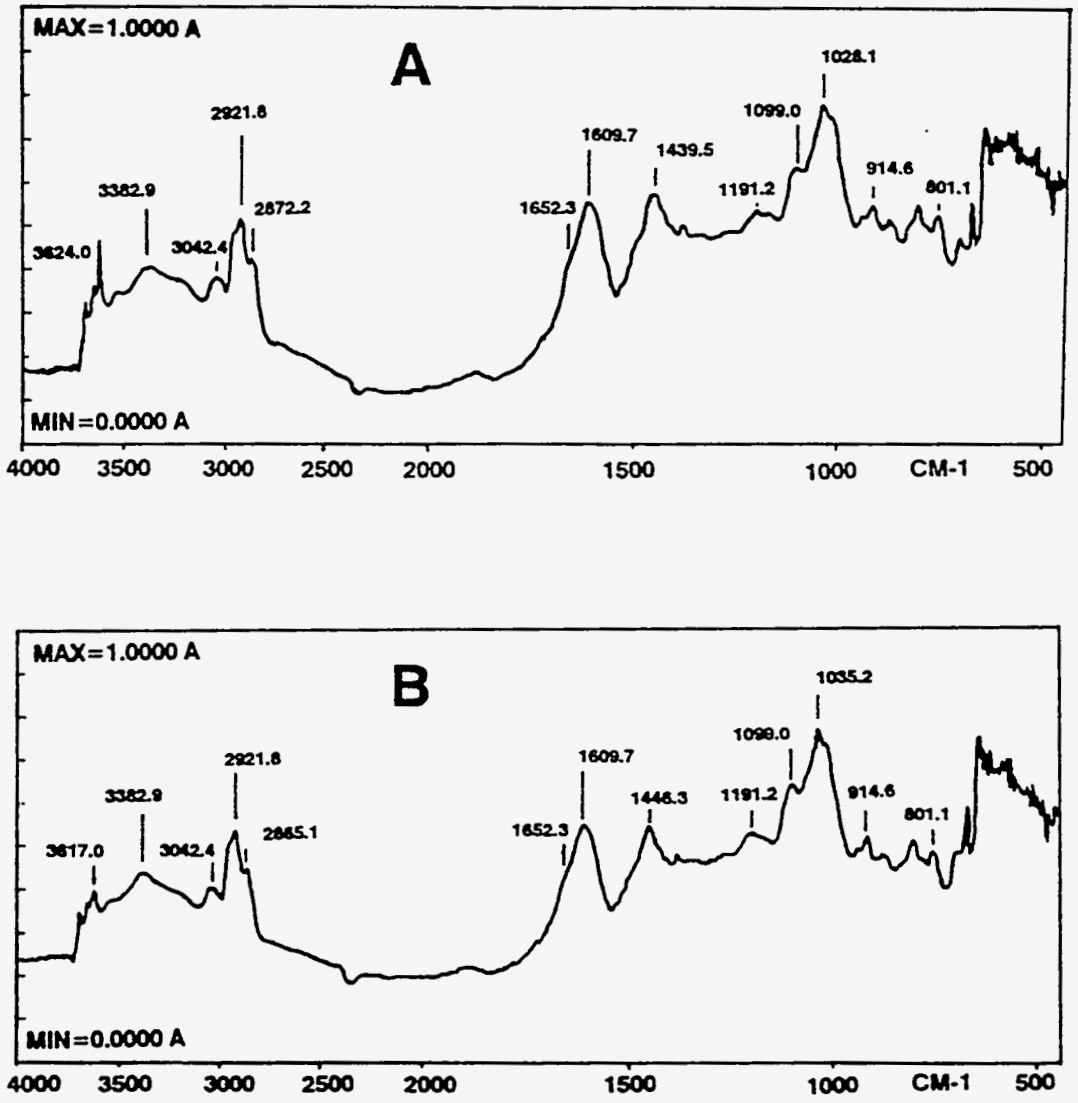

Figure 58. DRIFT spectra of MV bituminous coal (PSOC-1527); (A):oxidized with 10% H_2O_2; (B) oxidized with 0.05M $Fe_2(SO_4)_3$ for 5 hours at room temperature.

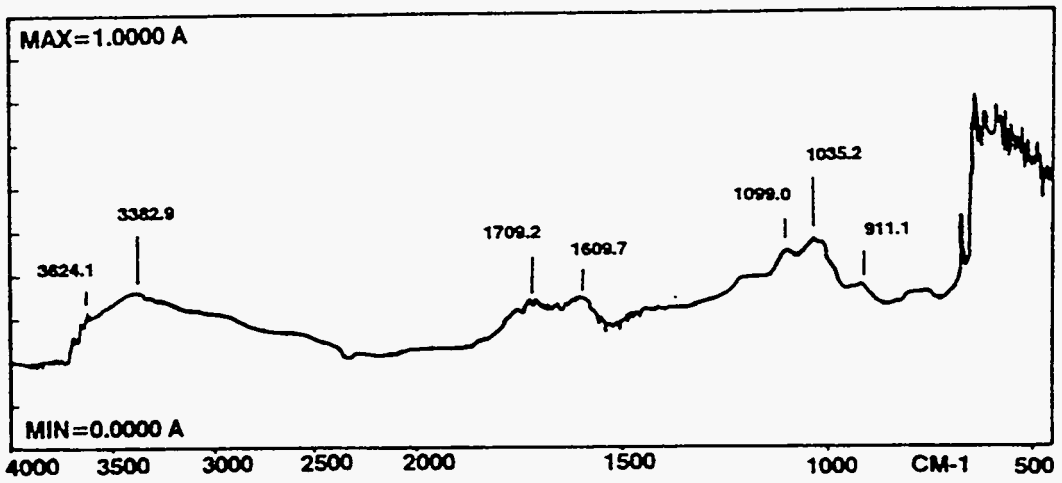

Figure 59. DRIFT spectrum of MV bituminous (PSOC-1527) coal oxidized with air at 230°C for 24 hours.

The presence of solution potentials above 0.7V during the oxidation tests and quinone structures detected by DRIFT suggests that this reaction likely occurred. In this reaction, hydroquinone structures are oxidized to quinone structures. As the hydroxyl species are consumed, sites with higher oxidation states are produced on the coal surface and other oxidation reactions could occur, leading for example to the formation of carboxylic groups.[112] A small peak was present at about 1191.2 cm^{-1}, probably due to C-O stretching vibrations, mainly of ether groups[200,201] or to C-OH species.[202] The peaks at 1099.0 cm^{-1} and 1028.1 cm^{-1} are probably due to kaolinite.[193,198] In the range between 900 and 650 cm^{-1} this MV bituminous coal exhibited at least nine different peaks of medium intensity which are characteristic of out of plane aromatic C-H deformations.

Figure 60 shows the spectra of anthracite (PSOC-1461) coal, as-received and oxidized with 1.0 M HNO_3. Table 17 summarizes the major features of Figure 60. The spectra indicates that this anthracite coal shows more uniform absorption in the region between 3000-1500 cm^{-1}. As reported earlier, no significant differences between the spectra are evident; this is consistent with the negligible oxidation experienced by this coal (Table 13). The peaks of oxidized coal are practically the same as those discussed in the analysis of dry thermal oxidation at 230°C. Similar spectra (not shown) were obtained for this coal oxidized with H_2O_2 and $Fe_2(SO_4)_3$.

DRIFT spectroscopic analysis is a sensitive technique for detecting changes in the structure of coal as a result of oxidation. A set of four as-received and oxidized coals of different ranks were characterized by DRIFT analysis; good qualitative information on the absorption of the main functionalities present in coals were obtained. The organic structural changes caused by oxidation of different coals in aqueous H_2O_2, HNO_3 or $Fe_2(SO_4)_3$ solutions were in general similar with the exception of the formation of aliphatic ethers in sub-bituminous C (PSOC-1442) and HVA bituminous (PSOC-1481)

Table 17. DRIFT absorption peaks of anthracite (PSOC-1461) coal, as-received and oxidized with HNO_3.

As-received		1.0 N HNO_3	
Peak cm^{-1}	Intensity	Peak cm^{-1}	Intensity
3638.2	0.42	3638.2	0.45
3255.2	0.41	3255.2	0.45
1588.5	0.37	1588.5	0.37
1425.3	0.36	1425.3	0.36
1028.1	0.46	1028.1	0.50
801.1	0.37	801.1	0.35

coals, and the formation of quinone-type structures and aromatic ethers in MV bituminous (PSOC-1527) coal. As expected, no significant differences between as-received and oxidized anthracite coal were detected. The results of this study are not in total agreement with the mechanism of interaction between coal and nitric acid proposed by van Krevelen.[109] He postulated that the first stage of oxidation involves the oxidation of the aliphatic coal chain to form quinone structures that later are transformed to carboxylic groups. Although in this study the presence of quinone-type structures and carboxylic groups was detected, the aliphatic structure of coals was not significantly altered, suggesting that there could be a direct oxidation of the aromatic structure of coals. Kinney *et al.*[46] proposed that at low temperatures the initial reaction of the coal involves the addition of nitric acid to unsaturated structures and the cleavage of other structures, such as phenolic ether linkages, possibly forming nitrophenols.

In the oxidation study by nitric acid, the potential of the coal slurry solutions showed several discontinuities, probably due to the fact that there would have been more than one redox couple in solution, and these need not have been at equilibrium. The behavior of the redox potential with time was an indicator of the complexity involved. The potential of

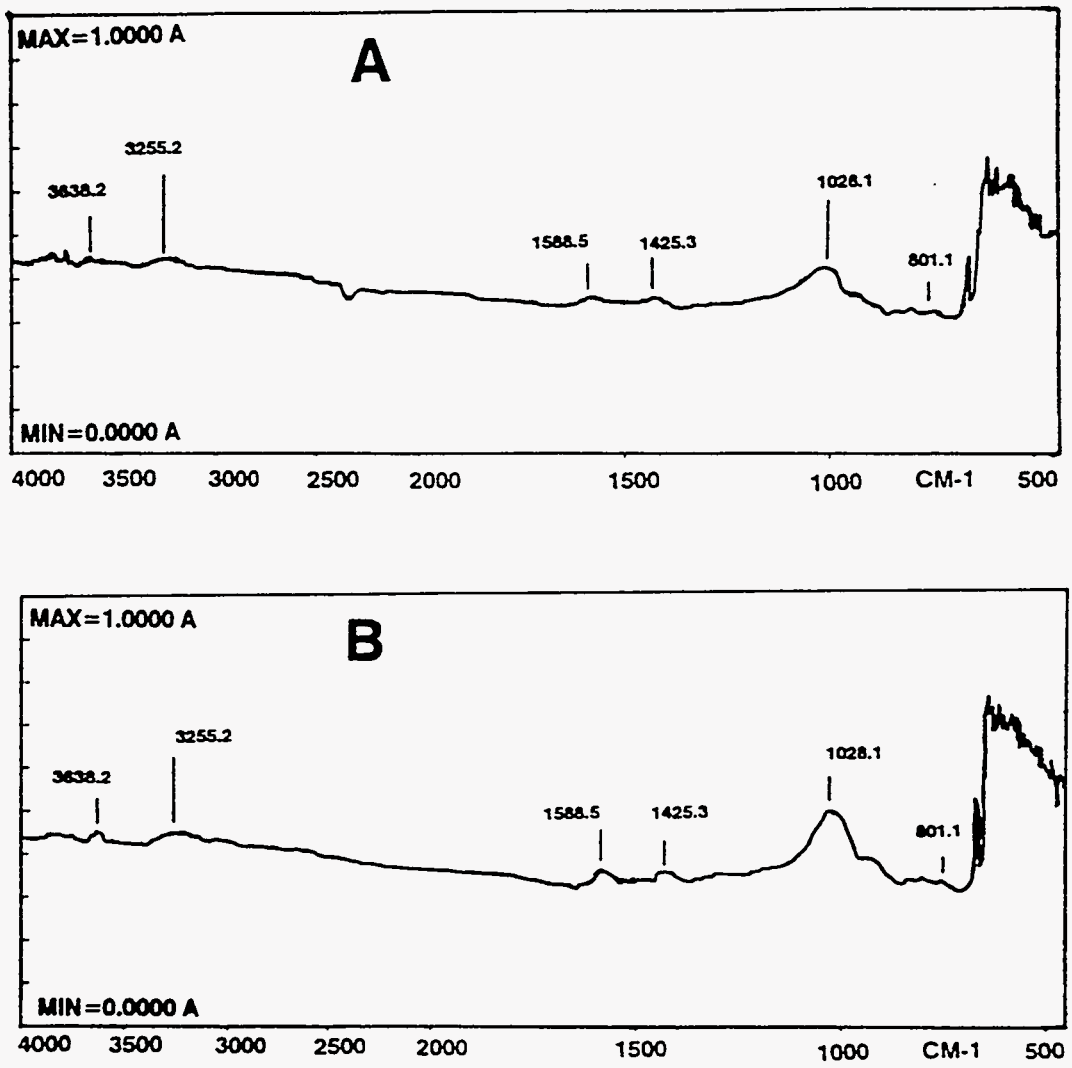

Figure 60. DRIFT spectra of anthracite (PSOC-1461); (A): as- received; (B) oxidized with 1.0M HNO_3 for 5 hours at room temperature.

the platinum working electrode could have changed, depending on the exchange current density, and polarization behavior of each redox couple.

Kaolinite and quartz present in MV bituminous and anthracite coals as ash constituents were unaltered by oxidation. In general, the most significant agreement between the results for oxidation of coals with air at 230°C and wet oxidation using different oxidizing agents was in the appearance of a band at about 1700 cm^{-1}, which is normally attributable to the carbonyl group in carboxylic acids. However, thermal oxidation at 230°C induced significant changes in the aliphatic structure of low rank coals whereas wet oxidation treatments were less severe. The mechanisms of oxidation at 230°C can be interpreted in terms of classical autooxidation reactions in which the first step of oxidation is the formation of hydroperoxide compounds by the oxidation of the aliphatic, olefinic, and ether structures that link the aromatic units present in coal.

According to the above results, oxidation of coals by different oxidizing agents induced changes in the content of oxygen functional groups and other functionalities that affect the surface characteristics of coals. Because of the complex nature of coals, the exact mechanisms of chemical changes that occur during oxidation are not known with certainty; therefore, the chemistry of oxidation is often described in generalities.

B.8 Low Temperature Dry Oxidation Studies on Coals

Coal samples from the Pennsylvania State Coal Bank were also oxidized at room temperature. Five g samples of coals, spread to about 1 mm, were oxidized at ambient humidity (50-70% relative humidity) at room temperature (mean 20^{o}C) for extensive time periods. Room temperature tests were also done at approximately 100 % humidity in a dessicator with water at the bottom . The dessicator valve was left slightly open, to ensure an adequate supply of oxygen. The extent of the oxidation was assessed by analyzing the carboxylic and phenolic functional groups.

Figure 61 shows the carboxylate and phenolic contents of sub-bituminous (PSOC-1442), HVA bituminous (DECS-12) and anthracite (PSOC-1461) coals oxidized at room temperature for 90 days at ambient humidity. The HVA bituminous coal experienced the highest increase in total acidity (carboxylic plus phenolic) in 90 days, whereas the anthracite coal experienced the lowest. The rate of carboxylic group generation appeared to be steady for all coals, with anthracite showing the slowest rate. The HVA bituminous coal had the highest rate of phenolic group generation. Figure 62 shows the carboxylate and phenolic contents for the same coals after oxidation at room temperature and 100% humidity. With the exception of anthracite, the rate of oxidation was initially low but increased markedly after 30 days. Comparing with Figure 61, it is clear that there was more extensive oxidation under humid conditions. Water could accelerate the oxidation of coal by a physical effect, or the oxidation mechanisms could involve surface hydroxyl groups. It has been demonstrated that during adsorption of oxygen on solid surfaces different forms of molecular and ionic oxygen can be formed.[103] As discussed earlier, these ionic forms of oxygen have the capacity to react with water to form hydroxide ions and radicals that can participate in the formation of hydroperoxide compounds and free radicals. Subsequent reactions can proceed to oxidize the surface of coal, generating

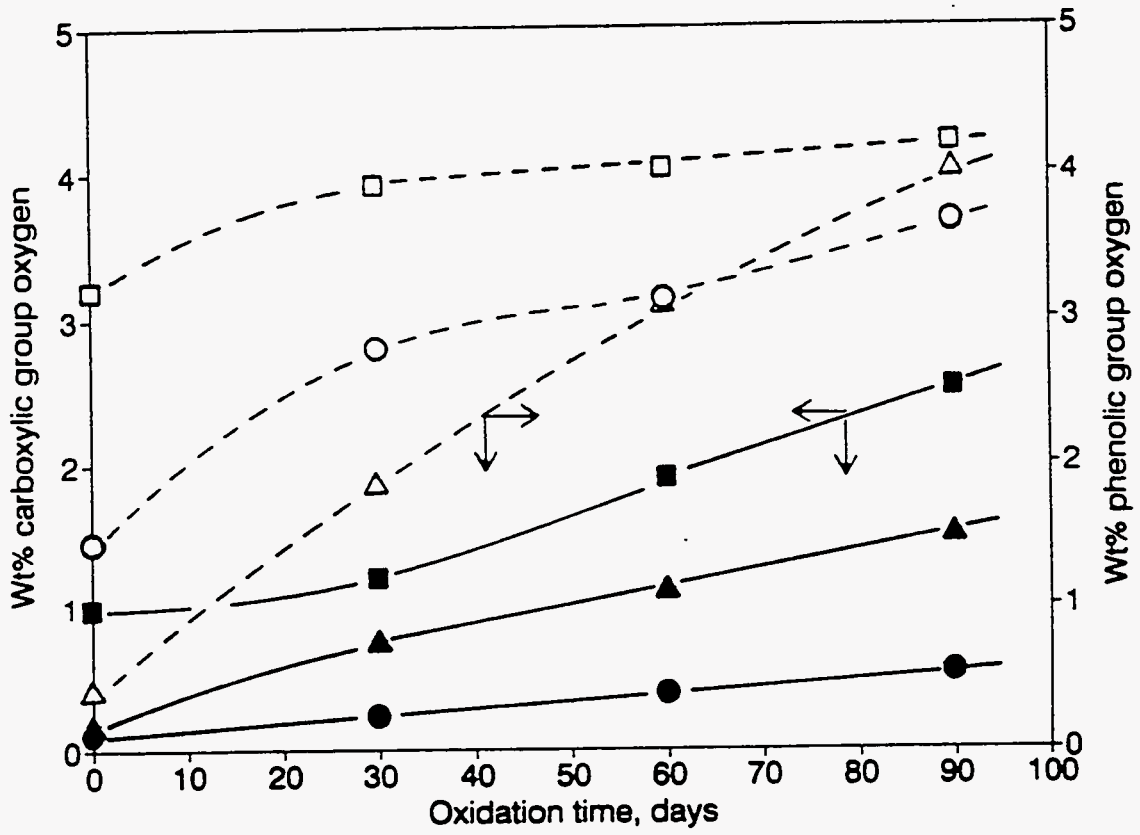

Figure 61. Wt% phenolic and carboxylic oxygen of coals oxidized at room temperature, ambient humidity.
Sub-bituminous (PSOC-1442): □: phenolic, ■: carboxylic;
HVA bituminous (DECS-12): Δ: phenolic, ▲: carboxylic;
Anthracite (PSOC-1461): ○: phenolic, ●: carboxylic.

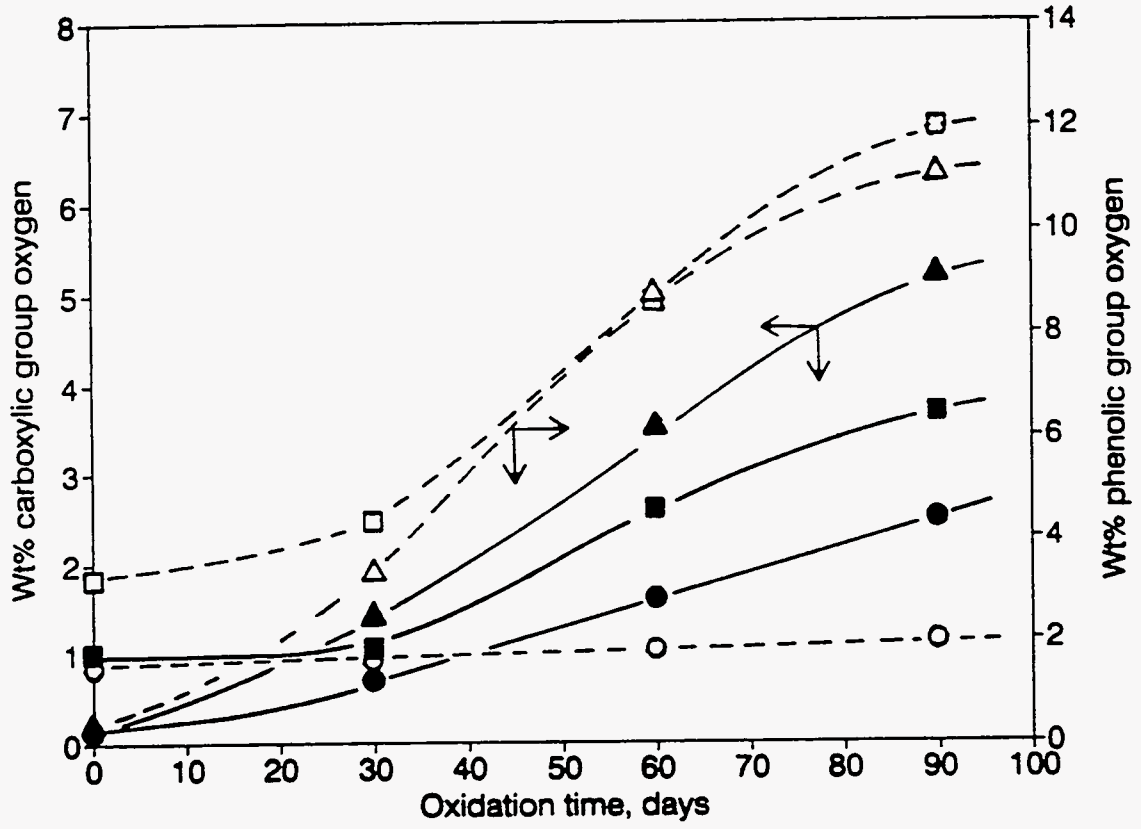

Figure 62. Wt% phenolic and carboxylic oxygen of coals oxidized at room temperature and 100% humidity.
Sub-bituminous (PSOC-1442): ❑: phenolic, ■: carboxylic;
HVA bituminous (DECS-12): Δ: phenolic, ▲: carboxylic;
Anthracite (PSOC-1461): ○: phenolic, ●: carboxylic.

oxygen group functionalities. Thus, water enhances oxidation of coal by catalyzing the formation of free radicals.

Minerals components present in coal are active water sorbents. Particularly in the case of pyrite, the interaction with oxygen and water occurs through sorption of the latter. Pyrite in the presence of water and oxygen is oxidized to form sulfuric acid.[156] It was noted in this study that Sub-bituminous B (PSOC-1539) and HVC Bituminous (PSOC 1486) coals had high susceptibility to sorb water, evidenced by the presence of a thin water layer at the bottom of the petri dishes that contain each coal. The pH of both water layers was estimated using indicator paper, and found to be acidic, suggesting that oxidation of pyrite had occurred. It has been reported that reactions involving peroxide compounds are pH dependent.[68] This could suggest that pyrite indirectly activates the oxidation of coal.

B.9 Flotation Tests

Flotation tests were done on as-received Upper Freeport coal and on coals from the Pennsylvania State Coal Bank. Table 18 shows the oxygen group analysis of each coal, because of the interest in the relationship between this parameter and wettability.

Table 18. Oxygen Group Analysis of Coal Samples Studied.

Sample	Origin	Rank	Wt% Phenolic Oxygen As rec'd	Wt% Carboxyl Oxygen As rec'd
PSOC-1442	Darco, Texas	Sub-bituminous C	3.23	0.99
PSOC-1538	Bottom, Texas	Sub-bituminous C	1.06	0.13
PSOC-1486	Big Dirty, Washington	Sub-bituminous B	1.80	0.30
PSOC-1487	Adaville#1, Wyoming	Sub-bituminous A	0.29	0.21
PSOC-1539	Illinois #6, Illinois	HVC Bituminous	1.68	0.62
PSOC-1497	Illinois #2, Illinois	HVC Bituminous	1.38	1.02
PSOC-1494	Kentucky #9, Kentucky	HVB Bituminous	1.07	0.50
PSOC-1481	Upper Clarion, Pennsylvania.	HVA Bituminous	2.84	0.81
DECS-12	Pittsburgh #8, Pennsylavnia.	HVA Bituminous	0.41	0.15
U.F.	Upper Freeport, Pennsylvania.	MV Bituminous	0.68	1.01
PSOC-1527	Upper Freeport, Pennsylvania.	MV Bituminous	1.22	0.25
PSOC-1516	Lower Kittanning, Pennsylvania.	LV Bituminous	0.02	0.35
PSOC-1515	Penn. Anthracite, Pennsylvania.	Semi Anthracite	0.42	0.11
PSOC-1461	Mammot, Pennsylvania.	Anthracite	1.47	0.11

In order to find a desired conditioning time, the fraction floated or flotation yield of Upper Freeport coal was determined for different conditioning time periods using a 0.5M NaCl solution at pH 5.6. Upper Freeport coal was used in this screening tests because relatively large quantities of this sample were available. Figure 63 shows that the flotation yield was independent of the conditioning time from 5 to 20 minutes. A conditioning time of 10 minutes was selected for this study, to ensure that the electrical charge could develop fully on the coal surface.

Figure 64 shows the flotation yield of Upper Freeport coal as a function of flotation time using a 0.5 M NaCl solution at pH 5.6 after conditioning for 10 minutes.

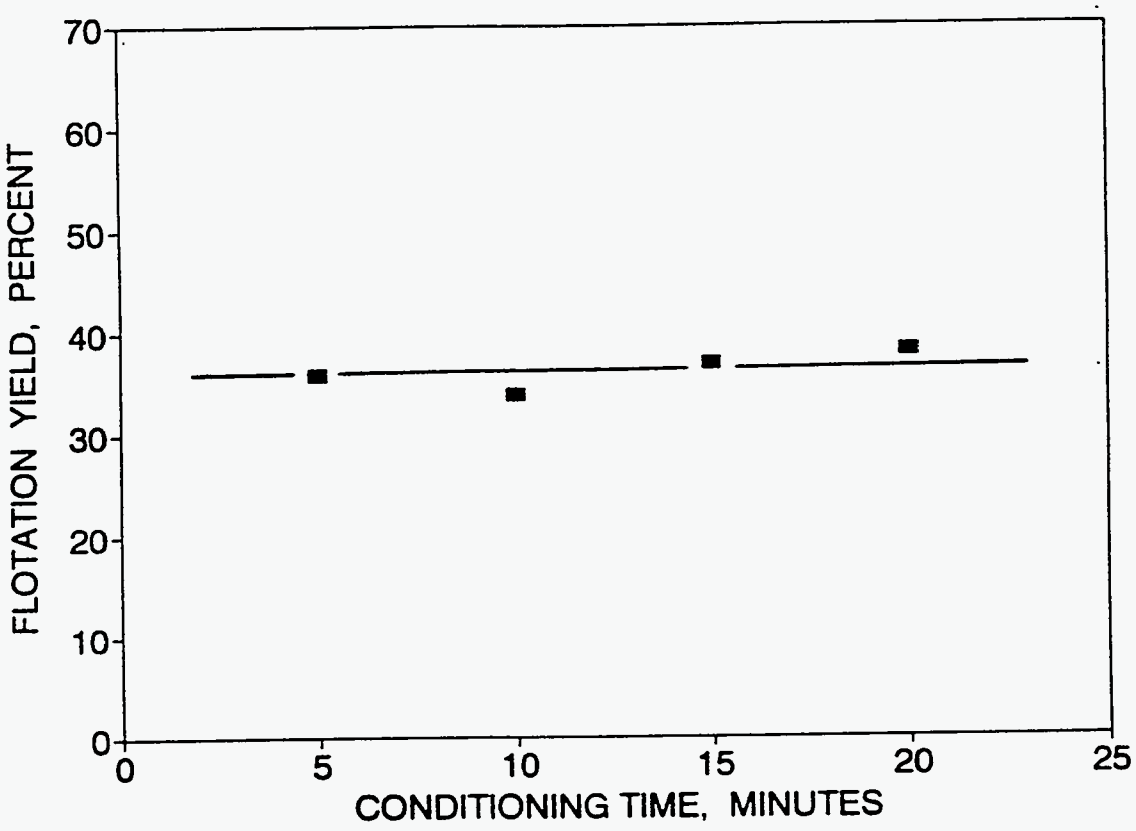

Figure 63. The effect of conditioning time on the flotation yield of as-received Upper Freeport coal in 0.5M NaCl solution at pH 5.6, in a modified Hallimond tube with 3 minutes of flotation.

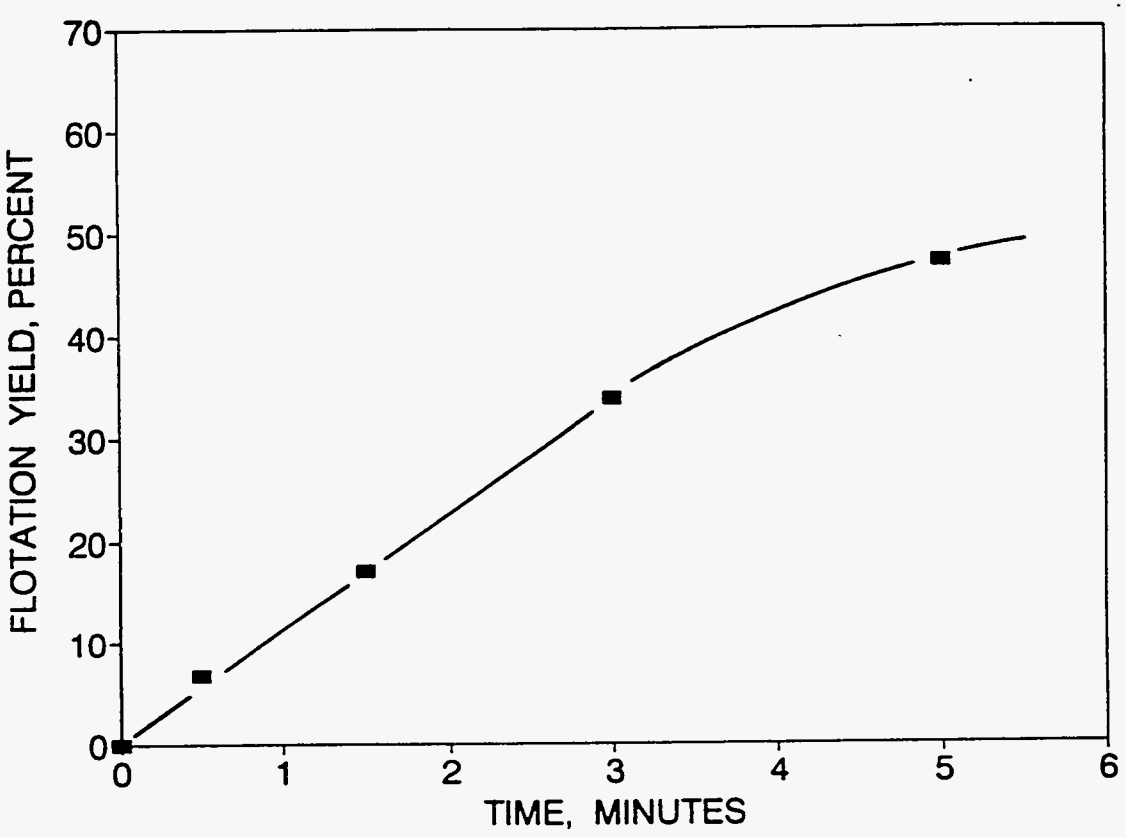

Figure 64. Flotation yield of as-received Upper Freeport coal in 0.5M NaCl solution at pH 5.6 as a function of time, in a modified Hallimond tube after 10 minutes of conditioning time.

Each data point represents a separate flotation test using a new sample. Figure 65 shows ln(1 - flotation yield) plotted as a function of the flotation time. The least-squares regression line shown had a correlation coefficient, r, of 0.9989. Flotation clearly follows first-order kinetics:

$$\ln (1\text{-flotation yield}) = - Kt \qquad (52)$$

where t is the flotation time and K is the flotation rate constant, in this case 0.129 $min.^{-1}$

The effect of the solution pH on the floatability of Upper Freeport coal was tested by salt flotation tests at different pH values. The pH was controlled by additions of HCl or NaOH and each sample was conditioned at the chosen pH for 10 minutes. Figure 66 shows that the flotation yield after 3 minutes reached a maximum of 44.9% at pH 3.1. There was some correlation between flotation yield and zeta potential; the greatest yield ocurred at pH values where the zeta potential was relatively small, although the maximum yield occurred at a pH below the PZR. This effect was probably associated with the ash content (17.6% ash). Some correlation is to be expected, both because the coal surface would become more hydrophobic with low surface charge, and because the rate of bubble/particle attachment would be fastest close to the PZR when there is no retarding force due to overlapping of double layers on the coal particle and nitrogen bubbles.[116,203]

Figure 67 shows the flotation yield versus pH of sub-bituminous (PSOC-1442), HVA bituminous (DECS-12) and anthracite (PSOC-1461) coals obtained in the Hallimond tube after 10 minutes conditioning and 3 minutes flotation. The HVA bituminous and the sub-bituminous coals showed the maximum flotation yield at pH about 3.0 and 2.4 respectively. The anthracite coal gave much lower flotation yield, with a maximum at about pH 3.3. Again, there was some correlation between the maximum

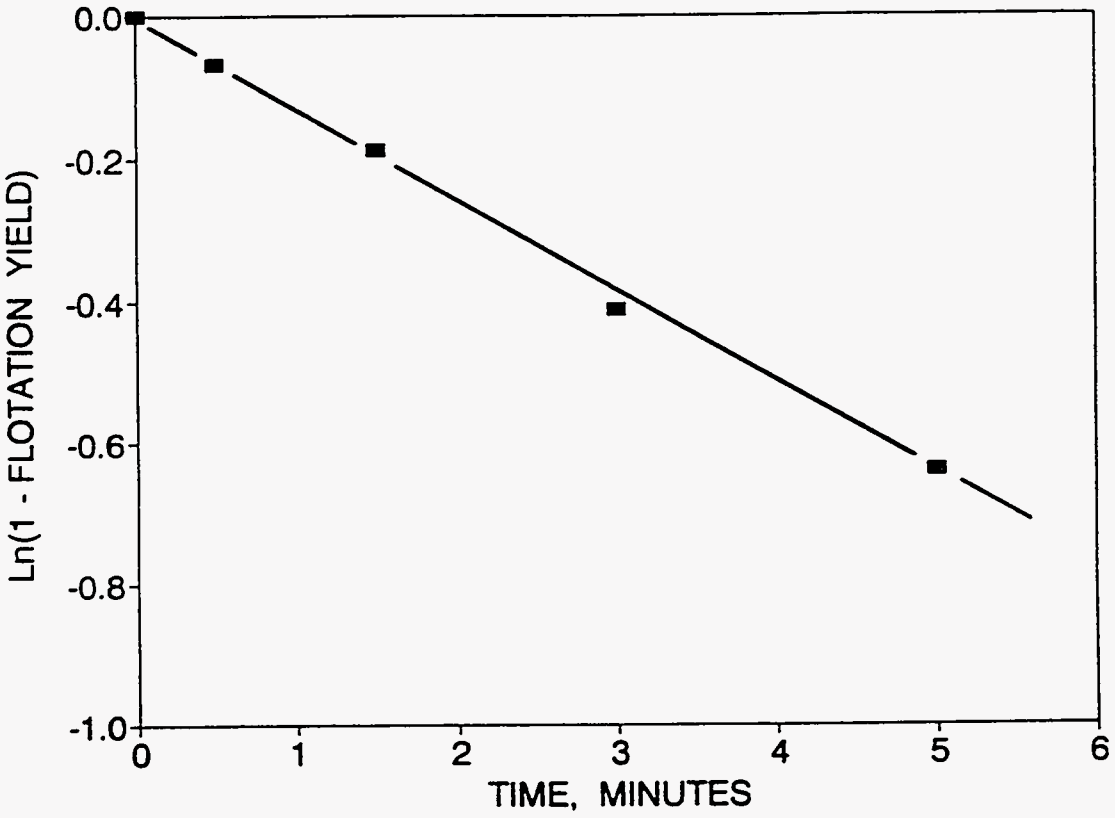

Figure 65. Verification of first order flotation kinetics for Upper Freeport coal in 0.5M NaCl solution at pH 5.6 in a modified Hallimond tube after 10 minutes of conditioning.

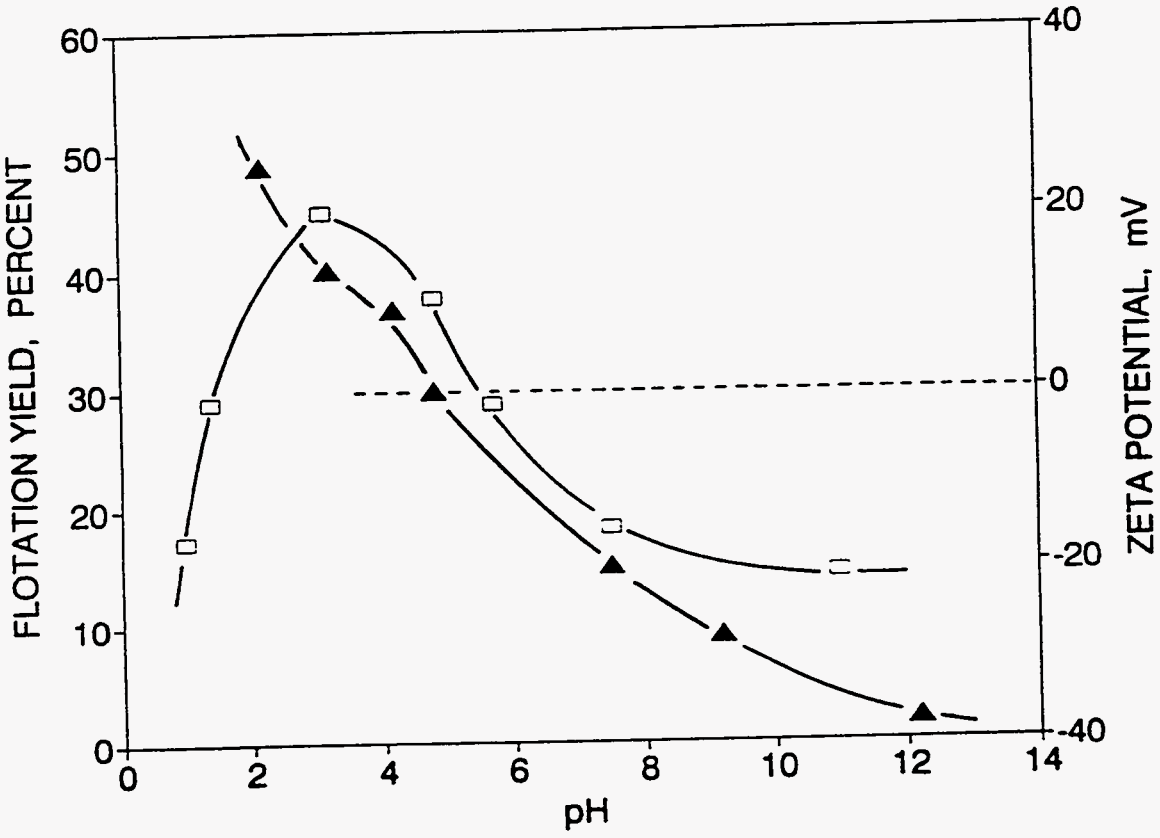

Figure 66. Zeta potential (▲) and flotation yield (❑) (in modified Hallimond tube after 10 minutes conditioning and 3 minutes flotation) of as-received Upper Freeport coal in 0.5M NaCl solution as a function of pH.

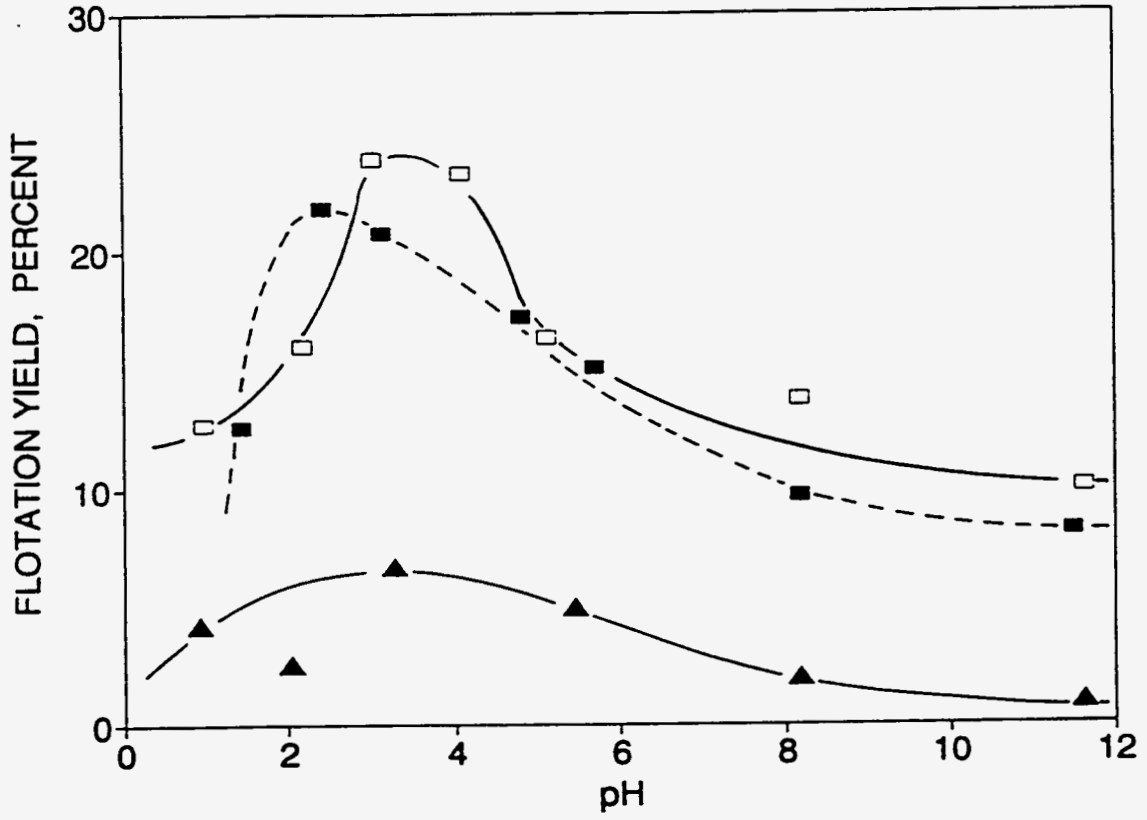

Figure 67. Flotation yields versus pH of coals in 0.5M NaCl solution, using a modified Hallimond tube, with 10 minutes conditioning time and 3 minutes flotation: ■: Sub-bituminous (PSOC-1442); ❑: HVA bituminous (DECS-12); ▲: Anthracite (PSOC-1461).

flotation yield and the reported PZR values of sub-bituminous C (PSOC-1442), HVA bituminous (DECS-12) and anthracite (PSOC-1461) reported earlier (Figures 39,40 and 41). It has been suggested that anthracite coal is more hydrophilic than bituminous coals because of the π electrons associated with the higher level of aromatization.[204]

Figures 68 shows the flotation yield versus pH of LV bituminous (PSOC-1516), MV bituminous coal (PSOC-1527) and HVA bituminous (PSOC 1481) coals. The flotation yields were much higher than those observed in Figure 67. LV bituminous coal had the highest flotation yield, with a maximum at about pH 4.7. The good floatability of this coal is attributed to its low content of nonfloatable components such as moisture, oxygen functional groups, and relatively low content of ash. The somewhat lower floatability of MV bituminous coal might be due to its higher ash content. The floatability of the PSOC-1481 HVA bituminous coal decreased steadily with increasing pH. It should be noted that this coal behaved quite differently from the DECS-12 HVA bituminous shown in Figure 67, which was very similar in composition, except for pyrite and total sulfur content. The reasons for the differences are not fully understood.

Because Hallimond tube salt flotation experiments provide a good measure of the floatability of coals, flotation tests were done on each coal. Table 19 summarizes the maximum flotation yields found for each sample, using 10 minutes of conditioning time and 3 minutes of flotation, along with the pH of flotation maximum. In an attempt to relate the floatability of the coal samples to their composition, chemistry and structure, the maximum flotation yield of each coal was plotted as a function of selected rank parameters from the proximate, sulfur and oxygen group analysis, to identify any parameters that correlated well with flotation yield, either positively or negatively. In each of these plots the coal samples have been identified by a number, as given in Table 19.

Table 19: Relative maximum flotation yields of coal samples studied.

Sample	Origin	Rank	Maximum Flotation Yield, %	pH of Maximum Flotation Yield	Plotting Symbol
PSOC 1442	Darco, Texas	Sub-bituminous C	21.80	2.4	1
PSOC 1538	Bottom, Texas	Sub-bituminous C	37.58	2.0	2
PSOC 1486	Big Dirty, Washington	Sub-bituminous B	11.73	1.2	3
PSOC 1487	Adaville #1, Wyoming	Sub-bituminous A	35.40	4.0	4
PSOC 1539	Illinois #6, Illinois	HVC-Bituminous	28.88	3.2	5
PSOC 1497	Illinois #2, Illinois	HVC-Bituminous	25.41	1.2	6
PSOC 1494	Kentucky #9, Kentucky	HVB-Bituminous	25.39	1.2	7
PSOC 1481	Upper Clarion, Penn.	HVA-Bituminous	43.83	1.0	8
DECS 12	Pittsburgh #8, Penn.	HVA-Bituminous	23.86	3.0	9
PSOC 1527	Upper Freeport, Penn.	MV-Bituminous	57.40	4.7	10
PSOC 1516	Lower Kittanning, Penn.	LV-Bituminous	78.38	4.7	11
PSOC 1515	Penn. Anthracite, Penn.	Semi-Anthracite	11.81	2.0	12
PSOC 1461	Mammoth, Penn.	Anthracite	6.69	3.3	13

Figure 69 shows that with the exception of Upper Freeport coal (PSOC-1527, denoted as 10), higher ash levels tended to decrease the flotation yield. Figure 70 shows that, in general, higher amount of volatile matter give better floatability due to the presence of larger amounts of waxy hydrocarbon components, although the correlation is rather weak. Figure 71 shows that as the fixed carbon content increases, the flotation yield rises to a maximum for low and medium volatile bituminous coals and decreases for the anthracite as discussed above. Figures 72 and 73 show poor flotation at high phenolic and carboxylic oxygen contents, but poor correlation of flotation with the oxygen content at low levels. The decrease in floatability at high oxygen levels is a consequence of the

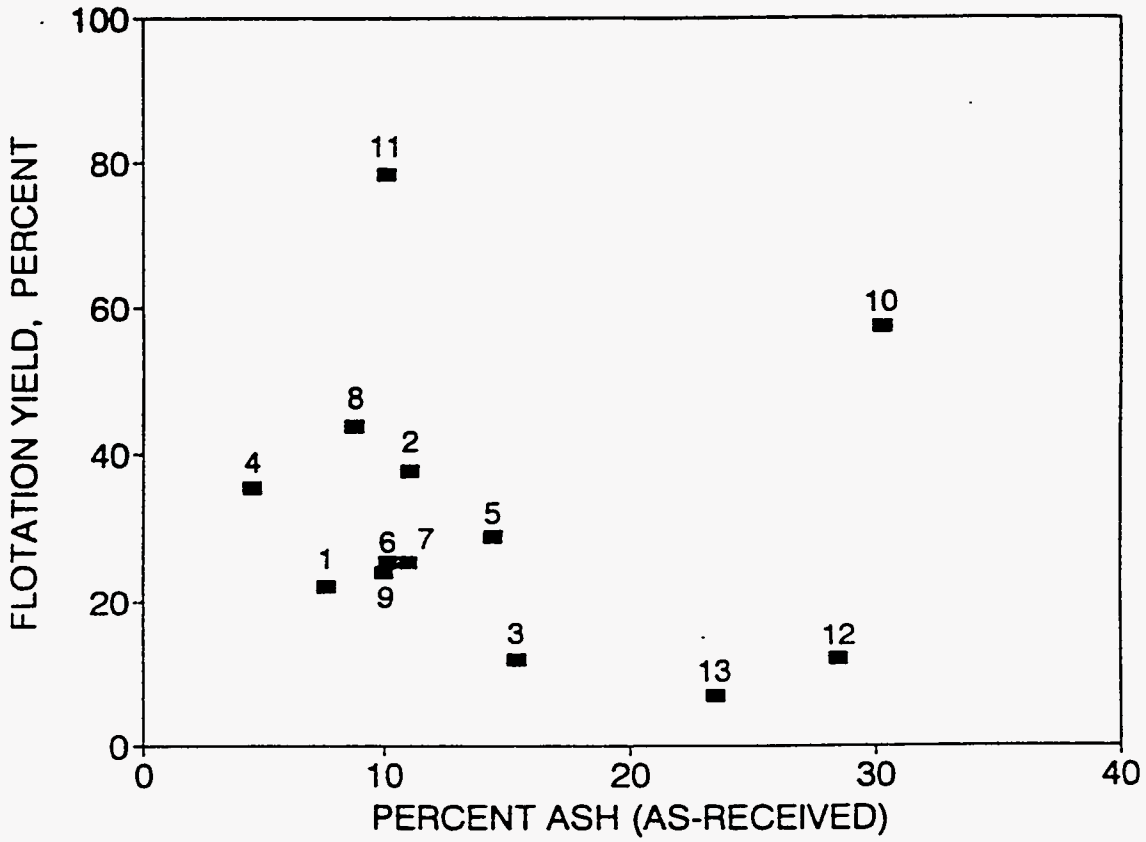

Figure 69. Maximum flotation yields versus ash content (as-received) of coals. Flotation performed in modified Hallimond tube, using 0.5M NaCl, 10 minutes conditioning time, 3 minutes flotation. See Table 19 for key to sample numbers and pH of maximum flotation yield.

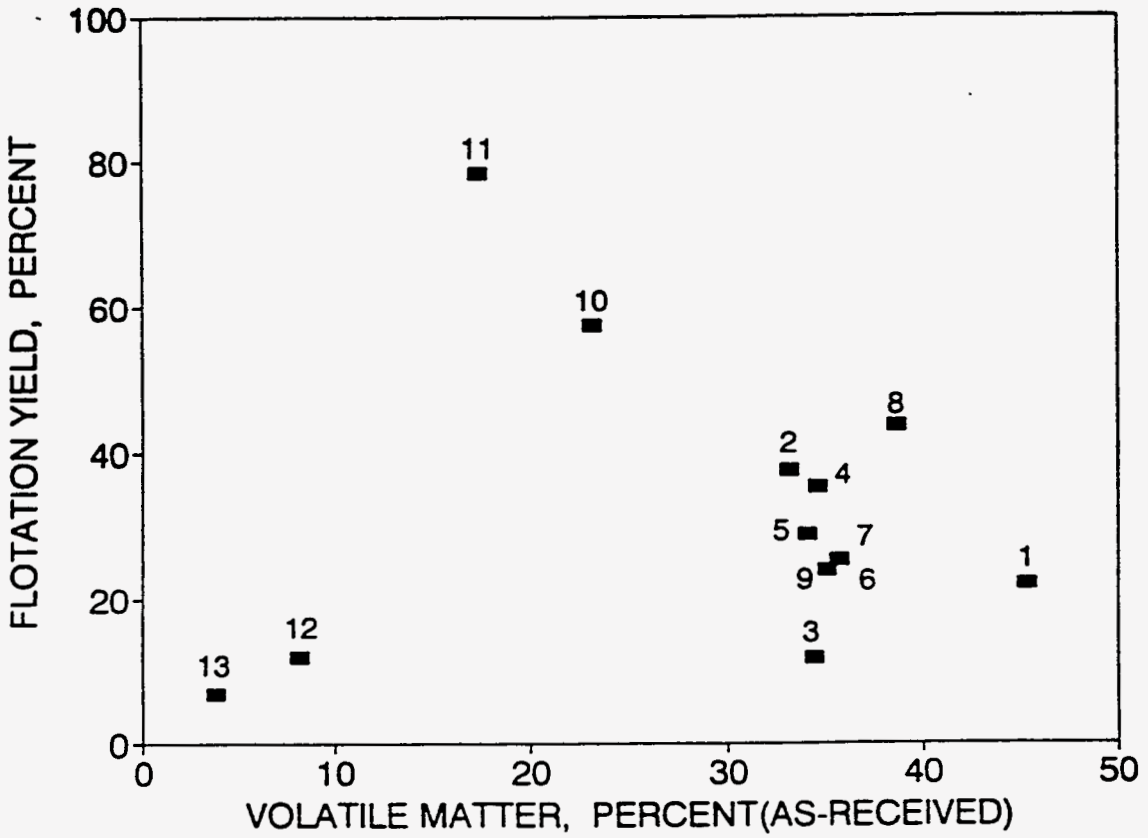

Figure 70. Maximum flotation yields versus volatile matter (as-received) of coals. Flotation performed in modified Hallimond tube, using 0.5M NaCl, 10 minutes conditioning time, 3 minutes flotation. See Table 19 for key to sample numbers and pH of maximum flotation yield.

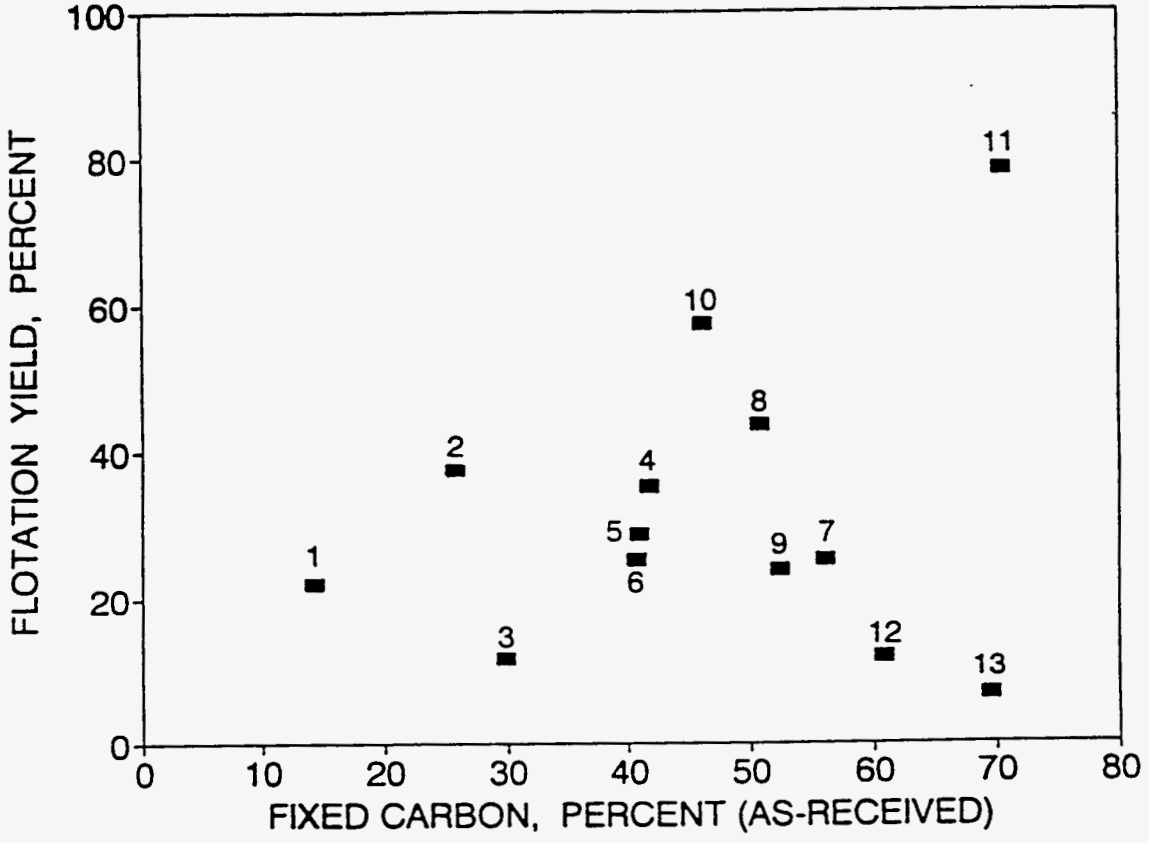

Figure 71. Maximum flotation yields versus fixed carbon content (as-received) of coals. Flotation performed in modified Hallimond tube, using 0.5M NaCl, 10 minutes conditioning time, 3 minutes flotation. See Table 19 for key to sample numbers and pH of maximum flotation yield.

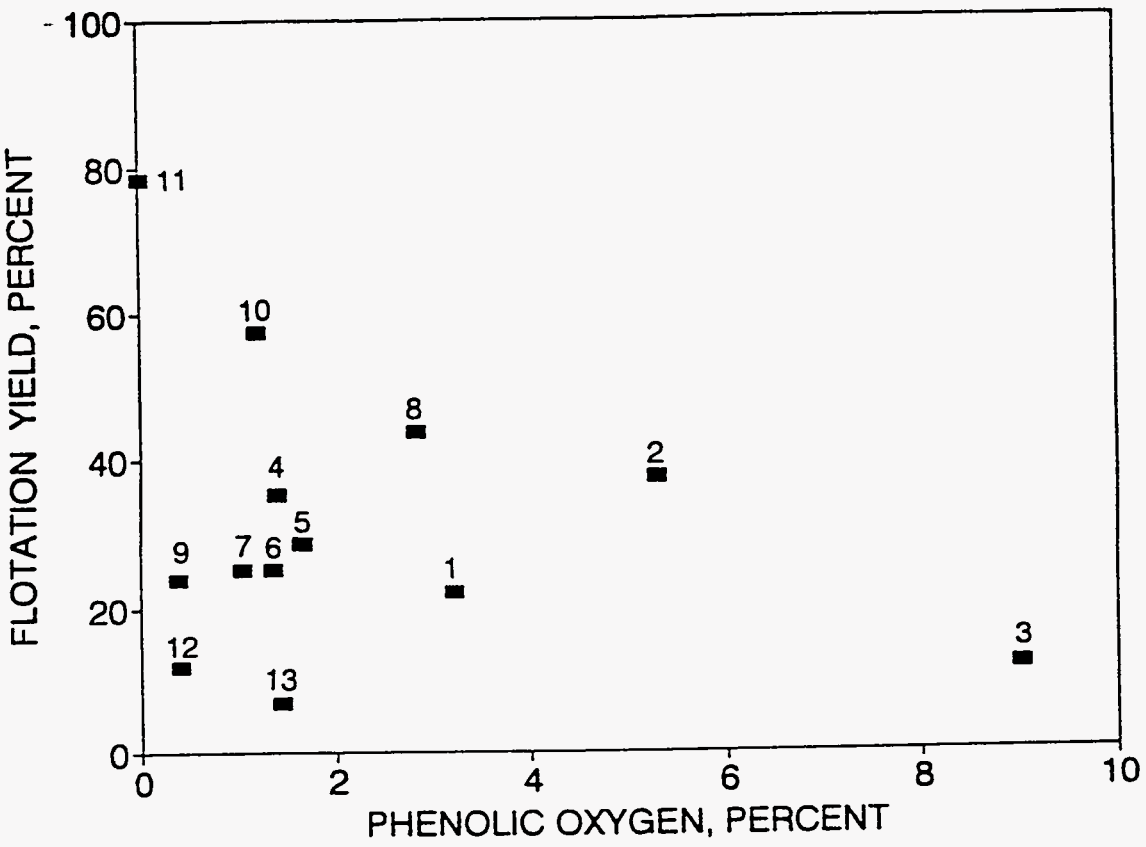

Figure 72. Maximum flotation yields versus phenolic oxygen content (as-received) of coals. Flotation performed in modified Hallimond tube, using 0.5M NaCl, 10 minutes conditioning time, 3 minutes flotation. See Table 19 for key to sample numbers and pH of maximum flotation yield.

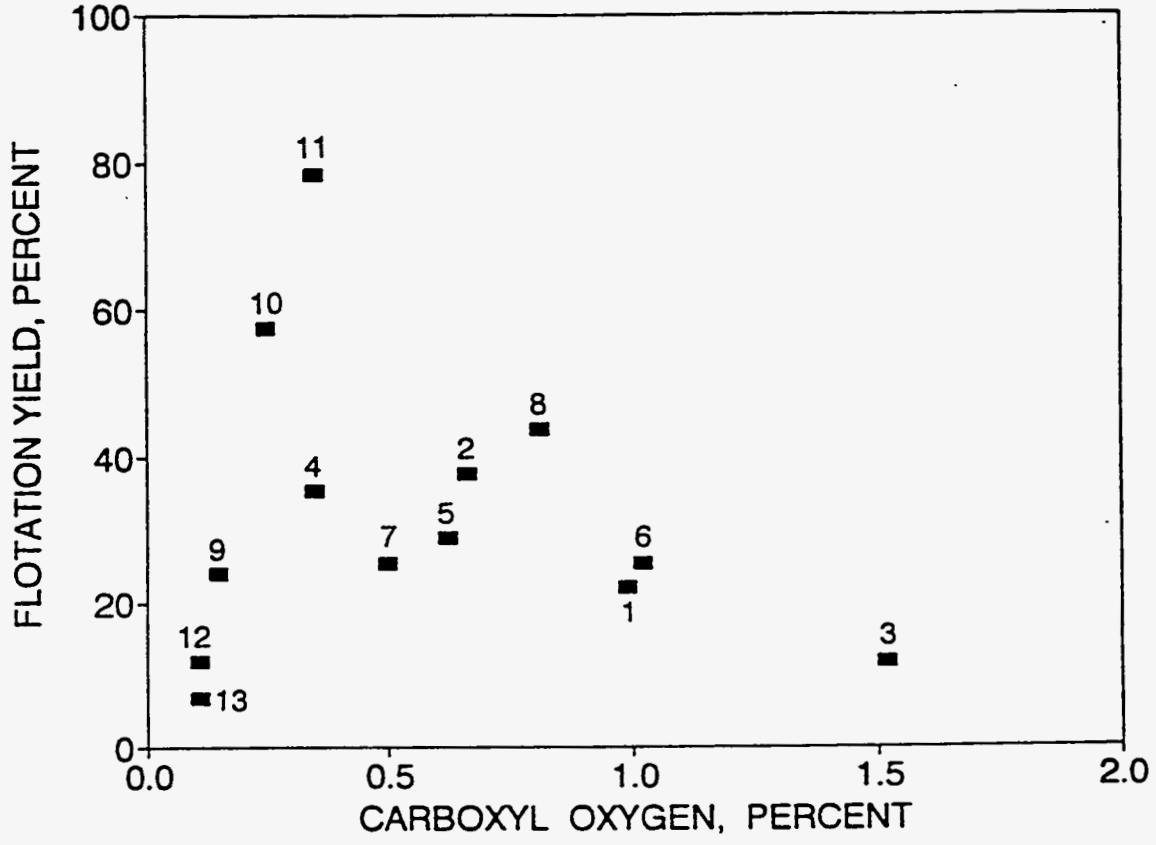

Figure 73. Maximum flotation yields versus carboxylic content (as-received) of coals. Flotation performed in modified Hallimond tube, using 0.5M NaCl, 10 minutes conditioning time, 3 minutes flotation. See Table 19 for key to sample numbers and pH of maximum flotation yield.

high affinity between polar water molecules and oxygen sites on the surface. Acidic oxygen functional groups also affect the electrical charge on the coal surface, which influences the rate of contact between bubbles and the coal particles. However, the maximum flotation yields tended to be at pH values lower than the pK_a's expected for the carboxylic acid present, so that this effect is probably weak. Figure 74 shows that with the exception of semi-anthracite and anthracite coals, high moisture content significantly reduced the floatability of coals. The amount of water generally correlates well with the content of phenolic and carboxylic groups. Thus, it is possible that most of the water present in coals is adsorbed on sites made hydrophilic by the presence of functional groups.

It should be noted that neither regressional nor statistical analysis were done with the data of flotation tests.

Figures 75 and 76 show the flotation yield versus pH of as received and oxidized sub bituminous C (PSOC-1442), HVA Bituminous (DECS-12), LV Bituminous (PSOC-1516) and anthracite (PSOC-1461) coals obtained in the Hallimond tube after 10 minutes conditioning and 3 minutes flotation. Clearly, in agreement with Figures 72 and 73, the floatability of coals samples oxidized at 230°C for 24 hours, is reduced significantly. The effect is particularly dramatic for sub-bituminous and bituminous coals.

Table 20 shows the percentage of total sulfur present on coal samples in the feed, concentrate and tailing fractions during salt flotation of as-received coals all at the pH of maximum flotation. With the exception of HVA bituminous coal (PSOC-1481), the total sulfur content of each coal sample (28x65 mesh size fraction) in the feed was lower than those reported in Table 7 for the whole coal sample. It should be noted, that different size fractions have different total sulfur content. Because coal samples have been under

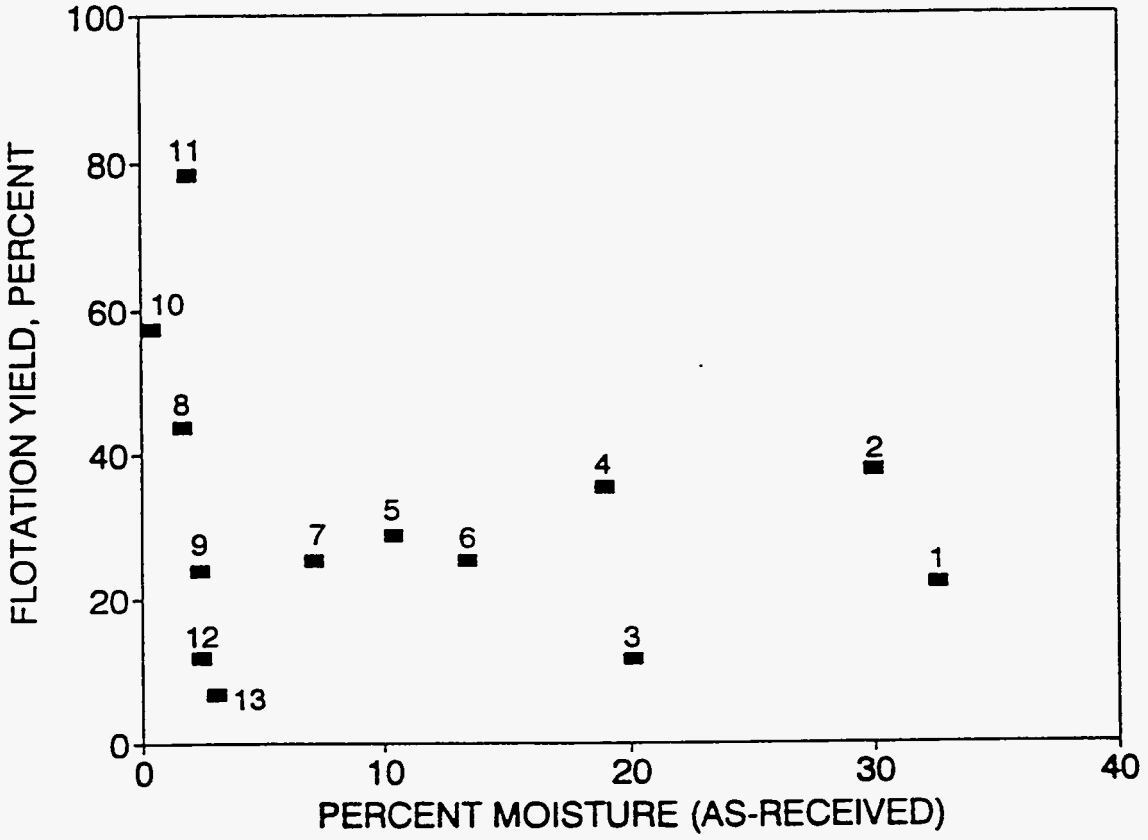

Figure 74. Maximum flotation yields versus moisture content (as-received) of coals. Flotation performed in modified Hallimond tube, using 0.5M NaCl, 10 minutes conditioning time, 3 minutes flotation. See Table 19 for key to sample numbers and pH of maximum flotation yield.

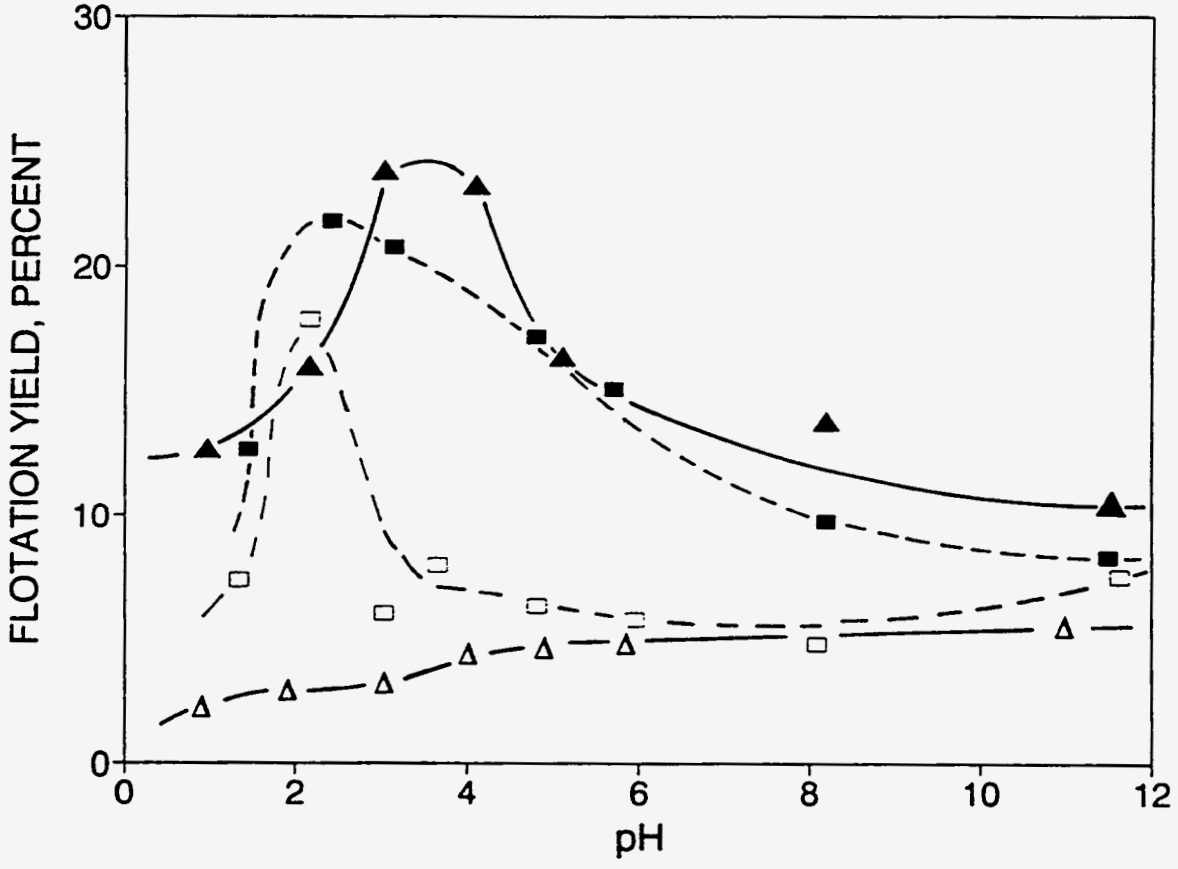

Figure 75: Flotation yield versus pH of coals in 0.5M NaCl solution, using a modified Hallimond tube, with 10 mins conditioning and 3 minutes flotation: HVA Bituminous (DECS-12):Δ:oxidized, ▲:as-received;
Sub-bituminous C (PSOC-1442): ❑:oxidized, ■:as-received.

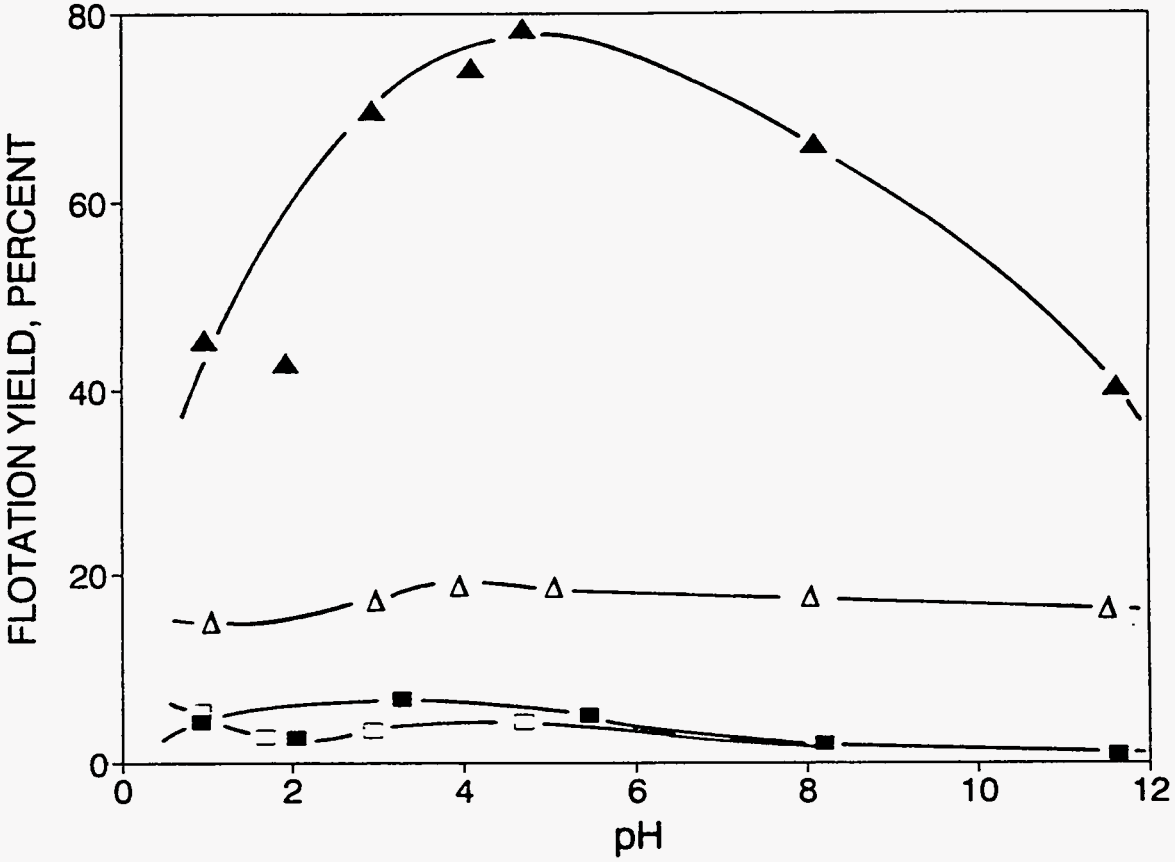

Figure 76: Flotation yield versus solution pH of coals in 0.5M NaCl solution, using a modified Hallimond tube, with 10 mins conditioning and 3 minutes flotation:
LV Bituminous (PSOC-1516):Δ:oxidized, ▲:as-received;
Anthracite (PSOC-1461): ❑:oxidized, ■:as-received.

Table 20: Sulfur percentage in the feed, concentrate, and tailing fractions in salt flotation of as-received coals all at pH of maximum flotation.

Sample	Maximum Flotation Yield, %	Wt% Sulfur Feed	Wt% Sulfur Concentrate	Wt% Sulfur Tailing	pH of Maximum Flotation Yield
PSOC 1442	21.80	0.40	0.26	0.45	2.4
PSOC 1538	37.58	0.37	0.43	0.32	2.0
PSOC 1486	11.73	0.29	ND	ND	1.2
PSOC 1487	35.40	0.76	0.42	0.85	4.0
PSOC 1539	28.88	2.66	2.41	3.16	3.2
PSOC 1497	25.41	2.10	2.00	2.12	1.2
PSOC 1494	25.39	4.12	2.20	2.23	1.2
PSOC 1481	43.83	6.00	1.64	1.87	1.0
DECS 12	23.86	0.49	0.39	0.57	3.0
Upper Freeport	44.90	0.62	0.37	0.58	3.1
PSOC 1527	57.40	0.57	0.74	ND	4.7
PSOC 1516	78.38	0.35	0.28	0.72	4.7
PSOC 1515	11.81	0.34	0.21	ND	2.0
PSOC 1461	6.69	ND	ND	ND	3.3

ND:Less than 0.1 wt% sulfur.

storage for extensive periods, it is possible that some gaseous sulfur compound such as H_2S had evolved, lowering the total sulfur content of coal samples.

Table 20 indicates that with the exception of sub-bituminous C (PSOC-1538) coal, the percentage of total sulfur was higher in the tailing than in the concentrate, suggesting that flotation of inorganic sulfur has been depressed by oxidation of pyrite despite all effort to minimize probably contact with air. HVB bituminous (PSOC-1494), HVA bituminous (PSOC-1481), and MV bituminous coals show higher percentage of total sulfur in the feed than in the concentrate and tailing fractions. The reason for these inconsistencies are not

Table 21. Sulfur percentage in the feed, concentrate, and tailing fractions in salt flotation of oxidized coals at 230°C for 24 hours, all at pH of maximum flotation.

Sample	Maximum Flotation Yield, %	Wt% Sulfur Feed	Wt% Sulfur Concentrate	Wt% Sulfur Tailing	pH of Maximum Flotation Yield
PSOC 1442	17.91	0.40	ND	ND	2.2
DECS 12	4.67	0.49	0.73	0.44	4.7
PSOC 1516	18.40	0.35	ND	0.47	4.0
PSOC 1461	2.71	ND	ND	0.5	1.7

ND:Less than 0.1 wt% sulfur

fully understood, although some sulfatic sulfur species could have been dissolved during the tests at low pH.

Table 21 gives the sulfur percentage in the feed, concentrate, and tailing fractions in the salt flotation of oxidized coals, all at the pH of maximum flotation. The total sulfur content of HVA bituminous (DECS-12) coal in the concentrate was higher than in the tailing fraction, indicating that coal particles in the concentrate were rich in hydrophobic organic sulfur, whereas coal particles in the tailing were rich in hydrophilic functional groups and oxidized coal pyrite.

Flotation studies under controlled potential and pH conditions were carried out to investigate the effect of polarization on the flotation of coal. The Hallimond tube used in this study had a platinum disk electrode fitted into the flotation zone. The electrical control was obtained by inserting a platinum counter electrode through the top of the tube while contact with the reference electrode was obtained through a fritted glass disk connecting the main tube with the reference electrode compartment. In each experiment, the flotation yield was studied as a function of the solution potential at the optimum pH of each coal sample given in Table 19.

Figure 77 shows the flotation yield versus solution potential of HVC Bituminous (PSOC-1497), HVB Bituminous (PSOC-1494) and HVA Bituminous (PSOC-1481) coalsobtained in a specially modified Hallimond tube after 10 minutes conditioning and 3 minutes flotation. As summarized in Table 7, these coal samples contain high amounts of pyritic sulfur and were used to check possible polarization effects. The results given in Figure 77 show that on reducing the solution potential, the flotation yield slightly increases, possibly due to the reduction of the functional groups on the coal surface which would cause the coal surface became more hydrophobic. Table 22 shows that at low potentials, the total sulfur content is higher in the concentrate fractions. The total sulfur in the tailing fraction must be rich in pyritic sulfur since at these negative potentials, the surface of pyrite is more hydrophilic (to be discussed later) due to the reduction of pyrite to FeS or Fe_{2-x}. On increasing the solution potential, the flotation yield decreased substantially for HVB Bituminous (PSOC-1494) and HVC Bituminous (PSOC-1497) coals. Table 22 indicates that at high potentials the total sulfur content was higher in the tailing fractions. The effect was particularly noticeable in the HVB Bituminous (PSOC-1494) and HVC Bituminous (PSOC-1497) coals with high content of pyritic sulfur. It was observed (to be discussed in the next section) that when pyrite was oxidized at high potential, its wettability was significantly reduced probably due to the formation of a hydrophilic oxide layer on its surface. Also, at high potential the flotation of coal is reduced by the presence of highly oxidized funtional groups on the coal surface.

In Figure 78, the flotation yield is presented as a function of solution potential of HVC Bituminous coal (PSOC-1539), MV Bituminous coal (PSOC-1527) and Upper Freeport (MV Bituminous) coals obtained in a specially modified Hallimond tube after 10 minutes conditioning and 3 minutes flotation. These plots indicate that only Upper Freeport coal exhibits similar behavior to those observed in Figure 77.

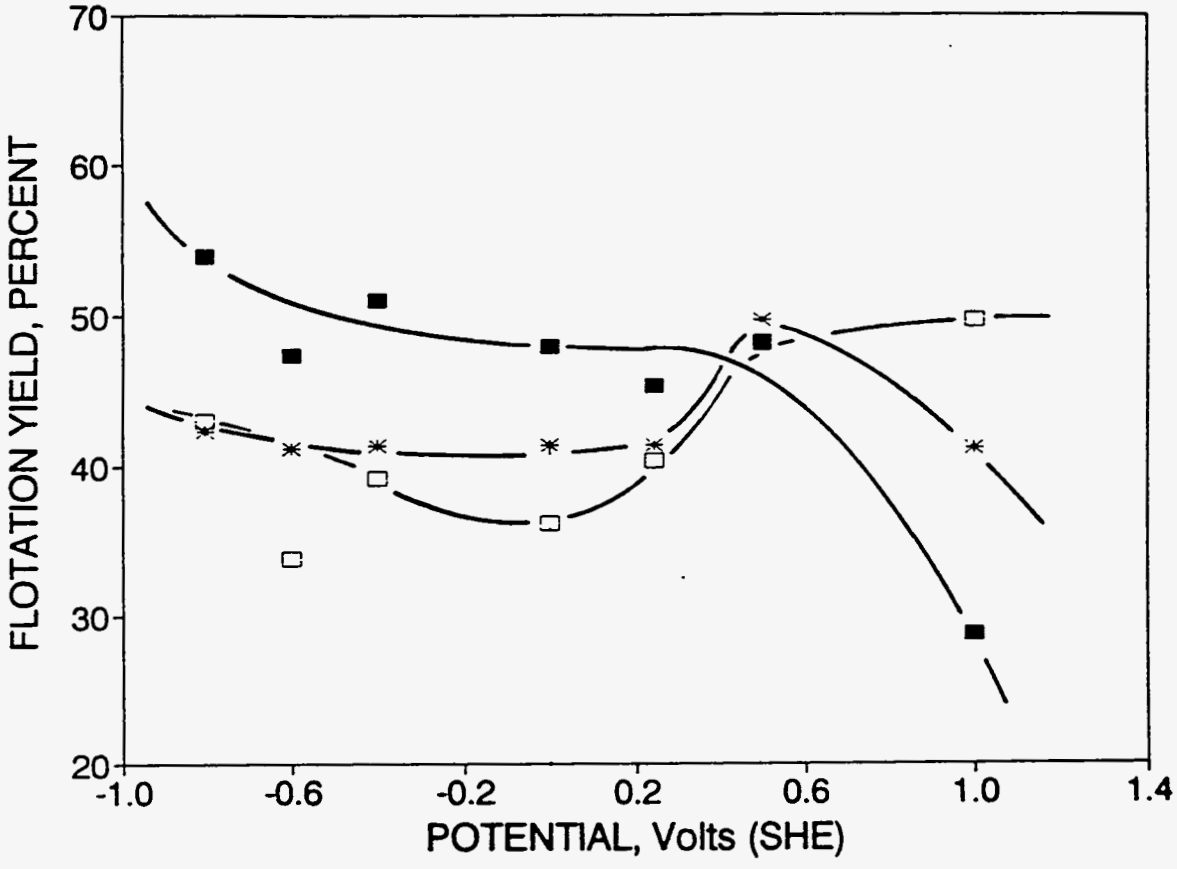

Figure 77: Flotation yield versus solution potential of coals in 0.5M NaCl solution, using a modified Hallimond tube, with 10 mins conditioning and 3 minutes flotation:
■: HVC Bituminous (PSOC-1497); :*: HVB Bituminous (PSOC-1494);
❑: HVA Bituminous (PSOC-1481).

Table 22. Sulfur percentage in the feed, concentrate, and tailing fractions in salt flotation of as-received coals as a function of the solution potential all at pH of maximum flotation.

Sample	wt%S Feed	-0.8 Volts (SHE)		-0.4 Volts (SHE)		0.5 Volts (SHE)		1.0 Volts (SHE)		pH
		Wt%S. Conc.	Wt%S. Tail.	Wt%S. Conc.	Wt%S. Tail.	Wt%S. Conc.	Wt%S. Tail.	Wt%S. Conc.	Wt%S. Tail.	Max. Flotation
PSOC 1497	2.10	1.66	1.64	1.96	2.64	1.97	2.12	1.47	2.55	1.0
PSOC 1494	4.12	2.30	1.82	NA	NA	2.42	4.45	1.71	5.10	3.0
PSOC 1481	6.00	1.67	1.46	1.53	2.65	2.10	2.79	NA	NA	1.0
Upper Freeport	0.62	0.20	0.25	NA	NA	0.26	0.42	ND	0.37	3.5
PSOC 1527	0.57	0.57	1.50	NA	NA	0.70	1.25	0.84	0.50	4.5
PSOC 1539	2.66	2.32	2.72	2.71	3.94	2.43	3 86	2.24	3.39	3.0

NA:Not available
ND:Less than 0.1 wt% sulfur

At negative potentials the flotation yield of HVC Bituminous coal (PSOC-1539) decreases in conjuction with a tailing fraction with higher total sulfur than the concentrate fraction. At positive potentials the flotation yield of MV Bituminous (PSOC-1527) coal increases, due to a oxidation of pyrite to hydrophobic polysulfide species at high potentials. The higher flotation yield is also consistent with a concentrate fraction more rich in sulfur.

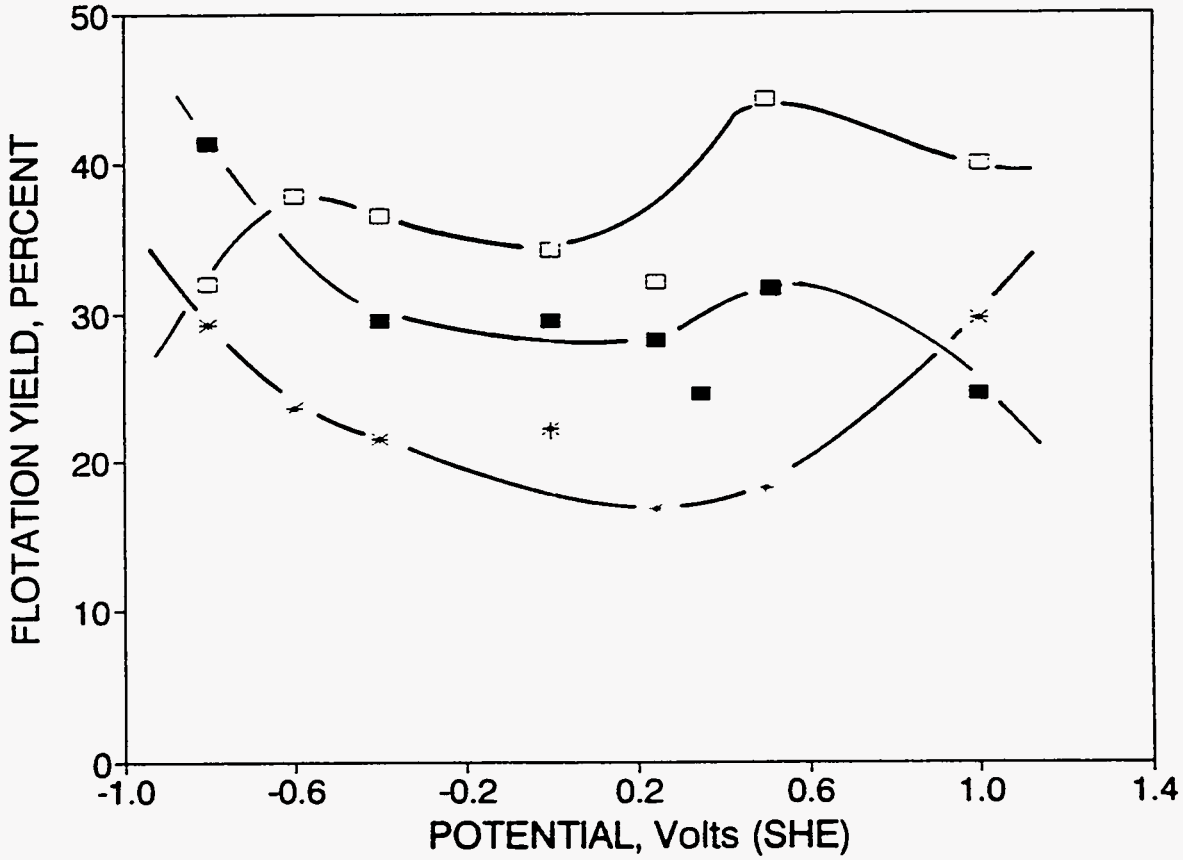

Figure 78: Flotation yield versus solution potential of coals in 0.5M NaCl solution, using a modified Hallimond tube, with 10 mins conditioning and 3 minutes flotation:
■: MV Bituminous (UF); :*: MV Bituminous (PSOC-1527);
❑: HVC Bituminous (PSOC-1539).

C. Electrochemical Studies on Coal Pyrite Samples.

C.1. Rest Potential Measurements

The potentials of both pyrite samples in the different buffer solutions at 0 and 24 hours is shown in Table 23. The potentials measured initially were relatively high, then

Table 23. Potentials of Coal Pyrite Electrodes (mV SHE ± 10 mV)

Pyrite Source	pH 1.0		pH 7.4		pH 9.3		pH 10.5	
	Initial	24 hrs	Initial	24 hrs	Initial	24 hrs	Initial	24 hrs
Upper Freeport	727	311	586	303	600	273	-	-
Pittsburgh	645	552	730	323	360	249	305	205

decreased, albeit to different extents. After 24 hours the potentials were fairly steady. Since there was no added oxidant or reductant in any of the electrolytes, the pyrite should have established an equilibrium potential rapidly, and remained at this potential. The steady decrease over the first 24 hours or so is indicative of some reaction or physical transformation. Recognizing this, we designate the potential after 24 hours as the "rest potential", with the caveat that this might not be characteristic of true equilibrium, or of the electrode surface at the point of immersion. These potentials are shown on Figure 79. In all cases, the potentials of the pyrite samples were well above the region of thermodynamic stability for pyrite, consistent with earlier reports in the literature.[113,155-157,167] One reason for this non-equilibrium behavior might be that despite all attempts to exclude oxygen, during grinding the pyrite surfaces form oxide films or polysulfides that are not removed by etching. Alternatively, the grinding procedure might introduce a large

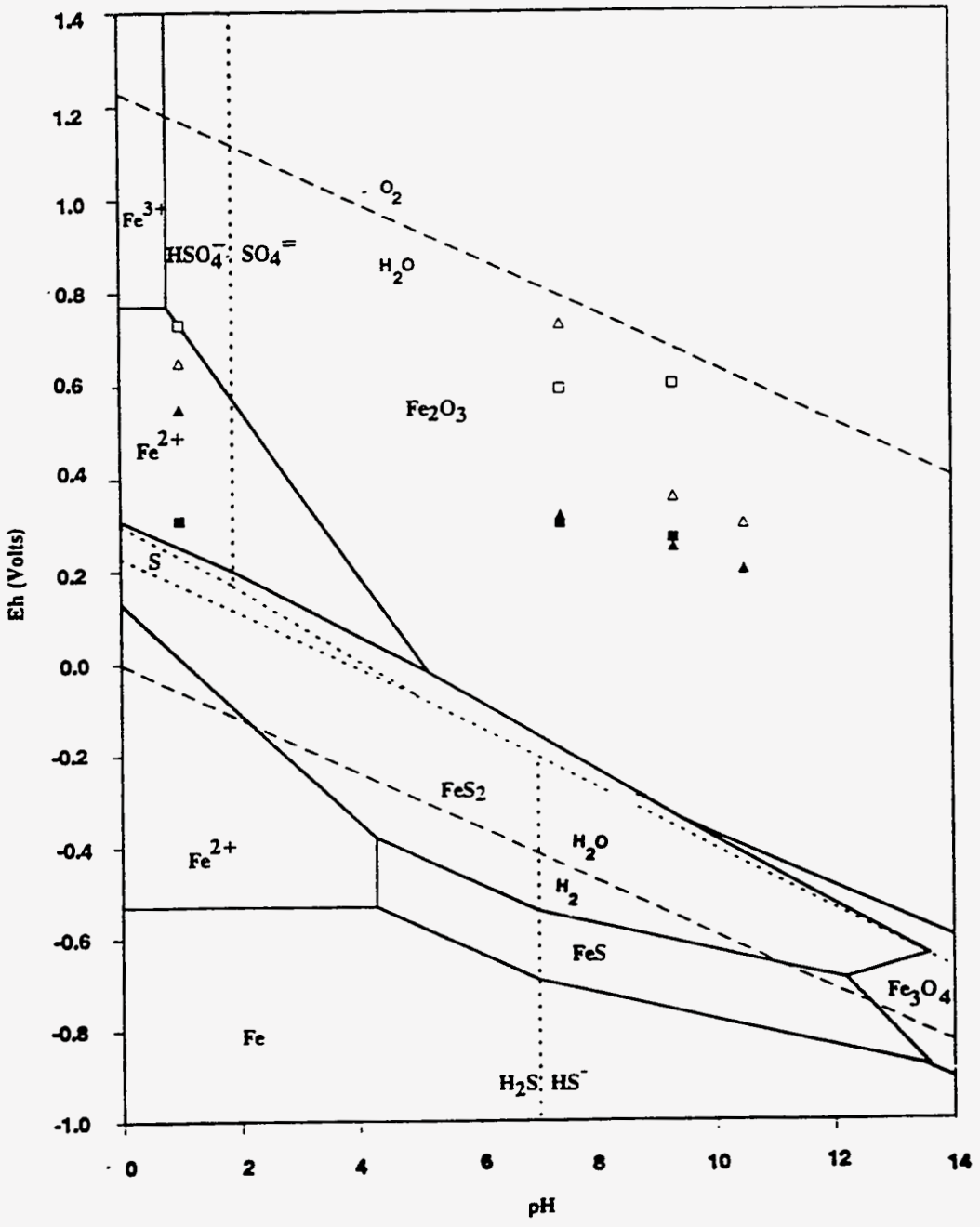

Figure 79. Experimentally measured electrode potentials of Upper Freeport coal pyrite: ❑: initial, ■: 24 hours; Pittsburgh coal pyrite: Δ: initial, ▲: 24 hours.

number of defects that alter the stability of the surface layers of pyrite. It is highly relevant that Tao *et al.*[166], and Richardson and Yoon[169] have observed that pyrite surfaces exposed by cleavage *in-situ* exhibit different electrochemical behavior to pyrite samples that have been ground.

The differences observed in the initial potentials of the two pyrite samples are likely to be due to differences in the level of trace oxygen impurities during grinding, or to differences in damage, although the intrinsic characteristics of the pyrite samples also can influence their behavior. At pH 1.0, oxide films would be expected to dissolve, which could account for the reduction in potential of both pyrite samples over 24 hours. However, the failure to reach the region of stability for pyrite suggests that there is also some influence from grinding defects, or that a polysulfide layer formed by acid dissolution during the "equilibration". The final potentials of both coal pyrite samples were close at both pH 7.4 and pH 9.3. This fact, in conjunction with observation made during cyclic voltammetry (discussed below), suggests that phosphate and borate replaced any original oxide coating during the 24 hours period. The potentials of both pyrite samples decreased with increasing solution pH. This is consistent with the pH dependence of the stability areas shown on the Eh-pH diagram (Figure 79).

C.2 Cyclic Voltammetry Tests

pH 1.0: Figure 80 shows the cyclic voltammogram obtained for a Pittsburgh coal pyrite electrode after 2 hours in contact with H_2SO_4 solution at pH 1.0 scanning at the relatively slow scan rate of 2.0 mV/s. At this scan rate, mobile species that are generated by electrode reactions, such as ions and dissolved gas, tend to be transported away from the electrode into the bulk solution, and are not present at the surface in sufficiently large concentrations to allow the reverse reaction to occur at an appreciable current density

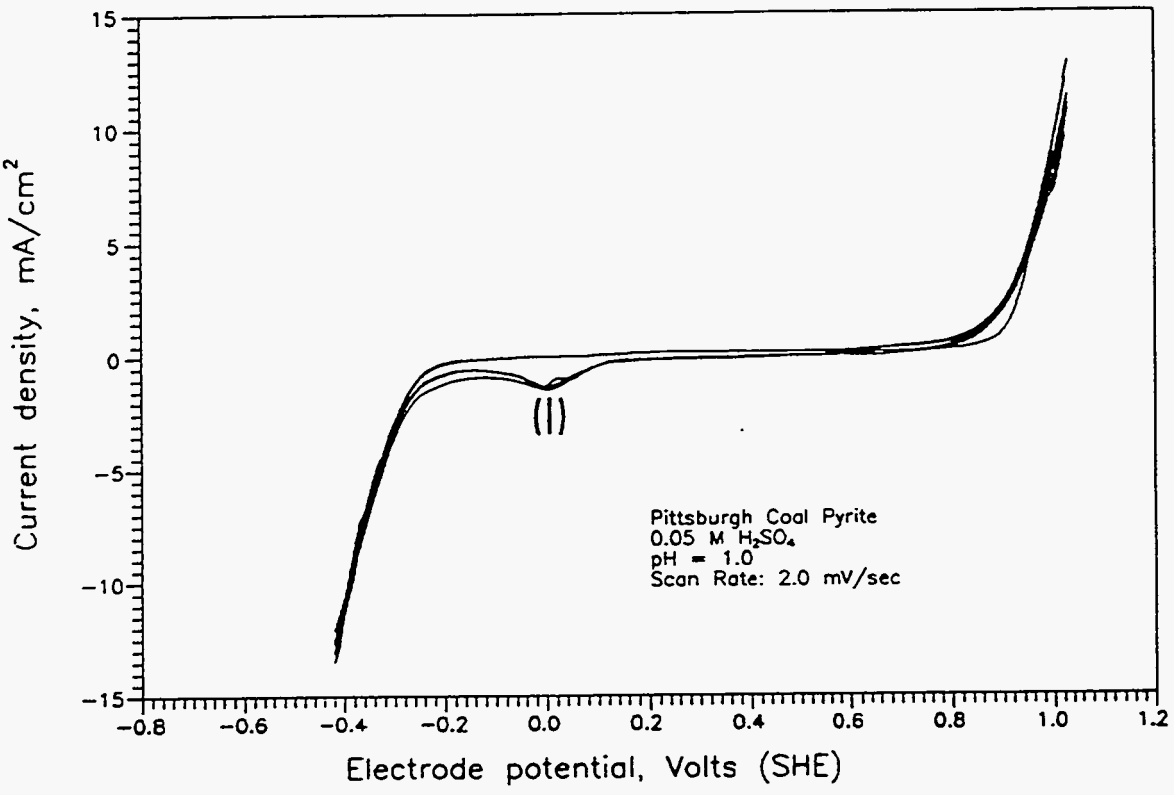

Figure 80. Cyclic voltammogram for Pittsburgh coal pyrite after 2 hours in contact with a pH 1.0 H_2SO_4 solution at 2.0 mV/s

when the potential returns to the required value during cycling. Thus, any peaks that are observed must be due to reaction of the solid alone, or the solid and electrolyte. On the first anodic sweep there was no significant anodic current until about 0.9 V SHE, when extensive oxidation occurred. The cathodic peak I, observed at about 0.0 V on reversing the scan, was probably due to reduction of the insoluble oxidation products that had been formed at the higher potentials, as opposed to reduction of *all* oxidation products, since the total charge associated with this reaction, which is proportional to the area under the current density-potential curve, was much lower than that for the extensive anodic oxidation. At pH 1.0 the insoluble products are more likely to be polysulfides than oxides, and the soluble species would be $Fe^{3+}$and HSO_4^-. The cathodic reaction that started at about -0.3V had a very high charge associated with it and probably corresponds to reduction of FeS_2 to FeS_{2-x} or FeS. On the returning anodic scan, the current density was greater than had been observed in the first anodic excursion, indicating that the new surface was more susceptible to oxidation than the original, ground and etched surface had been. Successive scans resulted in converging voltammograms.

For the same electrode, the plots given in Figure 81 shows that the characteristics of the cyclic voltammograms were changed markedly when the scan rate was increased to 20.0 mV/s under the same conditions used to generate Figure 80. At this scan rate mobile reaction products are still present at the electrode to participate in the reverse reaction when an appropriate potential is reached. On the first cycle (labeled 1) the current was low up to about 0.9 V, where extensive oxidation occurred. On reversing the scan direction, the cathodic peak II appeared at about 0.65 V. This is the correct potential for reduction of Fe(III) to Fe(II), and demonstrates that Fe(III) was produced at the highest current densities. Although there was no distinct peak at around 0.0V corresponding to peak I in Figure 80, there was a continual increase in current density, down to -0.4V, suggesting continual reduction of polysulfides, and then underlying pyrite. A broadening

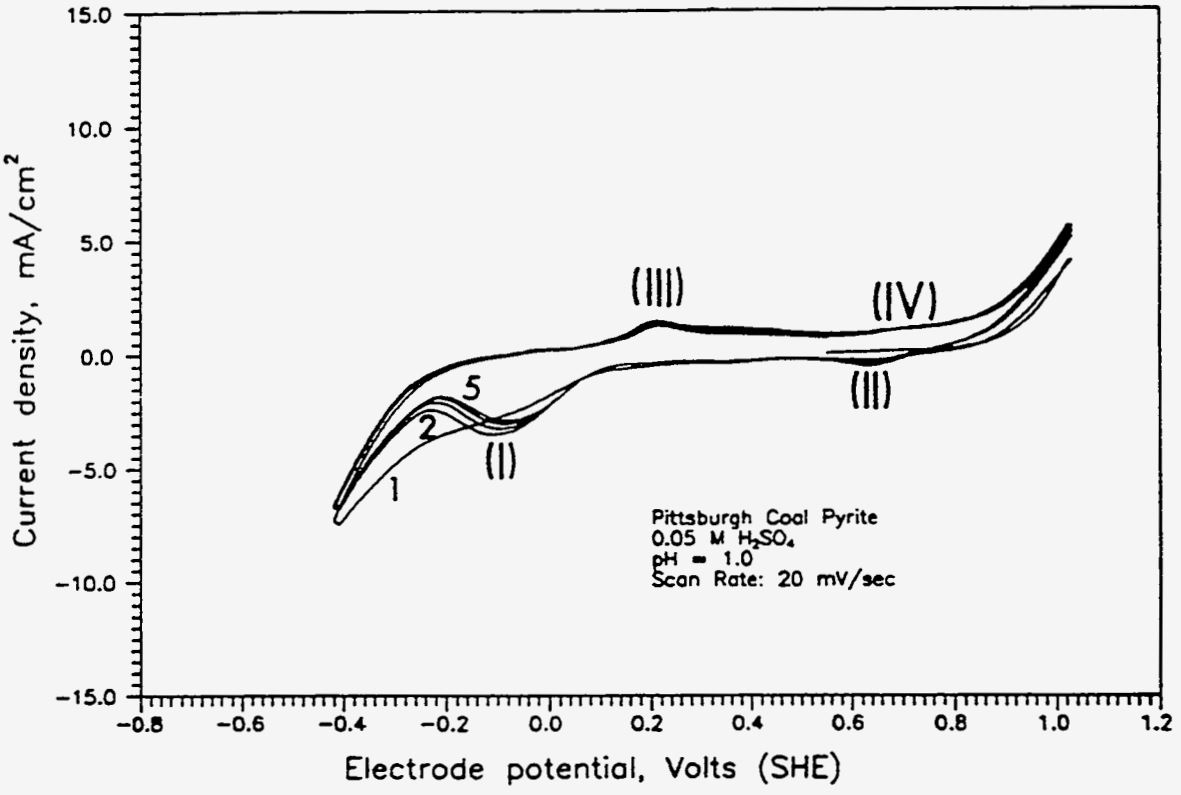

Figure 81. Cyclic voltammogram for Pittsburgh coal pyrite after 2 hours in contact with a pH 1.0 H_2SO_4 solution at 20.0 mV/s

of peaks and higher overpotentials are characteristic of rapid scan rates. The anodic peak III probably corresponds to re-formation of pyrite, by reversal of reaction:

$$FeS_2 + 2xH^+ + 2xe \leftrightarrow FeS_{2-x} + xH_2S \qquad 0<x\leq 1 \qquad (53)$$

The charge associated with this reaction is less than the cathodic charge, because some of the H_2S released on reduction would not be available at the pyrite surface. Consequently there would not be complete replacement of surface FeS or FeS_{2-x} with FeS_2, although the spatial distribution of sulfur in the surface layer is not known. The anodic current was again higher on the second and subsequent cycles, suggesting a change in surface reactivity. Peak IV is due to oxidation of Fe(II) to Fe(III). On the subsequent cycles, the cathodic peak I appeared at -0.1V, rather than the continuous increase in the current density seen on the first cycle. This suggests that the solid oxidation products produced during the second and subsequent cycles had a more distinctive composition than those present on the first cycle.

The same electrode was contacted with the acidic solution for 24 hours, and a cyclic voltammetry experiment was carried out at 20.0 mV/s. The results are shown in Figure 82, which is essentially similar to Figure 81. This shows that although the rest potential had decreased almost 100 mV in 24 hours (Table 20), this did not cause any fundamental change in the electrochemical reactivity of the surface.

Figure 83 shows the cyclic voltammograms obtained with the Upper Freeport coal pyrite electrode after 24 hours of contact with pH 1.0 H_2SO_4. On the first cycle the anodic current was extremely low up to about 0.6V, when oxidation occurred. A cathodic reaction was observed at about -0.4V that was probably due to dissolution of the oxidized layer, possibly a polysulfide. On the second anodic scan, the anodic current density

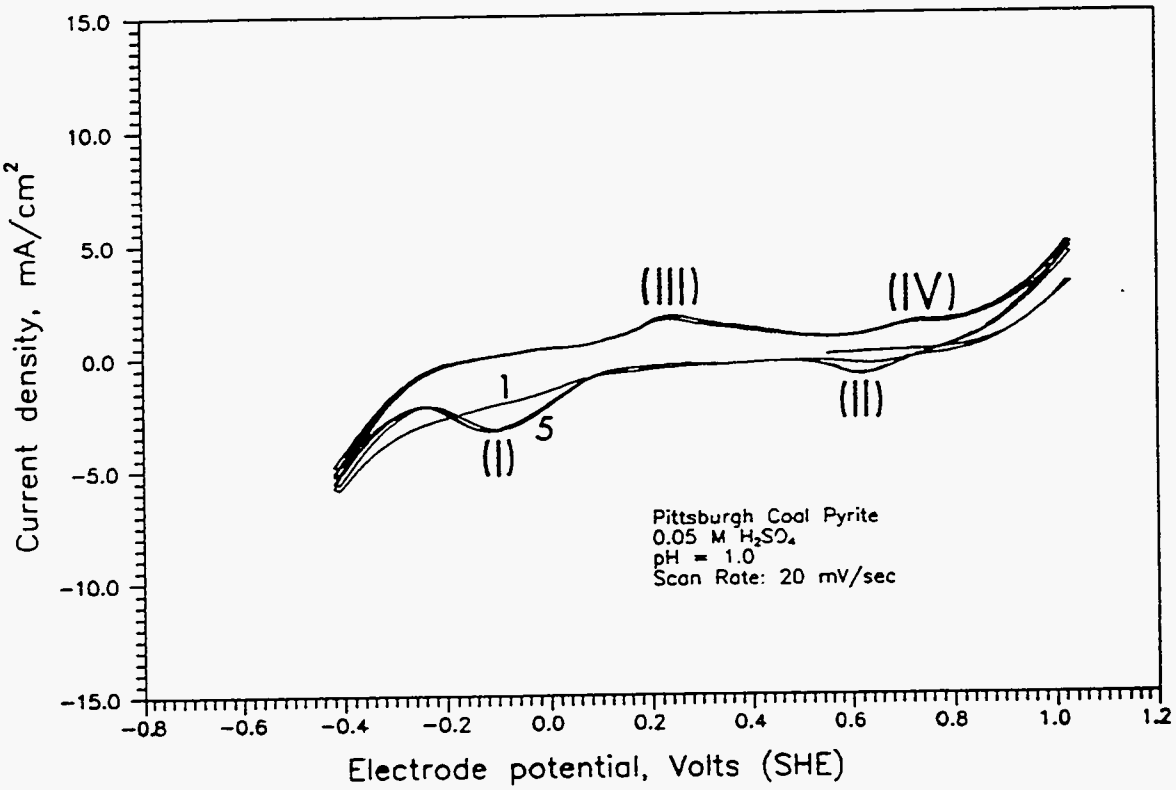

Figure 82. Cyclic voltammogram for Pittsburgh coal pyrite after 24 hours in contact with a pH 1.0 H_2SO_4 solution at 20.0 mV/s

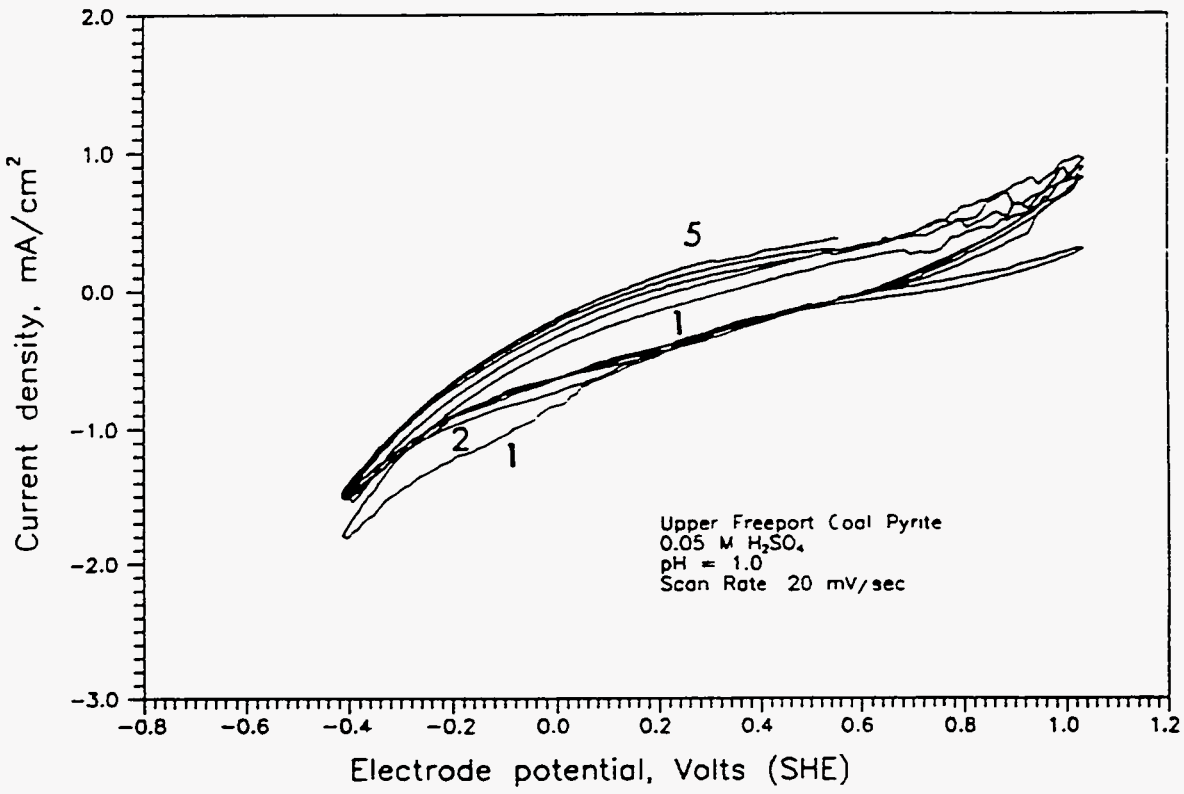

Figure 83. Cyclic voltammogram for Upper Freeport coal pyrite after 24 hours in contact with a pH 1.0 H_2SO_4 solution at 20.0 mV/s

started increasing at about 0.3V, and higher anodic currents were passed on subsequent scans, indicating that the electrochemical character of the pyrite surface changed during the course of cycling. The cathodic current was lower on the second and subsequent scans than in the first cycle.

pH 7.4, 9.3, and 10.5: The surface properties of coal pyrite are very sensitive to changes in the solution conditions. Because of this, the behavior of pyrite was studied at pH values closer to those used in flotation systems. Cyclic voltammetry experiments were done with Pittsburgh coal pyrite at pH 7.4, 9.3 and 10.5.

Figure 84 shows the behavior over 5 cycles at 2.0 mV/s after 2 hours of contact with a pH 9.3 borate buffer solution. On the first cycle the current was low initially and started increasing at about 0.4 V. This potential is lower than the potential where the anodic current density started to increase at pH 1.0, namely 0.9V (Figs 80-83), which is consistent with the pH dependence shown in Figure 79. A cathodic peak (I) was observed at -0.5 V. This must be due to reduction of oxidized layers, since the potential is too high for pyrite reduction. There was a small peak at -0.8V, probably corresponding to reduction of pyrite to form FeS and HS^- by the reaction:

$$FeS_2 + H^+ + 2e^- \leftrightarrow FeS + HS^- \qquad (54)$$

On the anodic scan, re-formation of FeS_2 by interaction of FeS layers on the electrode surface with HS^- would be unlikely, because of transport of HS^- from the electrode by both migration and diffusion. Thus peaks (II) and (III) in Figure 84 are probably due to electrochemical reactions involving the borate buffer. This possibility has been confirmed recently by Wang *et al.*[205], who reported that different borate and phosphate buffers react strongly with pyrite and other sulfide minerals, to form both

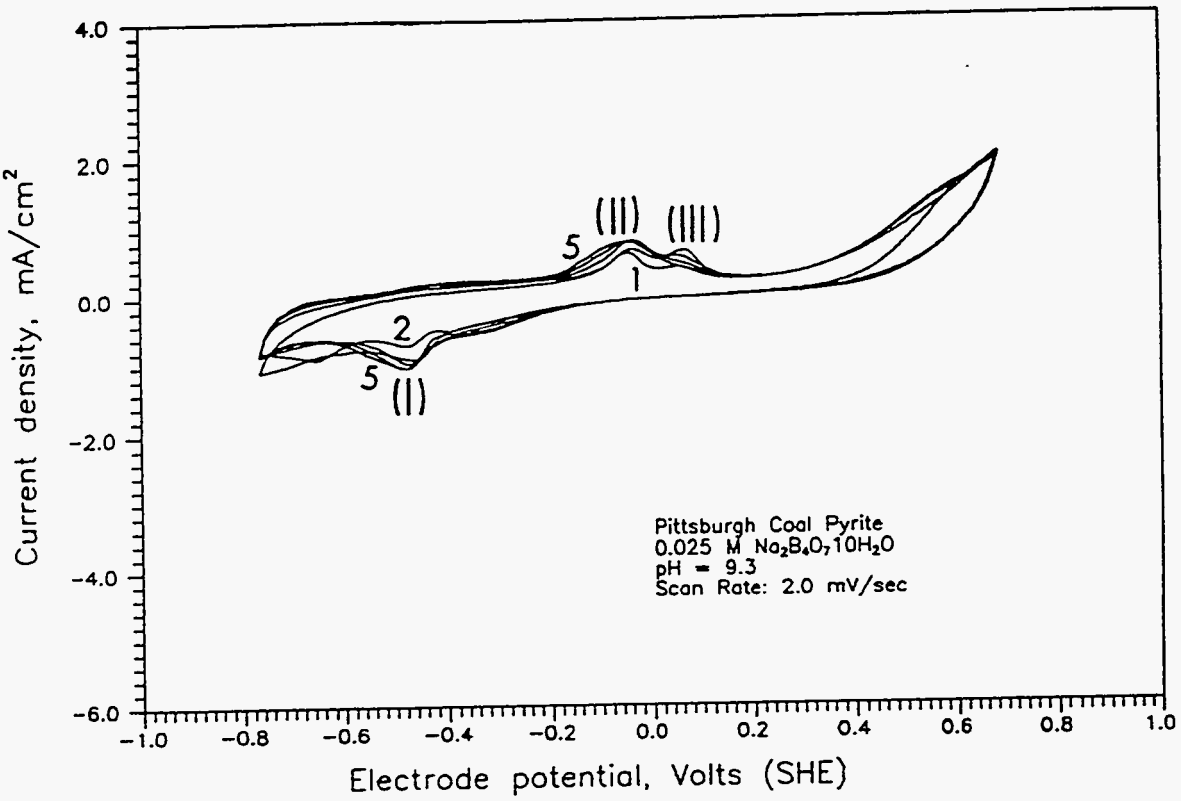

Figure 84. Cyclic voltammogram for Pittsburgh coal pyrite after 2 hours in contact with a pH 9.3 borate buffer solution at 2.0 mV/s

soluble and insoluble compounds. These reactions could either enhance or inhibit the oxidation of pyrite and its interaction with flotation reagents.

Figure 85 shows the cyclic voltammogram obtained with the Pittsburgh coal pyrite electrode after 2 hours of contact with pH 9.3 borate buffer at 20 mV/s. The anodic and cathodic current densities were higher than those observed at 2.0 mV/s (Figure 84). This is a general feature of rapid scan rates, reflecting the shorter time available for charge to pass while an electrode is in a particular potential range. During the first anodic excursion the current density started increasing at 0.4V. The cathodic peak observed at -0.75 V is probably due to the reduction of pyrite according to reaction 54. The anodic peaks II and III undoubtedly include components due to the same reaction observed in Figure 84. However, peak II was comparatively larger than III, suggesting that there might also be some recombination of HS^- and FeS at this potential. As noted in other voltammograms, the new surface passed higher anodic currents than the original pyrite surface. Because of the low solubility of iron species in basic solutions, no peaks were observed for the reduction of Fe(III) and oxidation of Fe(II). On the second cycle a very small cathodic shoulder (I) appeared at about -0.4 V and its magnitude was constant on subsequent cycles. This peak could be due to reduction of oxidation products or to an electrochemical interaction between the electrode and the buffer solution. This effect was not reported in previous electrochemical studies using buffer borate as electrolyte.[157,159,160,162,166-168,170]

The Pittsburgh coal pyrite electrode was also contacted with the same borate buffer solution for 24 hours before cyclic voltammetry at 20 mV/s. Figure 86 shows that peaks were obtained at the same potentials as those observed in Figure 85. The cathodic peak at -0.6 to -0.8V had a slightly higher current density than that in Figure 85, and the anodic peak II was dramatically higher, especially in the first cycle. This confirms that this

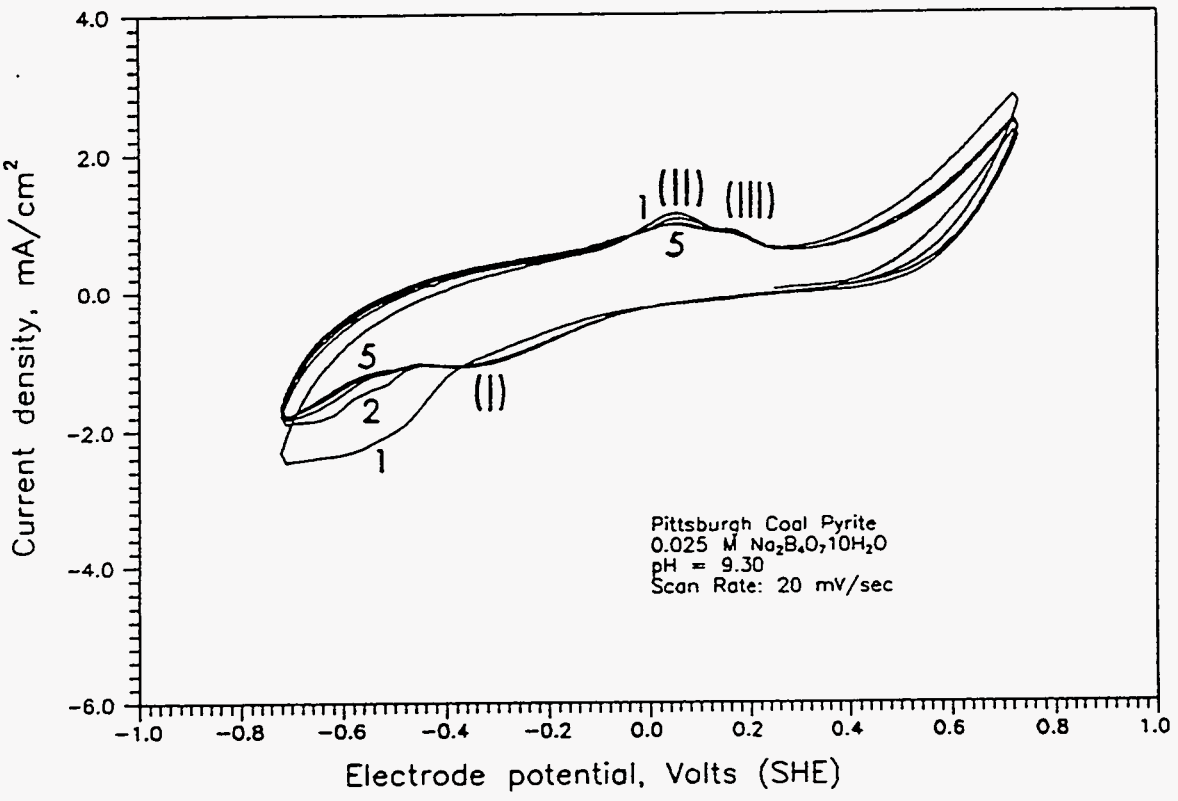

Figure 85. Cyclic voltammogram for Pittsburgh coal pyrite after 2 hours in contact with a pH 9.3 borate buffer solution at 20.0 mV/s

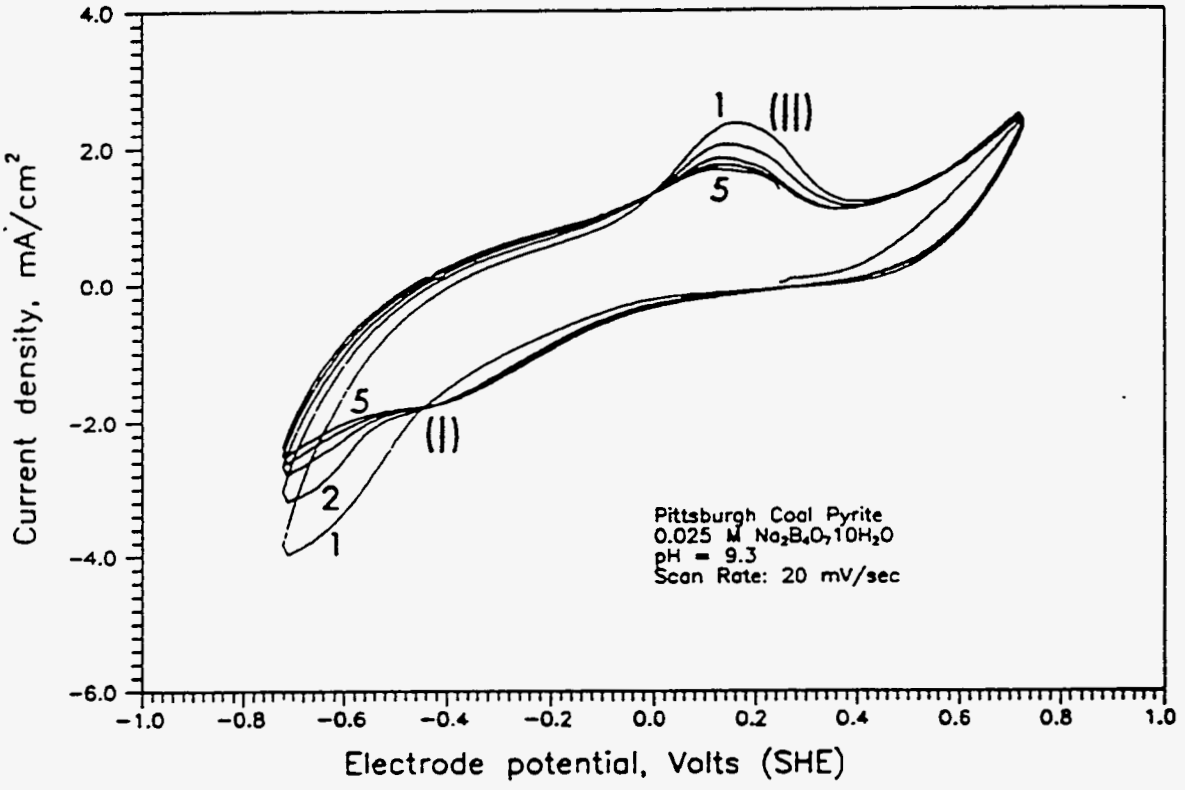

Figure 86. Cyclic voltammogram for Pittsburgh coal pyrite after 24 hours in contact with a pH 9.3 borate buffer solution at 20.0 mV/s

peak is largely due to some interaction with borate, and suggest that it is oxidation of a borate-containing layer that develops on exposure to the buffer.

Cyclic voltammograms at 20.0 or 2.0 mV/s with Pittsburgh coal pyrite in contact with pH 7.4 phosphate buffer and pH 10.5 borate buffer solution showed similar behavior to that observed at pH 9.3. This indicates that phosphate is also electrochemically active.

Figure 87 shows cyclic voltammograms obtained with the Upper Freeport coal pyrite electrode after 2 hours in contact with pH 9.3 borate buffer, scanning at the relatively slow scan rate of 2.0 mV/s. These are very similar to those for the Pittsburgh pyrite discussed above. On the first cycle, a cathodic current passed to about 0.45V, where the current reversed and increased. A cathodic peak I started developing at -0.4V, with a shoulder at -0.6V, probably due to reduction of oxidation products formed during electrode preparation, or reduction of borate species. A cathodic peak due to reduction of pyrite was established at -0.75V. The anodic peaks II and III are probably due to the same reaction of borate seen in Figures 84,85,and 86.

For the same electrode, Figure 88 shows the cyclic voltammograms obtained after 2 hours in contact with a pH 9.3 borate buffer scanning at 20.0 mV/s. The voltammograms indicate that even at relatively high potentials, the electrode is passing a cathodic, rather than the thermodynamically favorable anodic current. Even at the "rest" potential , a substantial cathodic current was being passed. Also, the currents observed for the Upper Freeport coal pyrite were less steady than those for the Pittsburgh coal pyrite under all conditions, suggesting that semiconductor or insulating layers were forming under certain conditions and giving erratic responses. This pyrite clearly has a very low propensity for oxidation, in marked contrast to the Pittsburgh coal pyrite. Such

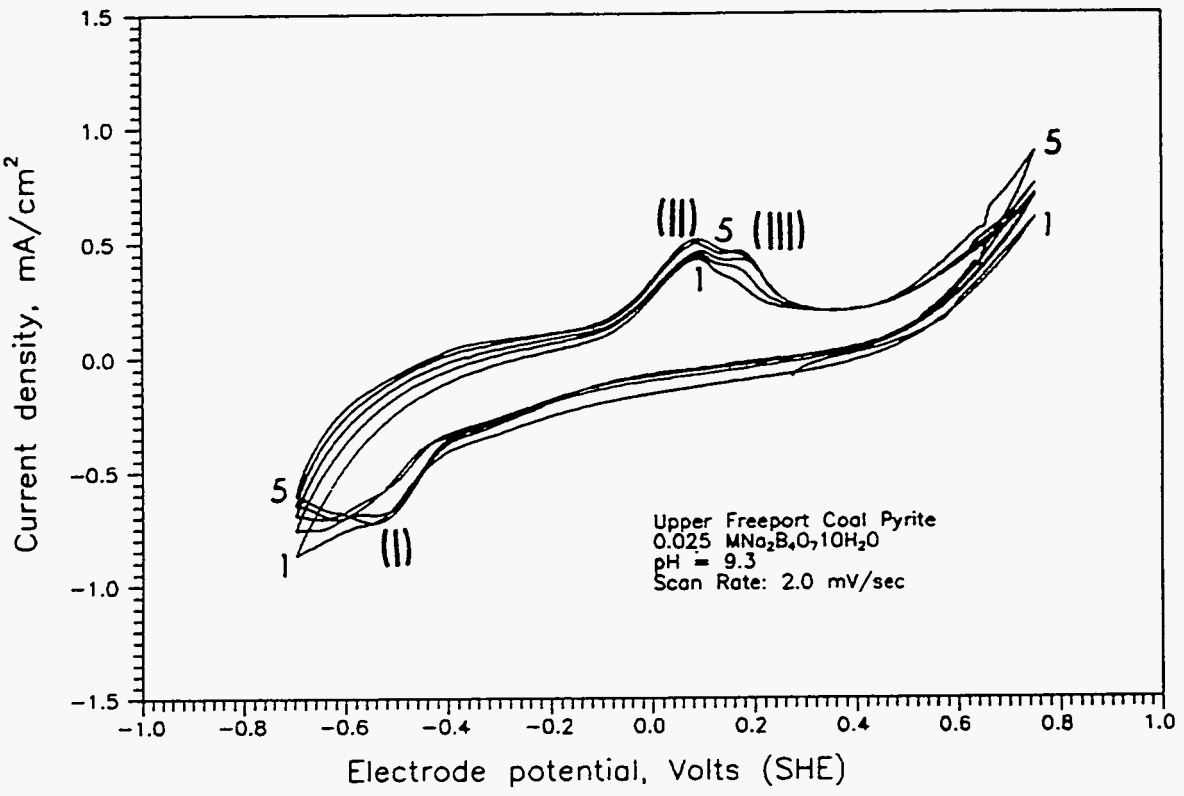

Figure 87. Cyclic voltammogram for Upper Freeport coal pyrite after 2 hours in contact with a pH 9.3 borate buffer solution at 2.0 mV/s

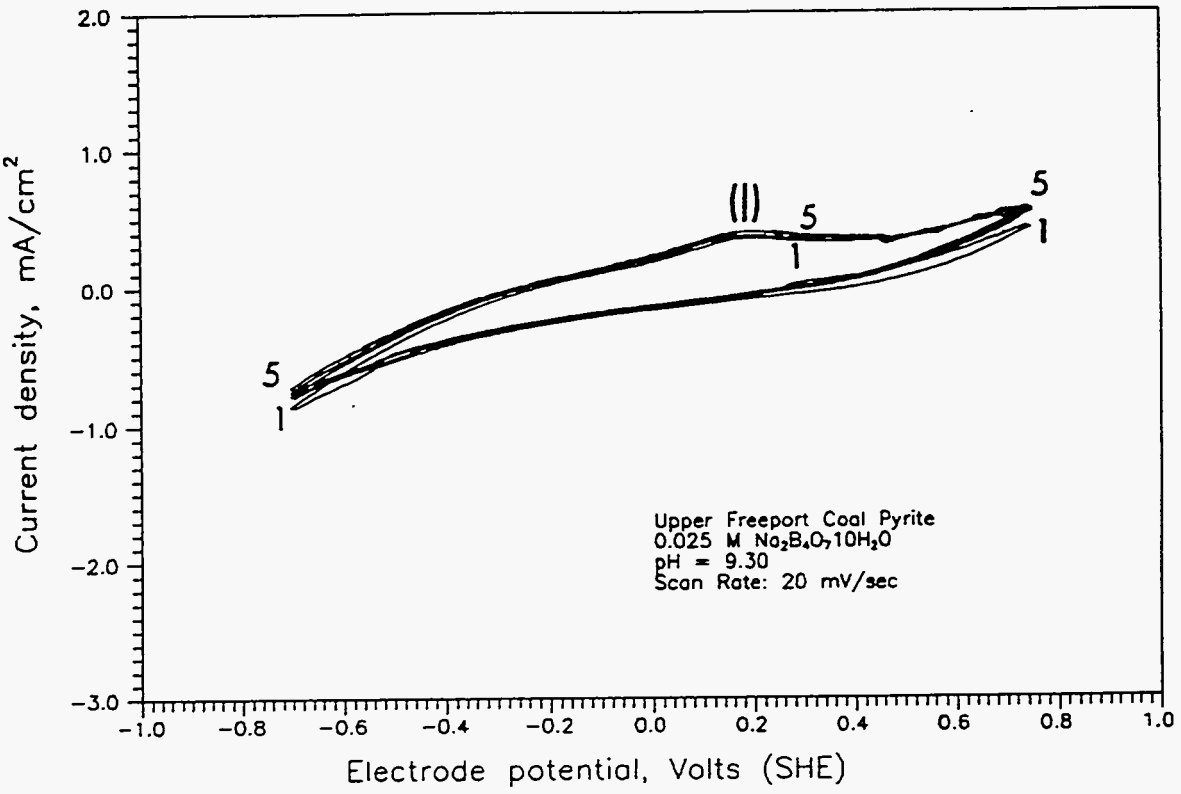

Figure 88. Cyclic voltammogram for Upper Freeport coal pyrite after 2 hours in contact with a pH 9.3 borate buffer solution at 20.0 mV/s

differences would be extremely important in determining the ability to desulfurize each coal after weathering.

C.3 Implication for Coal Cleaning

The experimental results of this study, in conjunction with previous work, clearly indicate that significant differences can be expected in the electrochemical behavior of coal pyrite samples, depending on their prior history. For example, grinding can introduce damage or defects in the surface layers, and traces of oxygen can readily oxidize their surface. These effects are more likely during commercial coal preparation as during idealized laboratory experiments. Any of these factors could alter the rest potential of pyrite samples from their intrinsic value. It is also possible that the reducing environment provided by coal actually increases the susceptibility of freshly exposed pyrite to oxidation, in the same way that the pyrite studied here was more susceptible after a cathodic excursion.

Coal pyrite undergoing weathering in storage piles may develop low pH values, according to reaction 46. The results obtained in this work would suggest that such weathering at low pH would make the coal pyrite surface more hydrophobic, because of the formation of sulfur and polysulfides. This would be undesirable, since cleaning methods such as flotation and oil agglomeration require the pyrite to be less hydrophobic than the coal. The problem is compounded by the concurrent oxidation of coal, which introduces hydrophilic carboxylic and phenolic groups.

Oxides form when pyrite oxidizes under basic conditions, although the effect of this on the surface properties would depend on whether non-equilibrium polysulfides also appeared. The borate or phosphate compounds that developed in the electrochemical

studies would not, of course, be expected in a coal flotation circuit where pH would be regulated with inexpensive bases.

C.4 Contact Angle Measurements.

Figure 89 shows the effect of the electrode potential on the wetting behavior of Pittsburgh coal pyrite at pH 9.3. As the potential of the electrode was increased, the surface became more hydrophobic at potentials between 250 and 450 mV(SHE). From our cyclic voltammetry results, this increase in hydrophobicity could be attributed to the formation of polysulfide species at the surface. When the electrode potential was further increased, the surface of the electrode became more hydrophilic, probably because of formation of oxide species that strongly interact with water. On reducing the electrode potential from 700 to 450 mV, the surface became more hydrophobic because of the reduction of the oxide layers formed during the anodic excursion. However, there was noticeable hysteresis, which is to be expected since diffusion of sulfate away from the electrode would preclude reversal of the chemical reactions that occurred during the anodic excursion. Upon further decrease in the electrode potential, reduction of the surface species made the electrode surface more hydrophilic. However, at the "rest potential" of the electrode, the surface was more hydrophobic than it had been at the beginning of the test, suggesting that not all of the oxidation products had been reduced on reversing the electrode potential. Between 250 and -200 mV the contact angle remained constant, then at more cathodic potentials the contact angle decreased continuously to about 9^{o}, mainly due to the reduction of pyrite to form FeS and HS^{-} according to reaction 54. Figure 90 shows the effect of the electrode potential on the wetting behavior of Pittsburgh coal pyrite at pH 1.0. As the potential of the electrode was increased up to 1000 mV the surface became more hydrophobic, due to the formation of polysulfides and sulfur. On reducing the electrode potential, the surface became more

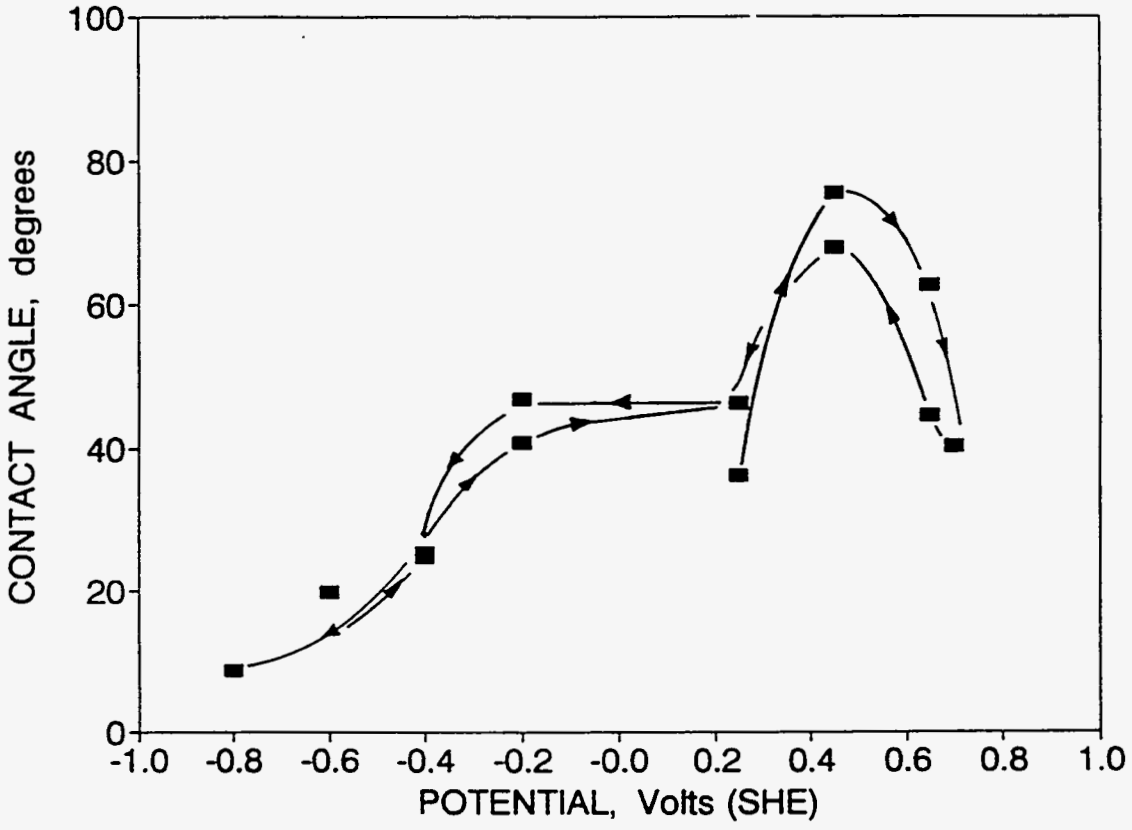

Figure 89. Contact angle of a nitrogen bubble on Pittsburgh coal pyrite as a function of the electrode potential in a borate buffer solution at pH 9.3. The potential was stepped, starting at the rest potential, and initially scanning anodically, then cathodically.

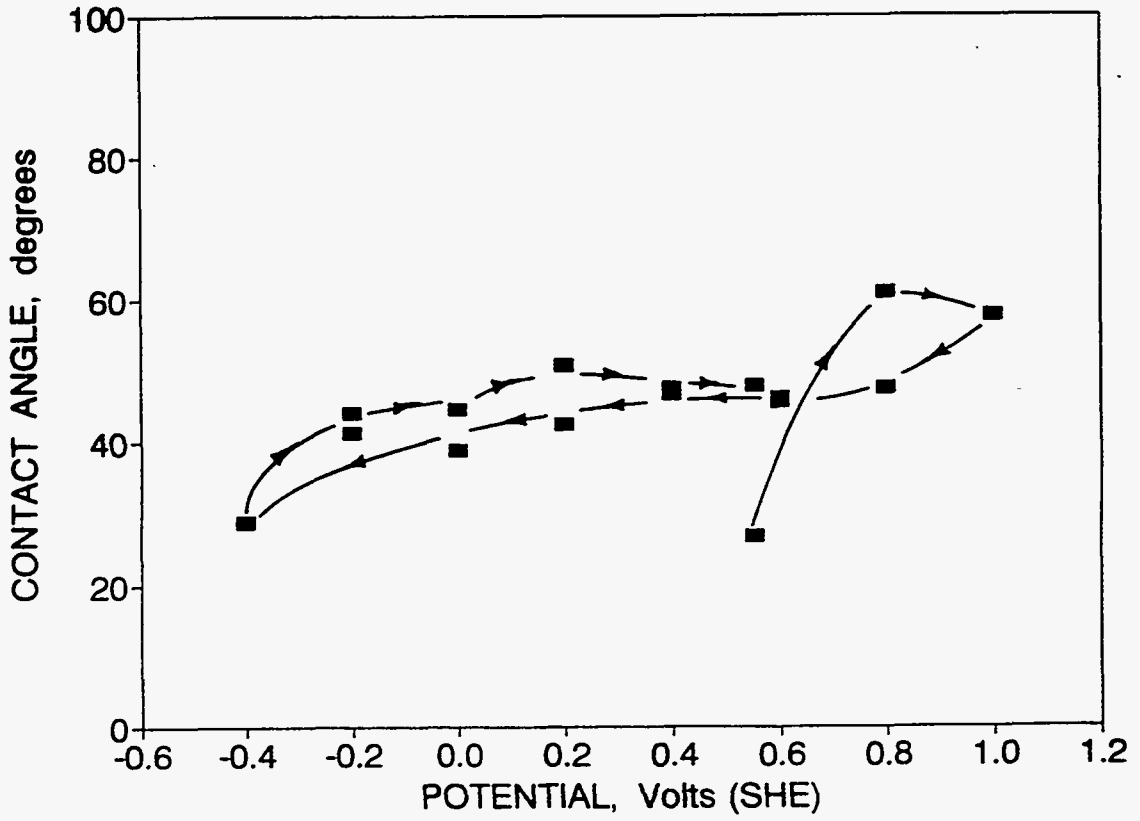

Figure 90. Contact angle of a nitrogen bubble on Pittsburgh coal pyrite as a function of the electrode potential in a sulfuric acid solution at pH 1.0. The potential was stepped, starting at the rest potential, and initially scanning anodically, then cathodically.

hydrophilic because of the reduction of the oxidation products. When the electrode potential was decreased beyond the rest potential, the contact angle decreased steadily, due to reduction of polysulfides and FeS_2 to FeS_{2-x} or FeS. On reversing the potential step direction, the surface became more hydrophobic due to the re-formation of pyrite. There was hysteresis, however, probably because there was incomplete replacement of the reduction products by FeS_2.

These results indicate that at least two products form when coal pyrite was oxidized at pH 9.3. These products are a hydrophobic polysulfide species and a hydrophilic oxide layer. The relative abundance and properties of these products determine the flotation response of coal pyrite. If the oxide layer is absent, that is, either it does not form or it is dissolved, coal pyrite is more hydrophobic. Oxidation of pyrite at pH 1.0 renders the surface more hydrophobic because of the formation of hydrophobic species such as polysulfide and sulfur, and the absence of an oxide layer. This behavior might be utilized in selective flotation for coal cleaning.

D. Chemical Oxidation of Upper Freeport Coal Pyrite

The purpose of these experiments was to study the reliability, reproducibility and suitability of different standard test methods used to determine the pyrite content of coal and its propensity to release acidic drainage.

D.1 The Peroxide Method (Smith *et al.*[173] ; Sobek *et al.*[174]).

Here, the validity of the assumption that all the pyrite in a sample reacts completely with hydrogen peroxide to produce acid was tested. The amount of iron released by pyrite oxidation was determined by atomic absorption spectrophotometry, and the amount of acid released was determined by titration with NaOH. The titration results were analyzed by assuming that all Fe(III), as determined by atomic absorption analysis, would consume three equivalents of OH^-, and that the residual OH^- consumption was due to the single H^+ ion released according to the reaction:

$$FeS_2 + 15/2\ H_2O_2 \leftrightarrow Fe(OH)_3 + 2SO_4^{2-} + 4H_2O + 4H^+ \qquad (55)$$

Although the hydrogen peroxide method is not a standard method for coal pyrite, it was tested to compare with ASTM D2492-84 method[172], and to understand the differences in the behavior of coal and ore pyrite samples.[206]

It is clear from Table 24 that for Upper Freeport coal, the AA (atomic adsorption) and titration analyses are totally inconsistent, and, in the case of acid titration, not realistic.

Table 24. Percentage of total pyrite in Upper Freeport coal reacted during peroxide oxidation processes (uncontrolled:PO:U, or temperature controlled at 40°C; PO:40 or 10°C; PO:10)

	PO:U		PO:40		PO:10	
	AA	Titration	AA	Titration	AA	Titration
Sample 1	8.94	374.7	8.18	316.1	10.82	356.1
Sample 2	8.40	357.5	8.34	310.7	9.04	360.0
Mean	8.67	366.1	8.26	313.4	9.93	358.1

Vigorous, exothermic reactions were observed between coal and hydrogen peroxide, with the temperature typically rising to about 95°C within a few seconds of adding peroxide, and the temperature only decreasing to room temperature after about 30 minutes. This caused release of little iron, and excessive acid. It is probable that much of the peroxide oxidized the coal, creating acidic groups on the surface of coal. Some of these were soluble, contributing greatly to the excess acid in solution, while surface acid groups may well have complexed some of the iron released by pyrite oxidation. It is clear that peroxide oxidation is an inappropriate method for analyzing the pyrite content of coal, and presumably of coal-containing wastes.

D.2 Nitric Acid Extraction Method (ASTM D2492-84)[172]

This method implicitly assumes that all the pyritic sulfur in a coal sample would be dissolved by this method. Upper Freeport coal pyrite samples were hand picked from broken coal before grinding. Because of the intimate association of coal with pyrite, samples of homogeneized, ground coal pyrite were ashed in duplicate in a proximate analyzer equipment (LECO-MAC-400) at 706°C under oxygen atmosphere. These samples contained 59.87% of ash. Pure pyrite would produce 66.55 wt% ash on oxidation to hematite (which would be expected in an oxygen atmosphere), which

suggests that homogeneized pyrite materials contained about 90% pyrite. When the ASTM Method D2492-84 was performed on four different pyrite nodules isolated from coal, the dissolved iron was equivalent to between 94.08 and 100% (mean 97.58%, standard deviation: 2.464) of the weight of pyrite used. Given that the homogeneized coal pyrite had contained a maximum of 90% pyrite, these results indicate that the test method is, indeed, capable of dissolving all the pyrite within the duration of the test, although it is implicit that the coal or other sample must be ground sufficiently fine to expose all pyritic material to the nitric acid oxidant. This requirement must be allowed for when analyzing coal samples with very small, encapsulated pyrite particles, which may end up being reported as organic sulfur. Despite this limitation, this test method seems to be adequate for normal analysis. However, the variant of this method indicates that samples can be left overnight at room temperature in order to dissolve all pyrite. Under this condition the kinetics of pyrite dissolution could be unfavorable and consequently might introduce erroneous pyritic sulfurdeterminations.

D.3 Oxidation Kinetics Studies.

Kinetic studies were made on the dissolution of coal and ore pyrite in 1.97M HNO_3 and 5% H_2O_2 solutions to gain insight into the kinetic features that could be incorporated into tests for predicting water quality during waste management.

D.3.1 Nitric Acid Test

Figure 91 shows the percentage of Upper Freeport coal pyrite and ore pyrite dissolved by 1.97M HNO_3 (concentration used in the ASTM method) as a function of time. Specifically, for these particular pyrite samples, it is clear that the coal pyrite was oxidized more rapidly than was ore pyrite. Such differences should be taken into account in kinetic models that predict the rate at which the acid potential and neutralization

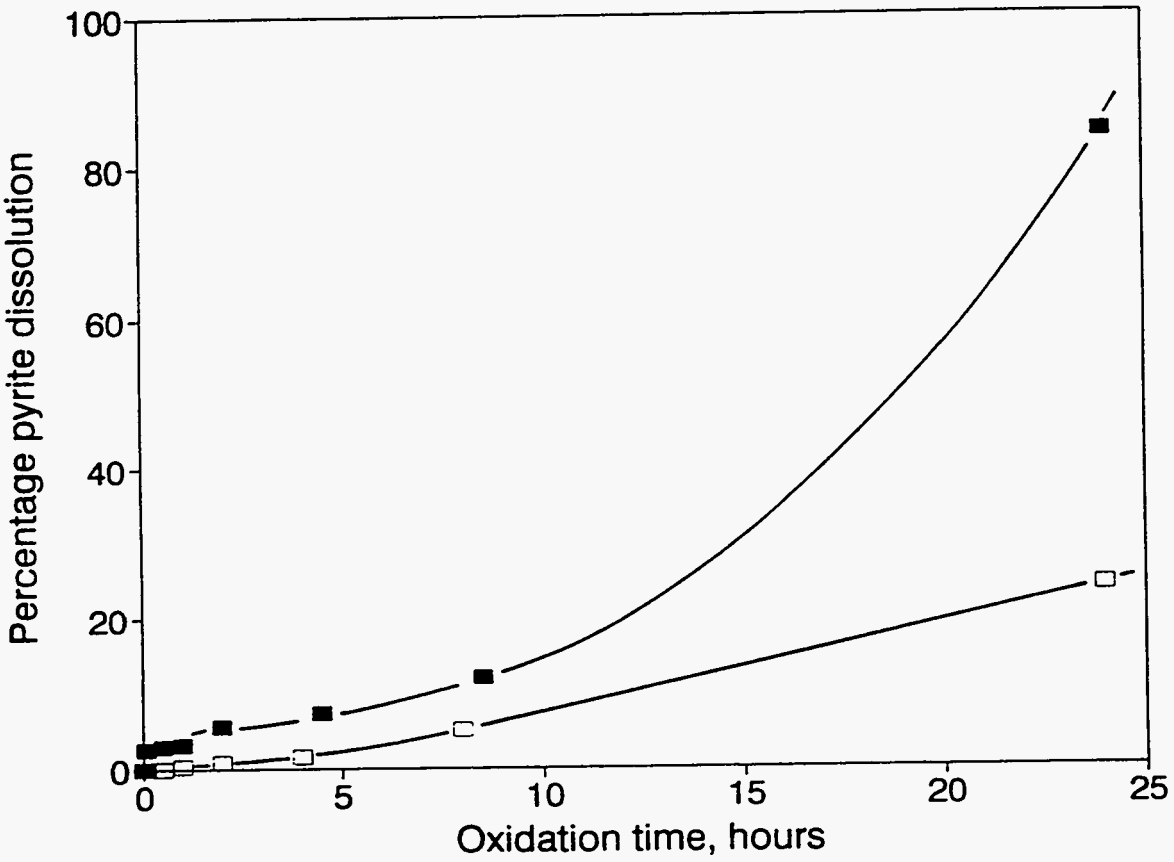

Figure 91. Percentage of pyrite samples dissolved by 1.97M HNO_3 at room temperature.
■:Upper Freeport coal pyrite; ❑: Huanzala, Peru ore pyrite

capacity of a given waste material are depleted. It should also be noted that ASTM Method D2492-84 states that samples can be left overnight in nitric acid at room temperature, instead of being boiled for 30 minutes. These results demonstrate that this treatment would not give complete oxidation of pyrite and hence, should be avoided.

D.3.2 Hydrogen Peroxide Test.

Figure 92 shows the percentages of Upper Freeport coal pyrite and ore pyrite dissolved by 5% H_2O_2 as a function of time. The coal pyrite gave 100% dissolution after about 10 hours, as analyzed by the iron content of the solution, whereas iron analysis had indicated only about 10% pyrite dissolution in the standard hydrogen peroxide oxidation technique. The discrepancy may have been due to the fact that there was more hydrogen peroxide present in this experiment to oxidize the pyrite, or that the reaction time here was longer than in the standard method, or that the temperature was lower, giving less thermal decomposition of peroxide. However, it is also highly probable that at the lower peroxide concentration, conditions were not sufficiently oxidizing to create soluble and surface acid groups by oxidation of the coal. Hence there would have been no side reaction consuming peroxide, or oxidized functional groups to adsorb iron from the peroxide solution.

E. Electrokinetic and Film Flotation Tests on Raw and Oxidized Coal Pyrite Samples.

In order to study the effect of oxidation on the electrokinetic behavior of coal pyrite samples, 3 g samples of -400 mesh Upper Freeport and Pittsburgh coal pyrite, spread to a depth of about 1 mm, were oxidized in a convection oven at 230°C for 24 hours. Figures 93 and 94 show the effect of oxidation on the zeta potential of coal pyrite samples. The results indicate that like the Upper Freeport coal samples the PZR shifts to

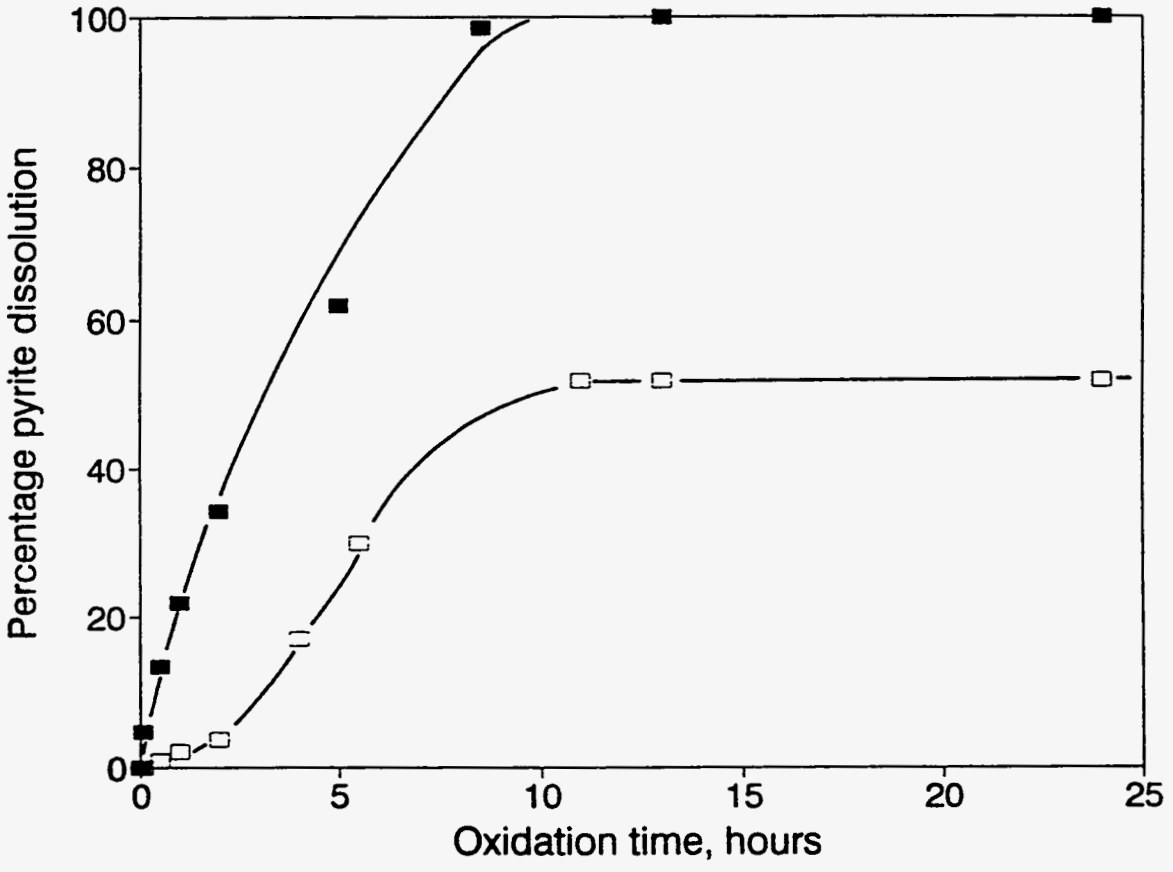

Figure 92. Percentage of pyrite samples dissolved by 5% H_2O_2 at room temperature.

■: Upper Freeport coal pyrite; ❑: Huanzala, Peru ore pyrite.

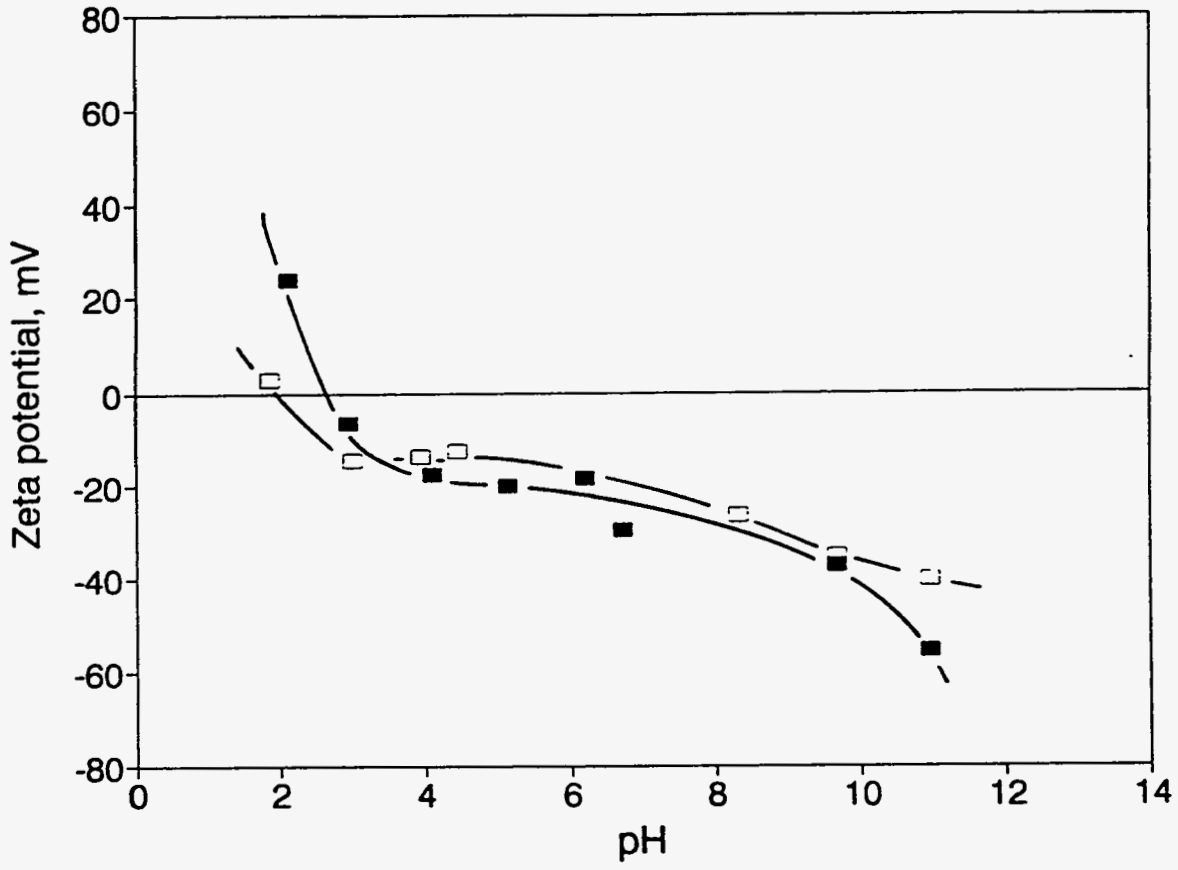

Figure 93. Zeta potential curves of as received and oxidized Upper Freeport coal pyrite at 230°C for 24 hours.: ■: as-received, ❑: oxidized.

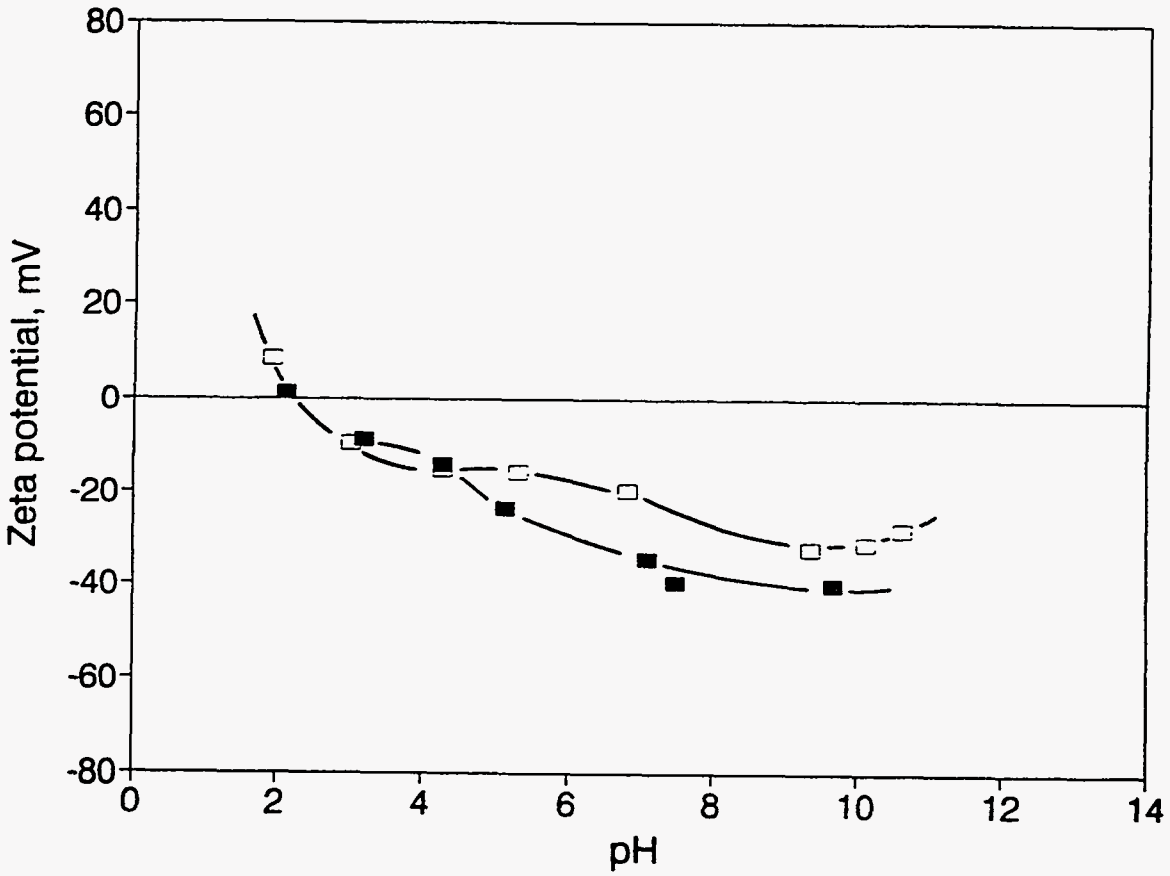

Figure 94. Zeta potential curves of as received and oxidized Pittsburgh coal pyrite at 230°C for 24 hours. ■: as-received, ❑: oxidized.

more acidic pH's values, probably due to the dissociation of some oxidation products at low pH. However, for Pittsburgh coal pyrite, there is no significant effect of oxidation upon the PZR. The PZR values of 2.2 seem to be in good agreement with some values reported in the literature,[118,207] but not with those reported by Fuerstenau *et al.*[208], who found a value of 6.2 for ore pyrite. The reason for this discrepances are possibly associated with differences in the surface composition of the pyrite samples. They also found that oxidation modify the interaction of pyrite with xanthate during flotation.

Upper Freeport coal samples oxidized at higher temperatures were negatively charged at all pH values (Figure 14). It is clear that this negative charge must be determined mainly by the acidic groups present on coal surface, rather than the oxidation products of pyrite.

Figure 95 shows the film flotation partition curves of coal pyrite samples as-received and oxidized at 230°C. Clearly, the critical surface tension increased dramatically on oxidation, reflecting a decrease in the hydrophobicity of pyrite samples with oxidation. This is undoubtedly due to the presence of hydrophilic iron oxide or hydroxide on the surface. Clearly this change with oxidation would affect the performance of coal cleaning processes.

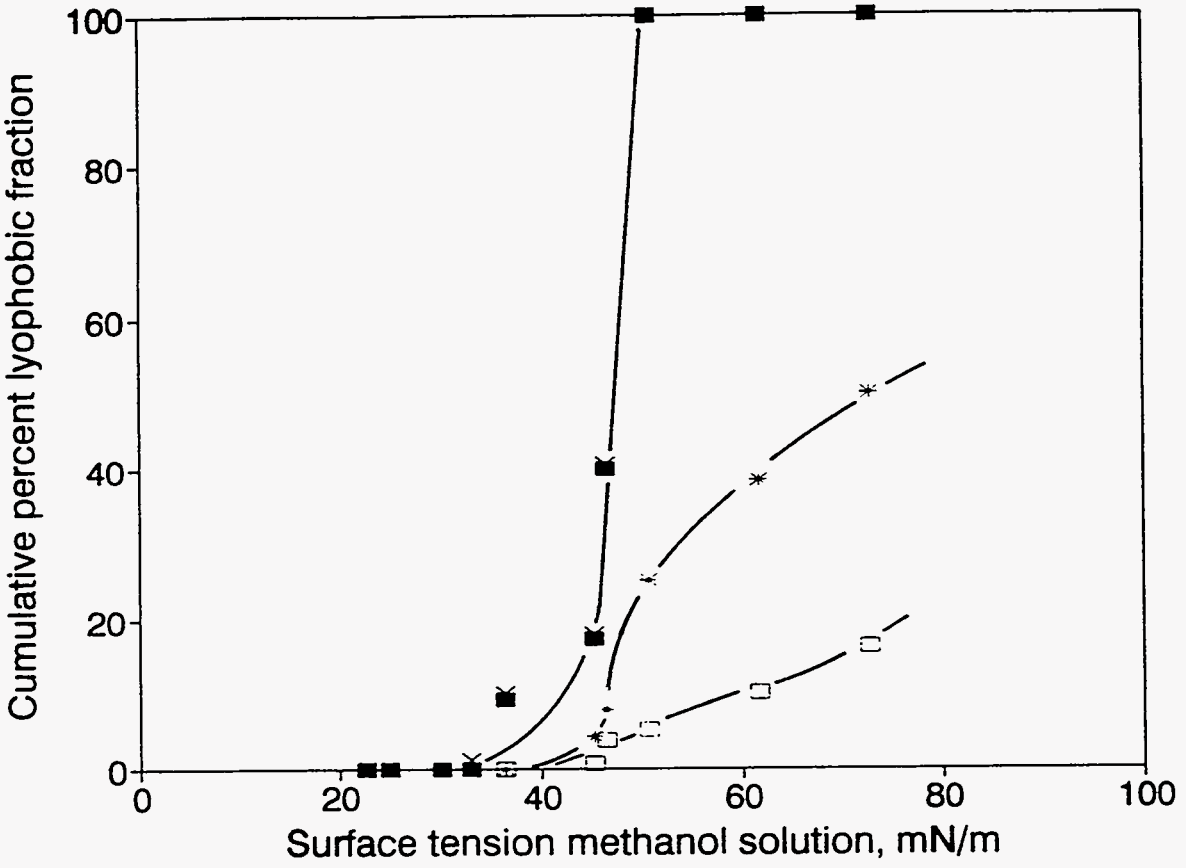

Figure 95. Film flotation partition curves of as received and oxidized Upper Freeport and Pittsburgh coal pyrite at 230°C for 24 hours. Upper Freeport: ■: as-received, ❑: oxidized; Pittsburgh: ×: as-received, * :oxidized.

VI. SUMMARY AND CONCLUSIONS

In this research, the influence of specific oxidation treatments on the surface properties that control the behavior of coal and coal pyrite in relation to physical cleaning processes was investigated. Fourteen coal samples of different ranks ranging from high to medium sulfur content were studied by dry oxidation tests at different temperatures and humidities, and by wet oxidation tests using different oxidizing agents. The wettability of as-received and oxidized coal samples were characterized by film flotation tests and electrokinetic behavior. Based on the results of the oxidation tests, possible mechanisms have been proposed to explain the changes on the coal surface induced by different treatments. Flotation tests were carried out on different coals under controlled pH and potential to investigate the effect of polarization on the flotation of coal, and the ability to separate pyrite from coal by selective flotation of either coal or pyrite. Finally, electrochemical tests were performed on two coal pyrite samples in order to obtain a better understanding of coal pyrite oxidation.

The effects of specific oxidation treatments on various surface properties of coals have been studied systematically. The concentration of oxygen functional groups increases as the temperature, humidity and oxidation time are increased. During oxidation at 230^{o}C, anthracite coals show only a small increase in the oxygen functional group concentration. This is consistent with the predominantly aromatic structure of anthracite coal and the fact that oxidation occurs preferentially on aliphatic groups. Conversely, sub-bituminous coals experienced severe oxidation with significant increase in the oxygen functional group concentration. These result are consistent with the fact that lower rank coals are more susceptible to oxidation than higher rank coals.

The wettability of as-received and thermally oxidized samples was studied by film flotation tests with a series of aqueous methanol solutions. In general, coals show wetting distribution curves that shift towards higher surface tensions with increasing oxidation. This decrease in hydrophobicity is attributed to the increase of functional groups that interact strongly with water and the evolution of volatile matter with oxidation. The decrease in hydrophobicity is more pronounced in bituminous coals, possibly due to more significant evolution of volatile matter.

With the exception of anthracite coal, electrokinetic tests on as-received and oxidized coals show that oxidation decreases the zeta potential and the PZR values shift to lower pH's. The shift is more pronounced as coals become more oxidized. This is due to the formation of more oxygen functional groups that dissociate at low pH. The presence of significant amounts of ash in the coal samples also affects the zeta potential. At basic pH, the zeta potential of coal samples became less negative, due to the formation and dissolution of humic acids.

The dry thermal oxidation of coals is accompanied by a change in the concentration of various functional groups. The DRIFT spectra of different coals show that the intensities of some specific absorption bands change during oxidation. With the exception of anthracite coal, in most of the cases, the intensity of the peak corresponding to the carboxyl functionality increases with oxidation. Also, the peaks corresponding to ester and anhydride functionalities was increased slightly, whereas the intensity of the peaks corresponding to aliphatic configurations decreased dramatically. The latter confirm the fact that thermal oxidation at 230^{o}C severely modifies the aliphatic structure of coal.

The mechanisms of oxidation at 230°C have been interpreted in terms of classical autooxidation reactions in which the first step could be the formation of hydroperoxide compounds by the preferential oxidation of the aliphatic units present in coal. The loss of aliphatic structure detected by DRIFT measurements suggests that this would be the initial site of abstraction of hydrogen and subsequent hydroperoxide formation. These products were not detected because they easily decomposed at the experimental oxidation temperature. Once hydroperoxide decomposition has occurred and released further radicals into the system, the range of reaction possibilities becomes extensive, and choosing between them is somewhat speculative. However, the presence of carboxylic acids, phenolic groups, esters and anhydrides detected in this study has been consistently explained according to coherent reaction sequences.

Wet oxidation studies using different oxidizing agents revealed that the extent of oxidation for the sub-bituminous C (PSOC-1442) and MV Bituminous (PSOC-1527) coals is comparable to that observed after dry thermal oxidation at 230°C. The susceptibility to oxidation by a given oxidizing agent varied from sample to sample in no obvious systematic way. Wet oxidation also reduced the hydrophobicity of the coal although to a lesser extent than dry thermal oxidation. Wet oxidation by hydrogen peroxide probably involves a Fenton reaction mechanism by which pyrite catalyzed the oxidation process by reducing H_2O_2 to form $OH^{\cdot}$ radicals that enhanced the oxidation of coal. Interaction between coal and nitric acid involves complex mechanisms characterized by a series of reactions such as oxidation of the organic and inorganic fractions of coal. In the oxidation of coal by ferric sulfate solution, the functional groups present in as-received coal and those generated by oxidation can interact with both ferric iron as well as ferrous iron generated by the oxidation of coal pyrite. The interaction is explained by an ion-exchange mechanism that is consistent with the marked decrease in the concentration of total iron in solution during the initial stage of oxidation.

Although the alteration of the inorganic and organic materials occurs simultaneously in coal exposed to the atmosphere, these processes had been generally regarded as independent. This study analyzed the importance of the role that the interaction of pyrite with water and oxygen plays in the oxidation of coal. Pyrite oxidation could promote and catalyze the oxidation of coal by the generation of sulfuric acid and ferrous iron. The role of sulfuric acid is very important because it participates in primary steps of coal oxidation, and it can leach trace toxic metals from ash minerals, promoting the alteration of other minerals present in coal that otherwise might be stable. The role of ferrous iron is related to its oxidation by oxygen to ferric iron, which in turn oxidizes pyrite and coal.

Oxidation of coal creates conditions for water sorption; water activates oxygen molecules that participate not only in the formation of free radicals, promoting the oxidation of the organic structure of coal, but also in the oxidation of pyrite. These concurrent oxidation processes produce an autocatalytic effect, thereby making the process self-propagating.

The complex nature of coals means that definitive results on coal oxidation are difficult to achieve. The results of the present work indicate that the oxidation mechanism is probably similar in all coals except, perhaps, for anthracite coal. The principal variations in oxidation are probably due to different relative proportion of the reactive species in different coals.

Bituminous coals exhibited the highest floatability, whereas sub-bituminous and anthracite coals showed poor floatability. No obvious reason could be found for the unexpectedly low flotation response of anthracite coals, however, similar behavior has been observed by other authors. The results of the oxidation, film flotation and salt

flotation studies indicate that the presence of oxygen functional groups, high ash and moisture contents may be responsible for the mediocre flotation behavior of some coals.

The effect of the solution potential on the flotation of coal and coal pyrite was studied on high sulfur coals. An important conclusion drawn from these flotation tests is that at reducing potentials, the functional groups present on the coal surface are reduced and consequently the hydrophobic character of the coal surface is partially restored. Moreover, at these potentials, the pyrite surface is more hydrophilic due to the formation of layers of sulfur-deficient (metal-rich) sulfides such as FeS or FeS_{2-x}. These concurrent effects contribute to potentially significant improvements in the separation of coal pyrite from coal, and should be considered in seeking more efficient conditions for flotation.

At oxidizing potentials, the flotation of coal decreases significantly due to the presence of highly oxidized functional groups on the coal surface. This phenomenon enhances the detrimental effect of oxidation on the surface properties of coal by decreasing its hydrophobicity. Moreover, at these oxidizing potentials the surface of pyrite is less hydrophobic due to the formation of a hydrophilic oxide layer on its surface. Therefore, it is clear that high potentials do not provide appropriate conditions for coal flotation.

This study showed that controlled experimental procedures can control the amount of carboxylic, phenolic and other functional groups on coal surface. This control provide a way to control for example: wettability, solvent penetration, ion-exchange capacity of coals, etc. Thus, for example, control of the surface characteristics of coals may allow the selective chemistry more commonly attainable with catalysts to be achieved with coals.

An important contribution of this study has been the extensive use of electrochemical tests at different pH to study the effect of different solution conditions on the behavior of coal pyrite. Results of these tests are very important since they provided insight on the behavior of pyrite in acid mine drainage and in flotation systems. It has been observed that significant differences can be expected in the electrochemical behavior of coal pyrite samples, depending on their prior history. For example, grinding can introduce damage or defects in the surface layers, and trace quantities of oxygen can readily oxidize their surface. These effects are even more likely during commercial coal preparation as during idealized laboratory experiments.

Pyrite samples studied here were more susceptible to oxidation after a cathodic excursion, suggesting that the reducing environment provided by coal actually increases the susceptibility of freshly exposed pyrite to oxidation. This finding constitutes important additional evidence to explain the reported higher reactivity of coal pyrite in comparison with ore pyrite.

Coal pyrite undergoing weathering in coal mines and storage piles may develop solutions of low pH values, according to reaction 46. The results of the present work would suggest that such weathering at low pH would make the coal pyrite surface more hydrophobic, because of the formation of sulfur and polysulfides. This transformation would be undesirable, since cleaning methods such as flotation and oil agglomeration require the pyrite to be less hydrophobic than the coal. The problem is compounded by the concurrent oxidation of coal, which introduces hydrophilic carboxylic and phenolic groups. Oxides form when pyrite oxidizes under basic conditions, although the effect of this on the surface properties would depend on whether non-equilibrium polysulfides also appeared.

Another observation in this work is that the borate or phosphate buffer solutions interacted with pyrite electrodes. This observation should be crucial in the interpretation of previous electrochemical studies using phosphates and borates as electrolytes. The compounds formed would not, of course, be expected in a coal flotation circuit where pH would be regulated with inexpensive bases.

There is no significant effect of thermal oxidation upon the PZR value of Pittsburgh coal pyrite; however, the PZR value of Upper Freeport coal pyrite shifted to more acidic pH with oxidation. The negative charge on coal surface must be determined mainly by the acidic groups present on coal surface, rather than the oxidation products of pyrite. The critical surface tension of both coal pyrite samples increased dramatically on oxidation, reflecting a decrease in the hydrophobicity with oxidation. This is undoubtedly due to the presence of hydrophilic iron oxide or hydroxide on the surface. Clearly, this change with oxidation would affect the performance of coal cleaning.

The reliability and suitability of standard test methods used to determine the pyrite content of coal and mineral wastes, and their propensity to release acidic drainage, were studied. The hydrogen peroxide method published by the U.S. Environmental Protection Agency is not reliable for materials containing coal, because of interference associated with coal oxidation itself. The nitric acid oxidation-extraction method described in ASTM D2492-84 is effective at dissolving coal pyrite. Coal pyrite oxidized faster than ore pyrite and, therefore, differences in the reactivity of pyrite samples should be taken into account in any pre-mine prediction of post-mining drainage quality.

VII. RECOMMENDATIONS FOR FUTURE WORK

The need to use energy resources in an acceptable environmental manner present crucial challenges and opportunities for coal beneficiation during the present and future years, particularly regarding the control of SO_2 and hazardous air pollutants. In this context, it is essentially important to develop cost-effective coal cleaning methods for sulfur removal and other precursors of hazardous air pollutants. The most promising methods for sulfur removal are advanced froth flotation and oil agglomeration, surface-based processes that are affected by oxidation. The results of this study confirm that oxidation affected the surface properties of coal and coal pyrite and consequently a detrimental effect would be expected on the separation efficiency. Although, this study has provided a basis for understanding the process of coal oxidation, more systematic examination of both mineral and maceral oxidation than was attempted in this study are required to elucidate the oxidation mechanisms. *In-situ* examination of coal during oxidation by infrared spectroscopy should be further developed in order to gather complementary information on the chemistry and behavior of individual coals. The study of the surface of pyrite during oxidation by using techniques such as X-ray photoelectron spectroscopy (XPS) and infrared spectroscopy would provide information on the nature and distribution of iron and sulfur species present on coal pyrite surfaces. This is very important because the wetting behavior of pyrite is controlled by the distribution of hydrophobic and hydrophilic species present on its surface, and oxidation products can also influence interactions with flotation collectors and reagents used in oil agglomeration. It is also necessary to carry out an in-depth study of the morphology, semiconductor properties, composition, size and distribution of the mineral matter in coal prior to beneficiation in order to find the most suitable methods and conditions for its removal.

Because chemical processes to remove sulfur from coal are not economically viable under present economic conditions, it is important to work on the improvement of the kinetic aspects associated with these processes. However, the use of microbial systems although slow, can be sufficiently effective and low in cost for practical utilization in coal cleaning.

Coal contains a wide range of trace elements, including Ni, Cu, Zn, As, Se, Mo, and Pb among others. The majority of these trace elements are associated with the inorganic mineral matter present in coal, and are released into the gas phase during coal combustion. It is important to study the behavior of these elements during combustion and their environmental significance, particularly the potential groundwater contamination from discarded fly ash. It should be noted that the removal of pyrite from coal, also reduces the concentration of some environmentally sensitive trace elements. It would be also interesting to determine the type and concentration of the trace elements associated with different coal pyrite samples and to correlate this with the electrochemical behavior of coal pyrite.

REFERENCES

1. Electric Power Research Institute Journal, "Quickening the Pace in Clean Coal Technology", **January/February**, 1989.

2. Energy Information Administration/Quaterly Report, **January-March,** 1993.

3. Diamond, S., "New Methods to Clean Coal", *New York Times,* 1985, **June 27**, 32.

4. International Energy Agency, "Sulphates in the Atmosphere", **December**, 1986.

5. Alloway, B.J., *Chemical Principles of Environmental Pollution,* 1993, Blockie Academic & Professional Ed., London, p. 129.

6. Phelps, R.W., "Clean Air in the United States-How?, *Engineering and Mining Journal*, 1991, **April**, p. 24.

7. Feeley, T.J. and McLean, V., "Advanced Physical Coal Cleaning as a Clean Acta Compliance Technology", *Mining Engineering*, 1993, **October**, p.1253.

8. ASTM Standard Test Number D3172M, "Proximate Analysis of Coal and Coke."

9. ASTM Standard Test Number D3176M, "Ultimate Analysis of Coal and Coke."

10. Falcon, R.M.S.,"Coal in South Africa, Part II: The Application of Petrography to the Characterization of Coal", *Minerals Sci. Engng.*, 1978, **Vol. 10**, no 1, p. 28.

11. Slaghuis, J.H., "Some Interactions Between Various Minerals Occurring in South African Coal Types During Thermal Decomposition", in *Proceedings of the 7th International Conference on Coal Science*, K.H Michaelian, ed., 1993, **Vol. I**, p. 124.

12. Price, J.T., Gransden, J.F. and Yu Jingfeng, "Effect of Coal Properties and Processing Conditions on the Reactivity of Metallurgical Cokes", in *Proceedings of the 7th International Conference on Coal Science*, K.H Michaelian, ed., 1993, **Vol. I**, p. 493.

13. Diego-Marin, A., and Garbett, E.S.,"The Effect of Minerals on Ignition of Pulverised Coal Particles", in *Proceedings of the 7th International Conference on Coal Science*, K.H Michaelian, ed., 1993, **Vol. II**, p. 39.

14. Shah N., Huffman, G.P., Shah, A., and Huggins, F.E.,"Spectroscopic Investigation of Coal Mineral Transformation During Combustion", in *Proceedings of the 7th International Conference on Coal Science*, K.H Michaelian, ed., 1993, **Vol. II**, p. 197.

15. Ibarra, J.V., Miranda, J.L., Romero, C., and Gracia, M.,"Structural Changes in Stockpiled Coals Induced by Weathering", in *Proceedings of the 7th International Conference on Coal Science*, K.H Michaelian, ed., 1993, **Vol. II**, p. 601.

16. Huggins, F.E., Huffman, G.P., and Lin, M.C., "Observation of Low Temperature Oxidation of Minerals in Bituminous Coals", *International Journal of Coal Geology.*, 1983, **3**, 157.

17. Laskowski, J.S. and Parfitt, G.D.,"Electrokinetics of Coal-Water Suspensions", in *Interfacial Phenomena in Coal Technology.*, Botsaris G.D. and Glazman Y.M., Eds., Surfactant Science Series , 1989, **32**, Marcel Dekker Inc., New York, p.279.

18. Zwietering, P. and van Krevelen, D.W.,"Chemical Structure and Properties of Coals", *Fuel*, 1954, **33**, p. 331.

19. Lin, J.L., Hendricks, R.W., Harris, L.A., and Yust, C. S.,"Microporosity and Micromineralogy in Vitrinite of Bituminous Coal", *J. Appl. Crystallogr.*, 1978, **11**, p. 621.

20. Mahajan, O.P., "Coal Porosity", in *Coal Structure*, 1982, Meyer, R.A., Ed., Academic Press, New York, **Vol.1**, p. 51.

21. Dubinin, M.M., "The Potential Theory of Adsorption of Gases and Vapors for Adsorption with Energetically Nonuniform Surfaces", *Chemical Review*, 1960, **60**, p. 235.

22. Brunauer, S., Emmett, P.H., and Teller, E.,"Absorption of Gases in Multimolecular Layers", *Journal of American Chemistry Society.*, 1938, **60**, p. 309.

23. Marsh, H. and Siemieniewska, T.,"The Surface Areas of Coal as Evaluated from the Adsorption Isotherms of Carbon Dioxide using Dubinin-Polanyi Equation", *Fuel.*, 1965, **51**, p. 272.

24. Franklin, R.E.,"A Study of the Fine Structure of Carbonaceous Solid by Measurements of True and Apparent Density", *Trans. Faraday Soc.*, 1949, **45**, p. 274.

25. Mahajan, O.P.,"Adsorption and Pore Structure and Coal-Water Interactions", in *Sample Selection, Aging, and Reactivity of Coal.*, 1989, Klein R. and Wellek R., Eds., John Wiley & Sons, Inc., New York, p. 157.

26. Spitzer, Z. and Ulicky, L.," Specific Surfaces of Coals Determined by Small-Angle X-ray Scattering and by Adsorption by Methanol", *Fuel*, 1976, **55**, p.21.

27. Bangham, D.H. and Razouk, R.I.,"The Swelling of Charcoal. Part V. The Saturation and Immersion Expansions and The Heat of Wetting", *Proc. R. Soc. London, Ser. A.* , 1938, **166**, p. 572

28. Mahajan, O.P. and Fuller, E.L.,"Porosity of Coals and Coal Products", in *Analytical Methods for Coal and Coal Products*, 1978, Karr, C., Ed., Academic Press, New York, **Vol. 1**, p.125.

29. Maggs, F. A. P.,"Anomalous Adsorption of Nitrogen at 90 K",1952, *Nature*, **169**, p. 793

30. Grimes, W. R., "The Physical Structure of Coal", in *Coal Science,* 1982, Gorbaty, M., Larsen, J., and Wonder, I.,Editors., **Vol. 1**., p. 21.

31. Aplan, F. F., "Coal Preparation", 1992, 5th Ed., Leonard, J.W. and Hardinge, Eds., AIME-SME, Littleton, Colorado, **Chapters 4 and 7**.

32. Matoney, J.P., Harrison, K.E., and Kern, K., "Coal Preparation Plants-Past, Present and Future", 1988. in *Proceedings of the Industrial Practice of Fine Coal Processing Conference*, AIME-SME, Littleton, Colorado, p. 3.

33. Fuerstenau, D.W.. and Healy, T.W., "Principles of Mineral Flotation", in *Adsorptive Bubble Separation Techniques*, 1972, Lemlich, R., ed., Academic Press, New York, p. 92.

34. Fuerstenau, D.W., and Raghavan, S., "Some Aspects of the Thermodynamics of Flotation", in *Flotation, A.M. Gaudin Memorial Volume*, 1976, Fuerstenau, M.C., ed., A.I.M.E., New York, **Vol. 1**, p. 21.

35. Fuerstenau, D.W., "Chemistry of Flotation", in *Principles of Mineral Flotation*, 1984, Jones, M.H., and Woodcock, J.T., Editors., The Australian Institute of Mining and Metallurgy, Parkville, Victoria, Australia, p. 7.

36. Fuerstenau, D.W., and Herrera-Urbina, R., "Flotation Reagents", in *Advances in Coal and Mineral Processing Using Flotation*, 1989, Chander, S., and Klumpel, R.R., Editors, AIME-SME, Littleton, Colorado, p. 3.

37. Rosenbaum, J.M., "Characterization, Flotation and Selective Agglomeration of Western Coals", Ph.D. Thesis, University of California, Berkeley, 1981.

38. Aplan, F.F., and Fuerstenau, D.W., "Principles of Nonmetallic Mineral Flotation", in *Froth Flotation: 50th Anniversary Volume*, 1962, Fuerstenau, D.W., ed., A.I.M.E., New York, p. 174.

39. Meyers, R.A., "Removal of Pyritic Sulfur from Coal Using Solutions Containing Ferric Ions", 1973, US Pat. 3,768,988.

40. Vasilakos, N.P., and Clinton, C.S., "Chemical Beneficiation of Coal with Aqueous Hydrogen Peroxide-Sulphuric Acid Solutions", *Fuel*, 1984, **63**, p. 1561.

41. Ali, A.S., Srivastava, S.K., and Haque, R., "Chemical Desulphurization of High Sulphur Coals", *Fuel*, 1992, **71**, p. 835.

42. Boron, D.J. and Taylor, S.R., "Mild Oxidation of Coal. 1. Hydrogen Peroxide Oxidation", *Fuel*, 1985, **64**, p. 209.

43. Ahnonkitpanit, E., and Prasassarakich, P., "Coal Desulphurization in Aqueous Hydrogen Peroxide", *Fuel*, 1989, **68**, p 819.

44. Heard, I., and Senftle, F.E., "Chemical Oxidation of Anthracite with Hydrogen Peroxide via the Fenton Reaction", *Fuel*, 1984, **63**, p. 221.

45. Palmer, S., Hippo, E.J., and Dorai, X.A., "Chemical Coal Cleaning Using Selective Oxidation", *Fuel*, 1994, **73**, p. 161.

46. Kinney, C.R. and Ockert, K.F., "Nitric Acid Oxidation of Bituminous Coal", *Industrial and Engineering Chemistry*, 1956, **48 No 2**, p 327.

47. Yang, R.T., Subho, K. Das, and Tsai, B.M.C.,"Coal Demineralization using Sodium Hydroxide and Acid Solutions", *Fuel*, 1985, **64**, p. 735.

48. Chriswell, C.D., Markuszesku, R. and Norton, G.A., "Processing and Utilization of High-Sulfur Coals IV", in *Coal Science and Technology 18*, 1991, Dugan, P.R., Quigley, D.R., and Attia, Y.A., Editors, Elsevier, New York, p. 385.

49. Berkowitz, N., in *An Introduction to Coal Technology*, 1979, Academic Press., New York, **Chapter 5**.

50. van Krevelen, D. W., in *Coal*, 1961, Elsevier Amsterdam, **Chapters 7 and 8**.

51. Dryden, I.G.C., Landers, W.S,. and Dmaven, D.J., in *Chemistry of Coal Utilization*, 1963, Lowry, H. H. , Ed., Wiley New York , Suppl. Volume, **Chapters 6 and 7**.

52. Seki, H., Ito, O., and Lino, M., "Effect of Oxidation on Caking Properties: Oxidation of Extract and Residue", *Fuel*, 1990, **Vol. 69**, p. 1047.

53. Huffman, G.H., Huggins, F.E., Durmyre, G.R., Pignocco, A.J., and Lin, M.C., "Comparative Sensitivity of Various Analytical Techniques to the Low Temperature Oxidation of Coal", *Fuel*, 1985, **64**, p. 849.

54. Crelling, J. C., Schrader, R.H., and Benedict, L.G.,"Effect of Weathered Coal on Coking and Coke Quality", *Fuel*, 1979, **58**, p. 542.

55. Alvarez, R., Casal, M. D., Diez, M. A., Gonzalez, A.I., Lazaro, M., Suarez, C., and Pis, J.J., "Coal Weathering of an Industrial Coal Blend : Influence of the Caking Properties and the Coking Pressure Developed During Carbonization", in *Proceedings of the 7th International Conference on Coal Science*, K.H Michaelian, ed., 1993, Vol. II, p. 107.

56. Neavel, R. C., "Liquefaction of Coal in Hydrogen-Donor and Non-Donor Vehicles", *Fuel*, 1976, **55**, p. 237.

57. Song, C., Saini, A., and Schobert, H., "Positive and Negative Impacts of Drying and Oxidation on Low-Severity Catalytic Liquefaction of Low Rank Coal", in *Proceedings of the 7th International Conference on Coal Science*, K.H Michaelian, ed., 1993, **Vol I**, p. 291.

58. Reinecke, C.F., van Nierop, P., and Fullard, A.F., "The Correlation of Functional Group Composition with Oil Agglomeration and Froth Flotation Behavior of Coal", in *Proceedings of the 7th International Conference on Coal Science*, K.H Michaelian, ed., 1993, **Vol. II**, p. 499.

59. Reinecke, C.F., van Nierop, P., and Wolters, F., "The Correlation of Flotation Behavior and Coal Characteristics", in *Proceedings of the 7th International Conference on Coal Science*, K.H Michaelian, ed., 1993, **Vol. II**, p. 491.

60. Nandi, B.N., Brown, T.D., and Lee, G.K.,"Inert Coal Macerals in Combustion", *Fuel*, 1977, **56**, p.125.

61. Lee, G.K., and Whaley, H.,"Modification of Combustion and Fly-Ash Characteristics by Coal Blending", *J. Inst. Energy*, 1983, **Vol. 56 No 429**, December, p. 190.

62. Mahajan, O.P., Komatsu, M., and Walker, P.L.Jr.,"Low Temperature Air Oxidation of Coking Coals:1. Effect on Subsequent Reactivity of Chars Produced", *Fuel* ,1980, **59**, p. 3.

63. Gethner, J.S., "Kinetic Study of the Oxidation of Illinois #6 Coal at Low Temperature", *Fuel*, 1987, **66**, p.1091.

64. Meuzelaar, H.L., McClennen, W.H., Metcalf. G.S., Winding, W., Thurgood, J.R., Hill, G.R., "Pyrolisis Mechanisms and Weathering Phenomena in Rocky Mountain Coals", *Am. Chem. Soc., Div. Fuel. Chem.*, 1984, **29(5)**, p. 166.

65. Ludvig, M. M., Gard, G.L., and Emmett, P.H.,"Use of Controlled Oxidation to Increase the Surface Area of Coal", *Fuel*, 1983, **62**, p. 1393.

66. van Krevelen, D. W., in *Coal Science and Technology. Coal, Typology-Chemistry-Physics-Construction.*, 1981, 2nd edn., Elsevier Scientific, New York. p. 219.

67. Grossman, S.L., Davidi, S., and Cohen, H.,"Molecular Hydrogen Evolution as a Consequence of Atmospheric Oxidation of Coal: 1. Batch Reactor Simulation", *Fuel*, 1993, **72**, p.193.

68. Liotta, R., Brons, G., and Isaacs, J.,"Oxidative Weathering of Illinois No.6 Coal", *Fuel*, 1983, **62**, p. 781.

69. Swaan, P., and Evans, D.G.,"Low Temperature Oxidation of Brown Coal. 3. Reaction with Molecular Oxygen at Temperatures Close to Ambient", *Fuel*, 1979, **58**, p. 276.

70. Kister, J., Guiliano, M., Mille, G., and Dou, H.,"Changes in the Chemical Structure of Low Rank Coal After Low Temperature Oxidation or Demineralization", *Fuel*, 1988, **67**, p. 1078.

71. Landais, P., and Rochdi, A., "*In situ* Examination of Coal Macerals Oxidation by Micro-FTIR Spectroscopy", *Fuel*, 1993,**Vol 72.**, p 55.

72. Clemens, A.H., Matheson, T.H., and Rogers, D.E.,"Low Temperature Oxidation Studies of Dried New Zealand Coals", *Fuel*, 1991, **70**, p. 215.

73. Gethner, J.S., "The Mechanism of the Low Temperature Oxidation of Coal by O_2: Observation and Separation of Simultaneous Reactions Using *In Situ* FTIR Difference Spectroscopy", *Applied Spectroscopy*, 1981, **41**, p. 50.

74. Rhoads, C.A. , Senftle, J.T., Coleman, M.M., Davis, A., and Painter, P.C., "Further Studies of Coal Oxidation", *Fuel*, 1983, **62**, p. 1387.

75. Mielczarski, J.A., Denca, A., and Strojek, J.W., "Application of Attenuated Total Reflection Infrared Spectroscopy to the Characterization of Coals", *Applied Spectroscopy*, 1986,**Vol. 40 No7**, p. 998.

76. Dack, S.W., Hobday, M.D., Smith, T.D., and Pilbrow, J.R.,"Free-Radical Involvement in the Drying and Oxidation of Victorian Brown Coal", *Fuel*, 1984, **63**, p. 39.

77. MacPhee, J.A., Wieslaw, P.H., Giroux, L., Charland, J.P., and Price, J.T., "Characterization of Coal Weathering/Oxidation by TGA-FTIR", in *Proceedings of the 7th International Conference on Coal Science*, K.H Michaelian, ed., 1993, **Vol. I**, p. 590.

78. Painter, P.C., Snyder, R.W., Pearson, D.E., and Kwong, J., "Fourier Transform Infrared Study of the Variation in the Oxidation of a Coking Coal", *Fuel*, 1980, **59**, p. 282.

79. Estevez, M., Juan, R., Ruiz, C., and Andres, J.S., "Formation of Humic Acids in Lignites and Sub-bituminous Coals by Dry Air Oxidation", *Fuel*, 1990, **69**, p. 157.

80. Banerjee, A.K., Choudhury, D., and Choudhury, S.S.,"Chemical Changes Accompanying Oxygenation of Coal by Air and Deoxygenation of Oxidized Coal by Thermal Treatment", *Fuel*, 1989, **68**, p.1129.

81. Azik, M., and Yurum, Y., "Air Oxidation of Turkish Beypazari Lignite. 1. Change of Structural Characteristics in Oxidation Reactions at 150°C", *Energy and Fuel*, 1993, **7**, p. 367.

82. Huai, H., Gaines, A.F., and Flint, C.D.,"Scanning Electron Microscopy of Treated Bituminous Coals", *Fuel Processing Technology*, 1992, **32**, p. 25.

83. Gerard, L., and Landais, P.,"Combined Effects of Oxidation and Thermal Maturation on Coal Behavior", in *Proceedings of the 7th International Conference on Coal Science*, K.H Michaelian, ed., 1993, **Vol. II**, p. 303.

84. Kalema, W.S., and Gavalas, G.R., "Changes in Coal Composition During Air Oxidation at 200-250°C", *Fuel*, 1987, **66**, p. 158.

85. Pis, J.J., Moran, A., de la Puente, G, and Fuente, E., "Effect of Aerial Oxidation on the Reactivity of Coals", in *Proceedings of the 7th International Conference on Coal Science*, K.H Michaelian, ed., 1993, **Vol. I**, p. 664.

86. Mukherjee, P.N., Bhowmik, J.N., and Lahiri, A. "Mechanism of Oxidation of Coal with Special Reference to the Products of Oxidation", *Fuel*, 1956, **36**, p 417.

87. Cronauer, D.C., Ruberto, R.G., Jenkins, R.G., Davis, A. Painter, P.C., Hoover, D.S., Starsinic, M.E., and Schlyer, D.,"Liquefaction of Partially Dried and Oxidized Coals", *Fuel*, 1983, **62**, p. 1124.

88. Chen, X.D., and Stott, J.B., "The Effect of Moisture Content on the Oxidation Rate of Coal During Near-Equilibrium Drying and Wetting at 50°C", *Fuel*, 1993, **72**, p. 787.

89. Panaseiko, S.P., "Influence of Moisture on the Low Temperature Oxidation of Coals", *Khimiya Tverdogo Topliva*, 1974, **Vol 8**, **No 1**, p. 26.

90. Huggins, F.E., Huffman, G.P., and Lin, M.C., "Observations on Low Temperature Oxidation of Minerals in Bituminous Coals", *International Journal of Coal Geology*, 1983, **3**, p. 153.

91. Huffman, G.P., Huggins, F.E., Dunmyre, G.R., Pignocco, A.J., and Lin, M.Ch., "Comparative Sensitivity of Various Analytical Techniques to the Low Temperature Oxidation of Coals", *Fuel*, 1985, **64**, p. 840.

92. Petit, J.C., "A Comprehensive Study of the Water Vapour/Coal System: Application to the Role of Water in the Weathering of Coal", *Fuel*, 1991, **70**, p. 1053.

93. Czuchajowsky, L., "Infra-red Spectra of Coals Oxidized with Hydrogen Peroxide and Nitric Acid", *Fuel*, 1960, **Vol. 39 No39**, p. 377.

94. Kawakami, K., Fujio, K., Kusunoki, K., Kusakabe, K., and Morooka, S., "Kinetic Study of Coal Slurry Electrolysis: Oxidation and Desulfurization of Illinois No. 6 Coal by Aqueous Ferric Chloride", *Fuel Processing Technology*, 1988, **19**, p. 15.

95. Oshinowo, T, and Ofi, O., "Kinetics of Chemical Desulfurization of Coal in Aqueous Ferric Chloride", *The Canadian Journal of Chemical Engineering*, 1987, **65**, p. 481.

96. Fuerstenau, D.W., Diao, J., and Yang, G.C., "On the Dry Thermal and Wet Chemical Oxidation of Coal", *Fluid/Particle Separation Journal*, 1989, **2 No.3**, p. 136.

97. Berkowitz, N., "The Chemistry of Coal", *Coal Science and Technology*, 1985, Elsevier, **Vol. 7**, p. 148.

98. Volborth, A.,"Analytical Methods for Coal and Coal Products", 1979, Karr Jr., Ed., Academic Press, **Vol. III**, p.563.

99. Badin, E.J., "Coal Combustion Chemistry-Correlation Aspects" , *Coal Science and Technology*, 1984, **Vol. 6**, p.75.

100. Streitwieser, A., and Heathcock, C., "Introduction to Organic Chemistry", 1976, 2º Edition, Macmillan Publishing Co., Inc., New York, p.399.

101. Alberts, G., Lenart, L. and Oelert, H., "Spectroscopy Studies on Chemically Reacted (Oxidized) Coal", *Fuel*, 1974, **53**, p. 47.

102. Markova, K.Iv., "Change in Oxygen-Containing Functional Groups During Medium-Temperature Oxidation Of Coals with Different Degrees of Coalification", 1989, *Khimiya Tverdogo Topliva*, **Vol. 23, No4**, p. 41.

103. Iskhakov, Kh. A., "The Role of Sorbed Moisture in Coal Oxidation", 1990, *Khimiya Tverdogo Topliva*, **Vol. 24, No2**, p. 19.

104. Karyakin, A.V., Kriventsova, G.A., "The State of Water in Organic and Inorganic Compounds", 1973, Nauka Editors, Moscow.

105. Streitwieser, A., and Heathcock, C., "Introduction to Organic Chemistry", 1976, 2º Edition, Macmillan Publishing Co., Inc., New York, p.252.

106. Draganic, J.G. and Draganic, Z.D., "*The Reaction Chemistry of Water*", 1971, Academic Press, New York, p. 109.

107. Barb, W.G., Baxendale, J.H., George, P.,and Hargrave, K.R.,"Reactions of Ferrous and Ferric Ions with Hydrogen Peroxide: 1. Ferrous Iron Reaction", *Trans. Faraday Soc.*, 1951, **47**, p. 462.

108. Nonhebel, D. and Walton, J.C., "Free-Radical Chemistry: Structure and Mechanisms", 1964, Cambridge University Press, Cambridge, p. 358.

109. van Krevelen, D.W., "Graphical-Statistical Method for the Study of Structure and Reaction Processes of Coal", *Fuel*, 1950, **29**, p. 269.

110. Meyers, R.A., "Coal Desulfurization", 1977, Marcel Dekker, Ed., New York, p. 246.

111. Vetter, K.J.,"Elektrochemische Kinetik," 1961, Spring-Verlag, Berlin, p. 381.

112. Thomas,G., Chettar, M and Birss, V.I.,"Electrochemical Oxidation of Acidic Alberta Coal Slurry", *Journal of Applied Electrochemistry*, 1990, **20**, p. 941.

113. Peters, E., and Majima, H., "Electrochemical Reactions of Pyrite in Acid Perchlorate Solutions", *Canadian Metallurgical Quarterly*, 1968, **7**, p. 111.

114. Eligwe, Ch. A., and Okolue, N., "Adsorption of Iron (III) by a Nigerian Brown Coal", *Fuel*, 1994, **73**, p. 569.

115. Sennett, P., and Olivier., J.P., "Colloidal Dispersions, Electrokinetic Effects and the Concept of Zeta Potential", *Industrial and Engineering Chemistry*, 1965, **57 No.8**, p. 32.

116. Laskowski, J. and Parfitt, G., "Electrokinetic of Coal-Water Suspensions", in *Interfacial Phenomena in Coal Technology*, Botsaris, G.D., and Glazman, Y. M., Eds., 1988, p. 279.

117. Fuerstenau, D.W., Rosenbaum, J.M., and You, Y.S., "Electrokinetic Behavior of Coal", *Energy and Fuels*, 1988, **2**, p. 241.

118. Kelebek, S., Salman, T., and Smith, G.W., "An Electrokinetic Study of Three Coals", *Canadian Metallurgical Quarterly,* 1982, **21 No.2**, p. 205.

119. Wen, W.W., and Sun, S.C.,"Recovery of Fine-Particle Coal by Colloid Flotation", *Separation Science Technology*, 1981, **16(10)**, p. 1491.

120. Fuerstenau, D.W., and Pradip, "Adsorption of Frothers at Coal/Water Interfaces", *Colloids and Surfaces*, 1982, **4**, p. 229.

121. Rubin, A.J., and Kramer, R.J., "Recovery of Fine-Particle Coal by Colloidal Flotation", *Separation Science Technology*, 1982, **17(4)**, p. 535.

122. Yarar, B., "Correlation of Zeta Potential and Floatability of Weathered Coal", *Trans. SME/AIME*, 1982, **4**, p. 1978.

123. Coca, J., Bueno, J.L., and Sastre, H.,"Electrokinetic Behavior of Coal Particles Suspensions", *J. Chem. Tech. Biotechnology*, 1982, **32**, p. 637.

124. Celik, M.S., and Somasundaran, P., "Effect of Pretreatment on Flotation and Electrokinetic Properties of Coal", *Colloids and Surfaces*, 1980, **1**, p. 121.

125. Campbell, J.A.L., and Sun, S.C., "Anthracite Coal Electrokinetics", *Trans. SME/AIME*, 1970, **247**, p. 120.

126. Ferrell, D.P., and Huang, C.P., "The Removal of Fine Coal Particles from Water by Flotation", *Chem. Eng. Comm.*, 1985, **35**, p. 351.

127. Diao, J., "Surface Properties of Coal and Their Role in Fine Coal Processing", Ph.D. Thesis, University of California, Berkeley, 1990.

128. Zisman, W.A., "Relation of the Equilibrium Contact Angle to Liquid and Solid Constitution", in *Contact Angle, Wettability, and Adhesion.*, Gould, R.F., Ed.; Advanced in Chemistry Series 43, American Chemical Society: Washington, D.C., 1964, p.1.

129. Fuerstenau, D.W., J. Diao, and Hanson, J.S., "Estimation of the Distribution of Surface Sites and Contact Angles on Coal Particles from Film Flotation Data", *Energy and Fuels*, 1990, **4**, p. 34.

130. Parekh, B.K., and Aplan, F.F., "Critical Surface Tension of Wetting of Coal", in *Recent Developments in Separation Science*, Li, N.N., Ed., CRC Press, Florida, 1978, **4**, p. 107.

131. Glanville, J.O., and Wightman, " Wetting of Powdered Coals by Alkanol-Water Solutions and Other Liquids", *Fuel*, 1980, **59**, p. 557.

132. Widyani, E., and Wightman, J.P., "Thermodynamics and Kinetics of Immersion of Coal by n-Alcohols", *Colloids and Surfaces*, 1982, **4**, p. 209.

133. Omenyi, S.N., Smith, R.P., and Neumann, A.W., "Determination Solid/Melt Interfacial Tensions and Contact Angles of Small Particles from the Critical Velocity of Engulfing", *J. Colloid Interface Science*, 1980, **75**, p. 117.

134. Fuller Jr., E.L., "Structure and Chemistry of Coals: Calorimetric Analysis", *J. Colloid and Interface Sci.*, 1980, **75**, p. 77.

135. Fuerstenau, D.W., and Williams, M.C., "Characterization of the Lyophobicity of Particles by Film Flotation", *Colloids and Surfaces*, 1987, **22**, p. 87.

136. Williams, M.C., and Fuerstenau, D.W., "A Simple Flotation Method for Rapidly Assessing the Hydrophobicity of Coal Particles", *International Journal of Mineral Processing*", 1987, **20**, p. 153.

137. Fuerstenau, D.W., and Williams, M.C.,"A New Method for Characterization of the Surface Energy of Hydrophobic Coal Particles", *Particle Characterization*, 1987, **4**, p. 7.

138. Diao, J., "Characterization of the Wettability of Solid Particles by Film Flotation", M.S. Thesis, University of California, Berkeley, 1988.

139. Fuerstenau, D.W., Diao, J., Narayanan, K.S., and Urbina, R.H., "Assessing the Wettability and Degree of Oxidation of Coal by Film Flotation", *Energy and Fuels*, **2(3)**, p. 237.

140. Yang, G.C.C., "Interfacial Properties of Coal and Their Role in Coal Beneficiation", Ph.D. Thesis, University of California, Berkeley, 1983.

141. Horsley, R.M., and Smith H.G., "Principles of Coal Flotation", *Fuel*, 1951, **30**, p.54.

142. Fuerstenau, D.W., Diao, J., and Williams, M.C., "Characterization of the Wettability of Solid Particles by Film Flotation", *Colloids and Surfaces*, 1991, **60**, p.127.

143. Fuerstenau, D.W., Yang, G.C.C., and Laskowski, J.S.,"Oxidation Phenomena in Coal Flotation. Part I. Correlation Between Oxygen Functional Group Concentration, Immersion Wettability and Salt Flotation Response", *Coal Preparation*, 1987, **Vol 4**, p. 161.

144. Gutierrez-Rodriguez, J.A., Purcell Jr., J.R., and Aplan, F.F., "Estimating the Hydrophobicity of Coal", *Colloids and Surfaces*, 1984, **12**, p. 27.

145. Rosenbaum, J.M., and Fuerstenau, D.W., "On the Variation of Contact Angle with Coal Rank", *International Journal of Mineral Processing*, 1984, **12**, p. 313.

146. Cassie, A.B.D., and Baxter, S., "Wettability of Porous Surface", *Trans. Faraday Soc.*, 1944, **40**, p. 546.

147. Brown, D.J., "Coal Flotation", in *Froth Flotation*, Fuerstenau, D.W.; ed., 1962, AIME, New York, p. 518.

148. University of California, University of Utah, Columbia University and Praxis Engineers Inc., "Coal Surface Control for Advanced Fine Coal Flotation", *Final Report DE-AC22-88PC88878 Project*, March 1992, p. 5-3.

149. Fuller Jr., E.L., "Structure and Chemistry of Coals: Calorimetric Analysis", *Journal of Colloid and Interface Science*, 1980, **75**, p. 577.

150. Ye, Y., and Miller, J.D., "The Significance of Bubble/Particle Contact Time During Collision in the Analysis of Flotation Phenomena", *International Journal of Mineral Processing*, 1989, **25**, p.199.

151. Lowson, R.T., "Aqueous Oxidation of Pyrite by Molecular Oxygen", *Chemical Reviews*, 1982, **Vol 82 No 5**, p. 461.

152. Mirza, A., "Kinetics and Mechanisms of Pyrite (FeS_2) Oxidation in the Formation of Acid Mine Drainage", Ph.D. Thesis, University of California, Berkeley, 1993.

153. Tao, D.P., Richardson, P.E., Luttrell, G.H, and Yoon, R.-H., "An Electrochemical Investigation of Surface Reactions of Coal- and Mineral-Pyrite in Aqueous Solutions", in *Processing and Utilization of High Sulfur Coals V*, 1993, Parekh, B.K., and Groppo, J.G., Editors, Elsevier Science Publishers B.V., p. 219.

154. Latimer W.M., "Oxidation Potentials", 1952, Prentice Hall, New York, p. 392.

155. Shuey, R.T., "Semiconducting Ore Minerals", 1975, Elsevier, Amsterdam

156. Doyle, F.M., and Mirza, A., "Understanding the Mechanisms and Kinetics of Acid and Heavy Metal Release from Pyritic Wastes", in *Proceeding of the Western Regional Symposium on Mining and Mineral Processing Wastes*, Doyle, F.M., ed., Society for Mining, Metallurgy and Exploration, Inc., Littleton, CO, May-June 1990, p. 43.

157. Briceno, A. and Chander, S., "An Electrochemical Characterization of Pyrites from Coal and Ore Sources", *International Journal of Mineral Processing*, 1988, **24**, p.73.

158. Lai, R.W., Diehl, J.R., Hammack, R.W., and Khan, S.U.M., "Comparative Study of the Surface Properties and the Reactivity of Coal Pyrite and Mineral Pyrite", 1989, AIME Annual Meeting, Las Vegas, Nevada, SME Preprint 89-6.

159. Chander, S., and Briceno, A., "Kinetics of Pyrite Oxidation", *Minerals and Metallurgical Processing*, 1987, **4**, p. 171.

160. Zhu, X., Wadsworth, M., Bodily, D.M., and Hu, W.B.,"A Comparative Study of the Electrochemical Properties of Mineral and Coal Pyrite", in *EPD Congress '91*, 1991, Gaskell, G.R., Editor, TMS, Warrendale, PA, p.179.

161. Ogunsola, O.M., and Osseo-Asare, K, "The Electrochemical Behavior of Coal Pyrite. 1. Effects of Mineral Source and Composition", *Fuel*, 1986, **65**, p. 811.

162. Li, J., and Wadsworth, M.E., "Raman Spectroscopy of Electrochemically Oxidized Pyrite and Optimum Conditions for Sulfur Formation", in *Hydrometallurgy: Fundamentals, Technology and Innovation*, 1993, Hiskey, J.B. and Warren, G.W., Editors, TMS, Littleton, Colorado, p. 127.

163. Chander, S., and Briceno, A., "The Rate of Oxidation of Pyrites from Coal and Ore Sources-An AC Impedance Study", in *Mine Drainage and Surface Mine Reclamation*, 1988, Bureau of Mines Information Circular 9183, U.S. Department of Interior, **Vol. 1**, p. 164.

164. Biegler, T., "Oxygen Reduction on Sulphide Minerals. Part II. Relation Between Activity and Semiconducting Properties of Pyrite Electrodes", *J. Electroanal. Chem*, 1976, **70**, p. 265.

165. Ball, B.and Rickard, K.,"The Chemistry of Pyrite Flotation and Depression", in *Flotation. A.M. Gaudin Memorial Volume*, 1976, Fuerstenau, M.C., ed., AIME/SME , New York, **Vol I**, Chapter 15, p. 458.

166. Tao, D.P., Richardson, P.E., and Yoon, R.H., "Effect of Oxidation on the Hydrophobicity of Coal Pyrite", in *Proceeding of the 7th International Conference on Coal Science*, 1993, K.H. Michaelian, K.H., ed., **Vol. II**, p. 325.

167. Hamilton, I.C., and Woods, R., "An Investigation of Surface Oxidation of Pyrite and Pyrrhotite by Linear Potential Sweep Voltammetry", *J. Electroanal. Chem.*, 1981, **118**, p. 327.

168. Zhu, X., Li, J., Bodily, D.M., Wadsworth, M.E., "Transpassive Oxidation of Pyrite", *J. Electrochem. Soc.*, 1993, **140**, p. 1928.

169. Richardson, P.E., and Yoon, R.-H., "A Comparison of the Semiconducting Properties of Abraded and Fractured Sulfide Electrodes: Pyrite and Galena", in

Hydrometallurgy: Fundamentals, Technology and Innovation, 1993, Hiskey, J.B., and Warren, G.W.. Editors, TMS, Littleton, Colorado, p. 101.

170. Wadsworth, M.E.. Zhu, X., and Li, J., "Electrochemistry of Pyrite", in *Hydrometallurgy: Fundamentals, Technology and Innovation,* 1993, Hiskey, J.B., and Warren, G.W.. Editors, TMS, Littleton, Colorado, p. 85.

171. Aplan, F.F., "How the Nature of Raw Coal Influences its Cleaning", in *Industrial Practice of Fine Coal Processing*, 1988, TMS, Littleton, Colorado, **Chapter 13**, p. 99.

172. American Society for Testing Materials, *Annual Book of A.S.T.M Standards*, 1984, Part 26, Method D2492-84, ASTM, Philadelphia.

173. Smith, R.M., Grube, W.E., Jr., Arkle, T., Jr., and Sobek, A., in *Mine Spoil Potentials for Soil and Water Quality*, 1974, U.S. Environmental Protection Agency (EPA-670/2-74/070), Cincinnati, Ohio.

174. Sobek, A.A., Schuller, W.A., Freeman, J.R., and Smith, R.M., in *Field and Laboratory Methods Applicable to Overburdens and Minesoils*, 1978 U.S. Environmental Protection Agency (EPA-600/2-78-054), Cincinnati, Ohio.

175. Brooks, J.D. and Sternhell, S., "Chemistry of Brown Coals. 1. Oxygen Containing Functional Groups in Victorian Brown Coals", *Aust. J. Appl. Sci.,* 1957, **8**, p. 206.

176. Anon., "Operating and Maintenance Manual for the Surface Area and Pore Analyzer", Micromeritics Instrument Corporation, Norcross, Ga., 1973.

177. Adamson, A.W., "Physical Chemistry of Surfaces", 1982, 4th Edition, John Wiley and Sons, Inc., New York, p. 64.

178. Laskowski, J., "Surface Properties of Coals in Relation to their Flotation", *8th International Mineral Processing Congress*, Leningrad, U.S.S.R., 1968.

179. Fuerstenau, D.W., Metzge, P.H., and Seele, G.D., "How to Use this Modified Hallimond Tube for Better Flotation Testing", *Engineering and Mining Journal*, 1957, **158**, 93.

180. Friedman, L.D., Kinney, C.R.,"Controlled Air-Oxidation of Coals and Carbons at 150-400°C", *Ind. Eng. Chem.*, 1950, **42 No12**, p. 2525.

181. Williams, M.C., "Experimental Investigation and Mathematical Modeling of Multifeed Flotation Networks", Ph.D. Thesis, University of California, Berkeley, 1985.

182. Ignasiak, B.S., Clugston, D.M., and Montgomery, D.S., "Oxidation Studies in Coking Coal Related to Weathering: Part 2. The Distribution of Absorbed Oxygen in the Products Resulting from the Pyrolisis of Slightly Oxidized Coking Coal", *Fuel*, 1972, **51**, p. 76.

183. Schwartz, D., Hall, P.J., and Marsh, H., "Macromolecular and Chemical Changes Induced by Air Oxidation of a Medium Volatile Bituminous Coal", *Fuel*, 1989, **68**, p. 868.

184. Ramesh, R.,and Somasundaran, P., "Chemical and Wettability Studies on Coal Humic Acid and Cyclized Humic Acid", *Fuel*, 1989, **68**, p. 533.

185. Calemma, V., Iwanski, P., Rausa, R., and Girardi, E., "Changes in Coal Structure Accompanying the Formation of Regenerated Humic Acids During Air Oxidation", *Fuel*, 1994, **73**, p. 700.

186. Havens, J.R., Koening, J.L.,Kuehn, D., Rhoads, C., Davis, A., and Painter, P.C.,"Characterization of Coal Oxidation by Magic-Angle C^{13}n.m.r. Spectroscopy", *Fuel*, 1983, **62**, p. 936.

187. Barna, J., "Humic Substances-Clay Complexes in Hungarian Coals", *Fuel*, 1983, **62**, p. 380.

188. Perry, D.L., and Grint, A., "Application of XPS to Coal Characterization", *Fuel*, 1983, **62**, p. 1024.

189. Quast, K.B., and Readett, D.J., "The Surface Chemistry of Low Rank Coals", *Advances in Colloid and Interface Science*, 1987, **27**, p. 169.

190. Willard, H. H., Merritt, L. L., Dean, J. A., and Settle, Jr, F.A., "Instrumental Methods of Analysis", Seventh Edition, Wadsworth Publishing Company, California, 1988, p. 287.

191. Bellamy, L. J. "The infrared Spectra of Complex Molecules", Chapman and Hall, London, 1975, p. 137.

192. Rockley, M.G., and Devlin, J.P., "Photoacoustic Infrared Spectra (IR-PAS) of Aged and Fresh-cleaved Coal Surfaces", *Applied Spectroscopy*, 1980, **Vol. 34 No 4**, p. 407.

193. Garcia, A.B., Moinelo, S.R., Martinez-Tarazona, M.R., and Tacson, J.M.,"Influence of Weathering Process on the Flotation Response of Coal", *Fuel*, 1991, **70**, p. 1391.

194. University of California, University of Utah, Columbia University and Praxis Engineers Inc., "Coal Surface Control for Advanced Fine Coal Flotation", *Final Report DE-AC22-88PC88878 Project*, March 1992, p. 5-18.

195. Bellamy, L. J. "The infrared Spectra of Complex Molecules", Chapman and Hall, London, 1975, p. 82.

196. Meldrum, B. J. and Rochester, C. H., J.,"*In-situ* Infrared Study of the Surface Oxidation of Activated Carbon on O_2 and CO_2", *Chem. Soc. Faraday Trans.*, 1990, **86**, p. 861.

197. Lowry, H. H., "Chemistry of Coal Utilization", Lowry, H. H., Editor, New York, 1963, p. 67.

198. Pisupati, S.V., and Scaroni, A.W., "Natural Weathering and Laboratory Oxidation of Bituminous Coals: Organic and Inorganic Structural Changes ", *Fuel*, 1993, **72**, p. 531.

199. Painter, P.C., Starsinic, M., Squires,E., and Davis, A.A.,"Concerning the 1600 cm^{-1} region in the I.R. Spectrum of Coal", *Fuel*, 1983, **62**, p. 742.

200. Akhter, M. S., Chughtai, A. R. and Smith D. M., *Appl. Spectroscopy.*, 1985, **39**, p.143.

201. Starsinic, M., Taylor, R. L., Walker, R. L. and Painter, P. C., "FTIR Studies of Saran Chars", *Carbon*, 1983, **21**, p. 69.

202. Ishizaki, C. and Marti, I., "Surface Oxide Structures on a Comercial Activated Carbon", *Carbon*, 1981, **19**, p. 409.

203. Fuerstenau, D.W., Rosenbaum, J.M., and Laskowski, J., "Effect of Surface Functional Groups on the Flotation of Coal", *Colloids and Surfaces*, 1983, **8**, p. 153.

204. Sablik, J., "The Grade of Metamorphism of Polish Coals and Their Natural and Activated Floatability", *International Journal of Mineral Processing*, 1982, **9**, p. 245.

205. Wang, X.H., Jiang, C.L., Raichur,A.M., Parekh, B.K., and Leonard, J.W., "Pyrite Surface Characterization and Control for Advanced Fine Coal Desulfurization Technologies," in *Abstract and Research Accomplishments of University Coal Research Projects*, 1993, Pittsburgh Energy Technology Center, Pittsburgh, PA, p.30.

206. Mirza, A. H., Herrera, M.N., and Doyle, F.M.,"Characterization of Pyrite-Bearing Materials by Chemical Oxidation", in *Emerging Process Technologies for a Cleaner Environment*, 1992, Chander, S., Richardson, P.E., and Shaal, H., Editors, Society for Mining, Metallurgy, and Exploration, Annual Meeting, Phoenix, AZ.,p. 121.

207. Fornasiero, D., Eijt, V., and Ralston, T.,"An Electrokinetic Study of Pyrite Oxidation", *Colloid and Surfaces* , 1992, **62**, p. 63.

208. Fuerstenau, M.C., Kuhn, M.C., and Elgillani, D.A., "The Role of Dixanthogen in Xanthate Flotation of Pyrite", *Transaction. AIME*, 1968, **Vol 241**, p. 148.

209. Doyle F.M., "Oxidation of Coal and Coal Pyrite: Mechanisms and Influence on Surface Characteristics", *Technical Progress Report DE-FG22-90PC90287 Project*, June, 1991.